



<https://theses.gla.ac.uk/>

Theses Digitisation:

<https://www.gla.ac.uk/myglasgow/research/enlighten/theses/digitisation/>

This is a digitised version of the original print thesis.

Copyright and moral rights for this work are retained by the author

A copy can be downloaded for personal non-commercial research or study,
without prior permission or charge

This work cannot be reproduced or quoted extensively from without first
obtaining permission in writing from the author

The content must not be changed in any way or sold commercially in any
format or medium without the formal permission of the author

When referring to this work, full bibliographic details including the author,
title, awarding institution and date of the thesis must be given

Enlighten: Theses

<https://theses.gla.ac.uk/>
research-enlighten@glasgow.ac.uk

Early events of Jaagsiekte sheep retrovirus infection in the ovine lung

Henny Martineau
BVMS MRCVS

Submitted in the fulfilment of the requirements of the degree
of
Doctor of Philosophy
College of Veterinary, Medical and Life Sciences
University of Glasgow

September 2010

ProQuest Number: 10754023

All rights reserved

INFORMATION TO ALL USERS

The quality of this reproduction is dependent upon the quality of the copy submitted.

In the unlikely event that the author did not send a complete manuscript and there are missing pages, these will be noted. Also, if material had to be removed, a note will indicate the deletion.



ProQuest 10754023

Published by ProQuest LLC (2018). Copyright of the Dissertation is held by the Author.

All rights reserved.

This work is protected against unauthorized copying under Title 17, United States Code
Microform Edition © ProQuest LLC.

ProQuest LLC.
789 East Eisenhower Parkway
P.O. Box 1346
Ann Arbor, MI 48106 – 1346

GLASGOW
UNIVERSITY
LIBRARY:

Abstract

Ovine pulmonary adenocarcinoma (OPA) is a chronic respiratory disease of adult sheep caused by Jaagsiekte sheep retrovirus (JSRV). The primary route of disease transmission is by inhalation of the virus, which then infects respiratory epithelial cells initiating oncogenesis and tumour growth. Clinical signs are seen towards end stage disease and include laboured breathing and weight loss. In these animals, the production of copious amounts of virus rich fluid which pours from the nose when the hind legs are lifted is a common finding and pathognomic for OPA. Once these signs are apparent, the disease is invariably fatal.

The worldwide prevalence of OPA has both economic and welfare implications. However, there is currently no effective preclinical test or vaccine to control spread of disease. This is primarily due to the lack of detectable immunological response at any stage of disease pathogenesis. Theories of central and peripheral tolerance have been proposed as explanations for this. OPA is also regarded as a potential model for human lung cancer. As in sheep, clinical presentation in humans is not until tumour growth is extensive by which time treatment is unsuccessful. This makes it difficult to study the initial stages of disease, and identify potential markers for early detection or targets for therapeutics.

The aim of this study was to investigate these previously unexplored early stages of disease pathogenesis for OPA. The primary areas of interest were identification of the target cells for JSRV infection in the lung and analysis of the innate response following this infection.

Samples for analysis were provided by the intratracheal inoculation of specific pathogen free lambs with an infectious molecular clone JSRV₂₁. Lambs were euthanased 3, 10 and 72-91 days following inoculation and lung samples representing different stages of disease pathogenesis were collected from each lamb. Mock infected and non infected lambs were included as negative controls at each time point. Immunohistochemistry was used to localise virus expression to specific epithelial cell types within the ovine respiratory tract. The same techniques also offered a means of studying the postnatal development of the ovine respiratory

tract. The innate response to infection and subsequent tumour growth was measured in terms of cytokine production. RNA was extracted from adjacent samples to those used for IHC, and qRT-PCR measured mRNA levels of a number of inflammatory cytokines and chemokines at each time point.

Immunohistochemical analysis of the ovine respiratory tract found evidence of cytodifferentiation during postnatal development. This has implications for the susceptibility of lambs to infectious and noxious insults during this period. JSRV was found to target multiple cell types in the ovine lung. These included Clara cells, type II pneumocytes and cells which did not express either of these mature markers. Analysis of cytokine expression in lung tissue both before and during JSRV expression and tumour growth found little evidence of a host response to virus expression. Changes in the levels of cytokine mRNA were detected for those primarily involved in tumour growth and survival. These included IL-8 and IDO, both of which have been found to be increased in some cases of human lung tumour. These findings increase the understanding of the pathogenesis of OPA, and improve its validity as an animal model for human lung cancer.

Table of Contents

Title	i
Abstract	ii-iii
Contents	iv
List of Tables	viii
List of Figures	x
Acknowledgements	xiv
Authors declaration	xv
Abbreviations	xvi
Chapter 1 Introduction	
1.1 Lung anatomy	1
1.1.1 Developmental anatomy	1
1.1.2 Gross anatomy	2
1.1.3 Cellular anatomy	3
1.1.4 Lung maintenance and repair	12
1.1.5 Carcinogenesis and the lung progenitor cell	18
1.2 Ovine pulmonary adenocarcinoma	21
1.2.1 Clinical parameters of OPA	21
1.2.2 Pathology of OPA	24
1.2.3 Discovery of the aetiology of OPA	29
1.3 Retroviruses	34
1.3.1 Retrovirus classification	35
1.3.2 Retrovirus structure	36

1.3.3 Retroviral replication	38
1.3.4 Influential host factors for retroviral replication	42
1.3.5 Endogenous retroviruses in sheep	44
1.3.6 The immune response	46
1.3.7 Retroviral oncogenesis	50
1.3.8 Other exogenous retroviruses in sheep	56
1.4 Thesis overview	57
Chapter 2 Materials and methods	
2.1 Experimental infection with JSRV ₂₁	58
2.1.1 Preparation of JSRV ₂₁	58
2.1.2 Intra-tracheal inoculation of lambs with JSRV ₂₁	58
2.1.3 Post mortem of experimental animals	59
2.2 Slide staining protocols	63
2.2.1 Histochemical techniques	63
2.2.2 Immunohistochemical techniques	64
2.2.3 Antigen visualization systems	70
2.2.4 IHC quantification	72
2.3 Quantitative reverse transcriptase polymerase chain reaction	76
2.3.1 Preparation of samples for RNA extraction	76
2.3.2 qRT-PCR procedure	80

Chapter 3 Immunohistochemical analysis of the ovine lung during postnatal maturation

3.1 Introduction	86
3.2 Results	87
3.2.1 Histological categorisation of the lung	87
3.2.2 Histochemical analysis of the lung	90
3.2.3 Immunohistochemical analysis of the lung	92
3.2.4 Anatomical localisation of cell types	95
3.2.5 Numerical quantification of IHC labelling	96
3.2.6 Effect of age on proliferative index	101
3.3 Discussion	103

Chapter 4 Identification of the target cell for JSRV infection in the lung

4.1 Introduction	108
4.2 Results	109
4.2.1 Experimental infection of neonatal lambs with JSRV ₂₁	109
4.2.2 Post-mortem validation of experimental model	110
4.2.3 Proliferative cells in the sheep lung during postnatal development	113
4.2.4 Detection of cells expressing JSRV SU using IHC	117
4.2.5 Identification of JSRV target cell using serial sections	123
4.2.6 Identification of JSRV target cell using dual labelling	126
4.2.7 Identification of JSRV target cell using immunofluorescence	131
4.3 Discussion	146

Chapter 5	JSRV infection and the host cytokine response	
5.1	Introduction	151
5.2	Methods	152
	5.2.1 Sample collection and storage	152
	5.2.2 RNA extraction and purification	153
	5.2.3 Establishment of reference genes for qRT-PCR	154
	5.2.4 qRT-PCR candidate gene analysis	156
5.3	Results	
	5.3.1 Histological analysis of experimental samples	158
	5.3.2 Candidate gene analysis	159
5.4	Discussion	166
Chapter 6	General discussion and conclusions	171
Appendix 1		
	Table A1 A summary of experimental animal numbers and their corresponding age of euthanasia and infection status	179
Appendix 2		
	Figure A1 Alveolar region showing colocalisation of labelling for DC-LAMP and SP-C in type II pneumocytes	180
Bibliography		181

List of Tables

1.1	Comparison of epithelial cell distribution in the rabbit and sheep lung	4
1.2	Anatomical definitions of airways in the lung	5
1.3	Glossary of stem cell terminology	14
1.4	Markers for cancer stem cells in solid tumours	19
1.5	Summary of early experiments to determine the aetiology of OPA	30
1.6	Summary of early disease transmission experiments	31
1.7	General comparison of human and ovine lung tumours	55
2.1	Fixation procedure for all lung samples	60
2.2	Summary of antigen retrieval methods for IHC	66
2.3	Summary of primary antibodies and optimisation conditions tested in this study	67-9
2.4	Twelve steps taken to maximise RNA yield and purity from tissue samples	79
2.5	Details of primers selected for reference genes selected for geNorm analysis	83
2.6	Primers and probes for qRTPCR analysis of candidate genes	84
2.7	Reaction conditions for primers and probes	85
3.1	Anatomical regions of the lung as defined by Tyler 1983	87
3.2	Summary of histochemical stains used on ovine lung tissue	90
3.3	Optimised conditions for antibodies to label epithelial cells in the ovine lung	92
3.4	Summary of epithelial cell location in the ovine respiratory tract during postnatal development	95
4.1	Comparison of fixation methods and detection of single/clusters of cells expressing virus in OPA (E) lambs, 10 days PI using IHC	119
4.2	A summary of positive labelling for SU antibody on formalin fixed tissue from lambs 3 and 10 days PI	120
4.3	Summary of size and location of positive labelling cells in four lambs 10 days post inoculation	121
4.4	Summary of antibodies used for dual labelling	126

4.5	Optimised concentrations of antibody and fluorescent substrates / Fab fragments used for visualization	131
4.6	Summary of the protein expression of single SU positive cells in lambs 10 days post inoculation	140
4.7	Summary of protein expression of clusters of cells expressing virus in lambs 10 days PI	145
5.1	Summary of cytokines examined and their actions	157
5.2	Histopathological scoring of lung tissue for evaluation of infiltrating cell types and tumour pathology	158
5.3	Summary of changes in mRNA levels of a variety of cytokines	164
A1	A summary of experimental animal numbers and their corresponding age of euthanasia and infection status.	179

List of Figures

Figure 1.1	Schematic representation of ovine bronchial tree (A) lung (B)	2
Figure 1.2	Diagram of bronchial tree (A) and corresponding cellular anatomy (B)	11
Figure 1.3	Schematic representation of proliferative cells in a villus in the intestine	13
Figure 1.4	IHC labelling of Ki-67 positive cells in the intestine (A) and lung bronchiole (B)	13
Figure 1.5	Summary of stem cell types at different levels of the respiratory tract as defined in the mouse	16
Figure 1.6	Cancer stem cell model for tumour heterogeneity and propagation	19
Figure 1.7	Clinical signs of OPA in adult sheep	23
Figure 1.8	Post mortem findings in natural field cases of OPA	25
Figure 1.9	Histological findings in natural field cases of OPA	27-8
Figure 1.10	Phylogenetic tree showing the classification of retroviruses	35
Figure 1.11	Schematic diagram of JSRV virion structure	36
Figure 1.12	Structure of the JSRV genome	37
Figure 1.13	Replication cycle of JSRV, a general overview	38
Figure 1.14	A schematic representation of reverse transcription	41
Figure 2.1	Chart showing timings of lamb inoculations and PME	59
Figure 2.2	Photographic record of lungs from SPF lambs	61
Figure 2.3	PME template for lung sampling	62
Figure 2.4	Image J measures area of IHC labelling	73
Figure 2.5	NEB number calculation	74
Figure 2.6	Procedure for calculating proliferative index	75
Figure 2.7	Methods for optimization of primers and probes using the standard curve	81
Figure 3.1	Histological categorisation of the lung into five anatomical regions	88-9
Figure 3.2	Histochemical staining in the sheep lung and positive control tissue	91
Figure 3.3	IHC to identify specific cells in the ovine lung and positive control tissues	93
Figure 3.4	Graphs showing the variation in beta tubulin expression in four anatomical regions of the lung in different ages of lamb	97

Figure 3.5	IHC using anti-beta tubulin antibody to label ciliated cells in bronchiole from 9 (A) and 91 (B) day old lambs	97
Figure 3.6	Graph showing the variation in CCSP expression from two sites (1b, 5a) in four anatomical regions of the lung in different ages of lamb	98
Figure 3.7	IHC using anti-CCSP antibody to show labelling in the respiratory bronchioles of 9 day (A) and 91 day (B) old lambs	99
Figure 3.8	Graph showing variation of NEB per cm ² in a total of six lambs ages 9,16 and 91 days	100
Figure 3.9	Graph showing variation in % SP-C numbers in a total of six lambs aged 9,16 and 91 days	100
Figure 3.10	IHC using anti-Ki 67- antibody to compare proliferative index between intestine and lung	101
Figure 3.11	Graph to show the proliferative index of five anatomical regions in the lung in lambs aged 9, 16 and 91 days	102
Figure 3.12	Comparison of number of Ki-67 positive cells in the alveolar region of a 9 day (A) and 91 day old lamb (B)	102
Figure 4.1	Timing of experimental infection and euthanasia	109
Figure 4.2	Summary of lung weight as a proportion of bodyweight for all lambs 72 - 91 days PI	110
Figure 4.3	Gross appearance of lungs from experimental lambs	111
Figure 4.4	A whole transverse section of lung from case 2863 E, site 5a	112
Figure 4.5	IHC analysis comparing protein expression in cases of OPA-N (left column) and OPA-E (right column)	114
Figure 4.6	Optimisation of dual labelling IHC using anti-CCSP antibody (1/20 000) and anti-Ki-67 antibody (1/1000)	115
Figure 4.7	IHC to identify proliferative capacity of Clara cells, NEBs and type II pneumocytes on OPA-E 10 days PI	116
Figure 4.8	IHC using anti-JSRV SU antibody on cases from OPA-N and OPA-E	118
Figure 4.9	Variation in location of JSRV SU expression both within and between animals	121
Figure 4.10	IHC using anti JSRV SU Mab to label cells in lung tissue from lambs 10 days post inoculation	122
Figure 4.11	IHC of serial sections labelled with anti-JSRV SU Mab (A, B), anti-DC-LAMP antibody (C, D) and anti-pancytokeratin antibody (E, F)	124

Figure 4.12	IHC of serial sections labelled with anti-JSRV SU, anti-DC LAMP,SP-C and anti-pancytokeratin antibodies	125
Figure 4.13	Dual IHC on lungs from experimental infections	127
Figure 4.14	Dual labelling with anti-CCSP antibody (brown) and anti-JSRV antibody (purple)	128
Figure 4.15	Double IHC to determine the phenotype of single and clusters of cells positive for JSRV SU	129
Figure 4.16	Optimisation of fluorescent antibodies for single and multiple labelling techniques in OPA-E lambs 72-91 days PI	132
Figure 4.17	BADJ showing BASC-like cell in a negative control lamb	133
Figure 4.18	Sequential sectioning of lung tissue for multiple labelling using immunofluorescence	136
Figure 4.19	JSRV SU positive cell in respiratory bronchiole, which does not label with CCSP, SYN or SP-C	136
Figure 4.20	Single cell in terminal bronchiole with positive labelling for JSRV SU and CCSP only	137
Figure 4.21	Single cell in terminal bronchiole expressing JSRV SU and CCSP only	138
Figure 4.22	Single cell in alveolar region labels positively for JSRV SU and SP-C	139
Figure 4.23	Respiratory bronchiole showing two cells expressing JSRV SU only	142
Figure 4.24	Respiratory bronchiole from showing two cells adjacent to BADJ (arrow) expressing JSRV SU only	143
Figure 4.25	Phenotypic expressions of JSRV SU positive clusters	144
Figure 4.26	Schematic diagram to show possible target cells for JSRV infection in the ovine lung	149
Figure 5.1	Summary of animals sampled to investigate cytokine response to infection with JSRV	152
Figure 5.2	Summary of tissue sampling process before RNA extraction	153
Figure 5.3	Procedure for RNA extraction and analysis	153
Figure 5.4	geNorm analysis to determine the stability of reference genes in normal and diseased lung (A) and lymph node (B) tissue	155
Figure 5.5	Arrangement of samples on 96 well plate	156
Figure 5.6	Whisker box plots of relative amounts of cytokine mRNA in lung (A) and lymph node (B) of JSRV infected vs mock/uninfected animals at 3 days PI	160

Figure 5.7	Whisker box plots of relative cytokine expression in lung (A) and lymph node (B) tissue 10 days PI with JSRV ₂₁ vs. mock/uninfected animals	161
Figure 5.8	Whisker box plots of relative cytokine expression in lung and lymph node tissue versus controls, 8 weeks PI with JSRV ₂₁	162
Figure 5.9	Whisker box plots of relative cytokine expression in lung (A) and lymph node (B) tissue from naturally infected animals vs. control group	163
Figure 5.10	IHC showing labelling for IL-8 in lungs from OPA-N and OPA-E	165
Figure 5.11	Summary of possible cytokine interactions following JSRV infection of a lung epithelial cell	168
Figure A2	Alveolar region showing colocalisation of labelling for DC-LAMP and SP-C in type II pneumocytes	180

Acknowledgements

I would like to thank everyone that has helped me during the undertaking of this thesis. Firstly my supervisors David Griffiths, Mark Dagleish and Massimo Palmarini who helped and encouraged but were also patient with me. The experimental infection was made possible by Stuart Imlach for producing the JSRV₂₁, Manus Graham for inoculating the lambs, the staff in the High Security Unit for rearing the lambs, Arthur Watt and his team and Mike Malcom-Smith for coordinating and helping with post mortems. Clare Underwood, Val Forbes, Jeanie Finlayson and Stephen Maley worked tirelessly processing the many samples and slides that were required throughout the project and giving me invaluable advice on immunohistochemical techniques. Technical advice was given by Craig Watkins, Kim Willoughby, Dave Buxton, Alex Schock, Patricia Dewar, Julio Benavides and Gary Entrican. Chris Cousens was invaluable at all stages of the experiment providing hands on help and technical advice whenever needed. Finally, none of this would have been possible without extensive support and encouragement from my family and Gordy.

This thesis is dedicated to Gordon Watt and Tref y clawwd.

Authors declaration

I declare that all work included in this thesis is my own work. No part of this work has been, or will be submitted for any other degree or professional qualification.

Common Abbreviations

AAH	Atypical adenomatous hyperplasia
AHV	Avian haemangioma virus
ALDH1	Aldehyde dehydrogenase 1
APC	Antigen presenting cells
AR	Antigen retrieval
BAC	Bronchioloalveolar carcinoma
BADJ	Bronchioloalveolar duct junction
BALF	Bronchioloalveolar lavage fluid
BASC	Bronchioloalveolar stem cell
BMDSC	Bone marrow derived stem cells
CA	Capsid protein
CCSP	Clara cell secretory protein
CGRP	Calcitonin gene related peptide
C _T	Crossing threshold
CSC	Cancer stem cell
DAB	3,3'diaminobenzidine
DNA	Deoxyribonucleic acid
E	Eosin
EDTA	Ethylenediaminetetraacetic Acid
enJSRV	Endogenous JSRV
ENTV	Enzootic nasal tumour virus
ERV	Endogenous retrovirus
Fab	Fragment antigen binding
FS	Formal saline
GOI	Gene of interest
GPI	Glycosylphosphatidylinositol
H	Haematoxylin
HERV	Human endogenous retrovirus
HKG	Housekeeping gene
HRP	Horse radish peroxidase
Hyal-2	Hyaluronidase -2
IFN	Interferon

IHC	Immunohistochemistry
IN	Integrase
iv	Intravenous
JSRV	Jaagsiekte sheep retrovirus
LFB	Luxol Fast Blue
LTR	Long terminal repeat
MA	Matrix
Mab	Monoclonal antibody
MAPK	Mitogen-activated protein kinase
MHC	Major Histocompatibility complex
MMTV	Mouse mammary tumour virus
MPMV	Mason-Pfizer monkey virus
MRI	Moredun research institute
MVV	Maedi visna virus
NC	Nucleocapsid
NE	Neuroepithelial
NEB	Neuroepithelial body
NGS	Normal goat serum
NRS	Normal rabbit serum
NSCLC	Non small cell lung cancer
Oct 4	Octamer binding transcription factor 4
OM	Original magnification
OPA	Ovine pulmonary adenocarcinoma
OPA-N	Natural field case of OPA
OPA-E	Experimental case of OPA
PBS	Phosphate buffered saline
PAMP	Pathogen associated molecular pattern
PAS	Periodic acid Schiff
PBMC	Peripheral blood mononuclear cells
PBST	Phosphate buffered saline/0.05% Tween 20
PF	Paraformaldehyde
PI	Post inoculation
PME	Post mortem examination
PPT	Polypurine tract

PR	Protease
PRR	Pattern recognition receptors
PTAH	Mallory's phosphotungstic acid-haematoxylin
RIN	RNA integrity number
RON	recepteur d'origine nantais
RNA	Ribonucleic acid
RPMI	Roswell park Institute medium
RSV	Respiratory syncitial virus
RT	Reverse transcriptase
SN	Supernatant
SP-C	Surfactant protein C
SPF	Specific pathogen free
SU	Surface protein
tRNA	Transfer ribonucleic acid
TH1	T helper 1
TH2	T helper 2
TM	Transmembrane protein
TSA	Tyramide signal amplification
TEM	Transmission electron microscopy
WHO	World health organization
ZS	Zinc salts

Gene Symbol Gene name

B2M	Beta 2 microglobulin
CD 4	T-cell surface glycoprotein CD4
CD 8	T-cell surface glycoprotein CD8
GM-CSF	Granulocyte macrophage colony stimulating factor
IFN gamma	Interferon gamma
IFN alpha	Interferon alpha
IDO	Indoleamine 2, 3-dioxygenase
IL-1 Beta	Interleukin 1 beta
IL-2	Interleukin 2
IL-4	Interleukin 4
IL-6	Interleukin 6
IL-8	Interleukin 8
IL-10	Interleukin 10
IL-18	Interleukin 18
MCP-1	Monocyte chemoattractant protein-1
SDHA	Succinate dehydrogenase complex subunit A
TGF beta	Transforming growth factor Beta
TNF alpha	Tumour necrosis factor alpha
YWHAZ	Tyrosine 3-monooxygenase/tryptophan 5-monooxygenase activation protein, zeta

CHAPTER 1 INTRODUCTION

1.1 Lung anatomy

The functional anatomy of the lung has been a subject of scientific interest for many years. In the early literature of 1497, Alessandro Benedetti described the lung as an organ responsible for cooling the blood and '*changing breath into food for the vital spirit*'. A role in the psychology of the human body was also suggested: '*with the breath of the spirit from the hollow fistulae of the lung. Thus anger, otherwise implacable, is easily calmed*'. However, it was not until the 17th Century that the essential function as we know it today was recognised. '*Pre-eminence of the lung: nothing is especially so necessary neither sensation nor aliment. Life and respiratory are complementary. There is nothing living which does not breathe, nor anything breathing which does not live*' (William, 1961).

The anatomy of the lung is dictated by the efficiency of respiratory gas exchange required by the host. Single celled organisms can survive by simple diffusion of gases, fish utilise aqueous diffusion in their gills and insects have a well-branched respiratory trachea (Warburton et al., 2000). Birds have a unique system of lungs and air sacs which maximise gas exchange via parabronchi and atria while minimising the weight of the animal (Brackenbury, 1972). Air breathing amphibians and mammals have developed lungs which exchange gases with the circulation by diffusion through a single cell layer. As the metabolic needs vary between these species, so does the detailed anatomy of the lung.

1.1.1 Developmental anatomy

During embryogenesis, the lung arises from a bud in the ventral foregut endoderm, which divides and grows as a series of epithelial tubes and vascular structures (Cardoso and Lu, 2006). Its development is controlled by cross talk between the invading epithelial cells and surrounding mesenchyme and the regulated expression of numerous transcription factors (Cardoso, 2000; Cardoso and Lu, 2006; Deimling et al., 2007). The eventual pattern of the conducting and respiratory airways mimics the trunk and branches of a tree, hence the term bronchial tree (Figure 1.1A) (Metzger et al., 2008). The largest airway, the trachea, divides into two main stem bronchi at the thoracic inlet. These in turn bifurcate into smaller

intrapulmonary bronchi, bronchioles, terminal bronchioles and respiratory bronchioles before terminating in pouches called alveolar ducts. These are lined by alveolar sacs which bring inhaled gases into close contact with underlying alveolar capillaries so facilitating gas exchange.

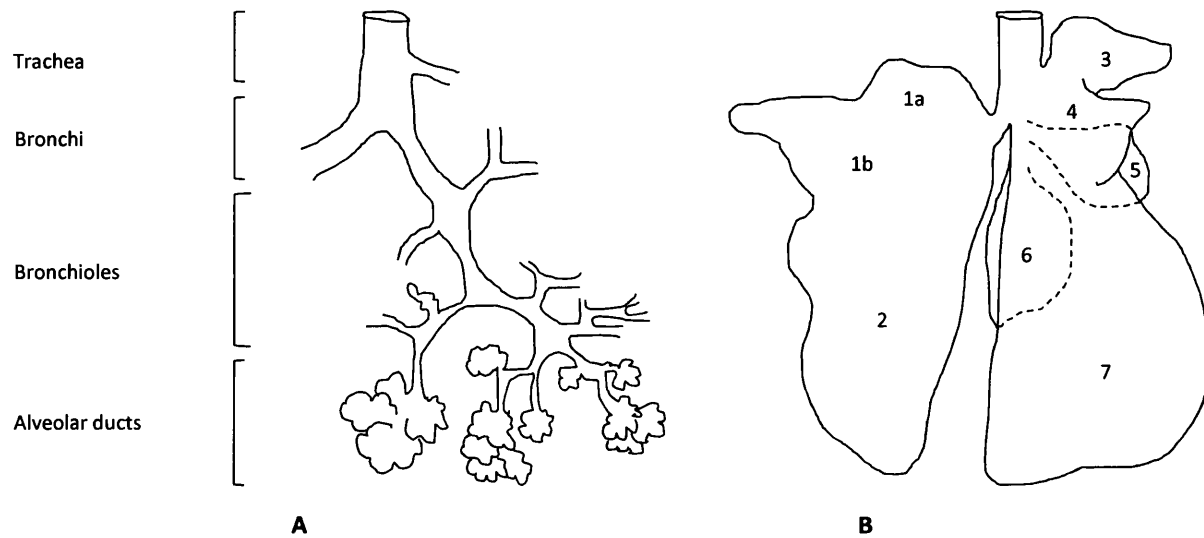


Figure 1.1 Schematic representation of ovine bronchial tree (A) and lung (B). Lung lobes (1a) left cranial apical, (1b) left caudal apical, (2) left diaphragmatic, (3) right apical, (4) cardiac, (5) mediastinal, (6) accessory, (7) right diaphragmatic

1.1.2 Gross anatomy

A thorough account of the general anatomy of the sheep lung has been described previously (Sisson and Grossman, 1975). It is a paired organ with left and right sides (Figure 1.1B). The left lung is made up of apical (cranial and caudal) and diaphragmatic lobes. The larger right lung is divided into five lobes by interlobular fissures and consists of the apical, cardiac, mediastinal, accessory and diaphragmatic lobes. Notable characteristics include the presence of a tracheal bronchus which branches to the right from the trachea at the level of the third rib, cranial to the division of the main stem bronchi. It supplies the right apical lobes and is common to other ruminants (Sisson and Grossman, 1975).

Techniques such as corrosion casting and microdissection have been used to study the gross anatomy of the lung (Mariassy and Plopper, 1983; Phalen et al., 1978; Plopper et al., 1983). Comparison of the lungs from five species shows variations in airway length, diameter, branching angle and number of generations (Plopper et al., 1983). For example, microdissection of five sheep lungs found there to be an average of 30 generations of axial pathways before reaching terminal bronchioles, which compares to 22 generations in the rabbit and 14 in the bonnet monkey. Differences between lung lobes in the same animal were also noted. An asymmetry in airway diameter at each branch point led to the development of a convenient binary system for airway numbering and accurate anatomical localisation within the organ (Phalen et al., 1978).

1.1.3 Cellular anatomy

The cellular structure and function of the mammalian lung was first investigated by light microscopists in the early 17th Century. The presence of an epithelial lining of the airways was noted by Laurentius in 1602, confirmed by Morgagni in 1712 (Breeze and Wheeldon, 1977) and further researched to identify ciliated cells, goblet cells and Clara cells (Clara, 1937; Kolliker, 1882). We now know there to be over 40 different cell types within the lung which are defined by their embryonic origin into mesenchymal and epithelial types. Epithelial cells act as the sentinels of the respiratory tract. They present a strong defence to inhaled particles both through barrier function and their ability to help maintain homeostasis during respiration. This preserves the sterile environment necessary for gas exchange. This study focuses on the epithelial compartment as it contains the majority of cells which have specialised functions specifically related to the lung (Wuenschell et al., 1996). Those of particular interest are ciliated cells, Clara cells, neuroepithelial bodies (NEBs) and type II pneumocytes.

Studies designed to quantify and locate epithelial cells within the lung are surprisingly scarce. This is most likely due to the difficulty the pathologist has in anatomical orientation when presented with a histological section of the lung, as depending on the cutting angle similar tubular structures in the lung can appear to be quite different. Before immunohistochemical techniques were widely available, pathologists had to rely on cell morphology with Haematoxylin and Eosin (H and E) staining, special histochemical stains and ultrastructural features to identify specific cell types (Azzopardi and Thurlbeck, 1969; Plopper et al., 1980a;

Plopper et al., 1980b; Roth, 1973). It was not until 1983 that a thorough study of the entire tracheobronchial epithelium in the sheep was carried out (Mariassy and Plopper, 1983). At that time, just two similar studies existed but these described rodent lungs only (Jeffery and Reid, 1975; Kennedy et al., 1978). The sheep lungs were examined using light microscopy and TEM to identify, quantify and locate eight major epithelial cell groups: four mucus type cells, ciliated, basal, Clara and serous cells (Mariassy and Plopper, 1983, 1984). By correlating cell type with anatomical location using the binary system, it was concluded that the epithelial distribution did not correlate with airway wall components, and that Clara cell distribution was based on airway generation and proximity to alveoli (Table 1.1). This was in contrast to the rabbit which appeared to have no Clara cells in the distal bronchioles.

Table 1.1 Comparison of epithelial cell distribution in the sheep and rabbit lung. Reproduced from Plopper et al 1983.

Airway generation	Basal cell %		Ciliated cell %		Mucous cell %		Clara cell %	
	Sheep	Rabbit	Sheep	Rabbit	Sheep	Rabbit	Sheep	Rabbit
Trachea	28.5	28.2	30.6	43.0	41.0	1.3	0	17.6
1° bronchus	18.0	27.1	48.2	43.0	33.8	1.1	0	21.8
5	18.7	2.3	39.1	49.2	42.3	0	0	41.3
10	16.4	0	48.4	50.0	34.9	0	0	50.0
15	19.2	0	42.6	43.7	38.0	0	0	56.3
20	10.6	0	47.6	46.0	42.0	0	0	54.0
24	0	NA	59.1	NA	19.8	NA	21.0	NA
30	0	NA	32.3	NA	0	NA	67.7	NA

Inspired by the increasing use of sheep as models of human disease, a similar experiment was conducted in 1993 to examine three sheep lungs with TEM (Bouljihad and Leipold, 1994). Instead of the binary system they applied criteria suggested by (Tyler, 1983). This uses airway wall components and proximity to alveoli to identify four types of bronchioles (Table 1.2). They found the primary and secondary bronchioles to contain four cell types: basal cells, intermediate cells, ciliated cells and Clara cells. The epithelium of terminal and respiratory bronchioles was made up of only ciliated cells and Clara cells, and the alveolar wall was

covered by type I and type II pneumocytes. The presence of Clara cells in primary and secondary bronchioles conflicts with the data of (Mariassy and Plopper, 1983, 1984), but both agree that terminal bronchioles only consist of ciliated and Clara cells. Previous publications had identified the intermediate cell type as a differentiating cell (Breeze and Wheeldon, 1977).

Table1.2 Anatomical definitions of airways in the lung (Tyler 1983)

Lung airway	Description
Bronchus	Complete walls formed by irregular plates or plaques of cartilage in loose connective tissue with elastic and collagenous fibers and smooth muscle. Mucous or mixed glands in the lamina propria or submucosa Ciliated pseudostratified columnar epithelium with mucous (goblet) cells.
Bronchiole	Walls of smooth muscle and loose connective tissue. No cartilage, no glands. Interalveolar septa attached to their abluminal surface. Ciliated columnar to squamous epithelium with no mucous (goblet) cells Terminal bronchioles are the most distal, highest generation bronchioles which are not alveolarised. Last of conducting airways.
Respiratory bronchiole	Transition between conducting airways and respiratory air spaces. Same structure as nonrespiratory bronchioles, except for the presence of openings in the walls for alveoli and shorter epithelium. Low generation respiratory bronchioles may be 'poorly alveolarised' ie. have few alveoli. Higher generation respiratory bronchioles are typically 'well alveolarised' ie. have numerous alveoli.
Alveolar ducts	Alveoli open into the lumen all around the circumference. Spiral smooth muscle and type I or II alveolar epithelium.

Interestingly, none of these studies mention the presence of neuroendocrine (NE) cells, also known as K cells or 'apparently unrelated endocrine cells' (APUD) cells (Balaguer and Romano, 1991; Breeze and Wheeldon, 1977). Initially identified as 'clear cells' due to their lack of affinity for H and E (Feyrter, 1938), they are also found in the gastrointestinal and genitourinary tracts and act as part of the peripheral endocrine epithelial system (Scheuermann et al., 1997). In sheep they were first identified in the trachea using TEM, Grimelius's silver nitrate method and fluorescence histochemistry (Cutz et al., 1975), but have since been found throughout conducting and respiratory airways as single cells or in groups called

neuroendocrine bodies (NEBs) (Balaguer and Romano, 1991). Immunohistochemistry (IHC) allowed quantification techniques to compare cell numbers in animals of different ages as well as localising them anatomically. Measurements either gave the total number of endocrine cells per surface area of sheep lung, or calculated them as a percentage of total number of cells counted. These studies demonstrated age related changes in number and location of cells during fetal and post natal development (Asabe et al., 2004; Balaguer and Romano, 1991; Van Lommel and Lauweryns, 1997).

The physiological functions of these different epithelial cell types are better understood for some than others. For example, it is well known that the mucous secreted by the goblet cells in the larger airways forms a sticky protective layer, the airway surface fluid, over the entire respiratory epithelium that captures unwanted inhaled particles (Snyder et al., 2009). These are then removed by the beating cilia of the ciliated epithelial cells, which continually walk the mucus carpet up out of the respiratory tract for external expulsion from the nose or swallowing (Corrin 2000). The role of type II pneumocytes as surfactant producers to maintain the patency of the distal airways, and type I pneumocytes as the site of gas exchange in the alveoli are also well recognised (Kotton and Fine, 2008). Clara cells and NEB/neuroendocrine cells appear to have a broader range of functions, not all of which are fully defined. The progenitor capabilities of these and less differentiated cell types is also a subject of much debate. The following section will discuss these points in more detail.

1.1.3.1 Ciliated epithelial cells

Ciliated cells are present in various proportions in all regions of the conducting airways (Plopper et al., 1983). They are easy to identify by using histological stains or IHC to highlight the cilia. Antibodies labelling beta tubulin or the transcription factor Foxj 1 are useful for specific identification (Dave et al., 2008; Park et al., 2006). The cilia act to transport mucus and unwanted inhaled particles out of the respiratory tract and they decrease in height to correspond with smaller airways and a change in viscosity of mucus (Corrin 2000).

There are conflicting reports regarding the progenitor capabilities of these ciliated cells. Lineage labelling techniques have shown them to be terminally differentiated during normal lung homeostasis (Rawlins et al., 2008). A transient change in morphology following lung

injury with naphthalene and SO₂ has been noted, but this was not accompanied by cellular proliferation or transdifferentiation (Rawlins et al., 2007). In contrast, an earlier report describes the transformation of ciliated cells into Clara cells following injury of the lung with bleomycin (Aso et al., 1976). Transdifferentiation and proliferation are also reported in another naphthalene injury model (Park et al., 2006). Here they describe squamous metaplasia of ciliated cells which spread beneath injured Clara cells to maintain epithelial integrity. Eventually these cells were seen to revert to their original ciliated phenotype (Park et al., 2006). Similar dynamic changes have been noted in the lung after unilateral pneumonectomy (Voswinckel et al., 2004). In models of acute asthma and viral infection transdifferentiation into mucus cells has also been demonstrated (Reader et al., 2003; Tyner et al., 2006). These reported variations in progenitor capacity are likely due to the different methods used for lung injury and cell identification. Although confusing, they do demonstrate the plasticity of ciliated cells in the lung.

1.1.3.2 Clara cells

Originally described as ‘non ciliated, non-mucous and non serous secretory cells’ (Clara, 1937), Clara cells are essential for normal maintenance and repair of the lung. They have a critical progenitor role and also contribute to homeostasis by secreting substances into the airway surface fluid. Ultrastructural characterisation shows them to have discrete electron-dense granules within the cytoplasm (Plopper et al., 1980a) which contain a 10-16 kDa protein called Clara cell protein – also known as uteroglobin, Clara cell secretory protein (CCSP), Clara cell 10/16-kDa protein, human protein 1, urine protein 1 (Singh and Katyal, 2000). It is the major product of these cells and comprises 7% of the total protein found in bronchioalveolar lavage fluid (BALF) in humans (Bernard et al., 1992). The precise role of this protein remains to be determined (Ryerse et al., 2001) but suggested functions include inhibition of phospholipase A2 and downregulation of inflammation, anti-viral activity, inhibition of leukocyte chemotaxis and immunomodulation by inhibiting interferon gamma (Singh and Katyal, 2000). It has also been shown to regulate cross talk between lung epithelium and macrophages (Reynolds et al., 2007). Other roles such as progesterone binding, retinoid binding, calcium binding and protease inhibition have been assigned to rabbit uteroglobin in the uterus, and are presumably transferable to the lung (Singh and Katyal, 2000).

Lung disease can affect the expression of CCSP. In humans, levels in BALF are generally increased in patients with sarcoidosis, and those at risk of or suffering from respiratory distress syndrome (Shijubo et al., 2000). In contrast, decreased levels are found in the BALF of asthma sufferers and smokers with normal lung function tests (Shijubo et al., 1997). The actual numbers of CCSP-positive bronchiolar epithelial cells in these patients are also reduced. Malignant transformation of cells tends to reduce expression and this has been shown in prostate, uterine and lung tumours (Linnoila et al., 2000; Patierno et al., 2002). Only 10-30% of lung adenocarcinomas were found to express CCSP, which was also at lower levels than seen in untransformed cells. In a model of lung cancer in the hamster, CCSP was only expressed during the early stages of tumour development. An excellent review by Linnoila et al details some of these experiments and proposes that CCSP downregulation contributes to carcinogenesis as CCSP antagonises the neoplastic phenotype (Linnoila et al., 2000). Clara cells have also been found to secrete other proteins. These are CC 55kDA protein, leukocyte protease inhibitor, beta galactosidase binding protein, phospholipase, Tryptase Clara and surfactant associated proteins A,B and D (SP-A,SP-B,SP-D) the latter of which have their own immunoregulatory and antibacterial properties (Singh and Katyal, 2000).

1.1.3.3 Solitary neuroepithelial cells and neuroepithelial cell bodies

Pulmonary neuroepithelial (NE) cells are a division of the diffuse neuroendocrine system and exist as solitary cells or in a cluster, termed a NE cell body (NEB). These specialised epithelial cells lie on the basal lamina and contact the airway lumen via microvilli in the apical membrane (Van Lommel, 2001). They are a primitive cell type and are found in invertebrate and vertebrate species (Linnoila, 2006), constituting less than 1% of the human airway epithelium (Castro et al., 2000). They possess endocrine and paracrine secretory mechanisms and are closely associated with intraepithelial nerve fibres (Linnoila, 2006). They are first functionally active during fetal development where they regulate lung growth and maturation via release of amine and peptide products (Sorokin et al., 1997). Later in fetal life and postnatally, they act as airway chemoreceptors that respond to airway hypoxia (Linnoila, 2006). Other reports emphasise their role in the regulation of airway tone and pulmonary blood flow during respiration (Peake et al., 2000).

Identification of NE cells by pathologists is both helped and hampered by their large number of secretory products. Immunohistochemical detection uses antibodies raised against paraneural activity (neurone specific enolase, synaptophysin, chromogranin A and protein gene product 9.5) and regulatory peptides (bombesin/ gastrin-releasing peptide, calcitonin, Leu-enkephalin, cholecystokinin, serotonin and somatostatin). However, the variation in levels of secretory products over time and between species may lead to errors in cell recognition using IHC. Synaptophysin, which is an integral membrane protein present in presynaptic vesicles of neuroendocrine cells, has been suggested as the most sensitive and specific marker for pulmonary NE cells by IHC (Kasprzak et al., 2007). Electron microscopy may be a more reliable technique as it recognises the dense core granules which reside in the basal pole, ready to discharge substances into the subepithelial corium (Balaguer and Romano, 1991; Van Lommel and Lauweryns, 1997). The secreted substances can influence nearby cells, or are taken up by the pulmonary capillaries to exert their effect on target cells elsewhere in the body (Van Lommel, 2001).

NEBs are often situated in strategic positions at airway bifurcations and bronchioalveolar duct junctions (BADJ). Lung disease has been shown to alter the distribution and number of detectable PNECs. Studies in humans have found increased numbers in chronic lung conditions such as bronchial asthma, pneumonia, chronic bronchitis and cystic fibrosis, and in sudden infant death syndrome (Linnoila, 2006). Two characteristic patterns of cell growth are seen. One shows increased numbers of interrupted rows of cells on the basement membrane of the epithelium, and the other appears as large aggregates of NE cells. This is described as neuroendocrine hyperplasia or tumourlets, and their role as a precursor to carcinoid and other lung tumours is under investigation (Rizvi et al., 2009). Studies in mice which used naphthalene to obliterate Clara cells, demonstrated a marked hyperplasia of NEBs following lung damage (Peake et al., 2000). This contradicts the original theory of these as terminally differentiated cells, and autoradiography found them capable of proliferating. However, they were not able to repopulate bronchiolar epithelium and therefore not capable of transdifferentiating into other cell types (Peake et al., 2000). Given the role these cells play in chemoreception, a body of literature has investigated cell numbers in humans and animals that live at high altitudes. There are mixed reports as to whether the location does or does not affect cell number (Gosney, 1990), but one consistent observation was that when cell numbers

did change, it was only the NEB which increased, not the solitary NE cells. This finding suggests the two cell types may have separate functions.

1.1.3.4 Type I and type II pneumocytes

Type I and type II pneumocytes are found in the respiratory airways of the lung. They constitute a continuous epithelial layer which is the final barrier between inhaled gases and the host circulatory system (Flecknoe et al., 2003). Type I pneumocytes are attenuated squamous epithelial cells with a flattened nucleus and an extremely thin, granular cytoplasm, through which the diffusion of respiratory gases occurs. Type II pneumocytes are plump and cuboidal and generally positioned in the corners of alveoli. Their hallmark is the presence of distinctive lamella bodies which contain surfactant. Immunohistochemical identification uses antibodies to aquaporin-5 for type I and SP-C or DC-LAMP for type II pneumocytes (Salaun et al., 2004; Warburton et al., 2000). They line the alveoli in a 1:2 ratio (type I : type II) although type I contribute to 86% of the total surface area (Otto, 1997).

Conventionally, type II pneumocytes are considered to be the alveolar progenitor cell as demonstrated using lung injury models and autoradiography (Evans et al., 1973). *In vitro* work also highlights the propensity of type IIs to produce cells with a type I phenotype. However during fetal development this hierarchy can be reversed, and changes in fetal lung expansion have been shown to induce transdifferentiation of type I pneumocytes into type II pneumocytes (Flecknoe et al., 2000). In addition, a recent study examining the phenotypes of rat type I pneumocytes *in vitro*, found 99% pure cultures to be capable of proliferation (50% were Ki-67 positive) and to express Oct-4, a potential stem/progenitor cell marker (Gonzalez et al., 2009). It was also possible to induce them to express SP-C and CCSP so illustrating their phenotypic plasticity. Proof of these properties *in vivo* remains to be shown. Also of interest is the question of the type II population homogeneity. Subsets of cells were found to be E-cadherin positive and negative (Reddy et al., 2004) and differences were noticed in their transgene expression (Perl et al., 2005; Roper et al., 2003). This suggests type II pneumocytes could be further categorised according to their different functional or progenitor capabilities (Kotton and Fine, 2008). A summary of the cellular anatomy of the lung is shown in Figure 1.2.

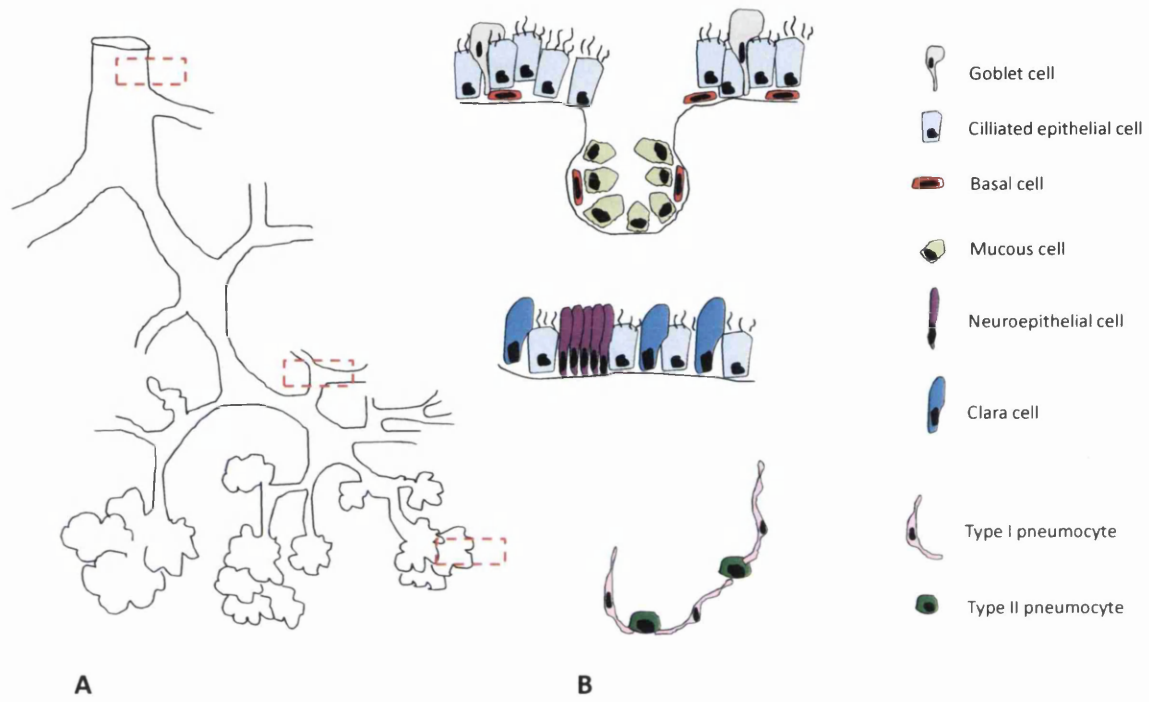


Figure 1.2 Diagram of bronchial tree (A) and corresponding cellular anatomy (B). The red dotted box in (A) represents the area denoted in (B).

1.1.4 Lung maintenance and repair

1.1.4.1 Lung progenitor cells

The finely tuned architecture of cells in the lung allows the organ to perform to its maximum efficiency for gas exchange. In humans the lungs process 10 000 litres of air per day, through a 300 m² epithelial gas interface. During exercise, 2.5 litres of oxygen are absorbed into the blood every minute (Otto, 1997). Any compromise to the functioning anatomy will be reflected in a reduced respiratory efficiency which may be life threatening.

The lung must be able to maintain normal architecture and react quickly to repair injuries from inhaled or systemic insults. To do this it has a reservoir of progenitor cells, each responsible for maintenance and repair of specific anatomical regions of the lung (Rawlins and Hogan, 2006). The term 'progenitor cell' describes all cells that have the ability to proliferate. Further classifications can be made when the product of this replication is examined. Does the cell self replicate? Does it produce an undifferentiated or terminally differentiated cell? Can it do both?

These distinctions can be made relatively easily when a tissue with rapid turnover is examined such as the gut (Figures 1.3 and 1.4A) (Kotton and Fine, 2008). As the adult tissue stem cell actively participates in normal tissue maintenance, a classical stem cell hierarchy based on proliferative frequency, self renewal and differentiation potential can be applied (Snyder et al., 2009). The adult tissue stem cell actively resides at the base of the crypt in the stem cell niche where it is protected from luminal contents. It has a lifelong ability to self replicate or produce relatively undifferentiated transit amplifying cells. Transit amplifying cells have a limited lifespan, during which they replicate to form terminally differentiated epithelial cells. There is constant shedding of differentiated cells from the tip of the villus which stimulates continuous proliferation of stem cells in the crypt, and there is a cell turnover rate of approximately five days (Snyder et al., 2009). This organisation appears fixed and if the adult stem cells are destroyed then the villus is lost. Commonly used stem cell terminology is summarised in Table 1.3.

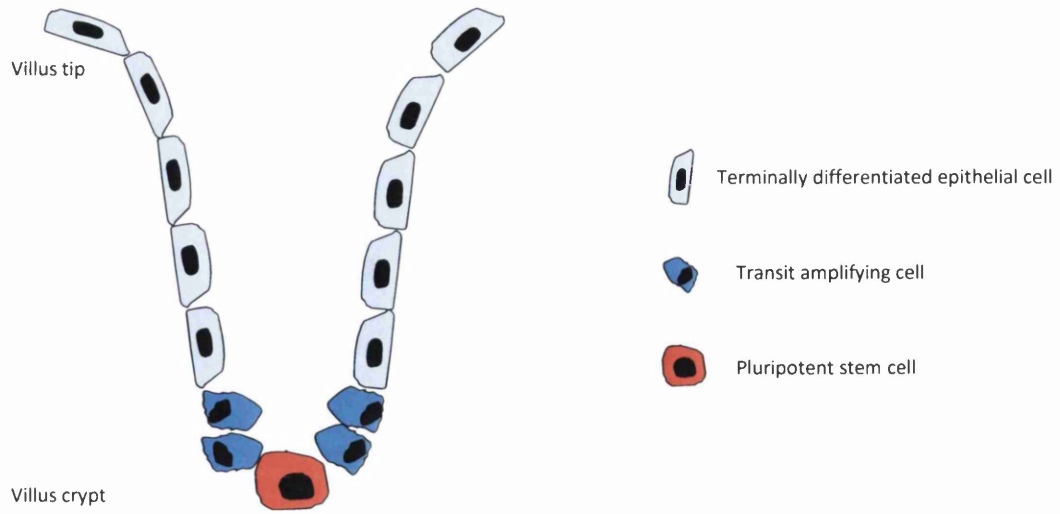


Figure 1.3 Schematic representation of proliferative cells in a villus in the intestine

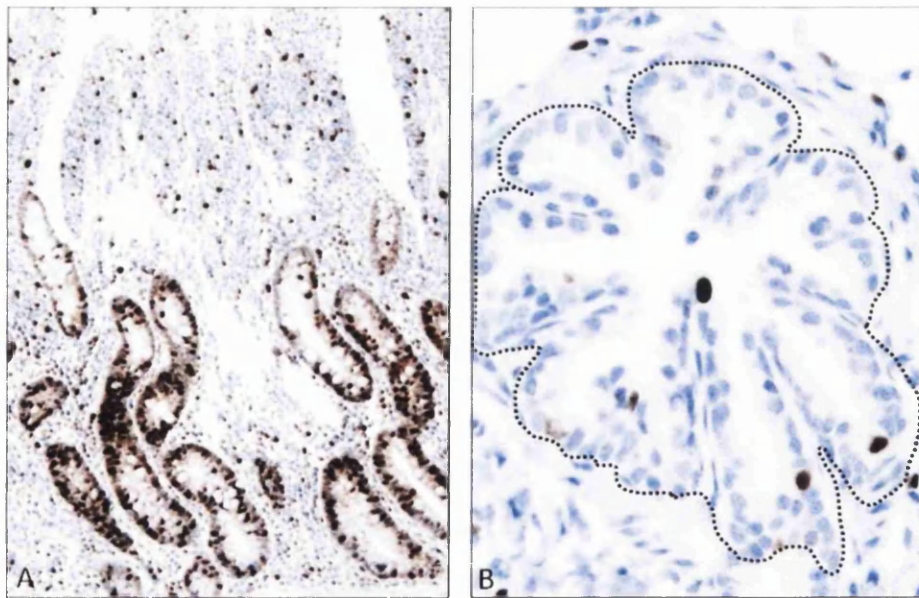


Figure 1.4 IHC labelling of Ki-67 positive cells in the intestine (A) and lung bronchiole (B). More cells are proliferating in the intestine

Table 1.3 Glossary of stem cell terminology (Fuchs et al., 2004; Stripp and Reynolds, 2008)

Definition	Description
Progenitor cell	Describes all cells that have the ability to proliferate.
Adult tissue stem cell	A relatively undifferentiated cell with the capacity for unlimited self renewal through stable maintenance within a stem cell niche. They have the differentiation potential of the tissue in where they are found.
Stem cell 'niche'	A specific area which provides the right environment for viability and function of stem cells
Transit- amplifying cell	The progeny of a tissue stem cell that retains a relatively undifferentiated character, generates specialised progeny for tissue maintenance and has a finite capacity for proliferation
Obligate progenitor	A cell that loses its ability to proliferate once it differentiates
Facultative progenitor	A cell that has differentiated features in quiescent state, but still retains the ability to proliferate for normal tissue maintenance.

In contrast, cell turnover in the lung is relatively slow (Figure 1.4B) and categorisation of cell types to these criteria has been more complicated (Kotton and Fine, 2008). For example, bronchial epithelial cells have an average lifespan of 100 days (Snyder et al., 2009), and ciliated cells are said to last for 17 months (Rawlins and Hogan, 2008). Clara cells are analogous to TA cells in the gut, but they are also able to be quiescent and have a differentiated function. Initial work used autoradiography to identify cell types capable of replicating. In the trachea and bronchi, basal cells were seen to incorporate H³ thymidine label (tritiated thymidine) (Wells, 1970) and were proposed as progenitor cells for ciliated and goblet cells (Blenkinsopp, 1967) which was later verified (Hong et al., 2004a, b). In bronchioles, injury models were necessary to demonstrate the dynamics of epithelial repair. Influential studies by Evans and colleagues recognised the Clara cell as a type of progenitor (Evans et al., 1976). They used NO₂ to damage terminally differentiated ciliated cells in rat lungs. Autoradiographic labelling of the remaining dividing cells showed them to be non-ciliated Clara cells (Evans et al., 1978). As the lung recovered, label retention was also seen in a proportion of newly formed ciliated cells (Evans et al., 1976). This showed Clara cells to be

capable of proliferation and differentiation into another cell type, hence their definition as a facultative progenitor/stem cell (Rawlins and Hogan, 2006).

Further morphological analysis using EM introduced the concept of an intermediate type Clara cell, which was called a type A cell (Evans et al., 1978). Distinguished by their lack of secretory granules and smooth ER, these were seen to increase dramatically in number following injury, and then reduce as more mature Clara cells and ciliated cells were formed. Type A cells were defined as a morphological derivative of the mature Clara cell, and the possibility was raised of it being a unique cell acting as a progenitor for the bronchial epithelium.

More recent experiments have created injury models which selectively ablate the Clara cell population using naphthalene (Peake et al., 2000; Stevens et al., 1997; Stripp et al., 1995). It was anticipated that by removal of these progenitor cells, a multipotent stem cell type would be activated and forced to repair the lung instead. In fact, two unique stem cell populations have since been identified in the mouse (Giangreco et al., 2002; Hong et al., 2001; Kim et al., 2005). The first contributes to the repair of proximal bronchioles and is located in a stem cell niche at the NEB. Commonly found at airway bifurcations, this site was previously identified as the first focus of epithelial regeneration following injury (Hong et al., 2001; Reynolds et al., 2000). These are variant Clara cells, and are defined by their expression of CCSP and deficiency in the phase 1 enzyme CYP450-2F2, which explains their resistance to naphthalene (Reynolds and Malkinson, 2010). Transgenic mouse models were used to demonstrate their critical role in facilitating epithelial regeneration after injury (Hong et al., 2001). Interestingly, a low proportion of cells in the NEB were seen to express both CCSP and calcitonin gene related peptide (CGRP), a NE marker.

The second population of naphthalene resistant cells was located at the BADJ (Kim et al., 2005). They were shown to express CCSP (using IHC and *in situ* hybridisation) and SP-C. Immediately after injury, autoradiography showed them to account for all proliferating cells in that area and repopulation of the terminal epithelium occurred proximally from this site. However, in contrast to the variant Clara cells, colocalisation studies found no association with CGRP expressing cells using IHC. They were suggested to be a separate population of

stem cells responsible for repairing terminal bronchioles, and have since been named bronchioloalveolar stem cells (BASC) (Kim et al., 2005) (Figure 1.5). Cells with this phenotype have yet to be described in animals other than the mouse.

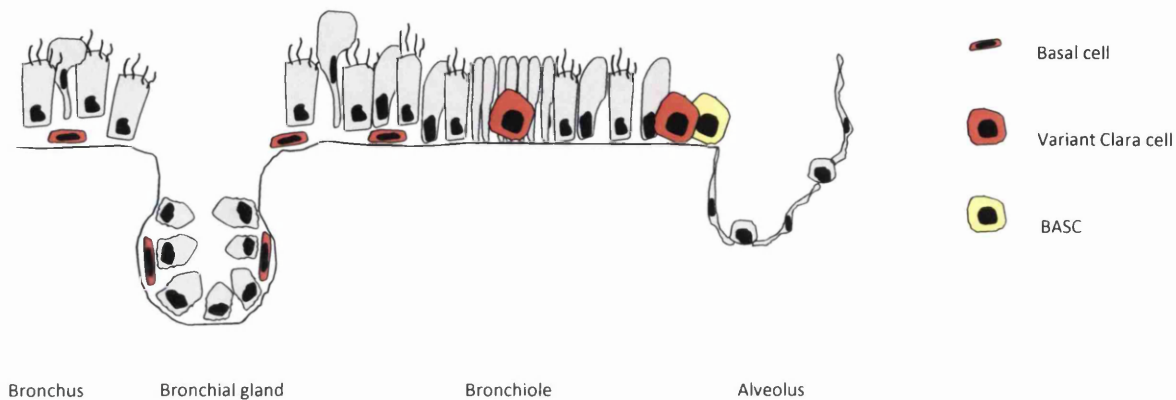


Figure 1.5 Summary of stem cell types at different levels of the respiratory tract as defined in the mouse

The distinction in role between abundant facultative progenitor cells and rare bronchiolar stem cells was further defined in an elegant experiment by Giangreco et al (2009). They used chimeric mice and a whole lung imaging method to show the relative contributions of each progenitor cell type to mouse lung during normal maintenance and following mild or severe injury. In normal and mildly injured animals, repaired lung showed chimeric patches to be small and randomly located. In contrast, when the lung had healed from a severe injury, large clonal patches associated with NEBs and BADJ were seen. This demonstrates the involvement of bronchiolar stem cells only when extensive repair is required in the lung (Giangreco et al., 2009).

Further characterisation of bronchiolar stem cells in mice has been attempted but with inconsistent results (Kim et al., 2005; Teisanu et al., 2009). Initial work used FACS analysis to isolate a population of cells which were Sca-1^{pos}, CD45^{neg}, Pecam^{neg}, CD34^{pos} and also positive for SP-C and CCSP. Immunofluorescence then verified their anatomical location at

the BADJ. The same cells were shown to exhibit stem cell properties in culture as defined by their ability to self renew and have multilineage differentiation potential (Kim et al., 2005). However, Stripp and his team claimed that these culture techniques enriched for alveolar epithelial cells, and the markers used would be unable to fractionate bronchiolar stem cells from a Clara cell rich pool (Teisanu et al., 2009). Instead, they used a lung cell preparation to include a broad population of cells from conducting and respiratory airways which would include variant Clara cells, and found that bronchiolar stem cells had a CD45^{neg}, CD31^{neg}, CD34^{neg}, Sca-1^{low} AF^{low} phenotype. They also commented that a proportion of cells which expressed CCSP and SP-C exhibited high autofluorescence, therefore not displaying the true BASC phenotype. This questions the use of CCSP/SP-C dual positivity to identify BASCs. More doubt has been raised concerning this classification in recent studies by (Rawlins et al., 2009). Using a 'knockin' mouse for lineage tracing CCSP-expressing cells, they suggested that there are subpopulations of Clara cells that differ in their ability to contribute to the ciliated cell population. They also queried the involvement of BASC populations at any stage in lung maintenance.

1.1.4.2 Bone marrow derived stem cells (BMDSC)

The bone marrow has also been suggested as a potential source of stem cells to aid in lung repair (Sage et al., 2008). An experiment which gave female mice with lethally irradiated bone marrow a single haematopoietic stem cell (HSC) from a male mouse, showed engraftment of donor-derived cells in the females bone marrow and lung, eventually making up to 20% of the parenchyma (Krause et al., 2001). When the experiment was repeated in humans, engraftment sites were concentrated to areas of lung injury, suggesting that BMDSC could repair damaged tissue by differentiating into epithelial cells (Kleeberger et al., 2003; Suratt et al., 2003). However, subsequent work produced conflicting results, with some studies showing no contribution of adult bone marrow stem cells to the epithelial compartment of the lung, and others suggesting engraftments as other stromal cell types. BMDSC are now thought to be of limited significance in their ability to contribute to epithelial repair in the lung (Sage et al., 2008).

1.1.5 Carcinogenesis and the lung progenitor cell

Research into lung stem cells is also fuelled by their associations with lung cancer. In fact, BASCs were originally discovered during an investigation of the cell of origin of lung adenocarcinoma and stages of tumour progression (Jackson et al., 2001). An inducible oncogenic *K-ras* mouse model found CCSP/SP-C double positive cells within adenomatous lesions which were continuous with the bronchiolar epithelium. They were thought either to be the product of transdifferentiated Clara cells following oncogene induced hyperproliferation, or the consequence of oncogene activation in a stem cell with the potential to develop into both cell types. Subsequent experiments found BASC hyperplasia and increased adenocarcinoma development in several lung tumour mouse models of disease and a role as a lung cancer stem cell was proposed for BASCs (Kim et al., 2005; Ventura et al., 2007; Yanagi et al., 2007).

The cancer stem cell (CSC) model was developed to explain the heterogenous nature of tumours (Eramo et al., 2010). It proposes that the same cellular hierarchical organisation that exists in normal tissues is also present in tumours (Figure 1.6). This means that CSC can self renew and produce differentiated progeny, so giving them the ability to initiate tumours and promote their progression. Ultimate proof of CSC identity is one of the most challenging aspects of this area of research. The most convincing experiments transplant CSCs into animal models, which then grow into tumours with phenotypic heterogeneity similar to the original tumour (Visvader and Lindeman, 2008). These cells must also show self renewing capacity on serial passaging. Various markers have been proposed for identifying these cells in solid tumours (Visvader and Lindeman, 2008).

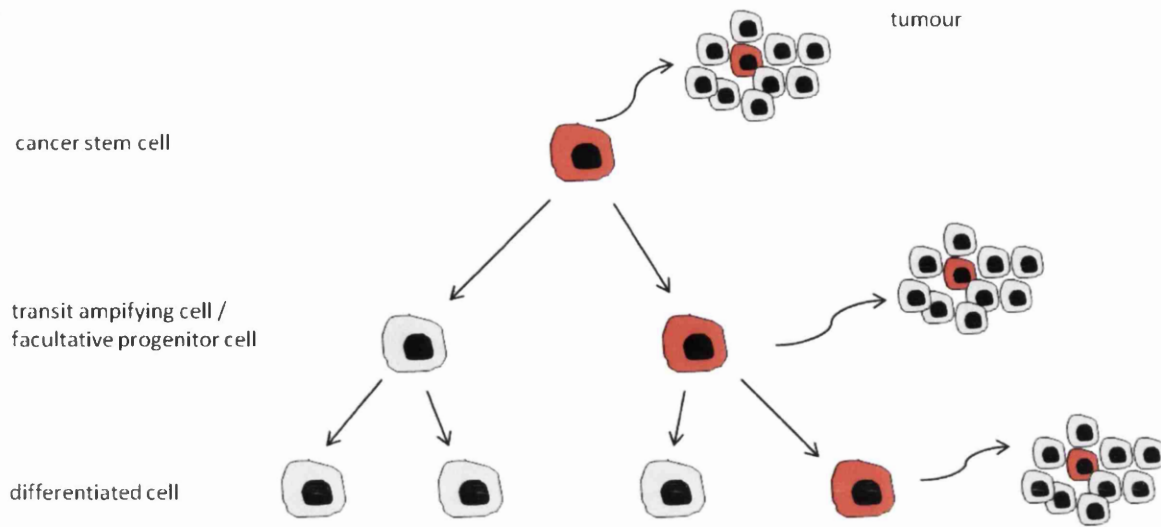


Figure 1.6 Cancer stem cell model for tumour heterogeneity and propagation. The tumour contains a cellular hierarchy, but only CSCs can generate a tumour

Table 1.4 Markers for cancer stem cells in solid tumours (Mallick et al., 2009; Visvader and Lindeman, 2008)

Target Gene	Function
CD133	CD133/prominin-1 is a transmembrane glycoprotein, which may participate in organisation of membrane topology. Expressed on CD 34 ⁺ stem and progenitor cells in fetal liver, endothelial precursors, fetal neural stem cells and developing epithelium. CD133 ⁺ cells highly expressed in cancers eg. prostate, colon carcinomas and have progenitor capabilities <i>in vitro</i> and <i>in vivo</i> .
Hoechst SP	Side population phenotype due to Hoechst ₃₃₃₄₂ efflux pump present on the plasma membrane in diverse cell types. Levels are low in stem cells
Oct 4	Octamer-binding transcription factor 4 ⁺ is a stem cell marker protein. It acts as a master switch in differentiation by regulating cells that have pluripotent potential
ALDH 1	It has a role in the conversion of retinol to retinoic acid which is important for proliferation, differentiation and survival.

Stem cells in human lung cancer have been isolated both from cell lines and primary tumours (Bertolini et al., 2009; Eramo et al., 2008; Ho et al., 2007; Jiang et al., 2009; Levina et al., 2008). Properties used for stem cell isolation vary between experiments and included side population phenotype (low Hoechst 33342 staining pattern), chemoresistance, Aldehyde dehydrogenase 1 (ALDH1) activity, ability to grow as spheres in serum-free medium and CD 133⁺ expression. The embryonic genes Oct-4 and Nanog are also expressed by some of these cells, so confirming their undifferentiated phenotype. Functions of some of these genes are summarised in Table 1.3.

In summary, it is clear that the lung is capable of efficient repair following a variety of insults. Injury models have shown there to be a hierarchy of progenitor cells and the severity of injury determines which 'type' is stimulated to proliferate. However, the situation is complicated by the cell plasticity exhibited in some injury models. Specific identification of these cells and how to define their 'stem cell' characteristics is a subject of much debate. Some are thought to be involved in lung carcinogenesis models, but the situation in animals other than the mouse has yet to be explored.

1.2 Ovine Pulmonary Adenocarcinoma

In the UK, the veterinary profession was first alerted to the emergence of this unique sheep disease in 1888 (Dykes and McFadyean, 1888). Mr Dykes was called to examine a flock of Oxford Downs where over 100 animals had been lost within the previous year. Some affected animals were said to be recumbent with an increased respiratory rate, whilst others died without any premonitory clinical signs. Common features at post mortem included generalised enlargement of lungs which were '*lighter in hue than natural, glistening and resistant to the knife*'.

Initially, the identification of large numbers of parasitic eggs and larvae within the tissue led to the suggestion that *Strongylus rufescens* (*Muelleriis capilariis*) was the aetiological agent. However, in a later publication when additional samples were taken from affected areas of '*dirty white fleshy tissue*', the histological picture detailed thickening of alveolar walls and transformation of the alveolar and bronchial epithelium (McFadyean, 1894). Matching histological descriptions were found in subsequent reports from different countries. In South Africa the disease was named Jaagsiekte, literally meaning driving (jagt) sickness (ziekte) (Robertson, 1904); in England it was called white pneumonia (McFadyean, 1920); and in Iceland it was named Deildartunga after the farm on which it was first discovered (Dungal et al., 1938). Similarities between these findings were recognised by Taylor in 1937 where he concluded that '*comparison of the detailed description of the microscopical appearance of lungs affected by this disease ... with those of Jaagsiekte and with sections of lungs affected by an epidemic disease of Icelandic sheep suggest that all three diseases may be one and the same, and that Jaagsiekte has occurred in Great Britain*' (Taylor, 1937). OPA has since been reported in countries all over the world. Exceptions include Iceland where it was eradicated by following a strict slaughter policy in the 1950s (Palsson, 1985), and New Zealand, Australia and the Falkland islands, where it has never been described.

1.2.1 Clinical parameters of OPA

As OPA has a long incubation period, naturally infected animals tend not to develop clinical signs until adulthood. A survey of sheep in Scotland found infected animals to show clinical

signs between nine months and seven years of age, with a peak of disease incidence between 3 and 4 years (Hunter and Munro, 1983). However, clinical cases have been reported in animals as young as 2-4 weeks old (Dungal, 1946; Shirlaw, 1959) and there is unpublished data which details tumour in a 3 day old lamb (De las Heras et al personal communication). The average mortality within flocks appears to depend on whether the disease is endemic (2% loss) or a recently acquired infection (up to 30% loss) (Sharp and Angus, 1990). Infection of goats has been reported but it is thought they are more resistant to developing clinical disease (De las Heras, 2003).

Clinical signs can be seen following forced exercise of those in the early stages of disease, or in severely affected animals at rest. This latter feature is responsible for the name Jaagsiekte (driving sickness), as these animals look like they have been overdriven. Movement of affected animals will bring on an exaggerated increase in respiratory rate and effort, causing them to lag behind a travelling flock (Robertson, 1904). Increased respiratory recovery time and coughing following exertion may also be clinical features. In severely affected animals laboured breathing can be accompanied by the sound of moist rales or '*boiling porridge*' resulting from the build up of fluid in the airways (Dungal et al., 1938). These animals can also have wet shiny nostrils, and in some cases when the head is lowered and hind legs lifted, translucent frothy fluid runs from the nares (Figure 1.7A). This manoeuvre is called the 'wheelbarrow test' and it is currently the only definitive way of diagnosing the disease in a live individual animal (Voigt et al., 2007). Up to 300 ml can be collected at any one time and the fluid has the appearance of watery egg whites which froth up on agitation (Palmarini and Fan, 2001).

Despite these respiratory signs, if left unstressed many affected animals can remain bright and appetent for 2-3 months until a critical tumour mass is reached and gas exchange is hugely compromised. Weight loss is marked in the terminal stages (Figure 1.7B), but pyrexia is not a noted feature unless secondary bacterial infections complicate. If this occurs, sudden death due to an acute bacterial pneumonia in an adult animal may be the first indicator that the disease is present in the flock. Concurrent infections with other viruses eg. ovine herpesvirus and maedi-visna virus (MVV) have also been recorded, but the disease course still remains chronic (Herring et al., 1983).



Figure 1.7 Clinical signs of OPA in adult sheep. (A) Arrow shows fluid pouring from nares in a positive wheelbarrow test. (B) Animals are in poor condition but remain bright and appetent.

Original observations of the disease by farmers found any form of chill or physical exertion to aggravate the condition (Dungal et al., 1938). This theory was reinforced following a clinical experiment in 1971 that confirmed cold stressing to be a predisposing factor for onset of clinical signs (Mackay et al., 1971). Differences in breed susceptibility have also been recorded, for example in Iceland the Gottorp breed was said to be more susceptible than the Adalbol breed (Dungal et al., 1938). A more recent study has implicated associations between sheep MHC-DRB1 alleles and susceptibility to OPA (Larruskain et al., 2010). Other surveys suggest specific breed predilection may be skewed by different management practices (Hunter and Munro, 1983) and a definitive survey of modern day breeds is lacking. Despite mention in early papers, reports of recovery are limited to one recent publication, but these animals were also infected with MVV (Hudachek et al., 2010). In the field, once clinical signs have been established the disease is assumed to be invariably fatal. Early attempts at vaccination were made using formalinised vaccines prepared from adenomatous lungs (Shirlaw, 1959; Tustin, 1969). While disease incidence was seen to reduce from 30-1% on some farms, administration also coincided with a change in management practice and culling of suspect cases (Shirlaw, 1959).

1.2.2 Pathology of OPA

1.2.2.1 Gross Pathology

The definitive diagnosis of this disease in an individual animal still relies on characteristic gross and histopathological post mortem findings. There are numerous descriptions in the literature (Al-Zubaidy and Sokkar, 1979; Blakemore, 1941; Cowdry, 1925a, b; Cuba-Cuparo et al., 1960; Cutlip and Young, 1982; de Kock, 1958; Demartini et al., 1988; Dungal, 1946; Nisbet et al., 1971; Nobel et al., 1969) From these it can be seen that there has been little change in the pathological presentation over the last 100 years (Sharp and DeMartini, 2003).

A typical post mortem examination of a naturally infected animal in the advanced stages of disease will find a thin carcass with frothy fluid exuding from the nares and filling the trachea as stable foam. On incision into the thoracic cavity, the lungs will fail to collapse and are enlarged, heavy and oedematous (Figure 1.8A, B). Palpation will find a large centre of consolidation in one or more lung lobes, which extends peripherally in a miliary distribution (Figure 1.8 C,D,E). Here, there is a clear distinction between normal and diseased lung. Neoplastic tissue appears solid, firm and darker in colour than the adjacent normal tissue which is often locally over inflated. The cut surface is uneven and granular and frequently exudes frothy fluid (Figure 1.8F). In larger masses the centre is more resistant to the knife and can feel almost gritty as accurately described by Robertson in 1904 '*in some cases it cuts like bacon, and in advanced cases like cartilage*'. Sometimes lesions are more focal, with single or multiple firm masses found within any lung lobe. The bronchial and mediastinal lymph nodes are generally enlarged and oedematous and histological examination has shown that up to 10% contain metastases (Demartini et al., 1988). Distant metastases have also been reported in liver, kidney, heart and skeletal muscle but are generally rare (Hunter and Munro, 1983). Animals which have died often have a secondary bacterial pneumonia (Figure 1.8D). In these cases detailed dissection is important as extensive pleurisy and adhesions can mask the underlying pathology of OPA.

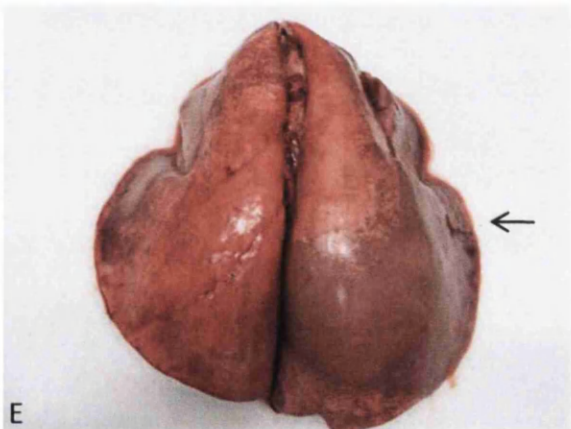


Figure 1.8 Post mortem findings in natural field cases of OPA. (A) Exposure of the thoracic cavity following removal of sternum. Lung lobes have failed to collapse as they are oedematous and infiltrated with tumour (arrows). (B) Frothy fluid exudes from the trachea (arrow). (C) Tumour infiltrating caudal region of the right diaphragmatic lobe (arrow). (D) Tumour infiltrating left caudal apical lobe (arrow). (E) Generalised enlargement of right diaphragmatic lobe due to tumour infiltration. Arrow points to section location for (F), which shows the grey, granular appearance of tumour tissue adjacent to normal pink aerated lung tissue.

1.2.2.2 Histopathology

OPA is described as an adenocarcinoma of mixed subtype when compared to the World Health Organisations classification for human tumours (Travis et al., 2004a). Non-encapsulated neoplastic foci emanate from alveolar and bronchial epithelium forming acinar and papillary proliferations which expand into adjacent structures (Figure 1.9A, B). The cells vary in shape and malignancy both within and between tumour nodules. Classically, they are cuboidal or columnar, with or without cytoplasmic vacuolation, and have a low mitotic index of 0.002% in any tumour (Platt et al., 2002) (Figure 1.9 C). In areas of increased malignancy, solid masses of pleomorphic cells with a high mitotic rate and scattered foci of necrosis can be found.

Neoplastic cells are supported by a fibrovascular connective tissue framework which can dominate the centre of large tumour nodules (Figure 1.9 D). This acts as a scaffold for infiltrating inflammatory cells which vary according to the size/age of the tumour and presence of secondary infectious agents. Occasionally, nodules of loose mesenchymal tissue appear alone or admixed with classical tumour, and these are also thought to be neoplastic tissue (Wootton et al., 2006b) (Figure 1.8 E).

IHC has shown virus expression to be limited to neoplastic tissue only (Figure 1.9 G) (Palmarini et al., 1995). Type II alveolar epithelial cells are the principal neoplastic cell type (82%) with Clara cells (7%) and undifferentiated cells (11%) making up the remainder (Figure 1.9 H) (Platt et al., 2002). Frequently, large numbers of foamy macrophages are seen to infiltrate alveolar spaces about mature neoplasms (Figure 1.9 I-K). These are often accompanied by neutrophils, assumed to be the result of secondary bacterial infection, and necrotic foci (Figure 1.9 L) (Platt et al., 2002).

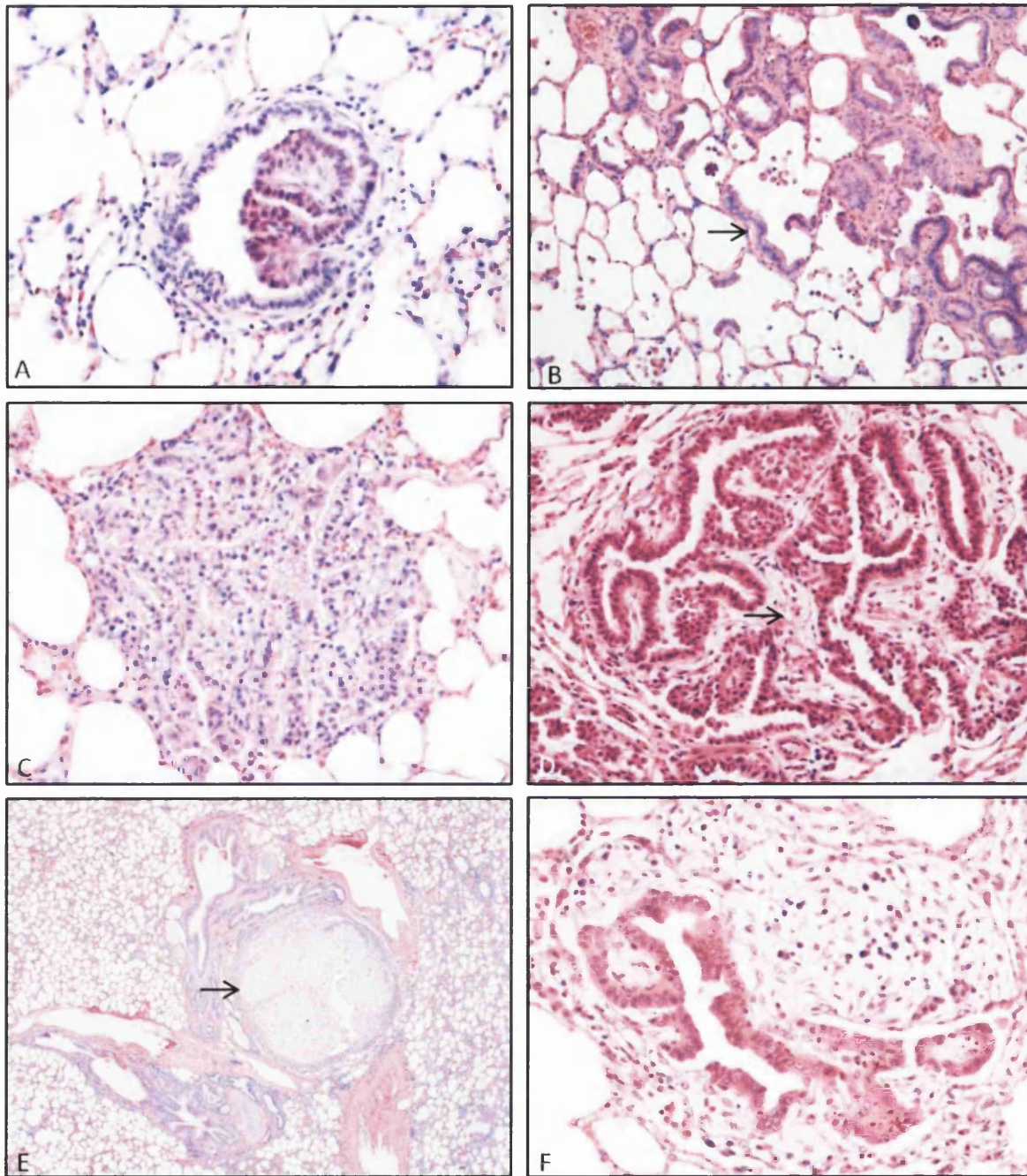


Figure 1.9 Histological findings in natural field cases of OPA. (A) Bronchiole with early neoplastic focus in lumen, OM x400. (B) Lepidic spread of tumour (arrow) along alveolar walls, OM x100. (C) Mature tumour focus with cytoplasmic vacuolation of neoplastic cells, OM x200. (D) Tumour with prominent fibrovascular connective tissue framework (arrow), OM x 400. (E) Large nodule of neoplastic mesenchymal tissue (arrow), OM x20. (F) loose myxomatous tissue about neoplastic focus, OM x600.

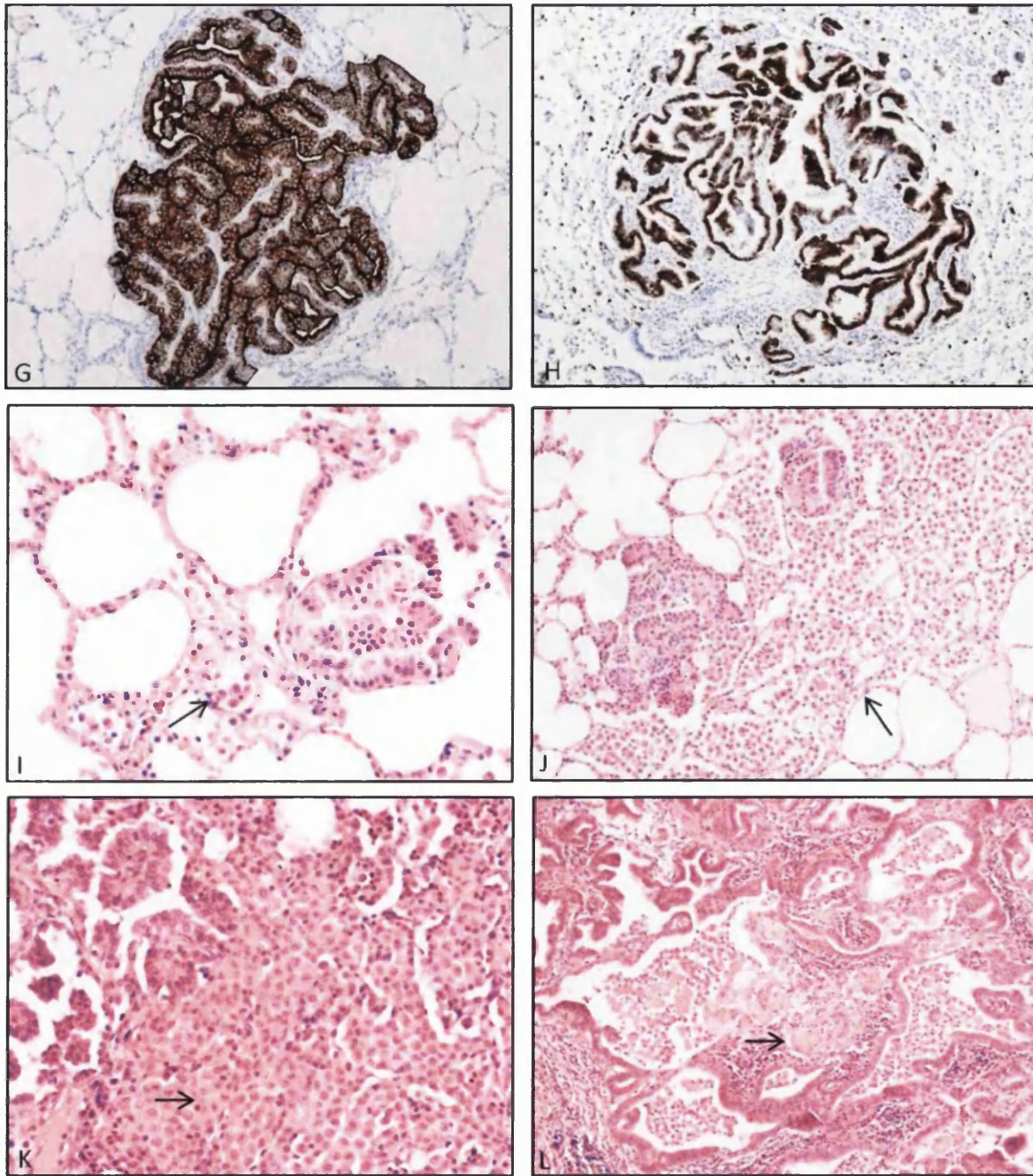


Figure 1.9 (cont.) Histological findings in natural field cases of OPA (G) IHC using anti-JSRV SU antibody to show positive labelling (brown pigment) of entire tumour nodule, OM x200 (H) IHC using anti-SP-C antibody to show positive labelling of neoplastic cells, OM x200 (I) Early neoplasm with occasional infiltrating macrophages (arrow), OM x400. (J) Growing neoplasms with a moderate macrophage infiltration (arrow), OM x 200 (K) Dense infiltration of macrophages (arrow) adjacent to tumour, OM x600. (L) Necrotic tissue (arrow) in the centre of a mature tumour nodule, OM x200.

1.2.2.3 Electron microscopy

Electron microscopy has also been used to document early growth of the tumour and identify ultrastructural characteristics of neoplastic cells (Payne and Verwoerd, 1984). Tumours are said to originate from paired cells resembling foetal pneumocytes, in the corner of alveoli. These proliferate to line alveoli with cuboidal or columnar cells, before forming papilliform or varicose clusters, which can extend into bronchioles. The cells have basal or centrally located nuclei, microvilli on all surfaces (reduced in older cells) and are connected by desmosomes. They contain variable numbers of secretory granules which can appear as electron-dense structures or are filled with myelinoid whirls, in comparison to the electron-lucent granules found in normal granular pneumocytes. The cells have rough endoplasmic reticulum (RER), large numbers of free polysomes, a well developed Golgi apparatus and hypertrophic mitochondria (Perk et al., 1971). Cytoplasmic glycogen granules have also been identified, sometimes in large quantities, and confirmed using Periodic Acid Schiff (PAS) staining. The macrophages identified on histology are highly ruffled and enlarged, confirming their activated status. They either attach to the surface of normal or neoplastic cells, or form separate clusters. As well as containing lysosomes and phagolysosomes, phagocytosed JSRV particles, bacteria and mycoplasma like organisms have also been found.

1.2.3 Discovery of the aetiology of OPA

Initial histological examination of lungs from diseased animals in 1888 found parasitic forms to be closely associated with areas of affected lung tissue. These were identified as *Muelleriis capillaris*, and were suggested to be responsible for the adjacent pulmonary pathology (Dykes and McFadyean, 1888). A few years later, 'peculiar crescent shaped bodies' were found in smears of lung from similarly affected animals, and a protozoal 'malarial-like' aetiology was proposed (Robertson, 1904). However, it was not until the autumn of 1936 that a thorough pathological investigation was performed at the request of the Icelandic government. This followed the importation of an infected ram from Germany, and the subsequent 50-80% mortality within sheep flocks in Iceland (Dungal et al., 1938).

1.2.3.2 Early transmission experiments

Early experiments followed the lead of Dykes and MacFadyean, but no association was found between parasitic burden and disease incidence or the distribution of both within the lung. Bacterial and viral aetiologies were then searched for *in vitro* and experimental transmission studies were also performed (Tables 1.8 and 1.9). These demonstrated disease transmission by the respiratory route and also by means of intrapulmonary injection of neoplastic lung tissue (Dungal, 1946). Injecting lambs with a glycerol saline filtrate which had been breathed into by infected animals, was also successful in transmitting disease and supported the theory of a viral aetiological agent (Dungal, 1946).

Table 1.5 Summary of early experiments to determine the aetiology of OPA

Experiment	Result	Reference
Assessed parasitic (<i>M Capillaris</i>) burden of 1000 lungs from OPA affected and non affected areas.	Parasitic burden similar	(Dungal et al., 1938)
Checked stage of larva in lung	Not fourth stage ie. not more pathogenic	(Dungal et al., 1938)
Bacterial culture of tissue from euthanased animal with clinical signs of OPA	No bacterial growth	(Dungal et al., 1938)
Bacterial culture of tissue animal that died with clinical signs of OPA	Cultured <i>Bacillus sp.</i>	(Dungal et al., 1938)
Cultivation of tumour tissue in chick embryos	No growth over 5-6 days	(Dungal et al., 1938)
Cultivation of tumour tissue in chick embryos	Evidence of growth	(Shirlaw, 1959)
Histochemical staining of sections with Giemsa/Castaneda	No protozoa/viral inclusions	(Dungal et al., 1938)
Dark ground illumination of sections	No spirochaetes	(Dungal et al., 1938)

Table 1.6 Summary of early disease transmission experiments

Experiment	Result	Reference
Hay fed from pastures grazed by infected animals	No disease transmission	(Dungal et al., 1938)
Faeces from infected animals fed to lambs via stomach tube	No disease transmission	(Dungal, 1946)
Parasite (<i>Melophagus ovinus</i> , <i>Muelleris capillaries</i>) transfer from infected to normal sheep	No disease transmission	(Dungal, 1946)
Housed eight healthy sheep with 20 sick sheep	7/8 developed disease in 8 months	(Dungal, 1946)
Sheep exposed to rear end only of infected sheep	No disease transmission	(Dungal, 1946)
Sheep housed above infected sheep in same airspace	3/5 got disease	(Dungal, 1946)
Intrapulmonary injection of homogenised tumour tissue into lambs	1/3 developed disease in 7 months	(Dungal, 1946)
Tumour tissue injected into mice, rabbits and guinea pigs	Adenomatous tissue growth in rabbit and guinea pig lung	(Cvjetanovic et al., 1972; Shirlaw, 1959)
Infected sheep breathed into 20% glycerol/saline for 30 minutes, injected into x3 lambs	1/4 infected	(Dungal 1946)
Addition of lung worms or <i>Bacillus</i> sp. to viral filtrate	Greater disease transmission	(Dungal et al 1938)

By this stage, it was clear that Jaagsiekte was an infectious disease of sheep, most likely of viral aetiology. The variability of successful disease transmission using conditions that we now know to be adequate, can be explained by inconsistencies in the age of animal used for infection and inadequate incubation periods. Whilst the virus typically has a long incubation period, some animals were only left a few months before being classified as free from disease and this may not have been long enough. An interesting observation made by Dungal in 1938 was that in the natural outbreak in Iceland not all animals exposed to infection developed disease. This suggests there may have been genetically related innate resistance or development of immunity in some cases.

1.2.3.3 Virus identification

Identification of the virus responsible for OPA was made difficult by the presence of multiple viruses in naturally infected animals. Herpes viral inclusions were frequently identified in macrophage cultures from infected animals and this virus was isolated from 24% of OPA cases examined (Malmquist et al., 1972; Martin et al., 1976). Work infecting fetal sheep lung cells also identified syncytia formation, a finding more consistent with the already known type C virus, maedi visna virus (MVV) (Malmquist et al., 1972). Attempts were made to produce disease with herpesvirus alone, but these failed and a multifactorial aetiology of Jaagsiekte was suggested (Cvjetanovic et al., 1972; de Villiers et al., 1975; Mackay, 1969; Martin et al., 1979). Further analysis using EM found type A and type C viral like particles to be associated with transformed epithelial cells (Perk et al., 1971). These were thought to be morphologically distinct enough from MVV particles to indicate the presence of a novel virus. In addition, sera from OPA sheep were not able to neutralise MVV (De Boer, 1970) and molecular hybridisation experiments indicated an absence of MVV RNA sequences in the polysome fraction of OPA tumours from Awassi sheep (Perk and Yaniv, 1977).

1.2.3.4 Virus classification

A retrovirus was suggested as the aetiological agent, as particles with a 60-70S RNA associated with reverse transcriptase (RT) were found exclusively in tumour tissue (Perk et al., 1974). A similar experiment was used to show the strong association between RT activity and the induction of OPA (Martin et al., 1976). Although it proved impossible to culture, *in vivo* transmission of disease using a cell line (JS 15.4) established from infected lung was effective (Coetzee et al., 1976). The experiment was successfully repeated using homogenised cells, which showed infection was due to actual transfer of genetic information rather than of neoplastic cells (Verwoerd et al., 1980a). Analysis of lung rinses from these animals by EM found electron dense particles with an average size of 80-150 nm and a close fitting membrane, similar in appearance to type B and D retroviruses. By using lung lavages concentrated by ultracentrifugation, incubation time of experimentally-induced OPA was reduced from 12 months to 3 weeks. This showed a dose-dependent response to infection, increasing the likelihood that the viral particles seen were responsible for disease (Verwoerd et al., 1980b).

Successful isolation and purification of this virus was achieved by the same group in 1983, and it was named Jaagsiekte Sheep Retrovirus (JSRV) (Verwoerd et al., 1983). Efforts to further classify it showed an immunological cross-reaction between the 25 kDa mol wt protein in OPA tumours and the 27 kDa mol wt core protein (p27) of Mason-Pfizer monkey virus (MPMV) and mouse mammary tumour virus (MMTV) (Sharp and Herring, 1983). Morphological comparisons with mouse mammary tumour virus (type B), murine sarcoma virus (type C) and squirrel monkey retrovirus (type D) found it to have a relatively electron-dense perinucleoidal space in comparison to other retroviruses and the nucleoid was eccentric. Surface spikes were longer than those seen on MMTV (Payne et al., 1983).

Up until the 1980's, the inability to culture the virus and complications with dual infections had hampered the progress of molecular studies. In 1991, York and his co-workers succeeded in isolating an 8.7 kb RNA molecule from washes of experimentally infected lungs (York et al., 1991). This was thought to represent the genomic RNA of JSRV, and transmission electron microscopy (TEM) of purified fractions containing this RNA revealed retroviral particles identical to those seen in infectious material. They also found sequence markers representative of a retrovirus, although only part of the genome was characterised. These included a polypurine tract, a TATA box, an inverted repeat and a poly A tail. By 1992 the complete genome had been cloned and its genomic organisation showed *gag*, *pro* and *pol* regions similar to type D retrovirus and *env* similar to type B (York et al., 1992).

The aetiological role of JSRV in OPA was not long to follow. Initially, a full length JSRV proviral clone, pJSRV₂₁, was isolated from a genomic DNA library of a natural case of OPA. Intratracheal inoculation of pJSRV₂₁ into newborn lambs and subsequent detection of proviral DNA in PBMCs demonstrated its infectious nature (Palmarini et al., 1999a). However, in order to use it as a source of infectious virus by transfecting *in vitro* cell lines, modifications were necessary. The U3 region of the upstream JSRV promoter was replaced with a powerful CMV promoter, to generate a plasmid designated pCMV2JS21. Transfection of pCMV2JS21 into human 293T cells resulted in release of JSRV into culture. This virus rich supernatant was used to inoculate three lambs, two of which developed disease, proving JSRV₂₁ was an infectious clone and sufficient to induce OPA *in vivo* (Palmarini et al., 1999a). This finding provided a solid platform on which to base further experiments.

1.3 Retroviruses

Retroviruses are a well established family of RNA viruses which comprise some of the most important human and animal pathogens known today (Coffin et al., 1997). They have a huge impact on human society worldwide and this has stimulated research into effective therapies and vaccine development for infection control. Each virus has a specific host range between which modes of transmission include transplacental, milk, respiratory, blood and sexual routes. Common manifestations of disease incorporate a wide range of immunological and neurological conditions and various cancers (Maeda et al., 2008).

Retrovirus diseases of animals were first documented in the 19th and early 20th century. Those associated with malignant disease were lung cancer in sheep in 1825 (Tustin, 1969), lymphosarcoma in cattle (Johnson and Kaneene 1992) and erythroid leukaemia and sarcoma in chickens (Ellermann and Bang, 1908; Rous, 1911). It took 40 years for the concept of viral oncogenesis to be truly accepted (Gross, 1951, 1957), but it was finally rewarded with a Nobel prize for Rous in 1966. By this time, *in vitro* methods for studying early stages of infection, cellular transformation and virus quantification were well underway (Temin and Rubin, 1958). It was not long before the discovery of reverse transcriptase, an essential enzyme required for retroviral replication, revised the Central Dogma theory of molecular biology (Baltimore, 1970; Temin and Mizutani, 1970). Assays to detect this enzyme as a marker for retroviral infection were rapidly developed and led to the finding of the first human retrovirus, Human T Lymphotropic virus-1 (HTLV-1) (Poiesz et al., 1981). Following this a novel T-lymphotropic retrovirus was detected in a patient with lymphoproliferative disease, and named HTLV-3 (Barre-Sinoussi et al., 1983). This was the first isolation of what we now know as human immunodeficiency virus (HIV) in humans and the start of the AIDS pandemic. It re-energised the hunt for new human retroviruses, which was enabled by the development of more sophisticated techniques such as bioinformatics and genomics (Voisset et al., 2008). For example, claims for a role of retroviruses in breast cancer, prostate cancer and myalgic encephalomyelitis have recently been made (Erlwein et al., 2010; Lombardi et al., 2009; Metzger et al., 2010). Proving Koch's postulates for these is the next hurdle (Voisset et al., 2008).

1.3.1 Retrovirus classification

Currently, retroviruses are classified according to their sequence similarity within the *pol* gene (Linial et al., 2005). This system divides the group into two subfamilies and seven genera as shown in Figure 1.10. Interestingly, other features such as virion size, structure and protein number also correlate well with this phylogenetic analysis. Before molecular details became available, viruses were categorised by their appearance on EM, associated disease or replication strategy. While these observations are all still valid, overlaps between groups reduce their effectiveness as a classification method.

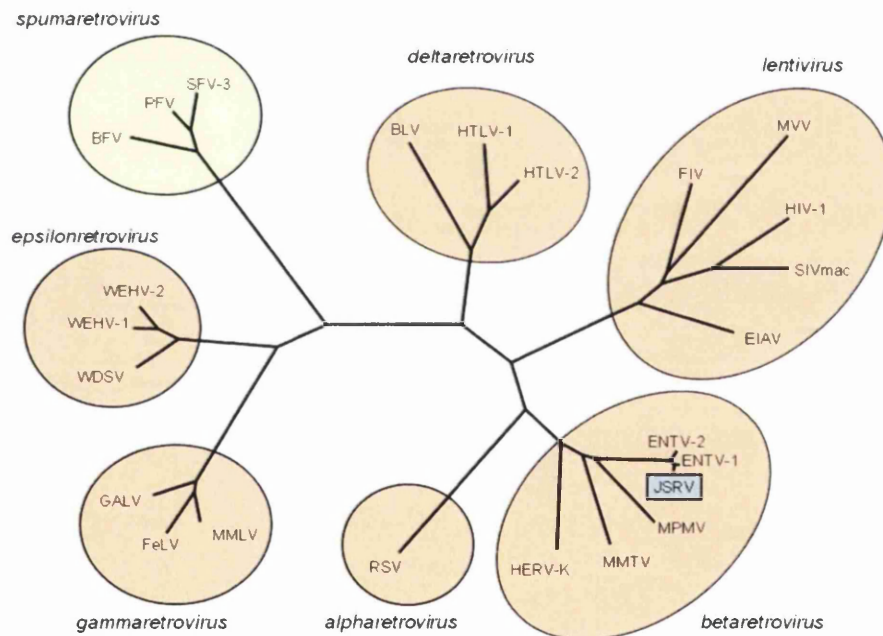


Figure 1.10 Phylogenetic tree showing the classification of retroviruses. The family Retroviridae is divided into two subfamilies: *orthoretrovirinae* (orange) and *spumaretrovirinae* (yellow). JSRV is a betaretrovirus and is highlighted in blue. (Griffiths et al 2010).

1.3.2 Retrovirus structure

Despite the variety of clinical disease, all retroviruses share similar structural properties. They are enveloped viruses with a diploid, single stranded positive sense RNA genome (Weiss, 2001). They encode only a few genes, and have evolved to maximise the use of the host cell machinery. The structural details of JSRV are outlined in Figure 1.11 and 12, and details of the replication cycle are in Figure 1.13.

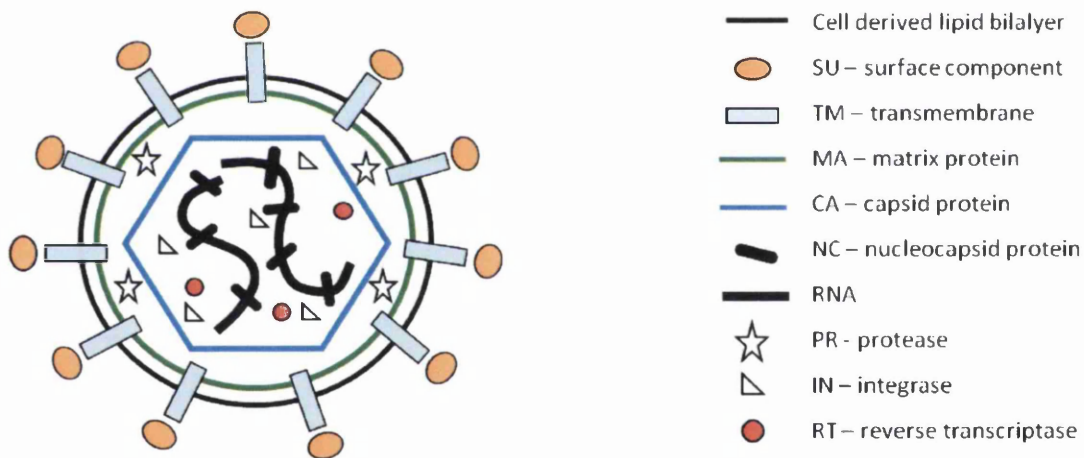


Figure 1.11 Schematic diagram of JSRV virion structure. The virion contains two identical copies of the RNA genome which are associated with the NC protein and enclosed within the virus CA and MA proteins. Enzymes involved in replication are also present within the viral core (PR, IN and RT). The whole structure is enclosed within a lipid bilayer envelope that is associated with SU and TM proteins.

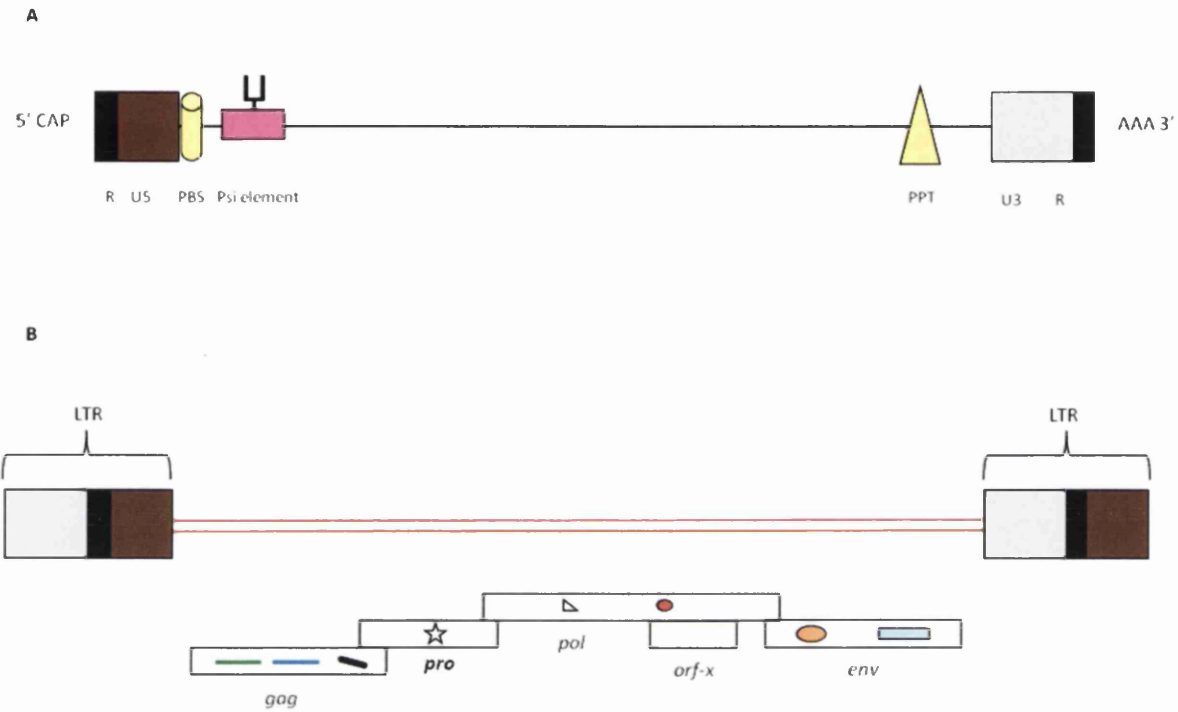


Figure 1.12 Structure of JSRV genome. The RNA genome of JSRV (A) is approximately 7,460 nucleotides in length. R represents the repeated elements at each end of the RNA genome. U5 and U3 are the unique elements close to the 5' and 3' termini of the genome respectively. The Ψ element is the packaging signal and PBS is the primer binding site for initiating reverse transcription. PPT is the polypurine tract which is the initiating site of positive strand synthesis. The DNA form of the JSRV genome (B) has long terminal repeats (LTR) at either end. These are made up of U3,R and U5 regions and contain promoter and enhancer elements. The retroviral LTR are generated by duplication of the end of the viral genome during reverse transcription and they regulate virus expression. The genome (B) contains four main genes which are *gag*, *pro*, *pol* and *env* (York et al., 1991, 1992). *Gag* encodes structural proteins matrix (MA), capsid (CA) and nucleocapsid (NC). *pro* and *pol* encode enzymes necessary for replication including protease (PR), reverse transcriptase (RT) and integrase (IN), and *env* encodes the surface (SU) and transmembrane (TM) envelope proteins. *Env* has also been shown to be an oncogene, and is capable of inducing tumours in lambs (Caporale et al., 2006) and immunocompromised mice (Wootton et al., 2006b). A highly conserved open reading frame (*orf-x*) also lies within the *pol* region but the function of this is unknown (Bai et al., 1999; Maeda et al., 2001; Rosati et al., 2000).

1.3.3 Retroviral replication

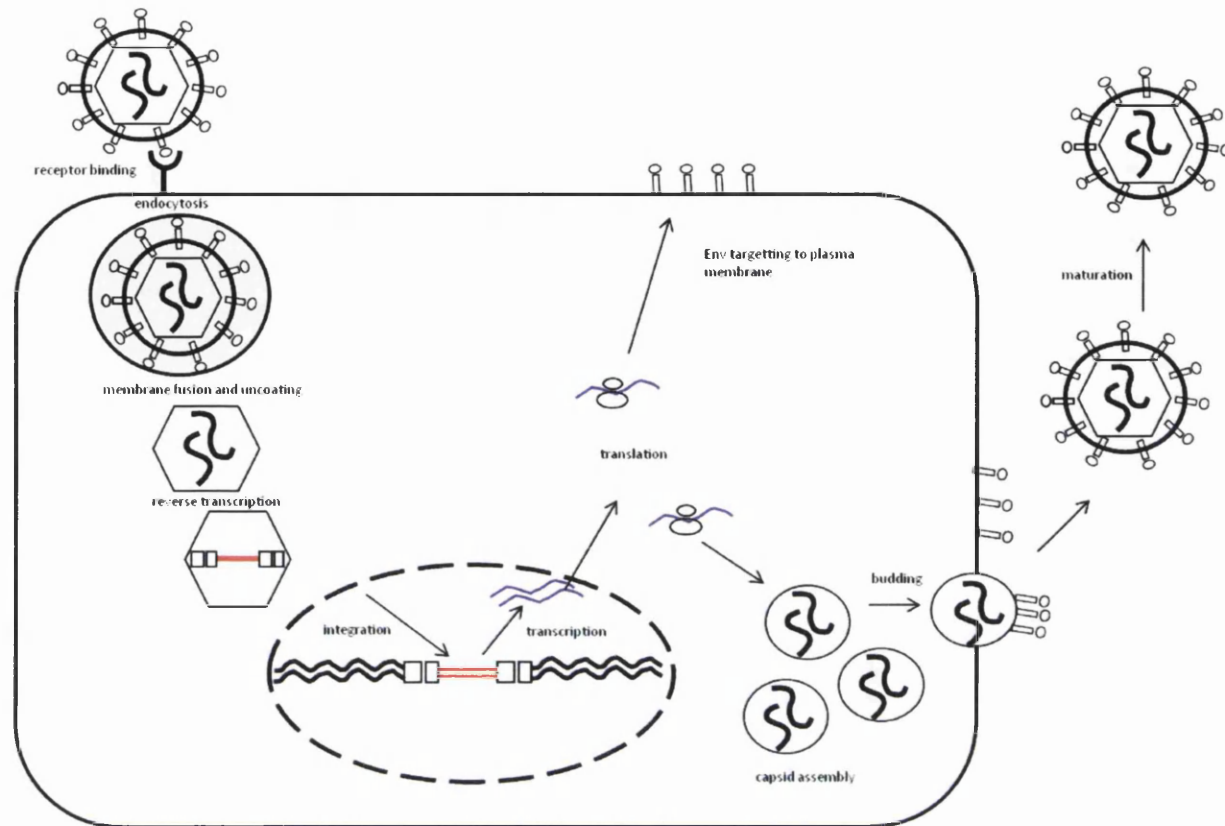


Figure 1.13 Replication cycle of JSRV, a general overview. JSRV entry into the cell is facilitated by fusion of viral and cellular membranes. This is initiated by the binding of the SU subunit of the Env glycoprotein to the cell surface receptor molecule Hyaluronidase -2 (Hyal-2), which induces a conformational change resulting in endocytosis of the virus and fusion of the membranes to release the viral core into the cell cytoplasm. The viral core then uncoats and reverse transcription is triggered. As this complex matures and DNA synthesis is completed, microtubules facilitate transportation through the cytoplasm towards the nuclear membrane. Mitosis provides an opportunity for nuclear entry, and integration of the double stranded DNA into the host genomic DNA using the viral integrase (IN) enzyme. This “provirus” is slightly longer than the original RNA genome as it is flanked on either end by the LTR derived from the 5’ and 3’ ends of the original RNA template during reverse transcription. Once the provirus is integrated, host RNA polymerase II is used to transcribe genomic length RNA which is packaged to make the RNA viral genome. Gag, Pro and Pol are translated from this while Env is translated from a singly spliced transcript. Structural proteins gather at the microtubules and are transported to the cell surface, where they are packaged with the remaining proteins and genomic RNA. The viral Gag polyprotein mediates JSRV assembly and release. At this point, these immature virions are non infectious and larger in size, and it is not until proteolytic cleaving of the polyproteins by protease (PR) enzyme occurs that the correct morphology is assumed and they are infectious.

1.3.3.1 Cell entry

The presence of a specific correct receptor on the host cell is the first step necessary for successful retroviral entry and replication. Initial work to determine the JSRV receptor showed it to be present on a wide variety of ovine cell types and cells of various species including human, monkey, cow, dog and rabbit cell lines (Holland et al., 1999; Palmarini et al., 1996; Palmarini et al., 1999b). However, rodent cell lines were found not to be transducible, and by using phenotypic screening of human/hamster hybrid cell lines, localisation of the receptor to the 3p21.3 region of the human chromosome was possible (Rai et al., 2000). This region was shown to contain a glycosylphosphatidylinositol (GPI) - anchored cell-surface protein called Hyaluronidase -2 (Hyal-2). Absolute proof of its receptor function for JSRV was shown by expressing Hyal-2 in previously resistant cell lines so rendering them susceptible to JSRV vector transduction. Equally, removal of Hyal-2 from susceptible cells by cleaving GPI linkages, blocked JSRV vector transduction (Rai et al., 2001). Hyal-2 has also been implicated in the transformation of some cell lines. In the human bronchial epithelial cell line BEAS-2B, Hyal-2 acts as a tumour suppressor by binding to the receptor d'origine nantais (RON) receptor tyrosine kinase and rendering it inactive (Danilkovitch-Miagkova et al., 2003). A similar role for RON has been proposed in sheep, although in mice at least, RON expression is limited to bronchial epithelial cells (Miller, 2008; Sakamoto et al., 1997). Other GPI anchored cell surface proteins have also been shown to participate in cell signalling and mitogenic activation, and the role of Hyal-2 in cell fusion during embryogenesis has been suggested (Dunlap et al., 2006).

1.3.3.2 Reverse transcription

Once the virus has gained access to the cell cytoplasm, all intracellular events take place within the nucleoprotein complex derived from the viral core. Reverse transcription is triggered by the uncoating of the viral core, and involves a series of highly related strand transfer reactions. The net result is the conversion of the diploid RNA genome to a single double stranded DNA form. A specific cellular tRNA molecule anneals to a complementary sequence in the viral RNA at the PBS, and initiates DNA synthesis. This forms the minus-strand strong stop DNA which contains R and U5 sequences. It is transferred to the 3' of the viral RNA genome following RNase H degradation of the viral genomic RNA. This process is

called the first strand transfer. The minus strand is then extended to copy the remaining RNA sequence, which is degraded by RNase H. The PPT sequence is preserved, and acts as a primer for the formation of the plus-strand strong-stop DNA which extends 18 nucleotides into the tRNA primer. The latter is removed by RNase H, and the second strand transfer acts to anneal the plus strand strong stop DNA with the 3' end of the minus strand. Subsequent extension of these plus and minus strands yields a linear ds cDNA which contains a copy of U3-R-U5 sequences. These are known as the long terminal repeats (LTRs).

1.3.3.3 Nuclear entry and integration

Integration into the host DNA acts to stabilise the viral DNA and enables efficient transcription of viral DNA into the viral genome and mRNAs encoding viral proteins. For all retroviruses, entry into the cell nucleus is essential to allow viral DNA integration. Early observations found that apart from lentiviruses, all retroviruses required actively dividing cells for efficient integration and replication (Lewis and Emerman, 1994; Temin and Rubin, 1958). *In vitro* work has shown that during mitosis the nuclear membrane is disassembled, and this provides the opportunity for viral DNA entry into the nucleus (Harel et al., 1981). Although not yet proven, this requirement for cell division is assumed to apply to JSRV, and the infection of quiescent cells is thought to be a rare and inefficient event (Griffiths et al., 2010). Once viral DNA synthesis is complete, the viral integrase cleaves the 3' termini of the viral DNA, exposing OH groups which help to attach the provirus to the host DNA. Integration sites for JSRV were investigated in several natural cases of OPA. Most were found to have multiple integration sites with a random distribution, although two integration sites from independent tumours were found on chromosome 16 (Cousens et al., 2004).

1.3.3.4 Trafficking and assembly

Retroviral assembly and release are both mediated by the viral Gag polyprotein. For betaretroviruses, immature particles known as Type-A particles assemble at microtubules in the cytoplasm. They are then transported to the cell surface for envelopment at the plasma membrane during budding. These immature particles are non infectious. Gag maturation occurs after assembly and budding, and involves the proteolytic processing by protease of the Gag polyprotein to yield the internal structural proteins matrix, capsid and nucleocapsid.

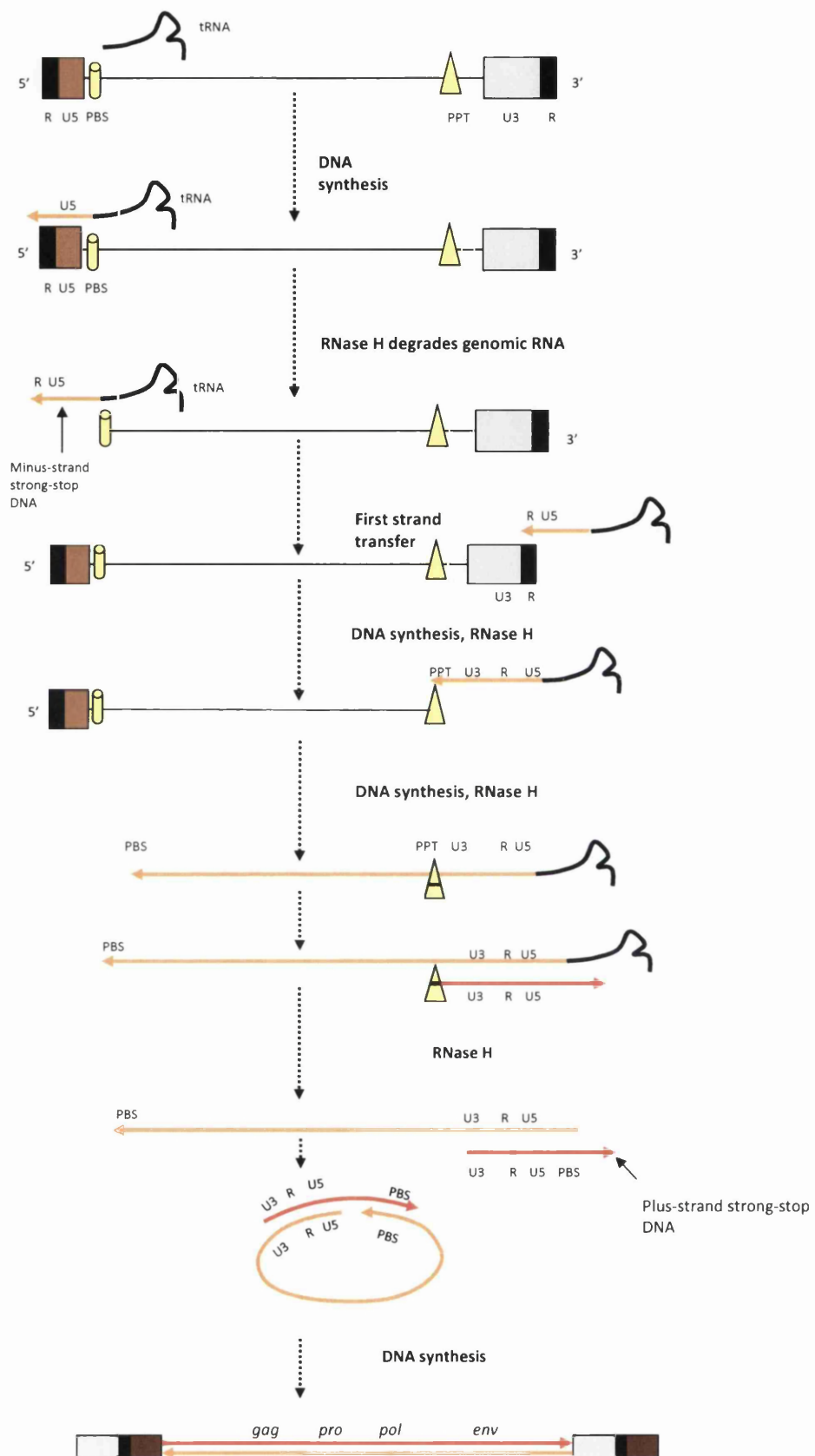


Figure 1.14 A schematic representation of reverse transcription. Described in section 1.3.2.

1.3.4 Influential host factors for retroviral replication

A diagram of the JSRV replication cycle is shown in Figure 1.13. As the virus has a limited genetic coding capacity, it is highly dependent on the host cell for provision of some essential 'permissive factors' to enable replication. However, the host has also evolved to produce factors that can actively inhibit retroviral replication, denoted 'restriction factors'. The balance between these two influences is a major determinant of the outcome of infection.

1.3.4.1 Transcription factors

Successful retroviral replication is also dependent on cellular transcription factors. These are essential host proteins which bind to promoter and enhancer elements located in the U3 region of the long terminal repeats (LTR) of the proviral DNA. They facilitate the transcription of proviral DNA by RNA polymerase II, in order to produce genomic viral RNA (Coffin et al., 1997). Core transcription factors are required for transcription initiation and bind together with RNA polymerase II and other proteins near the TATA box in the promoter region. Regulatory transcription factors bind either near to (promoters) or far (enhancers) from this region, and act to control the rate of transcription. Some transcription factors are ubiquitous while others are found only in specific cell types and each retrovirus has its own requirements for particular combinations. Their presence, along with the differentiation and physiological state of the host cell, will have a major influence on the transcription rate and hence the level of virus expression at a cellular level.

As far as we know, expression of JSRV is limited to transformed cells within the lung and occasional lymphocytes (Holland et al., 1999; Palmarini et al., 1999a). To investigate the role of transcription factors in this restricted expression, several cell lines were transiently transfected with a luciferase reporter plasmid driven by the JSRV LTR (denoted pJS21-luc), and its activity was determined relative to appropriate controls (Palmarini et al., 2000a). The experiment showed preferential activity of the JSRV LTR in murine type II pneumocyte (MLE-15) and Clara cell (mtCC1-2) lines. In addition, two putative enhancer binding motifs for Hepatocyte Nuclear Factor (HNF)-3B were identified within the U3 region, and the addition of HNF-3 was capable of enhancing pJS21-luc in some cell lines (McGee-Estrada et al., 2002; Palmarini et al., 2000a). HNF-3B is a lung and liver specific transcription factor

(McGee-Estrada and Fan, 2007). Further binding sites for the more ubiquitous transcription factors NF- κ B and C/EBP α were demonstrated in the mid and proximal promoter enhancer regions (McGee-Estrada and Fan, 2006). These were also shown to be important for LTR activity. In another experiment, the U3 regions of three closely related betaretroviruses (JSRV, ENTV and enJSRV) with different cell tropisms *in vivo* were aligned and compared. The differences that were identified by this experiment, supported the vital role that LTR enhancer elements play in tissue specific expression of betaretroviruses (McGee-Estrada and Fan, 2006). The cellular specificity of the LTR *in vivo* was studied by generating transgenic mice to carry a bacterial B-galactosidase gene under the control of JSRV LTR (Dakessian and Fan, 2008). The authors anticipated that this would identify the target cells for infection in mice, but excessive transgene silencing in several generations made it difficult to interpret the results meaningfully. From these experiments we can conclude that cell tropism is determined by the presence of specific transcription factors, both *in vitro* and *in vivo*. However, only three binding motifs have so far been identified, and it is likely that transcriptional control relies on additional factors that have yet to be found.

1.3.4.2 Restriction factors

During evolution, retroviral infections have led to the development of protective mechanisms in the host to control virus spread and cross species transmission. An example of these are restriction factors (Goff, 2004). They are proteins produced by the cell, some of which derive from inherited endogenous retroviruses (Mura et al., 2004). As they are constitutively expressed, they are regarded by some as a form of intrinsic immunity (Bieniasz, 2003). Expression of restriction factors may also be triggered by interferon α following viral infection. They are therefore considered to be part of the innate response of the host (Sauter et al., 2010).

Work on a number of retroviruses has discovered a variety of restriction factors including APOBEC 3 (A3), TRIM5 α (T5), and tetherin. A3 proteins are incorporated into newly assembled viral particles, and inhibit infection of subsequent target cells by a number of mechanisms including cytidine deamination of single stranded DNA. This results in hypermutation and instability of the viral genome (Bieniasz, 2003). T5 blocks infection by

targeting the incoming capsid for degradation by proteasome, and tetherin blocks the release of newly formed virions. To date, nothing has been published on T5 or A3 and JSRV, but ovine tetherin is able to block JSRV release *in vitro* (Arnaud et al 2010). In addition in pregnant sheep, tetherin expression is upregulated specifically within the endometrial stromal cells by the pregnancy hormone tau interferon, and is capable of blocking the release of viral particles produced by intact enJSRV and exJSRVs (Arnaud et al., 2010). *In vitro* work has shown that endogenous JSRV proteins are also capable of viral interference to protect the host from exogenous retrovirus infection (Mura et al., 2004).

1.3.5 Endogenous retroviruses in sheep

Endogenous retroviruses (ERVs) have evolved due to the ability of retroviruses to integrate into the host cell DNA during replication (Arnaud et al., 2007a). They result from chance infections of sperm or egg cells with exogenous retroviruses, which stably integrate into genomic DNA and are inherited in a Mendelian fashion. ERVs have accumulated over millions of years and now all vertebrate genomes are heavily colonized. In humans they account for up to 8% of the genome (Griffiths, 2001) and this degree of evolutionary success was demonstrated in recent experiments where the necessity for ERV expression to allow trophoblast cell fusion and placental development in humans, mice and rabbits was recognized (Dupressoir et al., 2009; Heidmann et al., 2009; Vargas et al., 2009). Unfortunately, occasional negative impacts have also been reported. High levels of HERV-W Env and HERV-H Env expression were detected on the surface of B cells from patients with active multiple sclerosis, suggesting an involvement in disease pathogenesis (Brudek et al., 2009). They have also been implicated in some autoimmune diseases, but these are mostly in experimental models where specific phenotypes have already been selected for (Varela et al., 2009).

The ovine genome contains several families of ERVs related to gamma and betaretroviruses (Klymiuk et al., 2003). One of these is closely related to JSRV and is denoted enJSRV. There are at least 27 enJSRV proviruses, all of which have been sequenced (Arnaud et al., 2007a). A majority of them are unable to express infectious virus or proteins, but a few contain intact open reading frames for one or more of gag, pro, pol and env (Palmarini et al., 2004). They

have a high degree of similarity with their exogenous counterparts displaying an 85-89% identity at the nucleotide level (Varela et al., 2009). Differences are predominantly found in the U3 region of the LTR, and variable regions (VR) 1-2-3 in gag and env (Palmarini et al., 2000b). Distinguishing between these highly related exJSRV and enJSRV is an ongoing challenge for scientists when developing molecular techniques for genome analysis (Cousens et al., 2004). In contrast, the similarities provide an effective assay for gene function analysis when different properties of these viruses are compared (McGee-Estrada and Fan, 2006).

Similar to other mammals, enJSRV play a vital role during placental morphogenesis and mammalian reproduction in the sheep. Expression is confined to the genital tract during oestrus and early pregnancy and transcription appears to be regulated by progesterone levels (Palmarini et al., 2001a). enJSRV *env* mRNA levels are highest in the endometrial luminal epithelium, glandular epithelium and trophoblast giant binucleate cells. Peak expression coincides with a type I interferon release which is the pregnancy recognition signal released from the developing fetus (Arnaud et al., 2010; Dunlap et al., 2005). During embryogenesis, it is thought that enJSRV binds to Hyal-2 so mediating cell fusion events and the formation of trinucleate cells and placental multinucleate syncytial plaques (Dunlap et al., 2006). Consequently, experiments which inhibit enJSRV transcription with antisense techniques result in compromised trophoderm growth and fetal death (Dunlap et al., 2006).

Interestingly, proteins encoded by enJSRV have been found to interfere with replication of exogenous JSRV in *in vitro* transfection studies (Arnaud et al., 2007b; Murcia et al., 2007; Spencer et al., 2003). enJSRV blocks JSRV entry, presumably by binding Hyal-2 and thereby reducing receptor availability on the cell surface. This phenomenon is termed receptor interference, and has been described for other retroviruses (Coffin et al., 1997). The Gag protein of at least one enJSRV provirus is able to block JSRV assembly and release. It has been proposed that the ability of enJSRV to block JSRV replication may have been responsible for a switch in tissue tropism of exJSRV from the reproductive tract to the lung during evolution of the virus (Arnaud et al., 2010; Palmarini et al., 2004).

1.3.6 The immune response

While restriction factors are relevant for replication at the cellular level, innate and acquired immune responses act to provide protection at the level of the host. The innate response is immediate and has no immunological memory. It is triggered by the recognition of pathogen-associated molecular pattern (PAMP) molecules present in a large number of microorganisms, by genetically determined Pattern Recognition Receptors (PRRs). A well studied class of PRRs are the Toll like receptors, and these are expressed by innate immune cells including macrophages, dendritic cells, neutrophils and lung epithelial cells (Mayer et al., 2008).

Following infection recognition, these cells release cytokines which further activate phagocytes of the innate immune cell population including antigen presenting cells (APC) like dendritic cells or local macrophages (Akira et al., 2006).

APCs migrate through afferent lymphatics to the draining lymph nodes to present antigen to CD 8+ cytotoxic T cells with MHC class I molecules and CD 4+ T helper cells with MHC II molecules (Larruskain et al., 2010). Once activated, the CD4+ helper cells interact with naive B lymphocytes or CD 8+ lymphocytes to induce clonal proliferation of antigen specific lymphocytes and production of antibody (Delves and Roitt, 2000a, b). These CD4 + helper cells can be divided into T helper 1 (TH1) and T helper 2 (TH2) cells. TH1 secrete IFN gamma IL-2 and GM-CSF to drive the clonal expansion of CD 8 + cells, and TH2 cells secrete large amounts of IL-4, IL-5, IL-6 to drive clonal expansion of B cells.

The immunological memory of the acquired response ensures an improved reaction of the host to the specific virus on each exposure. The innate and adaptive immune response act together to rid the host of infection as quickly as possible, and to prevent reinfection (Kawai and Akira, 2006). The specific cytokine responses associated with various arms of the immune response can be useful indicators when evaluating immune reactions during disease pathogenesis.

1.3.6.1 Immunity in the lung

Although this basic process of immune activation is identical in all areas of the body, cellular responses and their activation thresholds are modified to suit the local environment of each tissue (Raz, 2007). In the lung, the default immune response is non-inflammatory (Holt et al., 2008). As the microarchitecture is such that the respiratory airways are continually exposed to a myriad of antigens, maintenance of immunological homeostasis and a sterile environment suitable for efficient gas exchange is a priority. This requires a sensitive surveillance system to discriminate between the inhaled non-pathogenic and pathogenic particles, and immunomodulatory mechanisms to dampen down excessive reactions which might interfere with respiratory function. Respiratory epithelial cells are key players in this balancing act. They provide a physical barrier to deter incoming pathogens, and secrete an array of regulatory and effector molecules including surfactant proteins, antimicrobial peptides, cytokines and chemokines. These act to limit innate inflammation and raise the threshold for macrophage activation (Hussell and Goulding, 2010). This immunoregulatory environment is overcome by the loss of epithelial integrity and subsequent release of inflammatory mediators. Local immune cells including lymphocytes and dendritic cells in the bronchial epithelium and dendritic cells and macrophages residing in alveoli, are then activated (Guth et al., 2009).

1.3.6.2 Immune response to neoplasia

Similar to a viral infection, the presence of a tumour activates the host innate and adaptive immune response (de Visser and Coussens, 2005). Tumour growth is accompanied by release of a complex cytokine and chemokine network which manipulates the host to recruit endothelial cells, fibroblasts and inflammatory cells. In order to isolate these different cell types and understand whether they are pro tumour or host survival, sequential stages of carcinogenesis in mouse models have been examined. These experiments show pre-malignant lesions to be associated with a chronic infiltration of innate immune cells, inhibition of which (in knock-out mice) results in reduced tumour growth. Similarly, mice with reduced macrophage recruitment capabilities developed less malignant tumours with a lower metastatic potential. In these examples, the innate immune cells appear to promote cancer development. In contrast, some cancers with high numbers of infiltrating lymphocytes have a more favourable prognosis for the host. This was recently highlighted in a study looking at

colorectal tumours, where they found that the collection of immunological data ie. number, type, location of infiltrating immune cells to be a better predictor of patient survival rates than the standard malignancy criteria (Galon et al., 2006). Collectively, these studies demonstrate that tumour growth and metastasis are greatly influenced by the balance between the tumour microenvironment and the host immune response. These characteristics will vary between different hosts and individual tumour types (Whiteside, 2006).

Again similar to viruses, tumours have developed means of evading the host immune response (Whiteside, 2006). This is achieved either by 'hiding' from immune cells or disabling them. For example downregulation of cell surface molecules like tumour associated antigens or alterations in antigen processing machinery can prevent recognition by tumour specific T-cells. Suppressor cell populations such as regulatory T cells (T reg) also inhibit the reaction of T cells specific for autoantigens, and prevent the generation of immunity to tumour antigens. In addition the release of cytokines (TGF beta, IL-10, GM-CSF) small molecules (PGE2, INOS) or enzymes (IDO) from cells in the tumour microenvironment all act to modulate the systemic immune response in some way. Immunosuppressive effects of tumours are generally best seen at the tumour site, and an understanding of their intricacies will help aid therapeutic strategies aimed at combating cancer.

1.3.6.3 Immune response to JSRV

In contrast to infection with many other respiratory viruses, the detection of an immune response following infection with JSRV has proved somewhat elusive. Most experiments have failed to identify any JSRV-specific T cell or antibody responses in blood samples from experimental or naturally infected animals (Ortin et al., 1998; Summers et al., 2002). Anti-beta-retroviral Gag antibodies detected by immunoblotting in some studies (Kwang et al., 1995) are now thought to be due to antibodies to the glutathione-S-transferase fusion partner of the recombinant Gag antigen used in the assays (Ortin et al., 1998). The most popular explanation for the lack of immune response is a mechanism of central tolerance due to expression of closely related enJSRV proteins which are expressed in the thymus at the time of T lymphocyte development during fetal growth (Palmarini et al., 2004; Spencer et al.,

2003). This results in any JSRV-reactive T cells being recognised as anti-self and subsequently removed (Garcia-Goti et al., 2000; Summers et al., 2005).

However, vaccination studies for JSRV which use recombinant proteins and adjuvants, have generated humoral and cellular immune responses to JSRV antigens (Summers et al., 2006). Evidence of an adaptive response was also indicated when increased expression levels of interferon gamma and MHC II upregulation were detected using IHC in experimentally induced OPA (Summers et al., 2005). However, this was not accompanied by an increase in dendritic cells, B cells or $\gamma\delta$ T cells and a minimal CD4 and CD8 T cell infiltrate. This lack of expected immune response which commonly follows MHC II upregulation was attributed to peripheral tolerance due to local immunosuppressive properties of surfactant proteins (Summers et al., 2005). A more recent study found low levels of anti-JSRV Env antibody in a few experimentally infected animals, although they were concurrently infected with MVV (Hudachek et al., 2010). This suggests that JSRV can actually be recognised by the ovine immune system, and questions the central tolerance theory. In support of this, a role for a T cell-mediated immune response against JSRV was suggested following evidence of a marked CD3⁺ T cell infiltration in animals with partial tumour regression (Hudachek et al., 2010). However, whether this cellular infiltrate was directed against viral expression (JSRV or MVV) or tumour growth is still uncertain.

In OPA, as the tumour grows macrophage like cells are the predominant infiltrate (Demartini et al., 1988; Dungal et al., 1938; Payne and Verwoerd, 1984; Platt et al., 2002) The precise function of these macrophages is unclear but some suggest they are phagocytosing excess surfactant produced by the tumour cells (Payne and Verwoerd, 1984). Other experiments have noted the presence of lymphocytes and plasma cells infiltrating mature tumours (Garcia-Goti et al., 2000).

1.3.7 Retroviral oncogenesis

Traditionally, oncogenic retroviruses were divided into two groups according to their mechanism of tumour induction (Maeda et al., 2008). Acute-transforming retroviruses induce rapid neoplastic transformation of host cells *in vivo* forming tumours of polyclonal origin. Their genome contains an oncogene which is a captured form of a normal gene from the host (Coffin et al., 1997; Liu and Miller, 2006) In general, these are replication defective viruses because the incorporation of the oncogene sequence almost always results in deletion or disruption of viral genes which are essential for replication (Rous Sarcoma virus being one exception) (Coffin et al., 1997).

A second group of oncogenic retroviruses are designated insertional/ cis-transforming retroviruses. These integrate close to existing host proto - oncogenes and induce clonal tumours as the LTR drives unregulated expression of the proto-oncogene (Maeda et al., 2008). The slow nature of tumour induction can be explained by the number of rounds of infection it takes for the provirus to insert in an appropriate location for proto-oncogene activation. The importance of research in this area is reinforced by the fact that several human cancers share similar oncogenes and signal transduction pathways (Yeatman, 2004). More recently, a third mechanism by which retroviruses induce tumours using expression of the structural Env protein was discovered. We now know that Avian Hemangioma virus (AHV), Mouse Mammary Tumour virus (MMTV), Enzootic nasal tumour virus (ENTV) and JSRV are all members of this group (Maeda et al., 2008). Some rely solely on Env for transformation (JSRV, ENTV) while others have additional oncogenic mechanisms (MMTV).

1.3.7.1 JSRV oncogenesis

During JSRV replication, the *env* gene is expressed as a polyprotein that is glycosylated and transported through the endoplasmic reticulum (ER) to the cell surface. It is cleaved into SU and TM, which are connected by disulfide bonds. SU is anchored to the virus by binding to TM which spans the lipid bilayer of the plasma membrane into the cell cytoplasm. For JSRV, proof that the envelope gene had transforming potential was demonstrated using plasmids expressing JSRV Env where the *gag*, *pol* and *orf-x* coding sequences were deleted.

Transfection into rodent fibroblast cell lines resulted in the formation of transformed foci

(Maeda et al., 2001; Rai et al., 2001). Further experiments identified that mutations in the cytoplasmic tail of TM could abolish transformation in rat fibroblasts (Palmarini et al., 2001b). The specific region concerned (YXXM motif) was known to be recognised by phosphatidylinositol 3-kinase (PI-3K) which phosphorylates Akt, and activation of this pathway was proposed as a route of transformation. However, another study showed PI-3K independent transformation of mouse fibroblasts, and phosphorylation of Akt following the binding of a different protein to the TM tail (Maeda et al., 2003). Interestingly, elimination of this binding site in an avian fibroblast line failed to prevent Env-induced transformation (Allen et al., 2002), which was also shown to be Akt independent in this cell line (Zavala et al., 2003).

SU has also been shown to have a role in transformation of cells *in vitro*, the means of which is highly dependent on cell line and available surface receptors (Danilkovitch-Miagkova et al., 2003; Hofacre and Fan, 2004). In a human bronchial epithelial cell line, binding of SU to the cell surface receptor Hyal-2 was shown to activate RON receptor tyrosine kinase and mediate transformation via the Akt and mitogen-activated protein kinase (MAPK) pathways (Danilkovitch-Miagkova et al., 2003). However, infection of other epithelial cell lines eg. Madin-Darby Canine Kidney epithelial cells and IEC-18 shows similar findings to the rat fibroblast cell lines, with receptor independent signalling and activation of PI-3K/Akt pathway (Liu and Miller, 2005; Varela et al., 2006). Recent work using tissue from naturally and experimentally infected sheep has identified activated proteins of the MAPK Erk 1/2 pathway using IHC of fixed tissue (De Las Heras et al., 2006).

Whichever pathway is activated, tumourigenesis is a multistep process and mechanisms in addition to the initial expression of JSRV Env are likely to be involved (Hanahan and Weinberg, 2000). For example, HTLV-1 has a unique regulatory protein, Tax, which also functions as a viral oncogene. While Tax has been shown to be a primary determinant of tumourigenesis, further protein interactions are required for late stage and tumour cell maintenance (Maeda et al., 2008). With JSRV, the role of insertional mutagenesis was proposed following an analysis of 70 JSRV integration sites from natural cases of OPA (Cousens et al., 2004). Most were found to have multiple integration sites with a random distribution. However, two integrations sites from independent tumours were found on

chromosome 16, less than 200 kb from the gene MAPK31, activation of which has since been implicated in OPA tumour cells using IHC (De Las Heras et al., 2006). These were not clonal suggesting that they may not be involved in tumourigenesis, or that multiple tumours arise independently but contain integration sites in a preferred area, (Cousens et al., 2004; Philbey et al., 2006). Other mechanisms involving the inactivation of cellular senescence by increased telomerase activity have been suggested to maintain tumour growth in OPA (Suau et al., 2006).

In vivo experiments have successfully used Env, expressed from a replication incompetent vector, to induce rapid tumour formation in the lungs of immunocompromised mice and normal lambs within four months of inoculation (Caporale et al., 2006; Wootton et al., 2005). F1 progeny of mice containing the SPA-Env-HA, a transgene of JSRV driven by the SP-A promoter, have been reported to develop subdermal lipomas expressing transgene (Dakessian et al., 2007). Interestingly the closely related Env protein from Enzootic Nasal Tumour Virus - 1 (ENTV-1) is also capable of inducing lung tumours in sheep (Wootton et al., 2006a), even though this causes a nasal tumour in natural infection (De las Heras et al., 2003). This suggests that the oncogenic mechanisms of Env-mediated transformation are not cell type specific, and that Env is not directly involved in tissue specificity of the tumour.

These experiments have given us crucial information about the behaviour of JSRV *in vitro*, and provide useful infection assays for future work. While some of the findings will reflect the situation *in vivo*, the way in which results vary according to the infected cell lines or species is confusing. In order to understand the true pathogenesis of disease there is no substitute for looking at disease progression in the natural host itself.

1.3.7.2 OPA as a model for human lung adenocarcinoma

The study of retroviruses has provided additional tools to use in other experimental areas. For example, the ability of retroviruses to stably integrate into the nuclear DNA of target cells has been exploited to create retroviral vectors for use *in vitro* and *in vivo*, and the reverse transcriptase enzyme is widely used in cloning and RNA quantification methods. The molecular dissection of retroviral oncogenesis has also transformed our understanding of the

pathogenesis of non-viral cancer. Through the unravelling of cancer pathways numerous proto-oncogenes and potential therapeutic targets have been identified.

Lung cancer has the highest mortality rate of all cancers worldwide. It has an extremely poor therapeutic response with an overall five year survival rate of less than 15% (Eramo et al., 2008). Unfortunately, by the time patients show clinical signs and the disease is diagnosed, the tumour is already well established and refractory to treatment. If earlier diagnostic tests and treatment for lung cancer are to be developed, then the initial pathogenesis of tumour growth must be established.

Cancers are classified by their cell of origin, and in the lung they are either small cell lung cancers (originating from neuroendocrine cells) or non small cell lung cancers (NSCLC). The NSCLC are further categorised into squamous cell carcinoma, adenocarcinoma and large cell carcinoma (Snyder et al., 2009). Histological similarities between OPA and human lung adenocarcinoma were recognised early in disease discovery (Bonne, 1939; Watson and Smith, 1951), and this led to the suggestion of using OPA as an animal model for human disease (Mornex, 2003; Mornex et al., 2003; Palmarini and Fan, 2001; Perk and Hod, 1982). Several studies have investigated the involvement of JSRV in human lung tumours. One study found 30% of human lung adenocarcinomas to label positively with antisera raised against JSRV CA using IHC (De las Heras et al., 2000; De Las Heras et al., 2007). Others looked for JSRV related sequences using PCR but the results were inconclusive (Hiatt and Highsmith, 2002; Morozov et al., 2004; Yousem et al., 2001). Most recently, a study has confirmed the expression of a JSRV Gag-related protein in some human lung tumours using IHC, but was unable to provide additional evidence of betaretroviral infection with RTPCR, immunoblotting and DNA library screening techniques (Hopwood et al., 2010). The conclusion was that if a retrovirus was involved in disease pathogenesis then it is unrelated to known betaretroviruses. Recent experiments have used the OPA model to investigate the effects of Hsp90 inhibitors in lung adenocarcinoma (Varela et al., 2008). A summary of comparisons between the two diseases are shown in Table 1.7.

Although the mature tumours have several shared characteristics, the difference in precursor morphology is interesting to note in the context of disease pathogenesis. According to the

WHO, atypical adenomatous hyperplasia (AAH) is a putative precursor of bronchioloalveolar carcinoma (BAC) in humans. It is described as being a '*discrete parenchymal lesion arising often in the centriacinar region close to respiratory bronchioles. The alveoli are lined by rounded, cuboidal low columnar or 'peg' cells which have round or oval nuclei*' (Travis, 2004). Analysis of mature human adenocarcinomas often finds more than one pattern of tumour present, typically more malignant cells in the centre with BAC or AAH towards the periphery (Raz et al., 2006). This and recent studies using a mouse model of disease suggests that AAH and BAC may act as precursors to the development of invasive adenocarcinomas (Jackson et al 2001). There is little evidence of a similar progression in OPA, with epithelial hyperplasia being the only precursor lesion noted so far.

In humans, the current WHO lung cancer classification has been deemed inadequate (Chilosi and Murer, 2010). There is a move to incorporate immunophenotypic and molecular features of neoplastic cells with classic morphology and relevant stem cell biology information to improve the recognition of specific tumour profiles for adenocarcinomas. For example, microarrays have been used to further classify tumour subgroups, and additional markers of malignancy/ cellular origin have been identified (Bhattacharjee et al., 2001). Proteomic profiling is also being used to identify potential serological antigens which might indicate early tumourigenesis (Madoz-Gurpide et al., 2007). Applying these techniques to OPA would improve its value as a model for human BAC.

Table 1.7 General comparison of human and ovine lung tumours. OPA-N natural field cases, OPA-E experimental tumours (Bertolini et al., 2009; Beytut et al., 2008; Demartini et al., 1988; Eramo et al., 2008; Hudachek et al., 2010; Platt et al., 2002; Travis et al., 2004b; Verwoerd et al., 1983).

Parameter	Human Adenocarcinoma	OPA-N	OPA-E
Aetiology	Multiple factors	Viral	
Localisation	Peripheral, central, diffuse, pleural, post fibrosis	Peripheral, central	
Number	Single/multiple	Single/multiple	Multiple
Distant metastasis	Haematogenous/lymphatic 20% - brain, bone, adrenal gland, liver	Haematogenous/lymphatic Rare - liver, kidney, heart	NA
WHO classification	Adenocarcinoma (MS) = 80% Acinar, Papillary, BAC, solid acinar with mucin production	Adenocarcinoma mixed subtype (MS)	
Fibrosis	Yes	Yes	No
Tumour precursor	Atypical Adenomatous hyperplasia (AAH), Bronchoalveolar Carcinoma (BAC)	Not definitively identified	
IHC			
Capsid protein	30%	71% tumours 17%	71%
CC-10			
SP-A	60%	70%	Unknown
SP-C			
TTF	60%	80%	Unknown
CK7 : CK20			
	75% in well differentiated	Unknown	Unknown
	High:low	Unknown	Unknown
Genetic alterations	K-ras mut 25-50% P53 overexpression 35-53% <i>Survivin</i> < BAC cv AAH Laminin- 5, 38% E cadherin/B catenin decrease as malignancy increases. Ki67 < invasive cancer P27 < differentiation	No mutations in tyrosine kinase domain of epidermal growth factor receptor, KRAS codons 12/13 or DNA binding domain of p53 in tumour DNA	Unknown
Expression profiles	Microarray SAGE Proteomic profile	Unknown	
Stem cells identified	In human tumours only	Unknown	

1.3.8 Other exogenous retroviruses in sheep

There are additional exogenous retroviruses capable of infecting sheep and causing chronic respiratory disease in the adult animal. These include MVV and ENTV-1, both of which have genetically related forms which are pathogenic in goats (caprine arthritis-encephalitis virus and ENTV-2 respectively) (Phylogenetic tree Figure 1.10). MVV is a non-oncogenic lentivirus which targets cells of the monocyte/macrophage and myeloid dendritic system (McNeilly et al., 2008). Pathology in the lung is characterised by lymphoid hyperplasia and an interstitial infiltration of mononuclear cells. ENTV-1 is an oncogenic beta retrovirus which targets respiratory and olfactory epithelial cells to cause a low grade adenocarcinoma in the upper airways (Cousens et al., 1999; De las Heras et al., 2003; Ortin et al., 2003). Genome sequence analysis has shown significant genomic stability between isolates and a 75% sequence similarity to JSRV (Ortin et al., 2003; Walsh et al., 2010). The cytoplasmic tail of the transmembrane subunit is an area of difference between JSRV and ENTV-1, and it influences the low pH requirements for fusion and entry into the target cell when compared to JSRV, despite use of the same surface receptor Hyal-2 (Cote et al., 2009; Van Hoeven and Miller, 2005). ENTV Env-positive cells have also been demonstrated in the lung of some affected animals (Walsh et al., 2010). Concurrent infections of JSRV with MVV or ENTV-1 have been reported and it would be of interest to determine whether coinfection affects the host immune response to JSRV (De las Heras et al., 2000; Hudachek et al., 2010; Ortin et al., 2004; Rosadio et al., 1988a; Rosadio et al., 1988b).

1.4 Thesis overview

This thesis describes an investigation of the early interactions between the pathogen Jaagsiekte Sheep Retrovirus (JSRV) and its ovine host. Tissues from experimentally infected lambs are used to define the target cell for JSRV in the lung, and the host response to viral expression and tumour growth in terms of cytokine expression. It is hoped that by examination of these initial stages of infection, our understanding of the overall pathogenesis of OPA will be improved.

CHAPTER 2 MATERIALS AND METHODS

2.1 Experimental infection with JSRV₂₁

2.1.1 Preparation of JSRV₂₁

Infectious inoculate was produced by *in vitro* transfection of the human 293T cell line with a plasmid encoding an infectious molecular clone, pCMV2JS₂₁ (Palmarini et al 1999). The supernatant was collected 48 hours later and concentrated by centrifugation onto a glycerol cushion. Tubes of concentrated 293T cell supernatant (SN) were made up to 37.8 ml with phosphate buffered saline (PBS) and divided into 3 equal aliquots. It was predicted, using qRT-PCR, that 4 ml of this solution would contain 10¹⁰ RNA copies of JSRV₂₁. Mock inoculate was collected from the supernatant of untransfected 293T cells and processed in the same way.

2.1.2 Intratracheal inoculation of lambs with JSRV₂₁

All animal experiments were approved by the Moredun Research Institute (MRI) Ethical Review Committee and carried out in accordance with the Animals (Scientific Procedures) Act 1986. Pregnant ewes were hysterectomised, and twenty six full term Scottish Blackface lambs were passed through a disinfectant tank while still in the uterus. Following resuscitation, bottle feeding was initiated and animals were separated into two equal groups. They were housed in different rooms under specific pathogen free (SPF) conditions. At six days old, the lambs were prepared for intratracheal inoculation by shaving the hair thoroughly from the xiphisternum to the mandible. Two people were required for adequate restraint. One clasped the animal almost vertically under the arm while extending the head back and clamping the front legs to the belly, and the second stabilised the rump of the lamb. 18 gauge short Intraflon intravenous (iv) cannulae were used to deliver the inoculate. The trachea was stabilised between the thumb and forefinger by the injector and punctured with the cannula in a downwards direction. The plunger of an attached empty syringe was drawn back to confirm correct location in the tracheal lumen by the presence of air, and then quickly replaced with one containing the inoculate. Air was drawn back once more before injecting the inoculum over a period of 5 seconds. Post injection, the mouth and nose were covered for a few seconds

to encourage a deep inhalation on release. In occasional animals, the cannula puncture was unsuccessful and a half inch 18 gauge needle was used for delivery of the inoculum instead.

2.1.3 Post mortem procedure

Figure 2.1 summarises the inoculation and post mortem examination (PME) procedure. In Group 1 all twelve animals received 4 ml of JSRV₂₁. In Group 2 six animals received 4 ml of mock inoculate (293T SN). In Group 3 eight were left untreated. Clinical behaviour was monitored closely at least twice daily. Euthanasia was performed at 3 (n = 8) and 10 (n = 8) days post inoculation (PI), and then when clinical signs became apparent between 72-91 days PI (n = 8).

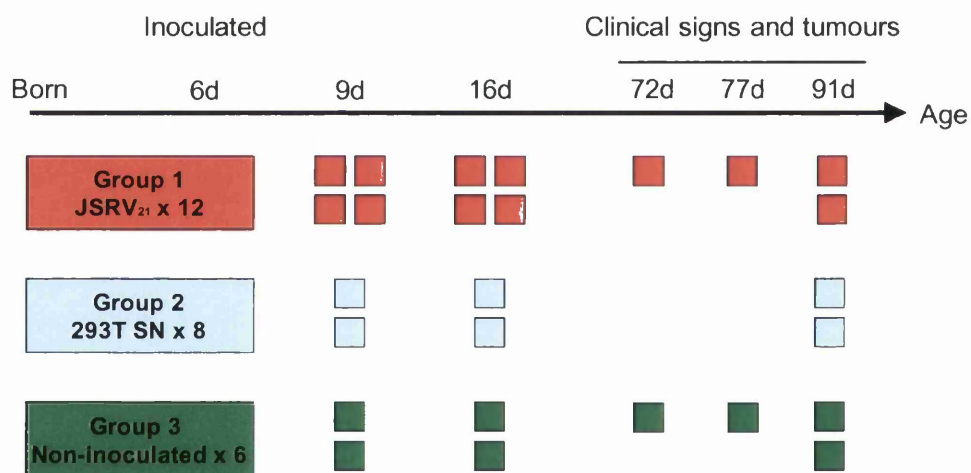


Figure 2.1 Chart showing timings of lamb inoculations and PME. Each coloured square represents a lamb PME. Red : lambs inoculated with JSRV₂₁. Blue: lambs inoculated with 293T. Green : lambs not inoculated. Groups 2 and 3 were negative control animals. d:lamb age in number of days.

2.1.3.1 Tissue sampling and fixation procedure

All lambs were euthanased by intravenous injection of barbiturate. The carcass was weighed, bled out and the pluck (heart and lungs) removed with the mediastinal lymph nodes attached. A photographic record was made for each animal (Figure 2.2, A-C). The procedure for tissue collection followed a fixed protocol and was carried out as quickly as possible to minimise post mortem artefact. Initially the lung was prepared using a sharp blade to section all lobes into thin segments about the horizontal axis (Figure 2.2 D). Tissue was then taken from 24 fixed sample sites (Figure 2.3). Four sequential tissue segments were taken from each of these locations in a cranial to caudal direction, trimmed, and placed in pre-labelled cassettes. These were immersed in formal saline (FS), zinc salts (ZS), paraformaldehyde (PF) and liquid nitrogen in that order. Additional samples from the mediastinal lymph node, mesenteric lymph node, liver (right lobe), spleen and kidney (right) were fixed in the same fashion. Fixation times and conditions were strictly adhered to and are shown in Table 2.1.

Table 2.1 Fixation procedure for all lung samples.

Fixative	Preparation	Procedure
4% buffered formalin (FS)	Prepared within last month	7 days fixation
4% paraformaldehyde (PF)	Prepared within last 12 hours and kept within 4°C	6 hours in fix, then re-trim and place in fresh solution for a total of 48 hours
Frozen (FZN)	Liquid nitrogen	Stored indefinitely in the -80°C freezer

2.1.3.2 Source of adult sheep with and without OPA

Adult animals showing clinical signs of OPA were collected from local farms. Twenty four such animals were examined and tissue was chosen from those with minimal secondary bacterial infection on gross inspection. Adult negative control animals were taken from MRI stock animals in which no case of OPA has been diagnosed in the previous 5 years.

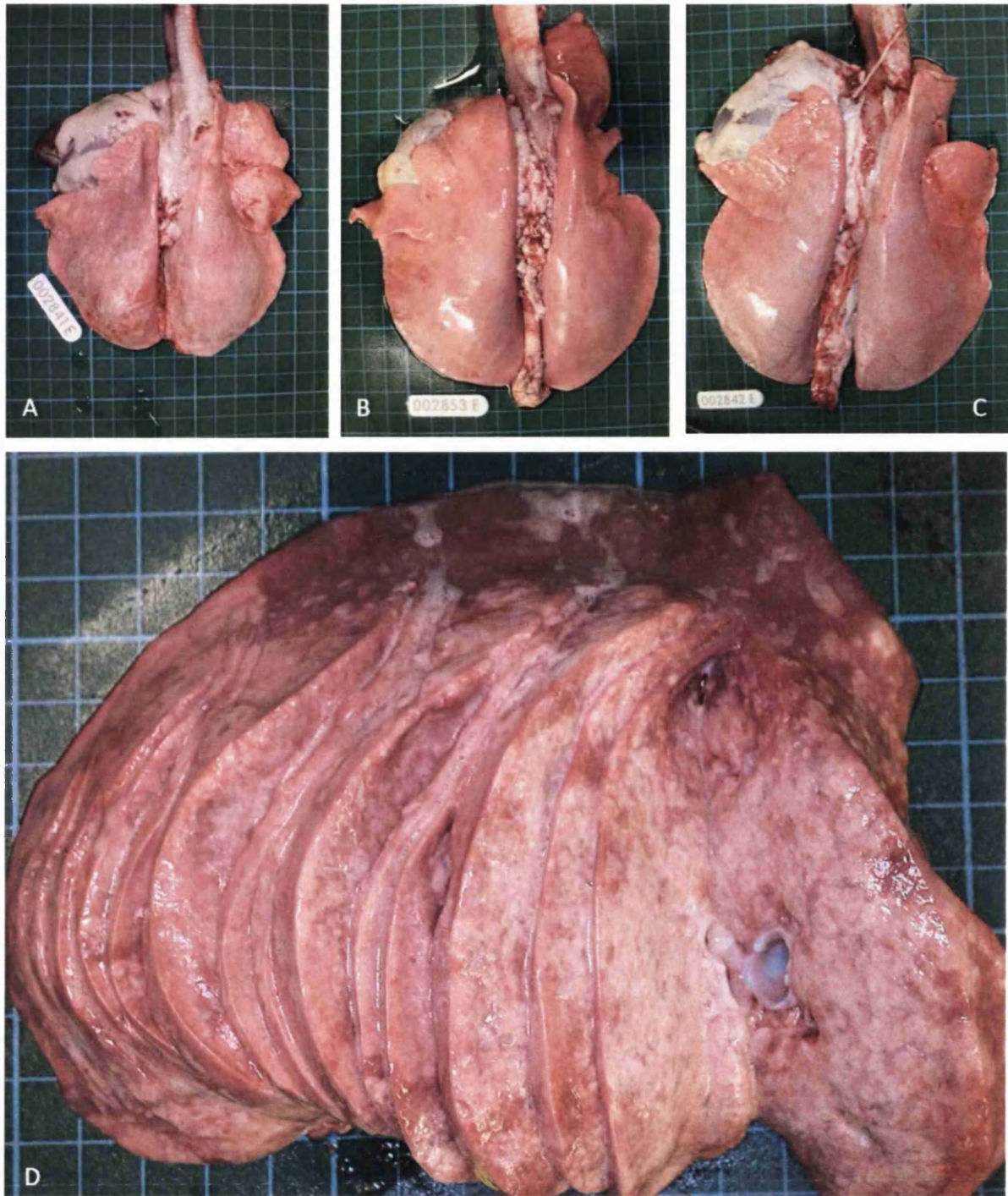
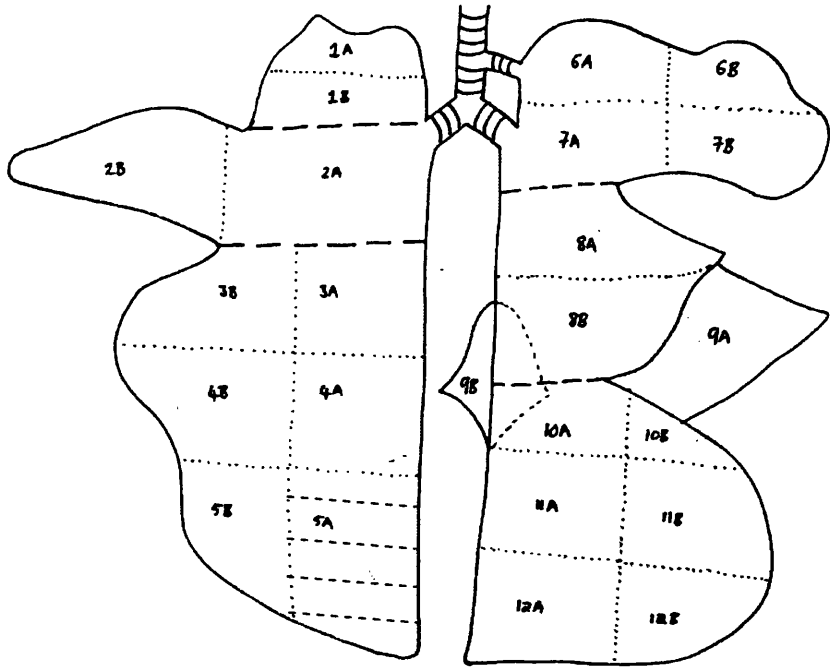


Figure 2.2 Photographic record of lungs from SPF lambs. (A) 2841E, group 1 infected lamb, 3 days PI. (B) 2853E group 2 mock infected lamb, 10 days PI. (C) 2842E group 3 control lamb, 72 days PI. (D) 2865E group 1 JSRV₂₁ inoculated lamb, 90 days PI.



Date	
Cont/Infect	
Eartag	
Casetle no	
Samples by	

TISSUE	Number	FS	ZS	PF	FZN
Left Apical	1A				
	1B				
Left Middle	2A				
	2B				
Left Diaphragmatic	3A				
	3B				
	4A				
	4B				
	5A				
	5B				
Mediastinal LN					
Ileal LN					
Liver					
Kidney R					
Spleen					
Tonsil					
Weight of left lung					

TISSUE	Number	FS	ZS	PF	FZN
Right Apical	6A				
	6B				
	7A				
	7B				
Right Cardiac	8A				
	8B				
Right Mediastinal	9A				
Accessory lobe	9B				
Right diaphragmatic	10A				
	10B				
	11A				
	11B				
	12A				
	12B				
Weight of lamb					
Weight of right lung					

Post mortem comments:

Figure 2.3 PME template for lung sampling. The red dotted lines represent orientation of tissue slices for fixation from each of the 24 sites.

2.2 Slide staining protocols

2.2.1 Histochemical techniques

2.2.1.1 Haematoxylin and eosin

Rehydrated sections were stained with Haematoxylin (H) stain (CellPath) for five minutes, washed well in running tap water and differentiated in 1% acid/alcohol for two seconds. Then they were washed in tap water and stained in 1% Eosin (E) stain (CellPath) for two minutes before washing in running tap water for two minutes, dehydrating and mounting. An automated staining machine, Shandon Varistain 24.4 (Thermo Scientific) was used for all sections stained with H and E.

2.2.1.2 Periodic acid Schiff technique

Rehydrated sections were incubated with periodic acid solution (BDH Chemicals) for five minutes then rinsed well in distilled water. They were then treated with Schiff's reagent (BDH Chemicals) for 30 minutes and washed in running tap water for 5-10 minutes. Nuclei were stained with Harris's haematoxylin solution for two minutes, rinsed with water, then immersed in Scott's Tap Water for one minute before washing in water again, dehydrating and mounting.

2.2.1.3 Luxol fast blue

Rehydrated sections were incubated at 71°C in Luxol fast blue (LFB) solution (BDH Chemicals) overnight. Slides were then rinsed in distilled water, differentiated in lithium carbonate (0.05%) (Hopkin and Williams) for 40 seconds and washed again in water. They were counterstained with 1% aqueous neutral red (BDH Chemicals) for five minutes, which was differentiated by pouring 80% ethanol over the slides, and finally washed in water before dehydration and mounting.

2.2.1.4 Grimelius silver method for argyrophil cells

Rehydrated sections were incubated in silver solution at 60 °C for three hours. The silver solution was drained from the slides before placing them in freshly prepared reducing solution at 45 °C for one minute. Sections were then rinsed in distilled water and examined under the microscope for the presence of black deposits. If these were not visible, the process was repeated by adding the slides to the silver solution for 5-10 minutes and then reducing them until the sections were well labelled. A green counterstain was used before washing the slides in tap water, dehydrating and mounting.

2.2.1.5 Mallory's phosphotungstic acid-haematoxylin (PTAH)

Rehydrated sections were treated with 0.25% aqueous potassium permanganate solution for five minutes before washing with water and bleaching with 5% aqueous oxalic acid solution. Then they were washed well in tap water, stained with PTAH (Cell Path Ltd.) solution for 12 hours at room temperature and washed in distilled water, before dehydrating and mounting in a DPX-type mountant.

2.2.2 Immunohistochemical techniques

2.2.2.1 Basic immunohistochemical protocol

Tissue sections were cut at 5 µm and placed on Superfrost Plus slides (Thermo Fisher Scientific). All sections were dewaxed in xylene and rehydrated through 100%, 75% and 50% ethanol to water. Antigen retrieval (AR) was performed at this point if necessary. Slides were then submerged in 3% (v/v) H₂O₂/methanol mix to block endogenous peroxidase activity for 20 minutes, and rinsed in running tap water for five minutes. Each slide was then taken individually, dried carefully with a paper tissue, and a Pap wax pen (ImmEdge Pen, Vector) was used to draw a continuous ring round the tissue sample. This area was then covered with 150 µl of 25% normal goat serum (NGS) (Vector) diluted with phosphate buffered saline/0.05% Tween 20 (PBST). Slides were incubated horizontally in a moisturising chamber for an hour at room temperature. The 25% NGS/PBST was replaced with primary antibody (diluted in 25% NGS/PBST) and incubated overnight at 4°C. Following this, individual slides

were rinsed with PBST three times, dried with paper tissue and incubated with the appropriate secondary antibody (goat anti-mouse/rabbit) for half an hour at room temperature. Sections were rinsed three times in PBST as before, and incubated with an appropriate antigen visualisation system.

2.2.2.2 Optimisation of primary antibodies

As few antibodies are specifically manufactured for use with sheep tissue, methods of validation and optimisation were necessary for each antigen labelled in each species. A summary of all conditions and dilutions trialled for each antibody is given in Table 2.3.

2.2.2.3 Positive and negative control tissue

Sections from known positive and negative tissue samples were required to validate the specificity of each antibody, and the non-specificity of the immune-labelling technique. Positive control tissues expressing the antigen under investigation proved the method and reagents were working. Sheep tissues were used when possible, but in some cases rabbit or mouse tissues were required. Negative controls included samples that were incubated with pre-immune/isotype matched/normal serum from the same species in which the primary antibody was raised. This allowed assessment of any non-specific binding or possible cross-reactivity between the tissue being examined and serum from the species which raised the primary antibody. In addition, the primary antibody was omitted to check for non-specific staining of the secondary antibody or the visualisation system. For multiple labelling techniques, primary antibodies were omitted from successive layers and substituted with 25% NGS/PBST or non-immune serum. The order of antigen detection was also reversed to ensure that antibodies were not masking each other.

2.2.2.4 Antigen retrieval

Tissue fixation processes often result in cross linking between antigens. AR techniques were required to break these down and improve antigen access for primary antibodies. Several methods were employed to ensure the best possible optimisation of antibodies in all experiments (Table 2.2). For heat induced epitope retrieval, rehydrated slides were placed in a

metal rack, fully immersed in one litre of sodium citrate / Tris Ethylenediaminetetraacetic Acid (EDTA) buffer, autoclaved at 121°C for 10 minutes and then left to cool to 50°C before blocking endogenous peroxidases. The pH of the buffer was varied from pH3-pH9. For enzyme induced epitope retrieval, 2 x 200 ml of distilled water was warmed in an incubator to 37°C and the slides were placed in one to warm up. 20 ml of frozen stock solutions of calcium chloride (1%) and trypsin (0.5%) were thawed, diluted in 160 ml of warmed water and adjusted to pH 7.8 with NaOH (1M). This solution was then reheated to 37°C in an incubator, and the slides were fully immersed in it for 5-20 minutes. They were then rinsed in running tap water before blocking endogenous peroxidases.

Table 2.2 Summary of antigen retrieval methods for IHC

Epitope retrieval	Buffer	Conditions
Heat induced	Sodium Citrate buffer (pH6)	Autoclave 121 degrees, 10 mins
Heat induced	Tris EDTA buffer (pH 3,6,9)	Autoclave 121 degree , 10 mins
Enzyme induced	0.1% Calcium chloride solution (pH7.8), Trypsin 0.05%, chymotrypsin 0.05%, Tris HCl	Incubator 37 degrees, 5-20 mins

Table 2.3 Summary of primary antibodies and optimisation conditions tested in this study. All antibodies were incubated overnight at 4°C

Cellular expression	Antibody	Antibody specificity, source animal and isotype	Dilution	Source	Fixation	Antigen retrieval	Positive control
JSRV infected cells	DJBH DJ01	Rabbit polyclonal anti-JSRV-CA	1/100-1/4000	MRI	FS	Heat citrate pH6 CaCl 0.1% trypsin	OPA-N lung
	DKPY DKOD	Rabbit polyclonal anti-JSRV-MA	1/100-1/4000	MRI	FS	Heat citrate pH6 CaCl 0.1% trypsin	
	JSRV p10	Rabbit polyclonal anti-JSRV-MA	1/1000	Prof. Massimo Palmarini	FS	Heat citrate pH6	
	405 F5 406 G9	Mouse monoclonal anti JSRV CA	1/10-1/100	MRI	FS	Heat citrate pH6	
	SU B3 +C9	Mouse monoclonal anti-JSRV SU IgG1	1/100-1/800	Dusty Miller	Cryostat ZS FS	Heat citrate pH6	
	Pancytokeratin (1-8, 10, 13, 14, 15, 16,19)	Mouse monoclonal anti-human CK IgG1 kappa	1/2000	DakoCytomation Clone AE1/AE3 M3515	FS	Heat citrate pH6	
Ciliated epithelial cells	beta tubulin	Mouse monoclonal anti- rat beta tubulin. IgM	1/100-1/40000	Abcam 40862 MC 3F3-G2	FS	Heat citrate pH6	Ovine lung
Type II pneumocytes	WRAB-SPC	Rabbit polyclonal anti-human N-terminal pro-SPC	1/100-1/20000	Gift from Jeffrey Whitsett R09337	FS, ZS	Citrate pH6	OPA-N lung Ovine lung
	DC-LAMP	Rat monoclonal anti-mouse DC-LAMP/CD 208 IgG2a	1/200	Dendritics Clone 10010E1.01	FS	Citrate pH6	
	SP-C	Rabbit polyclonal anti human pro- SP-C	1/1000	Chemicon AB 3786	FS	Citrate pH6	

Table 2.3 (cont) Summary of primary antibodies and optimisation conditions tested in this study

Cellular labelling	Antibody name	Antibody type	Dilution	Source	Fixation	Antigen retrieval	Positive control
Clara cells	WRAB-CCSP	Rabbit polyclonal anti-rat CCSP	1/200-1/20000	Severn Hills Bioreagents WRAB-CCSP	Cryostat, FS	None, Heat citrate pH 3,6 CaCl 0.1% trypsin Tris HCl 0.1% trypsin Tris HCl 0.05% trypsin/chymotrypsin	Ovine and rabbit lung
	GP-CCSP	Guinea pig polyclonal anti-CCSP	1/50-1/1000	Gift Jeffrey Whitsett	Cryostat, FS	Heat citrate pH 4,6,8 Tris EDTA pH9	
	CCSP	Rabbit polyclonal anti-bovine	1/200-1/20000	Prof Palmarini	FS	Heat citrate pH6	Ovine lung
	R41 -coupled to key-hole limpet haemocyanin	Rabbit polyclonal anti-mouse (synthetic 20-mer peptide)	1/100	Gift Jan Ryerse	FS	Tris HCl 0.1% trypsin	Mouse lung
NEBS	R42- coupled to tuberculin PPD	Rabbit polyclonal anti-mouse (synthetic 20-mer peptide)	1/500	Gift Jan Ryerse	FS	Tris HCl 0.1% trypsin	
	Chromogranin A	Rabbit polyclonal anti-human Chromogranin A	1/250-1/4000	DakoCytomation A0340	ZS FS	Heat citrate pH 6 Tris EDTA pH9	
	PGP 9.5	Mouse monoclonal anti-human PGP 9.5 IgG2a	1/10-1/40	Abcam 8189	FS	Citrate pH6	Ovine pancreas, intestine, cerebellum, lung
	Neurone specific enolase	Mouse anti-human NSE IgG1 kappa	1/100-1/3200	DakoCytomation	FS	Citrate pH6	
	Gastrin releasing peptide	Rabbit polyclonal anti 27 aa GRP (synthetic) IgG	1/100-1/4000	Abcam 22623	FS	Citrate pH6	
	Synaptophysin	Rabbit polyclonal anti human	1/25-1/100	Vector VPS284	FS	Citrate pH6	

Table 2.3 (cont) Summary of primary antibodies and optimisation conditions tested in this study

Cellular labelling	Antibody name	Antibody type	Dilution	Source	Fixation	Antigen retrieval	Positive control
Lung progenitor cells	CD133	Rabbit polyclonal anti-human (synthetic peptide)	1/200-1/1600	AB 19898	Cryostat ZS FS	Citrate pH6 Tris EDTA pH4,6,8 CaCl 0.1% trypsin	Ovine lung, OPA-N lung, MVV lung, pancreas, spleen, bone marrow, testis, liver tumour. Ovine fetal lung and liver. Mouse lung, bone marrow, testis, liver.
		Mouse monoclonal anti-human IgG1 kappa	1/10-1/800	BDP 550390	Cryostat ZS FS	Citrate pH6 CaCl 0.1% trypsin	
	Oct 3/4	Mouse monoclonal anti-human IgG2b	1/10-1/1000	Santa Cruz 5279	Cryostat ZS FS	Citrate pH6 CaCl 0.1% trypsin	
		Rabbit polyclonal anti-human (synthetic peptide)	1/10-1/1000	Abcam 19857	Cryostat ZS	None	
	Oct-4	Rabbit polyclonal anti-human (amino acids 1-140)	1/50-1/3200	AB18976	FS ZS	Citrate pH6 CaCl 0.1% trypsin	
	Proliferation marker	Ki-67	Mouse monoclonal anti-human (recombinant peptide 1002 bp Ki-67 cDNA fragment)	1/1000	DAKO M 7240 clone MIB-1	FS Cryostat	
IgG1 kappa							

2.2.3 Antigen visualisation systems

2.2.3.1 Indirect labelling techniques

Indirect labelling techniques were used to detect single antigens. Following incubation of the secondary antibody attached to horseradish peroxidase (HRP) enzyme with the section, antigens were visualized using the substrate chromogen 3,3'-diaminobenzidine (DAB). In the presence of HRP and H₂O₂, DAB is converted to an insoluble brown precipitate at the site of antigen expression. The supplied secondary antibody (Envision) has a long polymer backbone with multiple HRP molecules attached and so for each single antigen binding site, the visible signal is amplified.



Slides were incubated with DAB for 7 minutes, and then rinsed in water before staining with H and dehydrating on the automated machine.

A similar technique, the Tyramide Signal Amplification (TSA) kit (Molecular probes, Inc., Eugene, OR, USA) was used for single fluorescent labelling of antigen. In this case, the HRP enzyme activates a tyramide substrate which gives an amplified fluorescent signal. Alexa fluor® 488 and 568 – tyramide were used to detect the antigen, and a 4',6-diamidino-2-phenylindole (DAPI) counterstain was used to highlight cellular nuclei and as an anti-fade mountant (Prolong®Gold antifade reagent, Invitrogen).

2.2.3.2 Direct labelling techniques

In some experiments, fluorescence labelled fragment antigen-binding (Fab) fragments were used to detect antigen. This involved incubating the primary rabbit polyclonal antibody (anti-CCSP antibody) with a goat anti-rabbit Fab 649 fragment (Dylight™ 649-conjugated AffiniPure Fab Fragment, Jacksons Immunoresearch) at a 1:2 ratio for 5 minutes in the dark at room temperature. This solution was then mixed with 10% NRS (MRI) to bind to any free Fab, and the solution incubated in the dark for a further 10 minutes. Following this, the mixture was centrifuged for 10 minutes at 14 000 x g and then 150 µl was pipetted onto the

horizontal slide prior to overnight incubation at 4⁰C. Slides were washed three times in PBS before mounting and examining with the appropriate filter set.

2.2.3.3 Multiple labelling techniques

Combinations of these techniques were employed to label multiple antigens in one section. For double labelling using the indirect technique antibodies raised in different animals were used, e.g. mouse monoclonal and rabbit polyclonal antibodies. The experiment followed the same procedure as detailed previously for the first primary antibody, and was then repeated on the same slide for the second primary antibody. Conditions were re-optimised to determine in which order to use the antibodies and whether their concentrations required altering. Antigen visualisation was achieved using a combination of the chromogens DAB and VECTOR® VIP, or Tyramide Alexa Fluor 488 and Tyramide Alexa Fluor 568.

Triple labelling combined both direct and indirect techniques. Initially double labelling was performed as detailed above. Then the section was incubated overnight with CCSP antibody labelled with Fab 649 before rinsing and mounting.

2.2.3.4 Image acquisition and analysis

Images for bright field microscope were examined using an Olympus BX51 microscope and photographs were captured with an Olympus DP70 camera with analysis software. The fluorescent microscope was a Zeiss Axiovert 200M. Z stacking facilities and apotomes were used when necessary.

2.2.4 IHC quantification

Areas of DAB labelling for all antibodies were quantified using the deconvolution macro in Image J. This is a Java-based image processing programme developed at the National Institute of Health (Rasband W, 1997-2009). The colour deconvolution plug-in implements stain separation using the Ruifrok and Johnston method (Ruifrok and Johnston, 2001).

2.2.4.1 Beta tubulin

One sample site, 5a, was examined from each animal. From this section, the epithelium of four separate cross/longitudinal sections of each anatomical region (bronchus, bronchiole, terminal bronchiole, respiratory bronchiole) was outlined and an area measurement made. The percentage of this area that labelled positively for beta tubulin antibody was then calculated (Figure 2.4).

2.2.4.2 Clara cell secretory protein

Two sample sites, 1b and 5a, were examined from each animal. From both of these sections, the epithelium of four separate cross/longitudinal sections of each anatomical region (bronchus, bronchiole, terminal bronchiole, respiratory bronchiole) were outlined and an area measurement made. The percentage of this area that labelled positively for CCSP was then calculated.

2.2.4.3 Surfactant protein C

Type II pneumocytes were identified as cells in the alveolar region which labelled positively with SP-C. Images of six fields from the alveolar region of one section per animal were taken at x 400 magnification. Over 100 cells were examined per field. The number of cells labelling positively for SP-C were given as a percentage of the total number of nuclei counted in all fields.

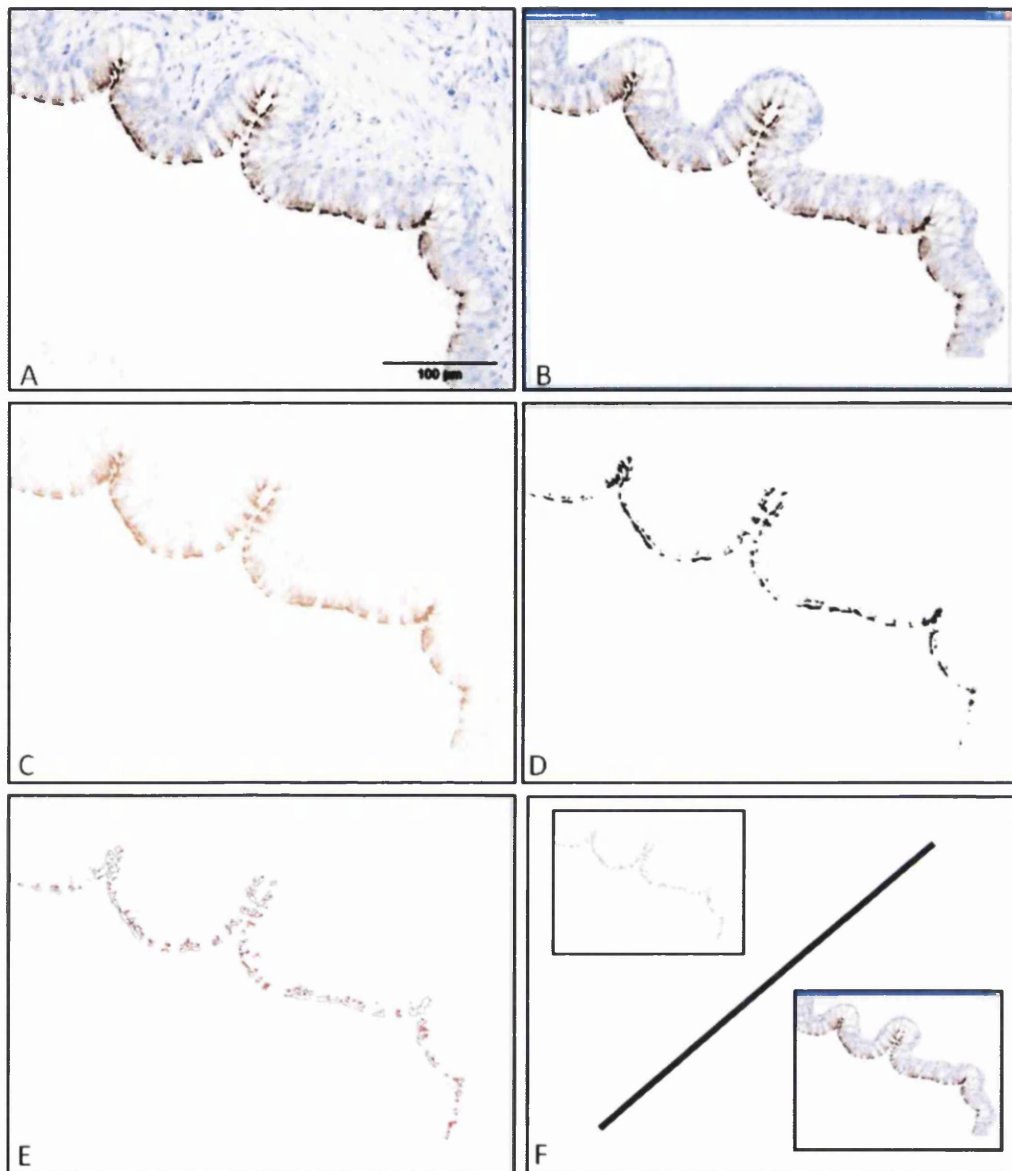


Figure 2.4 Image J measures area of IHC labelling. (A) Area for measuring is photographed with scale bar. (B) The epithelial region is isolated and the area measured. (C) The image is deconvoluted. (D) The area positive for IHC labelling only is isolated. (E) A total measurement for area of positive IHC is calculated by Image J. (F) The area of positive labelling is calculated as a percentage of the total epithelium.

2.2.4.4 Neuroepithelial bodies

Two sections per animal (1b and 5a) were examined for the presence of NEBs. Photographs were taken of the fixed tissue, and the gross area measured using Image J. The total number of NEBs labelling positively with synaptophysin antibody per whole section were identified microscopically. A final figure was given as the average number of NEB per cm^2 per animal.

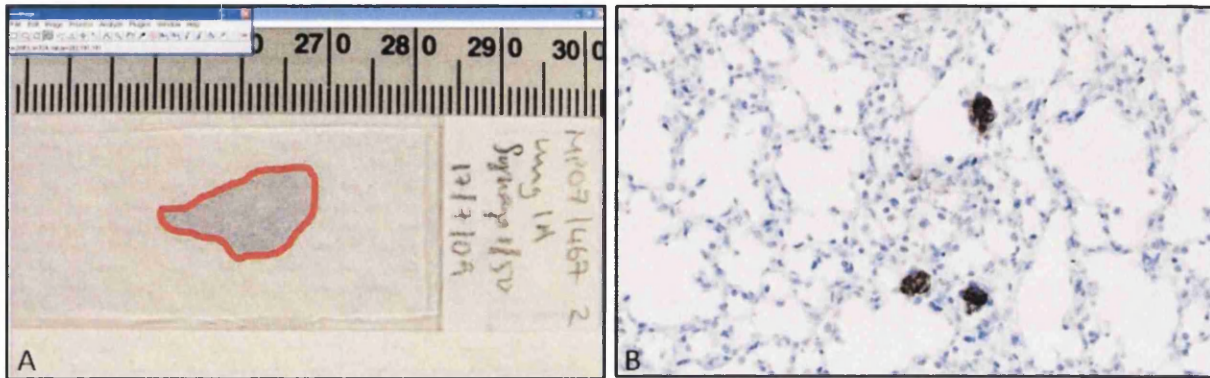


Figure 2.5 NEB number calculation. (A) The total surface area of fixed tissue was measured using Image J. (B) IHC anti-synaptophysin antibody, the total number of NEBS per cm^2 of tissue were calculated.

2.2.4.5 Ki-67, a proliferation marker

An antibody to Ki-67 was used to label the nuclei of all cells that were not in the G0 resting phase of the cell cycle, i.e., those that were proliferating. For each section examined (2-5 locations per animal), the lung was divided into five anatomical regions: bronchus, bronchiole, terminal bronchiole, respiratory bronchiole and alveolus. A total of 800 cells were counted per region per slide, and the percentage of these that labelled positively for Ki-67 was given as the proliferation index for that anatomical region (Figure 2.6). The mean per animal was calculated.

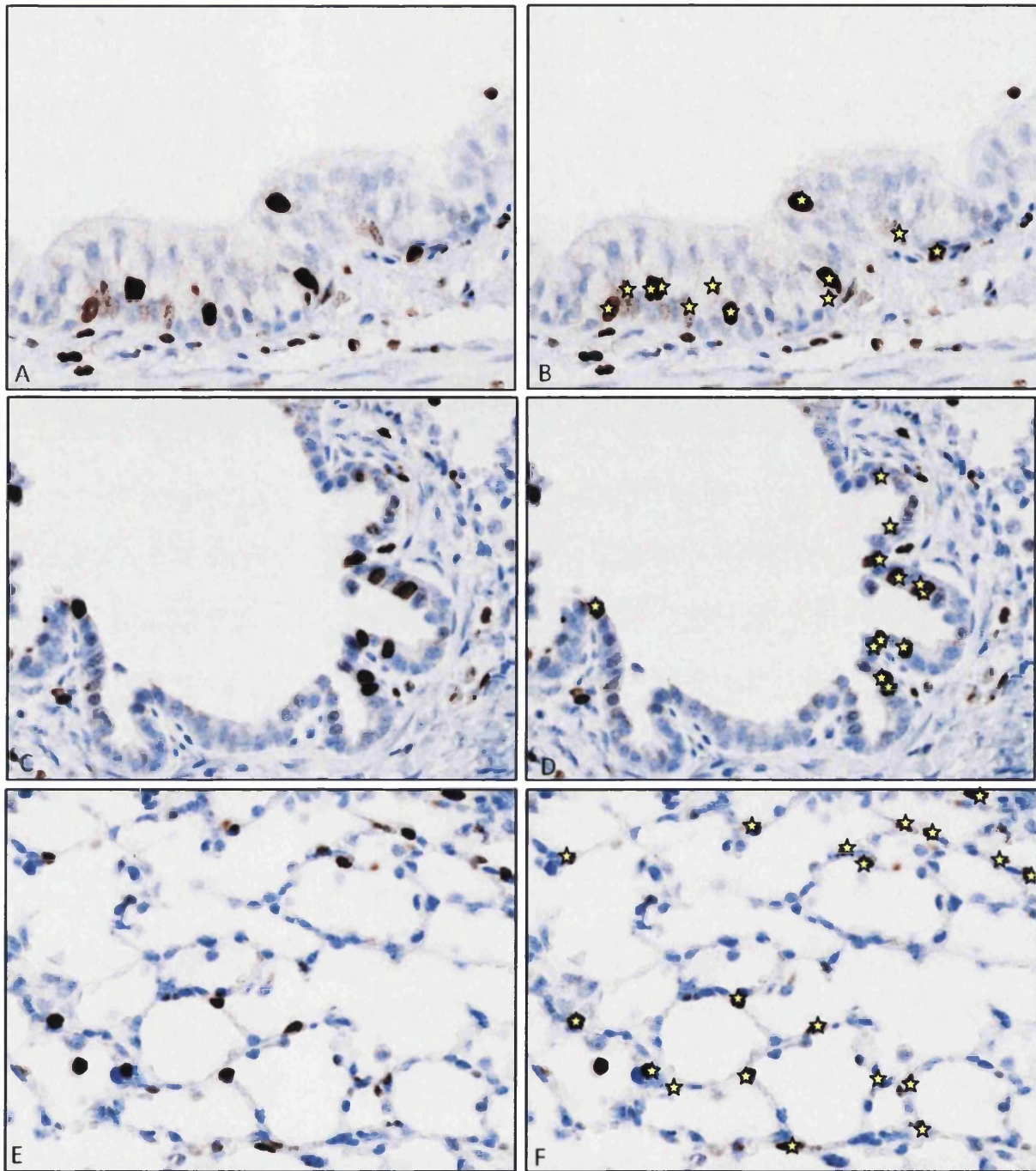


Figure 2.6 Procedure for calculating proliferative index. (A), (C), (E): all nuclei were counted. (B), (D), (F) all Ki 67 positive nuclei were counted (brown labelling, marked with yellow stars). Proliferative index is the percentage of the total number of nuclei counted that are positive for Ki 67. (A) Bronchial epithelium, total nuclei = 94. (B) Bronchial epithelium, total Ki67 +ve = 12. Proliferation index = 13%. (C) Bronchiolar epithelium total nuclei =100. (D) Bronchiolar epithelium, total Ki 67 +ve =12. Proliferation index = 12% (E) Alveolar region : total nuclei =163, (F) Alveolar region, total Ki 67+ve =19. Proliferation = 12%.

2.3 Quantitative reverse transcriptase polymerase chain reaction

2.3.1 Preparation of samples for RNA extraction

2.3.1.1 Experimental samples

Samples were taken from JSRV₂₁ infected and control animals as detailed in section 2.1 of this chapter. Four adult sheep with OPA and four without were also sampled in the same way. Tissues were placed in labelled plastic histological tissue sample cassettes, immediately immersed into liquid nitrogen and stored at -80 °C prior to analysis. When required, tissues were transported on dry ice to the cryostat machine (Thermo Scientific) and placed in the cutting chamber for 10 minutes for acclimatisation (chamber temperature: -22°C, specimen -16°C and cryobar -22°C). The machine had been thoroughly cleaned and fumigated prior to use and a fresh blade was used for each case. For the purposes of this study, only tissues from sites 1a, 1b, 2a, 2b and 5a in the lung and the mediastinal lymph nodes were examined. Each block of tissue was glued to the chuck using Optimal Cutting Temperature (OCT) compound (Bright Cryo-M-Bed, Embedding compound, Bright Instrument Company Ltd.) and trimmed until the cut surface was parallel to the blade. Between 5-10 cryostat sections of 20-40 µm thick slices of tissue were collected depending on the cellular density of the tissue.

2.3.1.2 Positive control samples

Positive controls for cytokine primer analysis were obtained from several sources. Concanavalin A (Con A) stimulated peripheral blood mononuclear cells (PBMCs) were a source of IFN gamma, TGF beta, IL-1Beta, IL-2, IL-4, IL-10, IL-18 and MCP-1. Plasmid DNA constructs were available for IL-8, TGF beta and IL-6 (McNeilly et al., 2008) and transfected Chinese Hamster Ovary cell lines expressed ovine IL-8, ovine TNF alpha and ovine GM-CSF (kindly gifted by Sean Wattedgera).

PBMCs were extracted from venous blood samples collected into 10 ml heparin tubes from healthy sheep. Each blood sample was transferred into a 50 ml tube with equal volumes of cold PBS, mixed and centrifuged at 623 x g for 20 minutes at 4°C with the brake off. The resultant buffy coat layer which collected on top of the red blood cells was aspirated using a

10ml pipette and transferred to a universal container with 7 ml of wash buffer. Any clots were broken up by pipetting the solution against the side of the universal. This solution was then layered onto 10 ml of prewarmed Lymphoprep™ (Axis-Shield) and centrifuged at 1107 x g for 30 minutes with the brake off. This produced an interface layer of the mononuclear cells which was transferred into a tube containing 5 ml of wash buffer. Cell clumps were disrupted, and wash buffer added to bring the volume up to 30 ml. This suspension was centrifuged at 276 x g for 10 minutes with the brake off. A cell pellet was formed which was resuspended and washed twice with 10 ml of RPMI (Roswell Park Institute medium) 1640 and again centrifuged at 276 x g for 10 minutes at 4°C. The pellet was resuspended in 2 ml of RPMI 1640, followed by a further 8 ml before introducing the suspension in to a flask. 50 µl of Con A was added to half of the samples, and then all were placed in an incubator at 37°C overnight. 12-15 hours later, the flasks treated with Con A were examined under the microscope to check for activation and PBMC by raft formation. All 10 ml of media with cells was removed from each flask, placed in a universal tube and centrifuged at 376 x g for 6 minutes. The supernatant was discarded, and the pellet resuspended in 10 ml of RPMI and centrifuged as before. This process was repeated twice before resuspending the pellet in 5 ml of RPMI. The concentration of cells was estimated by adding 90 µl of trypan blue to 10 µl of cell suspension and transferring this to a haemocytometer for counting. The solution was diluted to 1×10^7 PBMC prior to RNA extraction.

Chinese Hamster Ovary (CHO) cell lines stably expressing ovine cytokines were taken from liquid nitrogen and defrosted. The solution was placed in a chilled universal tube, and 9ml of cold culture medium slowly added. This was centrifuged at 4°C for 10 minutes at 276 x g. The culture medium was discarded and the cell pellet loosened by flicking the tube.

2.3.1.3 RNA extraction and purification

RNA extraction was performed on all samples using a commercially available kit (RNeasy mini kit, Qiagen) according to the manufacturer's instructions. Cryostats were immediately placed in Ribolyser tubes (Lysing Matrix D MP Bio) containing 800 µl of Buffer RLT (RNeasy kit) and beta mercaptoethanol. These tubes were shaken manually to ensure all tissue was covered by fluid and then stored on ice (maximum 1 ½ hours) until all the tissue from the

same animal was collected. Samples were then rotated in a ribolyser for 40 seconds and placed in a chilled centrifuge for three minutes at 12 000 x g. The lysate was removed from the beads and mixed with equal volumes of 70% ethanol in a 1.5 ml tube. 700 µl of this was pipetted onto an RNeasy column and centrifuged for 15 seconds at 10 000 x g. The filtrate was discarded and the remaining amount filtered in the same way. 350 µl of RW1 was filtered through the column by centrifuge (15 seconds at 10 000 x g), and then DNase digest (RNase-Free DNase Set, Qiagen) was pipetted onto the column and left for fifteen minutes at room temperature. Another wash with 350 µl of RW1 was followed by 500 µl of RPE for 15 seconds at 10 000 x g, and then 500 µl for 2 minutes at 10 000 x g. Then the tubes were spun into an empty eppendorf at full speed to remove excess ethanol. Finally, 50 µl and then 30 µl of RNase free water were centrifuged through the membrane in turn, and the filtrate placed on ice before long term storage in -80°C freezer.

Cell pellets were resuspended in 600 µl of buffer RLT and beta mercaptoethanol and thoroughly mixed. The solution was homogenized with a 20 gauge needle attached to a 5 ml syringe before adding one volume of 70% ethanol and mixing. 700 µl of this was transferred to an RNeasy spin column which was placed on a 2 ml collection tube and centrifuged for 15 seconds at 9000 x g. This step was repeated with any residual sample. The remaining procedure is identical to that for RNA extraction from tissue detailed in the section above.

2.3.1.4 RNA validation analysis

A small aliquot of all samples was analysed by the Nanodrop machine. This uses the absorption of UV radiation at 260 nm to determine the concentration of nucleic acid in a sample. The ratio of sample absorbance at 260 and 280 indicates the purity of RNA with a ratio of about 2 being accepted as pure for RNA. The Agilent 2100 bioanalyser was also used to obtain an RNA integrity number (RIN) for the sample. It estimates the integrity of total RNA samples by microcapillary electrophoretic RNA separation. This integrity is determined by the entire electrophoretic trace of the RNA sample, which includes the presence or absence of degradation products. Only those with a RIN above 8 were accepted. The stock RNA was diluted to 50 ng/µl and stored at -80°C until required.

All these processes aimed to maximise RNA yield and purity, so eliminating unwanted changes in the gene expression profile. Specific steps which ensure this are summarized in Table 2.5.

Table 2.4 Twelve steps taken to maximise RNA yield and purity from tissue samples

	Action	Effect
1	Environment preparation	RNAase ZAP all surfaces and equipment
2	Tissue preparation and handling	Immediate freezing and never let tissue samples thaw. Handle with gloves or sterile forceps. Process negative control tissues first, then mock and finally infected ones.
3	Cryostat machine	Cleaned and fumigated before use. Use a fresh blade for each animal.
4	Sample size	Under 30mg of tissue so as not to overload RNeasy column
5	Ribolyser beads	These simultaneously disrupt and homogenize tissue to maximise RNA release and reduce lysate homogeneity which increases column binding efficiency
6	Buffer RLT	Contains guanidine thiocyanate which inactivates RNases
7	Beta mercaptoethanol	Denature RNases
8	Ethanol	Promotes selective binding of RNA to RNeasy column
9	Silica based membrane on column	Removes DNA. Binds RNA over 200 nucleotides long, enriching mRNA quantity and eliminating shorter contaminants
10	On column DNA digestion	Eliminates DNA contamination from sample
11	Nanodrop	260/280 identifies contaminants
12	Agilent	RIN number indicates integrity of the sample

2.3.2 qRTPCR procedure

Quantification of virus and cytokine expression was determined using qRTPCR. Primers and probes for reference and target genes were selected from published literature Table 2.6 (Budhia et al., 2006; Garcia-Crespo et al., 2005; Harrington et al., 2006; Li et al., 2008; Palmarini et al., 1996). qRTPCR was performed using the ABI 7000 in 96 well plates (Applied Biosystems) with either Power SYBR® Green RNA-to C_T[™] *1-Step* Kit (Applied Biosystems) or TaqMan® one step RTPCR Master mix reagents kit (Applied Biosystems). All samples were run in duplicate with 100 ng of RNA in a 20 µl final reaction volume. Amplification conditions were 30 minutes (min) at 48°C for reverse transcription, 10 min at 95°C to activate the DNA polymerase and 40 cycles of 15 seconds (s) at 95°C (denature) and 1 min at 60°C (anneal and extend) unless otherwise stated. All SYBR runs included a melt curve to confirm the specificity of the amplicons (95°C for 15 s, 60°C for 20s and 95°C for 15s).

2.3.2.1 Primer and Taqman probe optimisation

Standard curves constructed from 10 fold serial dilutions of positive control mRNA were used to determine the primer set efficiency and replicate quality (R²). In some cases, further optimisation was necessary as the required efficiency of 70-110% with an R² value of 0.99 was not achieved with the published conditions. This involved altering primer concentrations, reaction conditions, reagents and occasionally primer sequences. In addition, it was ensured that the level of gene expression in experimental samples lay within the limits of the standard curve. Some examples of the optimisation process are given in Figure 2.7. Table 2.6 lists the final sequences and conditions used for each gene.

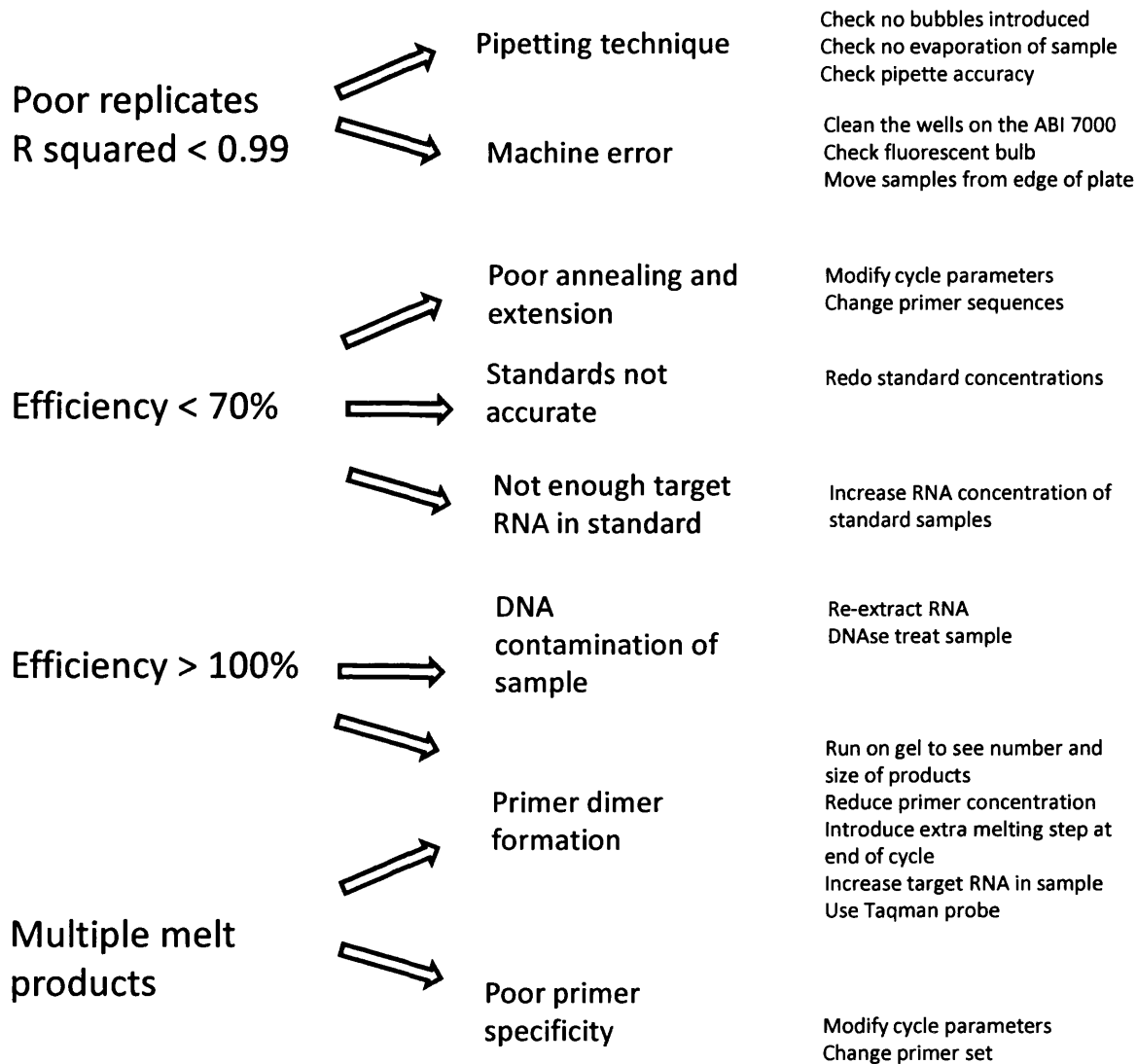


Figure 2.7 Methods for optimisation of primers and probes using the standard curve

2.3.2.2 Selection of optimal Reference genes

In order to obtain accurate gene expression measurements for target genes, stable reference genes for data normalisation were required. Primer sequences for five common reference genes were selected from published data (Table 2.6). Genes were chosen from different functional and abundance classes in order to avoid co-regulation. qRT-PCR was used to obtain crossing threshold (C_T) values for each gene in six samples of lung and lymph node tissue from normal and infected sheep. The stability in expression for each reference gene between normal/diseased tissue was determined using the programme geNorm. For each reference gene, this calculates the pairwise variation with all other reference genes as the standard deviation of the logarithmic transformed expression ratios. A reference gene stability value, the M value, can then be determined. The two reference genes with the lowest M value for each tissue were chosen for use in future experiments.

2.3.2.3 qRT-PCR procedure for analysis of JSRV and cytokine expression

Expression of virus and cytokines were compared between four infected, two mock infected and two control animals at three time points following experimental infection with JSRV₂₁. A group of eight adult animals with and without OPA were also examined. qRT-PCR of all lung samples for each gene of interest at a single time point was performed in a single 96-well plate. These contained replicate samples of RNA from five fixed sites in the lung per animal (80 wells), 10 fold serial dilutions of positive control mRNA (12 wells) and a water negative control (2 wells). The reaction efficiency (E) was calculated from the slope of the standard curve and incorporated into the final equation for relative quantitation of each gene of interest.

$$E = 10^{-1/\text{slope}}$$

2.3.2.4 Relative quantification of gene expression

The Pfaffl method was employed to quantify cytokine expression levels (Pfaffl et al 2002). This measures the relative change in mRNA expression levels between infected and control animals whilst taking into account the efficiencies of both reference and target genes. Two housekeeping genes (see section 4.5.6) were used to normalize data and control for experimental error. The relative expression software tool REST was used to analyse the data using the following equation:

$$\text{Ratio} = \frac{(\text{Efficiency GOI})^{\Delta C_T \text{ GOI (control-infected)}}}{(\text{Efficiency HKG})^{\Delta C_T \text{ HKG (control-infected)}}$$

The programme also provides a statistical test of the analysed C_T values using a *Pair-Wise Fixed Reallocation Randomisation Test*© (Pfaffl et al 2002). This test calculates the effect on expression ratio of randomly reallocating C_T values to the control or infected group. This is done over 2000 times, so providing a good estimate of P value (standard error < 0.005 at P=0.05).

Table 2.5 Details of primers selected for reference genes for GeNorm analysis

Gene	Accession numbers	Primers	Amplicon size (bp)	Primer conc nM	Reference
ACT B	NM_001009784	f- CTG AGC GCA AGT ACT CCG TGT r – GCA TTT GCG GTG GAC GAT	125	300 300	(Garcia-crespo et al., 2006)
SDHA	NM_AY970969 bases 1-90 part cds	f- CAT CCA CTA CAT GAC GGA GCA r- ATC TTG CCA TCT TCA GTT CTG CTA	90	200 200	(Garcia-crespo et al., 2006)
YWHAZ	AY970970 bases 1-102 part cd	f- TGT AGG AGC CCG TAG GTC ATC T r- TTC TCT CTG TAT TCT CGA GCC ATC T	102	100 100	(Garcia-crespo et al., 2006)
Beta 2 MCG	NM_001009284	f- AGA CAC CCG CCA GAA GAT GG r – TCC CCG TTC TTC AGC AAA TC	98	900 900	(Harrington et al., 2006)
GAPDH	AF 030943/AF035421	f- GCA TCG TGG AGG GAC TTA TGA r- GCC ATC ACG CCA	92	900 900	(Chris Cousens, MRI)

Table 2.6 Primers and probes for qRTPCR analysis of candidate genes

Gene	Accession numbers	Primers	Tm (°C)	Amplicon size	Reference
IFN gamma	X 52640	f- TTC TTG AAC GGC AGC TCT GAG r- TGG CGA CAG GTC ATT CAT CA	59.8 57.3	127	(Budhia et al., 2006)
GM-CSF	NM_001009805	f- GAT GGA TGA AAC AGT AGA AGT CG r- CAG CAG TCA AAG GGA ATG AT	58.9 55.3	261	(McNeilly et al., 2008)
IL-8	S74436	f- CAC TGC GAA AAT TCA GAA ATC ATT GTT A r- CTT CAA AAA TGC CTG CAC AAC CTT C	59.3 61.3	53	(Leutenegger et al., 2000)
TGF-beta	NM_001009400	f- GAA CTG CTG TGT TCG TCA GC r- GGT TGT GCT GGT TGT ACA GG	59.4 59.4	169	(McNeilly et al., 2008)
TNF alpha	NM_001024860	f- GCC CTG GTA CGA ACC CAT CTA r- CGG CAG GTT GAT CTC AGC AC	61.8 61.4	82	(Li et al., 2008)
IL-6	NM_001009392	f- TCC AGA ACG AGT TTG AGG r- CAT CCG AAT AGC TCT CAG	53.7 53.7	236	(McNeilly et al., 2008)
IL-2	NM_001009806	f- TGA AAG AAG TGA AGT CAT TGC TGC r- GAT GTT TCA ATT CTG TAG CGT TAA CC	59.3 60.1	138	(Li et al., 2008)
IL-4	NM_001009313	f- ACC TGT TCT GTG AAT GAA GCC AA r- CCC TCA TAA TAG TCT TTA GCC TTT CC	58.9 61.6	79	(Li et al., 2008)
IL-10	NM_001009327	f- AGC AAG GCG GTG GAG CAG r- GAT GAA GAT GTC AAA CTC ACT CAT GG	60.5 61.6	90	(Li et al., 2008)
IL-18	NM_001009263	f- ACT GTT CAG ATA ATG CAC CCC AG r- TTC TTA CAC TGC ACA GAG ATG GTT AC	60.6 61.6	100	(Li et al., 2008)
MCP-1	Predicted sequence in Dunphy	f- GCT GTG ATT TTC AAG ACC ATC CT r- GGC GTC CTG GAC CCA TT Probe AAA GAG TTT TGT GCA GAC CCC AAC C	58.9 57.6 63	-	(Dunphy et al., 2001; Kawashima et al., 2006)
IFN alpha	AY 802984	f- GCA CTG GAT CAG CAG CTC ACT G r- CTC AAG ACT TCT GCT CTG ACA ACC T	64 63	188	(Li et al., 2008)
IL-1 B	NM_001009465	f-CCT AAC TGG TAC ATC AGC ACT TCT CA r- TCC ATT CTG AAG TCA GTT ATA TCC TG	63.2 60.1	95	(Li et al., 2008)
IDO	NM_001141953	f- CAG AAG GCA CTG CTT GAC ATA TCT r- GGT TTG GGT CCA CAT ATT CAT GA	61 58.9	-	(Sean Wattegedera, MRI)
ACT B	NM_001009784	f- CTG AGC GCA AGT ACT CCG TGT r – GCA TTT GCG GTG GAC GAT	61.8 56	125	Garcia-crespo et al 2006
SDHA	NM_AY970969 bases 1-90 part cds	f- CAT CCA CTA CAT GAC GGA GCA r- ATC TTG CCA TCT TCA GTT CTG CTA	59.8 59.3	90	Garcia-crespo et al 2006
YWHAZ	AY970970 bases 1-102 part cd	f- TGT AGG AGC CCG TAG GTC ATC T r- TTC TCT CTG TAT TCT CGA GCC ATC T	62.1 61.3	102	Garcia-crespo et al 2006
Beta 2 MCG	NM_001009284	f- AGA CAC CCG CCA GAA GAT GG r – TCC CCG TTC TTC AGC AAA TC	61.4 57.3	98	Harrington et al 2006
GAPDH	AF 030943/AF035421	f- GCA TCG TGG AGG GAC TTA TGA r- GCC ATC ACG CCA	-	92	Chris Cousens MRI

Table 2.7 Reaction conditions for primers and probes. TCHO – transfected chinese hamster ovary cell lines

Gene	+ve control	Primer/ probe concentrations	Reaction conditions	Dissociation melting temp °C	R ²	Efficiency
IFN gamma	PBMC + Con A	f 300nM r 300nM	30 min 45°C, 10 min 95°C, (15s 95°C, 1 min 60 °C) x40	79	0.99	-3.15
GM-CSF	TCHO	f 500nM r 500nM	30 min 45°C, 10 min 95°C, (20s 94°C, 30s 57°C, 30s 72°C) x40	85.8	0.99	-3.4
IL-8	Plasmid DNA TCHO	f 500nM r 500nM	30 min 45°C, 10 min 95°C, (20s 94°C, 30s 55°C, 30s 72°C) x40	76.8/77.3	0.99	-3.9
TGF-beta	Plasmid DNA PBMC + Con A	f 500nM r 500nM	30 min 45°C, 10 min 95°C, (20s 94°C, 30s 55°C, 30s 72°C) x40	83.6	0.99	-3.1
TNF alpha	TCHO	f 200nM r 200nM	30 min 45°C, 10 min 95°C, (15s 95°C, 1 min 60 °C) x40	80.3	0.99	-3.4
IL-6	Plasmid DNA PBMC + Con A	f 500nM r 500nM	30 min 45°C, 10 min 95°C, (20s 94°C, 30s 52°C, 30s 72°C) x40	80	0.98	-3.7
IL-2	PBMC + Con A	f 200nM r 200nM	30 min 45°C, 10 min 95°C, (15s 95°C, 1 min 60 °C) x40	76.4	0.99	-3.5
IL-4	PBMC + Con A	f 200nM r 200nM	30 min 45°C, 10 min 95°C, (15s 95°C, 1 min 60 °C) x40	76	0.99	-3.6
IL-10	PBMC + Con A	f 200nM r 200nM	30 min 45°C, 10 min 95°C, (15s 95°C, 1 min 60 °C) x40	77.7	0.99	-2.9
IL-18	PBMC + Con A	f 200nM r 200nM	30 min 45°C, 10 min 95°C, (15s 95°C, 1 min 60 °C) x40	75	0.99	-3.7
MCP-1	PBMC + Con A	f 900nM r 400nM Probe 900nM	30 min 45°C, 10 min 95°C, (20s 95°C, 30s 58°C, 30s 60°C) x40	NA	0.99	-3.7
IFN alpha	PBMC + Con A	f 200nM r 200nM	30 min 45°C, 10 min 95°C, (15s 95°C, 1 min 60 °C) x40	-	-	-
IL-1 B	PBMC + Con A	f 200nM r 200nM	30 min 45°C, 10 min 95°C, (15s 95°C, 1 min 60 °C) x40		0.99	-4.1
IDO	Plasmid DNA	f 900nM r 900nM	30 min 45°C, 10 min 95°C, (15s 95°C, 1 min 60 °C) x40	76.5	0.99	-4.7
SDHA	Reference gene	f 200nM r 200nM	30 min 45°C, 10 min 95°C, (15s 95°C, 1 min 60 °C) x40	81	0.99	-3.15
ACT B	Reference gene	f 300nM r 300nM	30 min 45°C, 10 min 95°C, (15s 95°C, 1 min 60 °C) x40	84.3	0.99	-3.3
YWHAZ	Reference gene	f 100nM r 100nM	30 min 45°C, 10 min 95°C, (15s 95°C, 1 min 60 °C) x40	78.8	0.99	-3.2

CHAPTER 3 IMMUNOHISTOCHEMICAL ANALYSIS OF THE OVINE LUNG DURING POSTNATAL DEVELOPMENT

3.1 Introduction

During evolution the structure of the lung has developed to fulfil the specific requirements of each species. Subsequently, variations can be seen between mammals in the level of maturity of the lung at birth and the intricate anatomy in adulthood (Warburton et al., 2000). Early descriptions of lung anatomy date back to the 15th Century, and it is testament to its complex nature that we are still puzzling over details 500 years later. Popular areas of current research include lung morphogenesis studies to identify regulatory transcription factors, and injury models to analyse repair mechanisms and the role of progenitor cells (Stripp et al., 1995; Warburton et al., 2000). Much of this research is performed in mice and it is reliant on the availability of a robust panel of antibodies with which to identify specific cell types using immunohistochemical techniques (Dave et al., 2008; Lange et al., 2009).

A sound knowledge of the working anatomy in the lung is essential if lung development and the pathogenesis of respiratory disease are to be properly understood. Postnatal maturation is a critical stage of lung development. At this time cells are still differentiating and proliferating, and there is an increased vulnerability of the organ to injury from infectious or noxious insults (Castleman, 1984; Castleman and Lay, 1990; Fanucchi et al., 1997a; Plopper et al., 1994; Smiley-Jewell et al., 1998). In the sheep, there is no comprehensive account of lung cellular anatomy during this period. This is in part due to a lack of antibodies to identify specific cell types.

The studies described in this chapter aimed to characterise the postnatal development of the ovine lung using IHC to see how epithelial cell differentiation, distribution and proliferation varied between anatomical regions of the lung and different ages of lamb. Following optimisation of a panel of antibodies to identify specific epithelial cells, the results provided valuable information on the anatomy of the maturing lung. In addition, techniques developed were applied in subsequent chapters to increase our knowledge of the pathogenesis of OPA in the sheep lung.

3.2 Results

Lung tissue for histological analysis was taken from 6 SPF lambs aged 9, 16 and 91 days. Two animals were euthanased at each time point and a fixed post mortem procedure was followed (see section 2.4). Tissues were sampled from 24 sites per lung, immediately placed in labelled cassettes and fixed in buffered formalin for 7 days before further routine processing. The aim was to analyse the main epithelial cell types lining the conducting and respiratory airways, and to determine how these populations varied with age.

3.2.1 Histological categorisation of the lung

A standard H and E stain was used for basic microscopical analysis of lung sections to provide a means of localising each cell type to particular anatomical regions. The organ was divided into five distinct regions defined by airway wall components and proximity to alveoli as suggested by Tyler (1983) (Table 1.2). These were the bronchi, bronchioles, terminal bronchioles, respiratory bronchioles and alveolar regions, the histological appearance of which is shown in (Figure 3.1A-G).

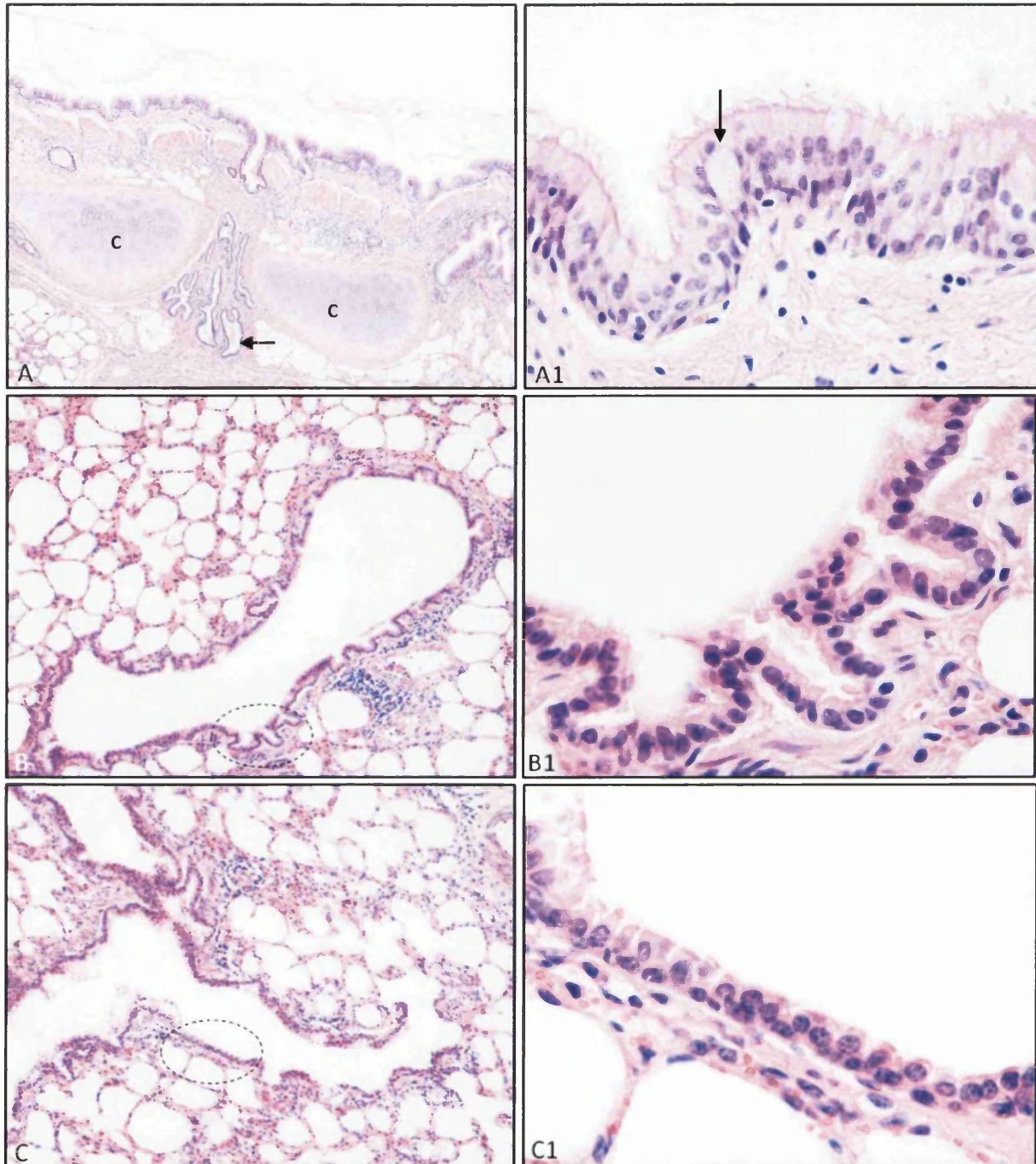


Figure 3.1 Histological categorisation of the lung into five anatomical regions.(A) Bronchus : epithelium with underlying cartilage (c) and mucous gland (arrow), OM x20.(A1)Bronchial epithelium: ciliated pseudostratified columnar epithelium with goblet cells (arrow), OM x400. (B) Bronchiole: walls of smooth muscle and loose connective tissue. No cartilage or glands, OM x100. (B1) Bronchiolar epithelium from B : ciliated columnar to squamous epithelium, OM x600. (C) Terminal bronchiole: most distal region of conducting airways, OM x100. (C1) Terminal bronchiole from C: ciliated columnar to squamous epithelium, OM x600. H and E stain.

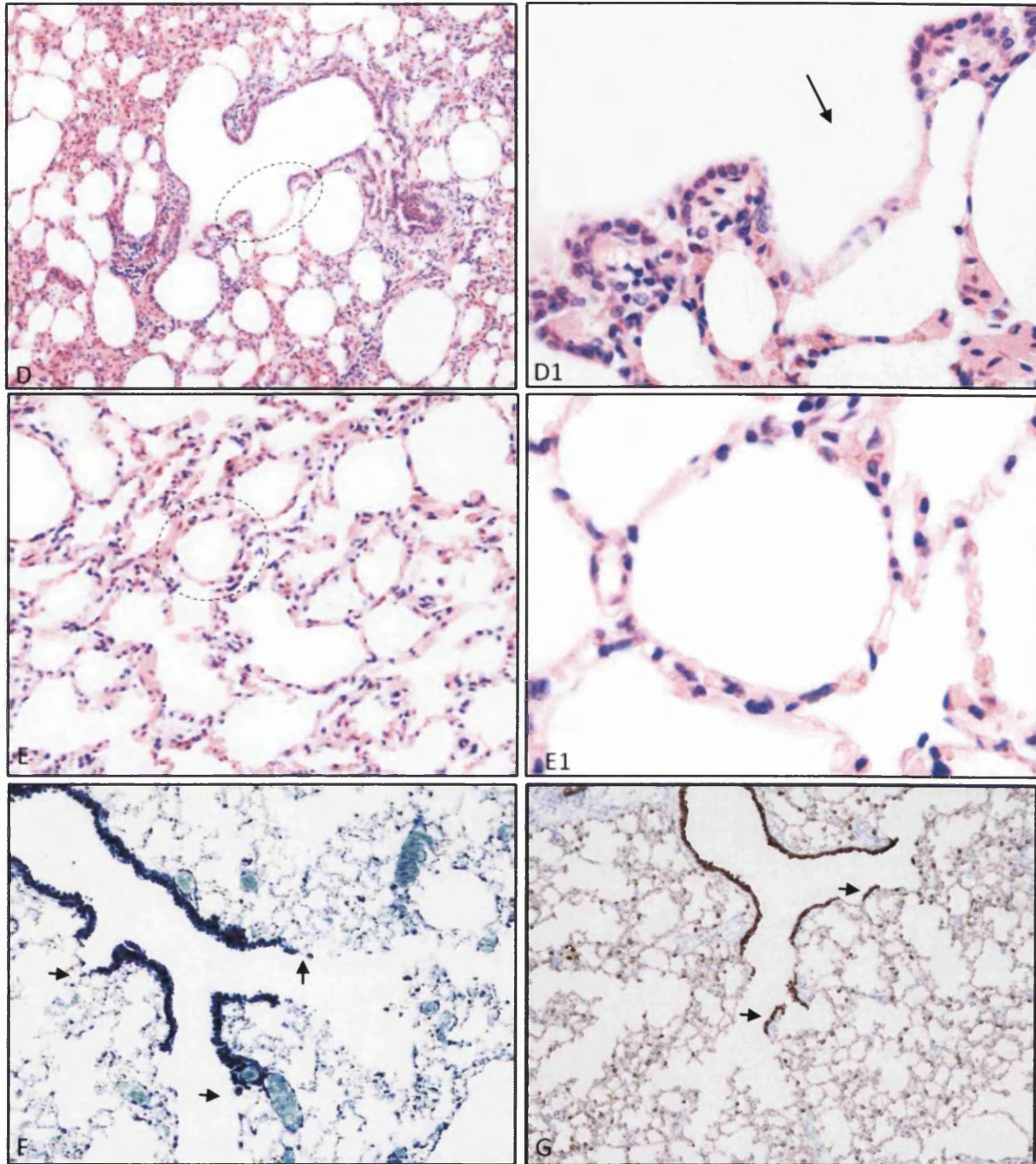


Figure 3.1 (cont). Histological categorisation of the lung into five regions. (D) Respiratory bronchiole: transition between conducting and respiratory airways, OM x100. (D1) Respiratory epithelium from D, interrupted by openings into alveoli (arrow), OM x400. (E) Alveolar region, OM x200. (E1) alveoli lined by type I and type II pneumocytes, OM x600. (F) Mouse lung showing abrupt junction of terminal bronchiole with alveoli (arrow). LFB stain, OM x400. (G) Ovine lung, showing respiratory bronchiolar epithelium (arrows) between terminal bronchioles and alveolar region. IHC anti-pancytokeratin antibody.

3.2.2 Histochemical analysis of the lung

Histochemical stains were used to further aid the recognition of ciliated cells, Clara cells, neuroepithelial bodies (NEBs) and type II pneumocytes in these anatomical regions. These cells were chosen as they have specialised functions specifically related to the lung (Wuenschell et al., 1996). Staining methods were taken from published literature (Bancroft J.D., 1994) (see section 2.5) and five stains were used to analyse tissue. Some of these had been specifically adapted for use in the lung (Azzopardi and Thurlbeck, 1969).

The results of histochemical analysis are summarised in Table 3.2 and displayed in Figure 3.2. Cilia were clearly visible in all regions using Grimelius (Figure 3.2A), PTAH and Luxol fast blue stains. PAS only highlighted the longer cilia in the bronchi. The distinctive domed cytoplasm of Clara cells stained strongly in all levels of bronchioles with PTAH, Luxol fast blue and PAS (Figure 3.2 C,E and G). Grimelius silver stain showed black stippling of occasional cells deep within the bronchial and bronchiolar epithelium (Figure 3.2A). These cells were assumed to be NE cells. No NEBs were detected in the alveolar region in any age of animal. Type II pneumocytes did not label specifically with any of the histochemical stains employed. From these results it was concluded that histochemical staining was only useful for detecting Clara cells and ciliated epithelial cells. However, while the Clara cell cytoplasm was highlighted with PAS, PTAH and LFB, the type of staining was not distinct enough to allow accurate quantitative analysis of specific cell types throughout the lung. Cilia were only detectable when at their longest in the bronchi, and NEBs and type II pneumocytes were not conclusively identified using any of the histochemical staining methods.

Table 3.2 Summary of histochemical stains used on ovine lung tissue

Stain	What does it stain	Ciliated cells	Clara cells	NEBs	Type II pneumocytes
H and E	Basophilic blue, acidophilic pink	Pink cytoplasm	Pink cytoplasm	Pink cytoplasm	Pink cytoplasm
PAS	Glycogen, neutral mucins and carbohydrates stain pink	Yes in bronchus	Yes	No	No
Grimelius	Argyrophil granules stain brown /black	Brown	No	Black stippling	No
PTAH	Many tissue structures	Yes	Yes	No	No
LFB	Phospholipids dark blue	Yes	Yes	No	No

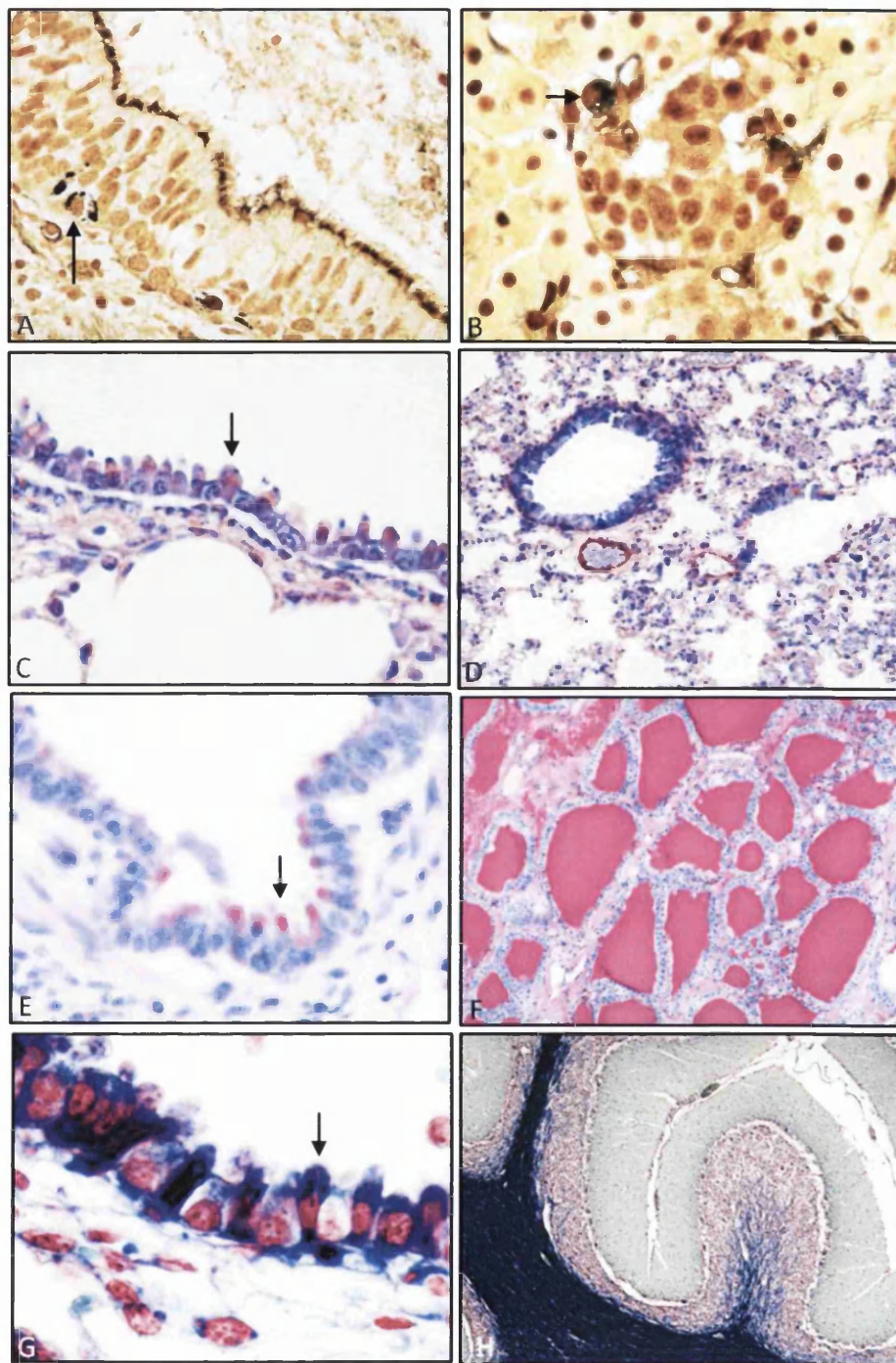


Figure 3.2 Histochemical staining in the sheep lung (left) and positive control tissue (right). (A) Bronchus, Grimelius silver stain: black stippled staining of NE cells (arrow) and brown cilia, OM x600. (B) Pancreas: black labelling of argyrophilic cells in the islet of Langerhans (arrow), OM x600. (C) PTAH, bronchiole: stains purple domed cytoplasm of Clara cells (arrow), OM x400. (D) Mouse lung: shows staining of a variety of structures, OM x400. (E) PAS, bronchiole: stains pink domed cytoplasm of Clara cells (arrow), OM x600. (F) Calf thyroid, pink colloid material in thyroid follicles, OM x200. (G) LFB, bronchiole : stains purple domed cytoplasm of Clara cells (arrow), OM x1000. (H) Mouse brain: purple staining of myelin.

3.2.3 Immunohistochemical analysis of the lung

3.2.3.1 Primary antibodies

Immunohistochemistry was used to improve the ability of identifying different epithelial cell types. This method is based on the binding of antibodies to specific antigens in the tissue (Ramos-Vara, 2005). Both commercially available and custom made monoclonal and polyclonal antibodies were optimised to label all epithelial cells, ciliated epithelial cells, Clara cells, NEBs and type II pneumocytes in the sheep lung (see Table 2.3). Immunohistochemistry was performed using the Envision™ system and indirect labelling techniques (see section 2.1). The final working dilutions and experimental conditions for each antibody are shown in Table 3.3. In order to minimise variations in antibody binding and visualisation between batches, all slides for each antibody were stained simultaneously.

Table 3.3 Optimised conditions for antibodies to label epithelial cells in the ovine lung

Cell phenotype	Primary antibody	Dilution	AR	Incubation	Source
Epithelial cells	Monoclonal mouse anti-human pancytokeratin	1/1000	Autoclave in citrate buffer pH6	Overnight 4°C	Dakocytomation M3515 Clone AE1/AE3
Ciliated epithelial cells	Monoclonal mouse anti-rat beta -tubulin	1/30 000	Autoclave in citrate buffer pH6	Overnight 4°C	Abcam 40862 Clone 3F3-G2
Clara Cells	Polyclonal rabbit anti- bovine CCSP	1/20 000	Autoclave in citrate buffer pH6	Overnight 4°C	Custom made
Neuroepithelial cells	Polyclonal rabbit anti-human Synaptophysin	1/50	Autoclave in citrate buffer pH6	Overnight 4°C	Vector VPS284
Type II pneumocytes	Polyclonal rabbit anti-human proSP-C	1/4000	Autoclave in citrate buffer pH6	Overnight 4°C	Gift from J Whitsett R09337

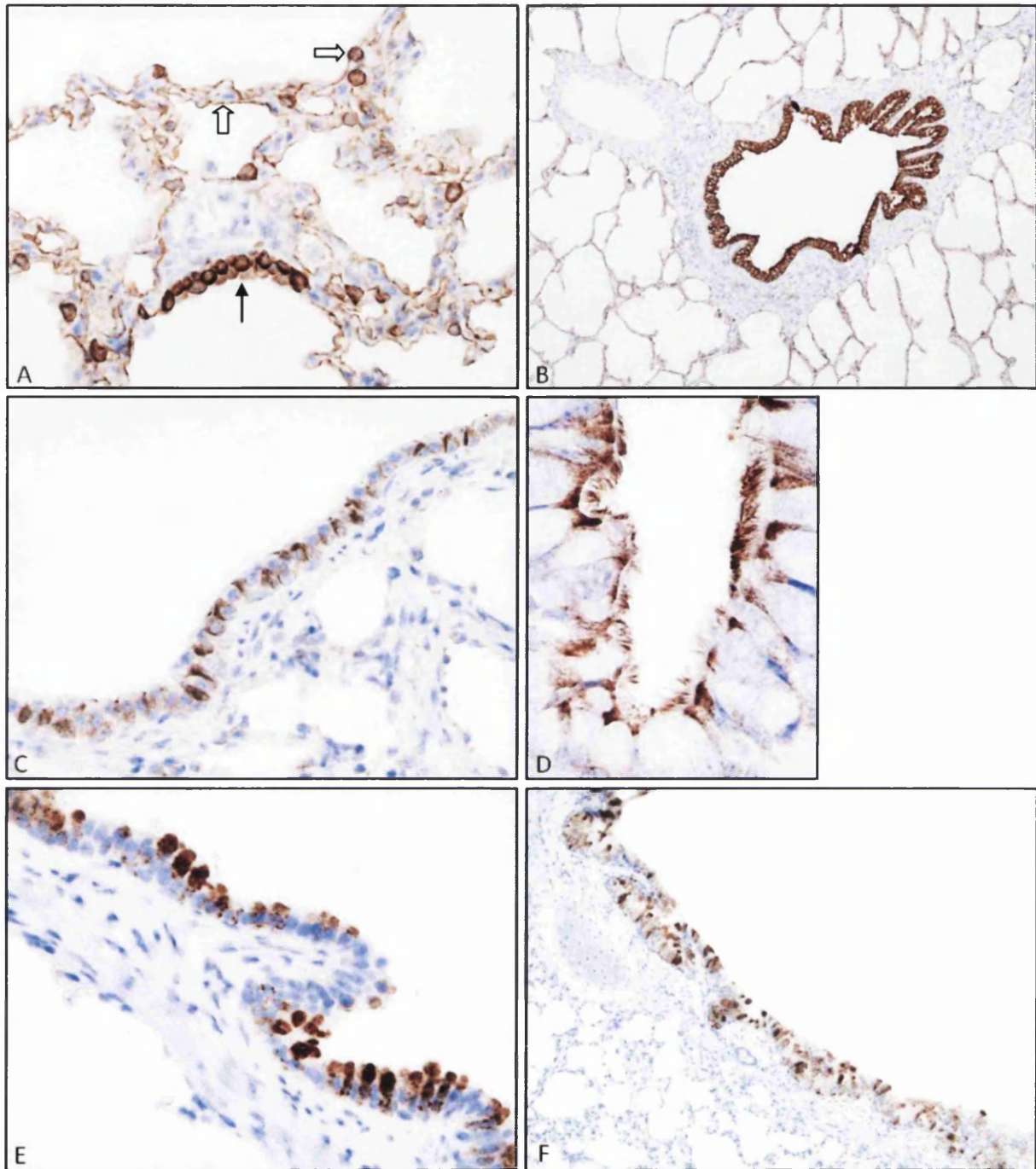


Figure 3.3 IHC to identify specific cells in the ovine lung (left) and positive control tissues (right). (A) anti-pan-cytokeratin antibody, labels respiratory epithelium (arrow), type I pneumocytes and type II pneumocytes, OM x400. (B) anti-Pan-cytokeratin antibody: strong labelling of bronchiolar epithelium, OM x40. (C) anti-beta tubulin antibody bronchiole : cytoplasmic labelling of ciliated epithelial cells, OM x400. (D) anti-beta tubulin antibody bronchus: labels long cilia of bronchial epithelium, OM x1000. (E) anti-CCSP antibody bronchiole : labels Clara cells, as identified on histochemical staining OM x600. (F) Bronchus: unexpected CCSP expression within multiple epithelial cells in the bronchus (cartilage present).

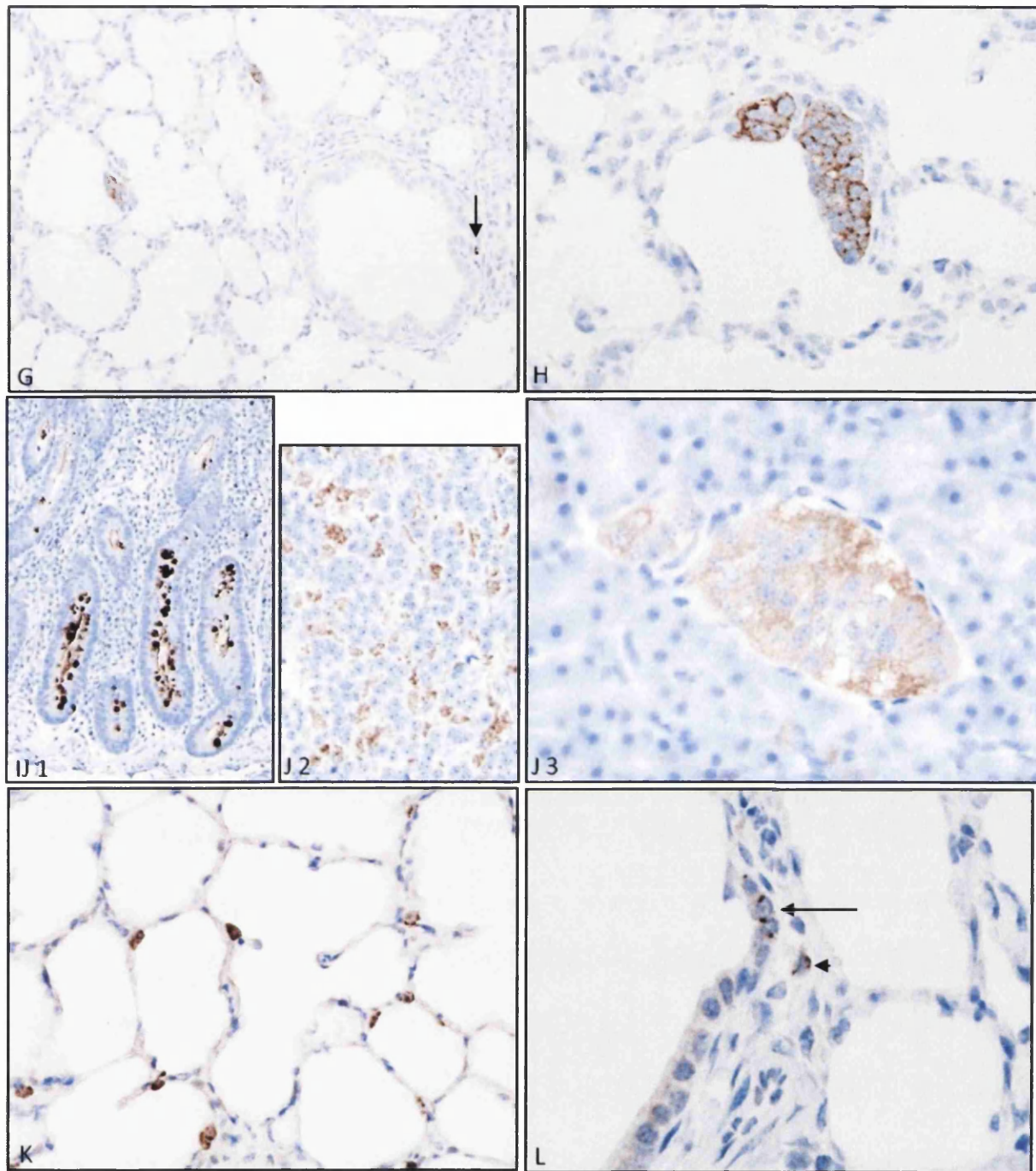


Figure 3.3 (cont). IHC to identify specific cells in the lung. (G) anti-synaptophysin antibody labels two NEBs in alveolar region and one NE cell within bronchial epithelium (arrow), OM x200. (H) anti-synaptophysin antibody labels large NEB in alveolar region, OM x600. (J1-3), positive controls for synaptophysin antibody. (J1) Ovine intestine, villus crypt, labelling of enterchromaffin cells. (J2) Ovine cerebellum, positive label of molecular layer. (J3) Ovine pancreas, positive labelling of islet of Langerhans. (K) anti-SP-C antibody alveolar region labels type II pneumocytes in alveolar walls. (L) Respiratory bronchiole: SP-C expression at BADJ (arrow). Type II pneumocyte acts as positive controls (arrow head).

3.2.4 Anatomical localisation of cell types

Using these antibodies, it was now possible to accurately assign different cell types to an anatomical location during post natal development (Table 3.4). For IHC interpretation, it was assumed that the proteins detected had been expressed by the cell in which they were localised. Cytokeratin labelling was found in the cytoplasm of epithelial cells throughout the respiratory tract from the bronchial epithelium to the type I pneumocytes (Figure 3.3A,B). Beta tubulin labelling was most intense in the cytoplasm of ciliated cells (Figure 3.3 C,D). Although there was faint cytoplasmic labelling in many other cell types, for the purposes of this study only ciliated epithelial cells were examined. CCSP labelling was cytoplasmic and found in characteristic dome shaped cells within the bronchioles (Figure 3.3E). These cells had the same morphology as those identified using histochemical stains (Figure 3.2 C,E,G). Unexpectedly, positive cells were also seen in the bronchial epithelium (Figure 3.2 F). Synaptophysin expression was strong in the cytoplasm of single (NE) cells and groups of cells (NEBs) in the conducting airways, although the presence of these cells was very sporadic, varying hugely between slides and animals. NEBs were more consistently found in the walls of alveolar ducts, and varied in size from 2-30 cells (Figure 3.2 G, H). SP-C labelling was seen in the cytoplasm of plump cuboidal cells in the angle of alveolar walls (Figure 3.3K). Occasional positive cells were also seen in sections of respiratory bronchial epithelium in all ages of lamb (Figure 3.3L).

Table 3.4 Summary of epithelial cell location in the ovine respiratory tract during postnatal development.

 : positive labelling for antibody : - no labelling

Location	Cytokeratin			Beta tubulin			CCSP			NE cells			NEBs			SP-C		
	9	16	91	9	16	91	9	16	72	9	16	91	9	16	72	9	16	91
Bronchus													-	-	-	-	-	-
Bronchiole																-	-	-
T Bronchiole																-	-	-
R Bronchiole																		
Alveolus				-	-	-	-	-	-	-	-	-						

3.2.5 Numerical quantification of IHC labelling

As these slides were being examined to identify the distribution of cell types in the lung, protein expression of CCSP and beta tubulin was seen to vary between different ages of lamb. In order to quantify this observation numerically, Image J deconvolution macro was used to measure the area of phenotypic protein expression as a percentage of the total epithelial area (see Figure 2.4). Image J software offered a consistent method for taking accurate measurements and providing numerical data for comparison between subjects. NEBs and type II pneumocyte numbers were counted manually.

3.2.5.1 Quantification of ciliated epithelial cells

Anti- beta tubulin antibody was used to label ciliated epithelial cells. The percentage of positive labelling was estimated in each of four regions of the lung: bronchus, bronchiole, terminal bronchiole and respiratory bronchiole at a single sample site (5a) from all 6 animals. For each anatomical region, labelling of four bronchi/bronchioles/terminal bronchioles and respiratory bronchioles was assessed. Image J software was used to calculate the area of positive labelling, and this was expressed as a percentage of the total epithelial area. An angular transformation of the data was performed to avoid misleading visual conclusions from error bars due to the original scale. This was because there was a tendency for animals with a higher mean percentage to show more variability between replicates. Error bars that represent 95% confidence interval of the mean were calculated. If these error bars do not overlap, then differences between data are considered to be statistically significant ($P < 0.05$). The data are presented in Figure 3.4. There was a significant increase in beta tubulin expression at 91 days in all four regions of the conducting airways when compared to the earlier time points. A representative photograph of IHC for beta tubulin expression is shown in Figure 3.5.

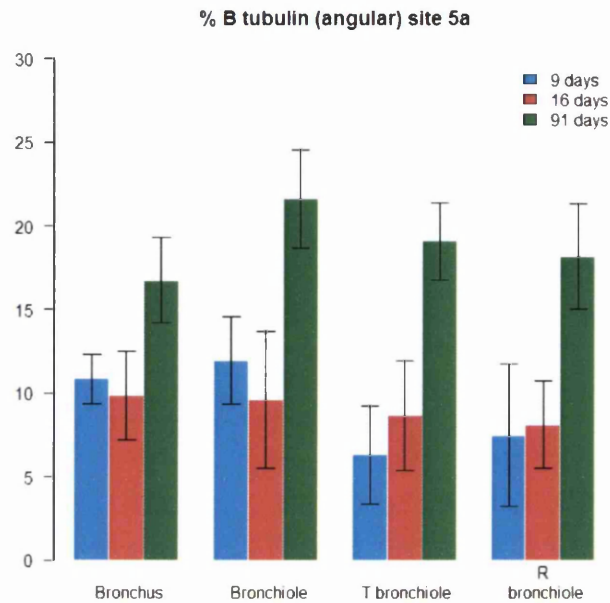


Figure 3.4 Graph showing the variation in beta tubulin expression in four anatomical regions of the lung in different ages of lamb. An angular transformation was carried out on the original data, and the y axis represents the mean of the transformed data. The error bars represent the 95% confidence interval of the mean. Higher levels of beta tubulin expression were found in 91 day old lambs than in younger animals ($P < 0.05$) in all four anatomical regions.

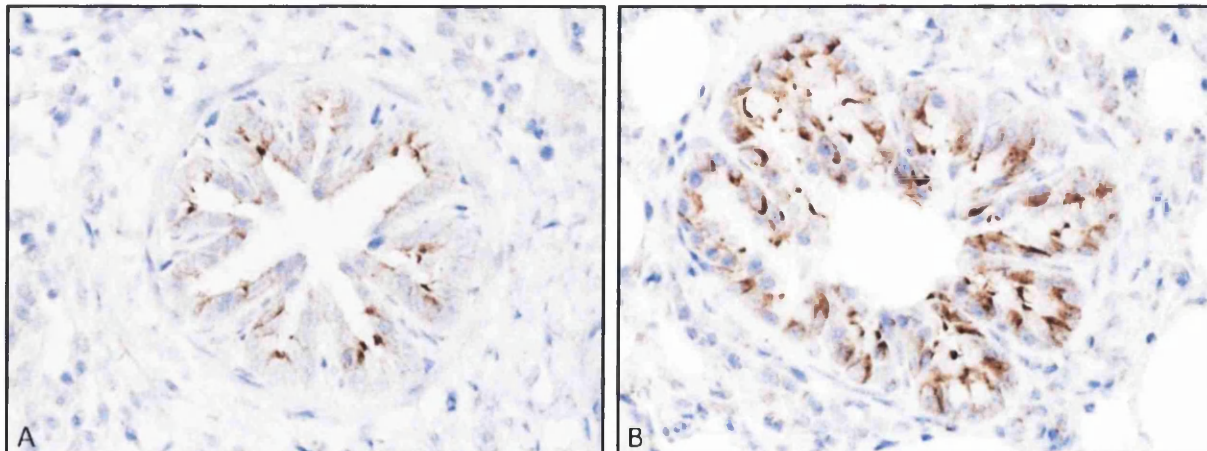


Figure 3.5 IHC using anti-beta tubulin antibody to label ciliated cells in bronchiole from 9 (A) and 91 (B) day old lambs. Increased labelling can be seen in the older animal (B).

3.2.5.2 Quantification of Clara cells

Clara cell protein percentages were estimated at two sites (1b and 5a) in each of four regions of the lung: bronchus, bronchiole, terminal bronchiole and respiratory bronchiole. This gave a total of eight observations per animal and all 6 animals were examined. The predicted mean percentages of Clara cell protein expression from the transformed scale are shown in Figure 3.6. Significant increases in CCSP expression in lambs between 9 and 91 days old are seen in bronchi, terminal bronchioles and respiratory bronchioles ($P < 0.05$). Increases in CCSP levels between 9 and 16 days are seen in the bronchiole and terminal bronchiole only ($P < 0.05$).

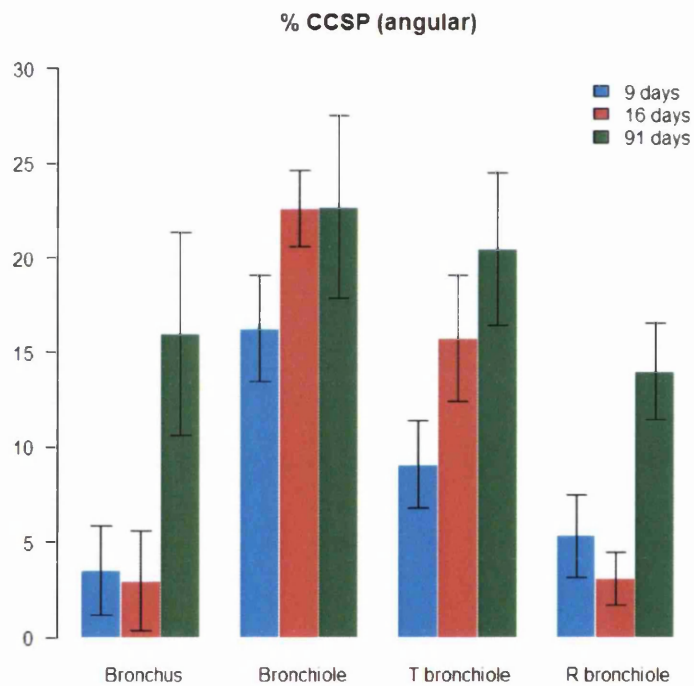


Figure 3.6 Graph showing the variation in CCSP expression from two sites (1b, 5a) in four anatomical regions of the lung in different ages of lamb. An angular transformation was carried out on the original data, and the y axis represents the mean of the transformed data. The error bars represent the 95% confidence interval of the mean. An increase in CCSP expression was found in the bronchi, terminal bronchioles and respiratory bronchioles in 91 day old lambs when compared to in 9 day old lambs ($P < 0.05$). The large error bars indicate the high variability in CCSP expression within the same anatomical region at the same site.

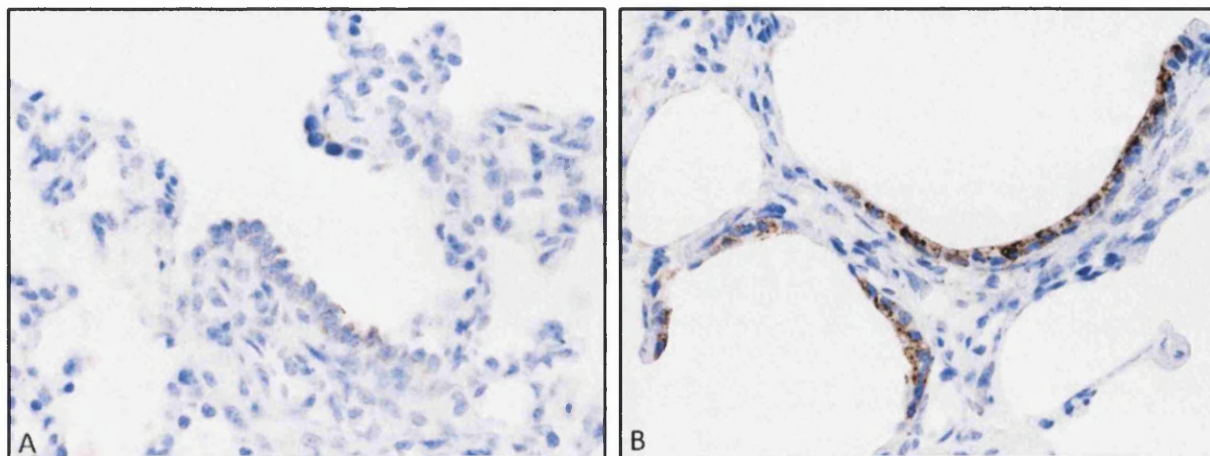


Figure 3.7 IHC using anti-CCSP antibody to show labelling in the respiratory bronchioles of 9 day (A) and 91 day (B) old lambs. Increased labelling is seen in the older animals.

3.2.5.3 Neuroepithelial cells

NEB were identified using an antibody to synaptophysin. Numbers were estimated at one or two sites (1b and 5a) in the lung from all 6 animals. Only those in the alveolar regions were counted, as those in the conducting airways were too sporadic to assess meaningfully. The final value was expressed as the total number of NEBs per cm² of fixed lung tissue (Figure 3.8). There was no consistent change in NEB number with age of lamb.

3.2.5.4 Type II pneumocytes

Type II pneumocytes were identified by their expression of SP-C. Between 500-1200 nuclei were counted in the alveolar region of a single site (5a) for each animal. The percentage of these cells that labelled positively for SP-C was calculated. The percentage of Type II pneumocytes were slightly higher at day 9, but this difference is marginal (Figure 3.9).

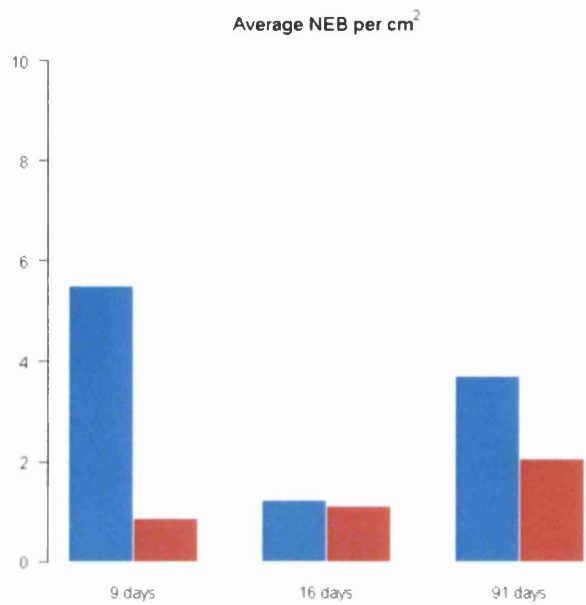


Figure 3.8 Graph showing variation of NEB per cm² in a total of six lambs ages 9,16 and 91 days. Red/blue represents a different animal at each time point.

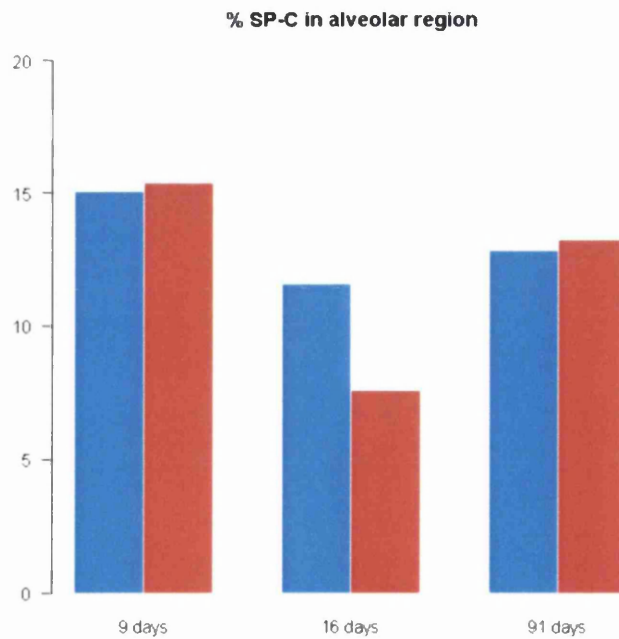


Figure 3.9 Graph showing variation in % SP-C numbers in a total of six lambs aged 9,16 and 91 days

3.2.6 Effect of age on proliferative index

Ki-67 antibody was used to identify the proliferative state of cells, in order to assess the growth rate of different anatomical regions of the lung during postnatal development. Ki-67 is a nuclear antigen expressed by cells which are not in the G₀/resting phase of the cell cycle. The antibody was optimised by labelling tissue with known differences in proliferation such as the intestine and the lung (Figure 3.10).

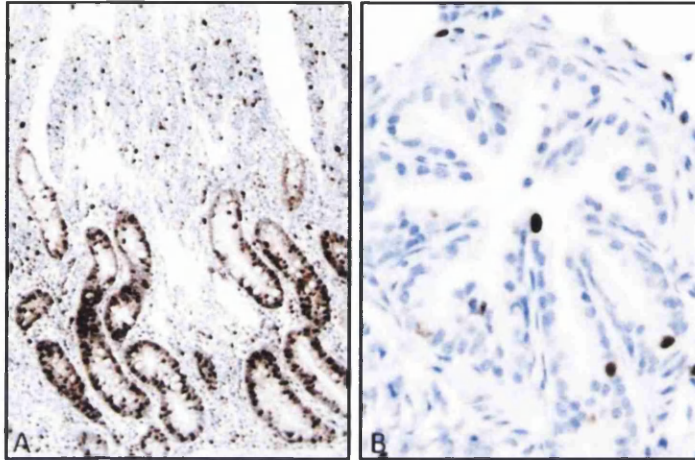


Figure 3.10 IHC using anti-Ki 67- antibody to compare proliferative index between intestine and lung. Intestinal epithelium (A) lots of Ki-67 positive cells, lung (B) few Ki-67 positive cells.

The proliferative index of the epithelial compartment from five regions of the lung was calculated in different ages of lamb. These were the bronchus, bronchiole, terminal bronchiole, respiratory bronchiole and alveolar region. In each of these regions, a total of 200 cells from each of four bronchi/bronchioles/terminal bronchioles and respiratory bronchioles were analysed. In the alveolar compartment, six fields of 200 cells were analysed. This took place in two sites (1b and 5a) from all 6 animals. The number of positive labelling nuclei for Ki-67 was recorded and expressed as a percentage for each 200 cells to give the proliferative index. An angular transformation was carried out on the data (Figure 3.11). Reductions in proliferative index with age are seen between 16 and 91 days in bronchus, bronchiole, terminal bronchiole and alveolar region. The biggest change is seen in the alveolar region (Figure 3.12).

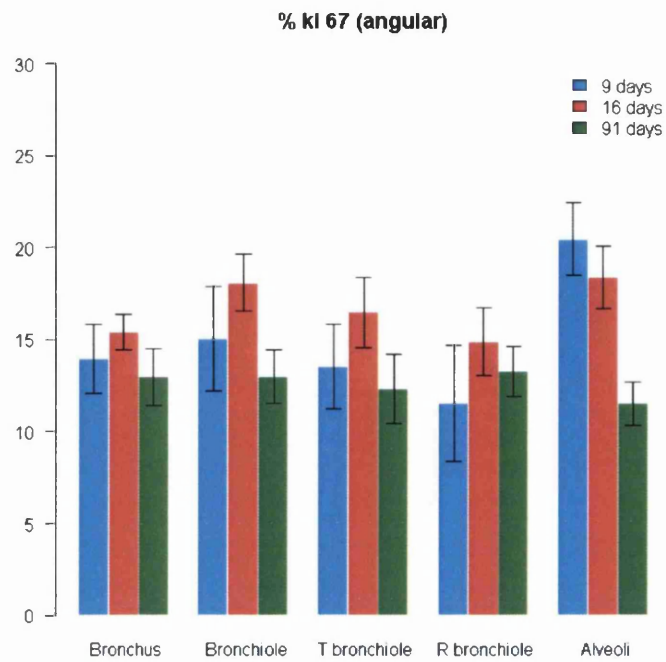


Figure 3.11 Graph to show the proliferative index of five anatomical regions in the lung in lambs aged 9,16 and 91 days. An angular transformation was carried out on the original data, and the y axis represents the mean of the transformed data. The error bars represent the 95% confidence interval of the mean. There is a significant reduction in proliferative index between 16 days and 91 days in the bronchus, bronchiole, terminal bronchiole and alveoli.

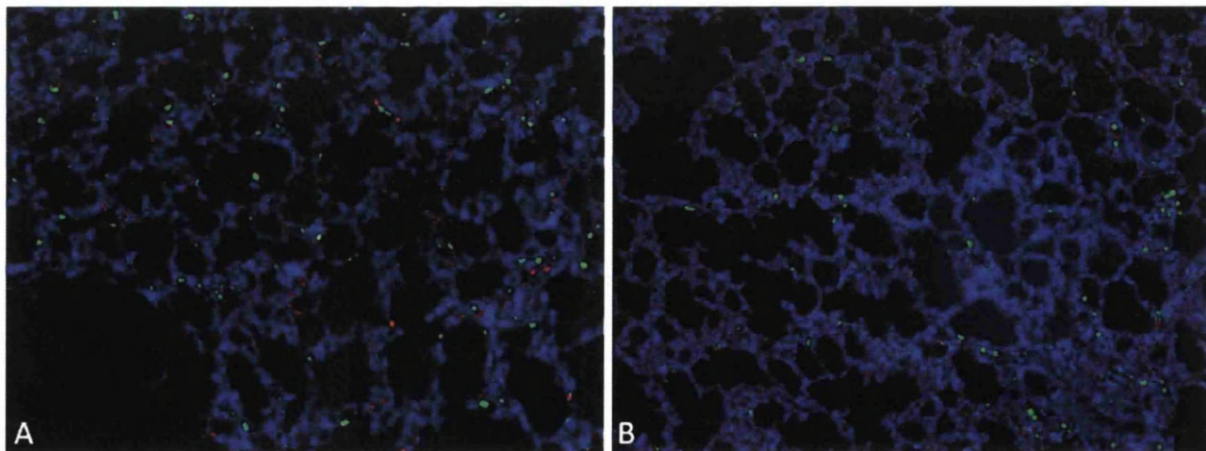


Figure 3.12 Comparison of number of Ki-67 positive cells in the alveolar region of a 9 day (A) and 91 day old lamb (B). Green, anti-Ki-67. Greater numbers of positive cells in the younger lamb (Red, anti-SP-C).

3.3 Discussion

This study provides data regarding the normal postnatal development of the respiratory epithelium in SPF lambs. It validates antibodies to identify specific epithelial cell types in the ovine lung, and uses immunohistochemical techniques to locate and quantify these cells and their proliferative state in predefined anatomical regions. Studies in other species have shown these parameters to vary according to the maturity of the neonate (Fanucchi et al., 1997b; Plopper et al., 1992). More accurate comparisons can now be made between these species and the sheep lung.

This analysis was performed in growing lambs which were 9, 16 and 91 days old. Clara cells and ciliated epithelial cells were detected in the bronchi, bronchioles, terminal bronchioles and respiratory bronchioles of all animals. Neuroepithelial cells and NEBs were found in conducting and respiratory airways. Type II pneumocytes were found predominantly in the alveolar compartment but were also detected in occasional areas of respiratory bronchiolar epithelium. As the animals aged there was an increase in detection of beta tubulin in the epithelium of all four regions of the lung ($P < 0.05$) (Figure 3.4). Increased CCSP was found in the bronchi, terminal bronchioles and respiratory bronchioles in 91 day old lambs when compared to 9 day old lambs ($P < 0.05$) (Figure 3.6). Numbers of NEBs and the % of type II pneumocytes showed no trend in variation over time. The proliferative index was seen to decrease in lambs between 16 and 91 days, with the biggest reduction in the alveolar compartment. This suggests that during postnatal development, there is maturation of the lung as defined by cytodifferentiation, and a reduction in proliferative index which is most apparent in the alveolar compartment.

Classification of cell phenotype using IHC to analyse protein production is a widely used technique (Ramos-Vara, 2005). Its reliability is dependent on the use of consistent tissue processing and antigen detection techniques, and the absolute specificity of antibodies. In this study, the strict tissue sampling and analysis protocols combined with appropriate positive and negative controls for IHC ensured that changes in protein expression were the result of biological variations only.

The use of Image J to provide numerical quantitative values for protein expression was another effort towards standardising these results. Traditionally, pathologists examine the tissue by eye and use a 3 or 4 point subjective scoring method to record the degree of positive labelling (Cregger et al., 2006). However, automated analysis offers a more objective means for quantitative scoring and increases the accuracy of data comparison between studies. Several methods have been used for quantification for IHC labelling in the lung (Arsalane et al., 2000; Bolton et al., 2008; Coppens et al., 2007; Fanucchi et al., 1997b). They include estimating the area of protein expression (by eye or automated analysis) as a fraction of the total epithelial area (Bolton et al., 2008; Coppens et al., 2007), or counting the number of positive cells in a given area (Arsalane et al., 2000; Bolton et al., 2008). For this study the former technique was applied. As the process of postnatal maturation in the sheep has not been fully defined, it was thought that assessing the overall amount of protein production would include both increased numbers of expressing cells and increased expression of protein by pre-existing cells, so being a more sensitive measure of cytodifferentiation. In addition, the complicated anatomy of the lung which leads to unavoidable tangential sectioning of respiratory epithelium in all levels of the tract, prevents an accurate assessment of cell number.

In the sheep existing histological studies on the lung use ultrastructural and histochemical staining techniques to analyse the process of cytodifferentiation and distribution of different cell types at maturity (Alcorn et al., 1981; Bouljihad and Leipold, 1994; Kikkawa et al., 1965; Mariassy and Plopper, 1983, 1984; Orzalesi et al., 1965; Plopper et al., 1980a). However, as changes in cellular morphology do not necessarily correlate with protein production (Coppens et al., 2007) the accuracy of these findings is questionable. They also mainly focus on the anatomy of fetal development and the adult animal, omitting the important process of postnatal maturation while cells are still differentiating and dividing.

Postnatal maturation in the lung has been examined in the mouse, hamster, rat, rabbit, rhesus monkey and human (Plopper et al., 1992). In the conducting airways, work has shown that fetal respiratory epithelial cells are typically filled with glycogen (Pinkerton and Joad, 2000). As the cells mature, this is gradually lost and expression of proteins associated with the differentiated phenotype increases. For example in the bronchioles, cytodifferentiation is characterised by a general loss of glycogen from undifferentiated cuboidal cells, and the

development of cilia which grow from basal bodies in the apical cytoplasm or an increase in Clara cell protein production (Marei and Abd el-Gawad, 2001). In the Clara cell, this corresponds with the formation of abundant amounts of smooth and rough endoplasmic reticulum in the basolateral and apical regions of the cell cytoplasm. The P450 isoenzymes which are involved in bioactivation and detoxification of xenobiotic compounds also develop postnatally (Fanucchi et al., 1997b). The type II pneumocyte is the only cell type which has been studied in detail during maturation of the sheep lung (Meyerholz et al., 2006). Here, glycogen loss was found to correlate with an increase in CD208 expression and the development of lamellar bodies and surfactant production.

The timing and pattern of epithelial differentiation is species specific (Cardoso, 2000; Castleman and Lay, 1990; Fanucchi et al., 1997b; Hyde et al., 1983; Pinkerton and Joad, 2000). For example in the rat and rhesus monkey Clara cells are fully differentiated by 1 week, but in the rabbit and calf this takes 4 weeks (Castleman and Lay, 1990). In the mouse, levels of CCSP and beta tubulin expression reach maturity by 14 days post partum (Fanucchi et al., 1997b). In the present study on ovine lung, beta tubulin expression did not increase until after 16 days in all regions of the lung. For CCSP, there was an earlier increase between 9-16 days in the bronchioles, and terminal bronchioles. No further change in the bronchioles suggests mature levels of CCSP expression were reached by 16 days, but in the terminal bronchioles expression had increased again by 91 days. In the respiratory epithelium CCSP expression did not increase until after 16 days. This indicates a proximal/distal graded maturation within the conducting and respiratory airways, although samples from additional time points are needed to see how protein expression varies within and after these time points.

These species specific timings are most likely influenced by the stage of lung development reached during gestation. Prenatal development of the lung goes through four stages of maturation: the pseudoglandular stage, the canalicular stage, the saccular stage and the alveolar stage. For example, marsupials are born with relatively primitive lungs in the canalicular or saccular stage and require significant postnatal maturation (Burri, 2006). Humans are born in the saccular stage, where airspaces are simple and their walls are thick septa with connective tissue and two capillary networks. The formation of alveoli (alveolarisation) occurs in the first 6 months and is followed by microvascular maturation for

up to 3 years. In contrast, the lamb is born with a more mature lung which is already alveolarised and the degree of postnatal microvascular maturation is unknown (Alcorn et al., 1981). Proportions of type I to type II pneumocytes are influenced by fetal lung expansion, and studies have shown a predominance of type I pneumocytes before birth, and type IIs after (Flecknoe et al., 2000; Flecknoe et al., 2003). In the present study the proportion of type II pneumocytes to other cells in the alveolar region of the ovine lung, showed little change with age increase. The finding that there was no postnatal increase in type II pneumocyte formation detected supports the theory of complete alveolarisation in the lamb.

This study identified additional locations for cells expressing CCSP and SP-C protein when compared to existing literature. CCSP expression in the bronchi has not been recorded in sheep (Figure 3.3A). Similar cells found in rat and human studies do not share the proliferative characteristics of Clara cells in the more distal conducting airways (Barth et al., 2000; Boers et al., 1999). Expression of SP-C in bronchioles is also a new finding. In mice, cells which express SP-C and CCSP called BASCs have been found at the BADJ (Jackson et al., 2001; Kim et al., 2005). Occasional SP-C positive cells in this study were also found in this anatomical region (Figure 3.3L). The absence of an obvious trend in NEB numbers during maturation is in contrast to other studies on the ovine lung where numbers are reported to reduce during maturation (Van Lommel and Lauweryns, 1997). This discrepancy may be due to the use of different antibodies for detection. It has been proposed that the endocrine function of these cells reaches maturity at birth, but the chemoreceptor function shows maturation in the postnatal period. In the sheep lung, variation in expression of specific markers with age has been recorded for NEBs (Asabe et al., 2004; Balaguer and Romano, 1991; Van Lommel and Lauweryns, 1997).

In this study, changes in proliferative state were used to assess the growth rate of separate anatomical compartments in the lung. The proliferation of cells during postnatal development was measured using Ki-67, which is a nuclear structure present exclusively in proliferating cells (Scholzen and Gerdes, 2000). It is a reliable indicator of cell proliferation and expression is closely correlated with other similar markers including thymidine labelling, bromodeoxyuridine incorporation and flow cytometry (Hall and Levison, 1990). The proliferative index is difficult to study in the normal lung as the cell turnover is so slow

(Kauffman, 1980). Therefore it is most commonly investigated in tissues during development, following injury or as a prognostic indicator in tumour biology (Hall and Levison, 1990). In this study, the largest reduction in PI was detected in the alveolar region. Here, as the measurement of Ki-67 expression potentially included type II pneumocytes, endothelial cells, fibroblasts and infiltrating leukocytes, it was not possible to pinpoint the phenotype responsible for this decrease in turnover. However, extrapolation of data from other animals indicates that microvascular maturation, which involves restructuring of the capillary network from double to single form, is the final stage of lung maturation (Burri, 2006). Measurement of Ki-67 expression in other areas of the lung directly reflects the proliferative capacity of epithelial cells lining the airways only as the epithelium is morphologically distinct. More subtle changes were seen in the conducting airways, with reductions in PI detected in the bronchi, bronchioles and terminal bronchioles between 16 and 91 days. Additional samples from between and outside these time points would help to map the proliferative state of these anatomical regions in the lung more thoroughly.

In summary, this study shows that in the lamb there is significant postnatal cytodifferentiation of Clara cells and ciliated epithelial cells in the respiratory airways. This may have implications for the pathogenesis of respiratory disease, as differentiation in other species coincides with development of lung xenobiotic metabolising enzyme systems (Pinkerton and Joad, 2000). This was demonstrated in studies on adult and neonatal mice and rabbits which exposed all animals to the same noxious insult and found injury to undifferentiated cells to be more severe. Subsequent maturation processes in the lung were also impaired (Fanucchi et al., 1997a; Plopper et al., 1994; Smiley-Jewell et al., 1998). Given the variation in timing and location of cell maturation in the lamb described in this study, particular regions of the lung may be more susceptible to injury at certain times than others. However, the data from this study must be interpreted with caution. Only a few animals were examined, and they were housed in an SPF environment where normal exposure to inhaled allergens was minimal. This may have affected the process of cell maturation. Analysis of many more lungs would overcome this problem.

CHAPTER 4 IDENTIFICATION OF THE TARGET CELL FOR JSRV INFECTION IN THE OVINE LUNG

4.1 Introduction

Initial interactions between virus and host have been poorly defined for OPA. As a first step towards investigating these early stages of disease pathogenesis, this chapter aimed to identify the target cell for JSRV infection in the ovine lung. Current theories on target cell identity for JSRV infection in the lung are based on the anatomical location and heterogenous phenotype of the resultant mature tumours. Such tumours are reported to emanate from bronchiolar and alveolar epithelium, and IHC shows the majority of the neoplastic cells to express SP-C or CCSP (see Figure 1.9H). Therefore, Clara cells, type II pneumocytes and an unidentified 'lung progenitor' cell have all been suggested as potential targets for JSRV (Platt et al., 2002).

Efforts to confirm these theories using experimental models of infection have been challenging. *In vitro* experiments were confounded by the difficulty of maintaining the required ovine cell phenotypes in culture (Archer et al., 2007; Jassim et al., 1987). Mouse models of OPA have only shown expression of JSRV in type II pneumocytes which does not accurately mimic natural disease in the sheep (Chitra et al., 2009; Dakessian and Fan, 2008; Wootton et al., 2005). Due to the lack of a pre-clinical diagnostic test for OPA, the study of OPA-N seldom provides tissues from an early enough stage of infection to identify the target cell in the lung.

In the present study lung tissue from experimentally infected lambs provided a source of material for analysis. Samples were taken shortly after inoculation before significant tumour growth occurred, and immunohistochemical techniques developed in the previous chapter were applied to identify the phenotype of single cells expressing viral protein. These pulmonary cells were assumed to be the target cell for JSRV in the lung.

4.2 Results

4.2.1 Experimental infection of neonatal lambs with JSRV₂₁

SPF lambs experimentally infected with JSRV₂₁ were used to provide lung tissue to identify cell types infected by JSRV at early stages post-infection (Figure 4.1). Twelve SPF lambs were challenged intratracheally with JSRV₂₁ (4 ml ~ 10¹⁰ RNA copies of JSRV₂₁) at 6 days old (Group 1). Four animals were euthanased at 3 and 10 days post-inoculation and the remaining four when clinical signs of disease were detected (72 -91 days). Age matched mock infected (Group 2) and non-inoculated (Group 3) lambs were included as negative controls. Samples collected at post-mortem were analysed as detailed in Materials and Methods (2.1).

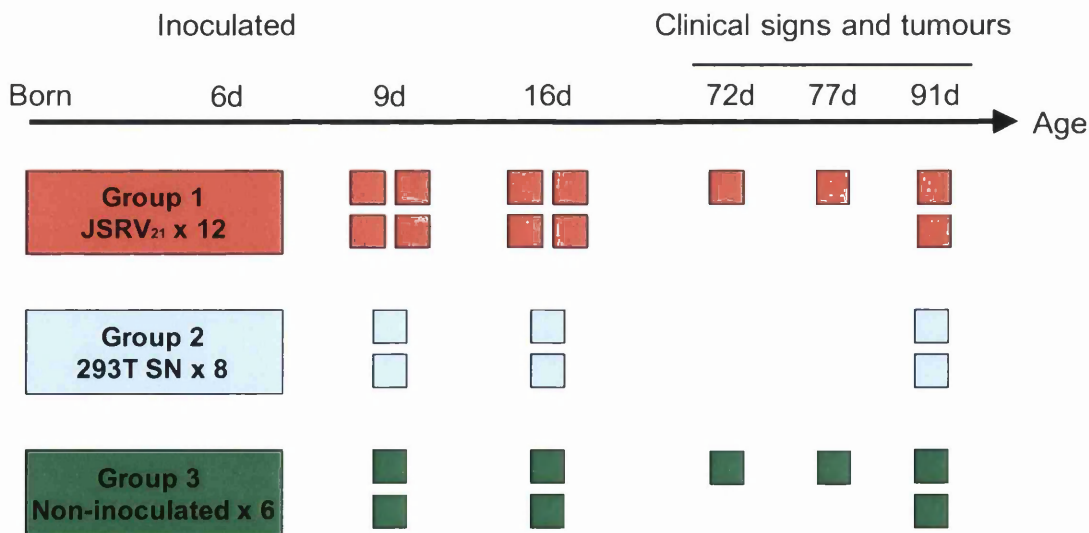


Figure 4.1 Timing of experimental infection and euthanasia. The letter d = days. Each coloured box represents a lamb post-mortem examination. Red: lambs JSRV₂₁ inoculated. Blue: mock inoculate (negative control) Green: no inoculate (negative control).

4.2.2 Post-mortem validation of experimental model

PME was used to confirm the efficacy of this experimental model. Lungs from all groups at 3 and 10 days post infection had similar gross appearances (Figure 4.3 A,B), and there were minimal differences in lung weight as a proportion of body weight between treatment groups. By 72-91 days post-inoculation infected lungs were enlarged and fluid filled (Figure 4.3 D,F). Frothy fluid exuded from the trachea of one animal (2863E) which is a common finding in OPA-N (Figure 4.3 D). Lung surfaces were mottled in colour, and some contained multiple subpleural pale foci surrounded by overinflated tissue (Figure 4.3 F). These were suspicious of neoplastic foci. Lung weight as a proportion of body weight was greater in infected animals when compared to mock and control (Figure 4.2). Histological examination confirmed the presence of tumour to be in infected animals only (Figure 4.4).

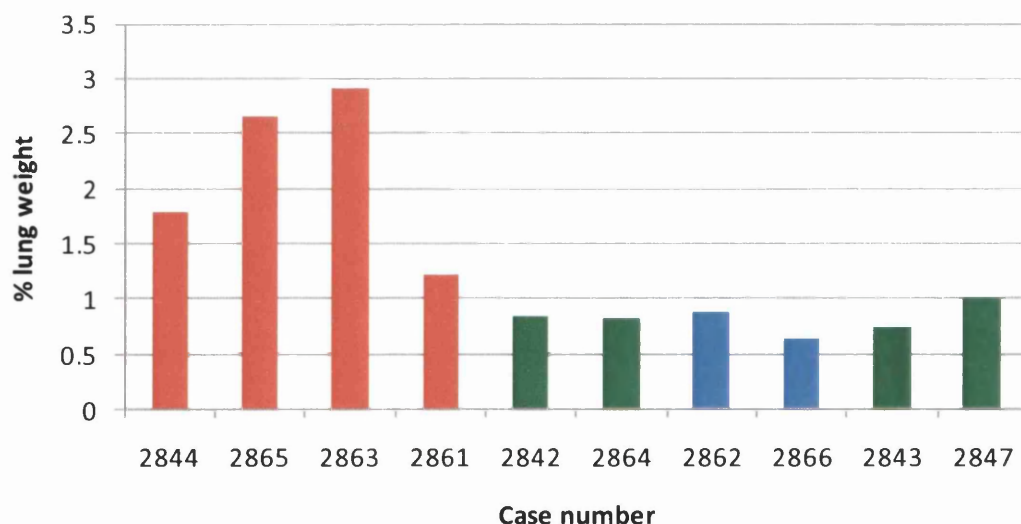


Figure 4.2 Summary of lung weight as a proportion of bodyweight for all lambs 72 - 91 days PI. Red: JSRV₂₁ infected lambs. Blue: mock infected control lambs. Green: non infected control lambs.

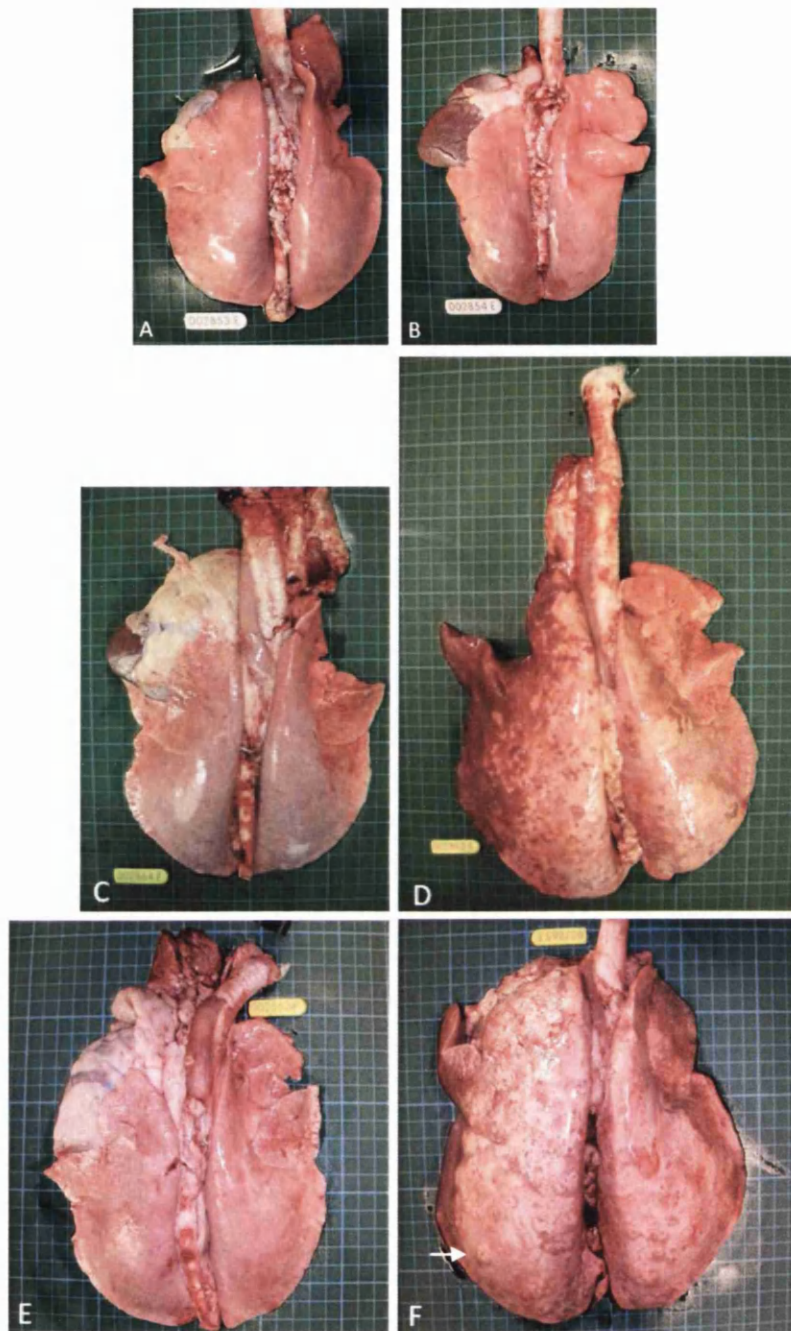


Figure 4.3 Gross appearance of lungs from experimental lambs. (A) mock infected lamb 2853 E and (B) JSRV₂₁ infected lamb 2854E lungs 10 days PI with a similar gross appearance. (C) Control lung from lamb 2864E, 77 days post non inoculation. Note uniform colour and collapsed nature of lung tissue. (D) Lung from lamb 2863E , 77 days post inoculation with JSRV₂₁. Note froth at tracheal opening and enlarged lung (compare with C using background grid) which is mottled in colour. It failed to collapse on opening of thoracic cavity. (E) Lung from lamb 2862E, 91 days post mock inoculation. Note uniform colour and smaller size when compared to (F) using the background grid. (F) Lung from lamb 2865E, 91 days post inoculation with JSRV₂₁. Note suspicious neoplastic dark foci surround by overinflated lung tissue (arrow).

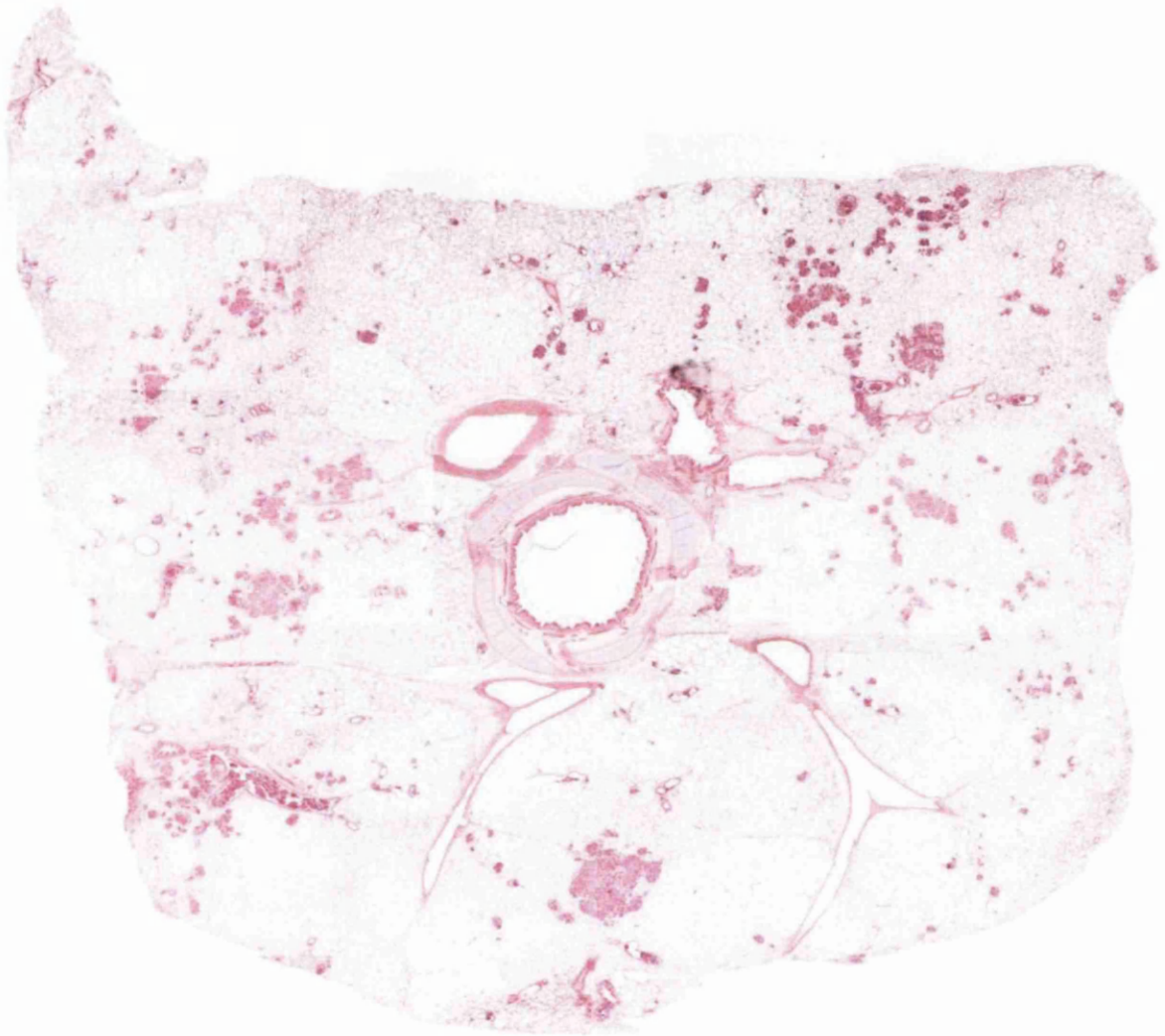


Figure 4.4 A whole transverse section of lung from case 2863 E, site 5a. The dark purple foci are neoplastic nodules which are consistent with a diagnosis of OPA. H and E stain, OM x20.

4.2.2.1 Comparison of experimental and natural OPA tumour phenotypes

In order to validate this experimental model of disease, the phenotype of experimentally induced tumours (OPA-E) were compared with those from natural field cases of OPA (OPA-N). Labelling for cytokeratin, SP-C, CCSP and synaptophysin proteins were assessed using previously optimised antibodies (see Figure 3.3). Similar labelling was seen for all except synaptophysin, which was not readily detectable in cases of OPA-N (Figure 4.5 A-H).

4.2.3 Proliferative cells in the sheep lung during postnatal development

Most retroviruses require actively dividing cells for efficient integration and replication (Coffin et al., 1997). Experiments on rodent lungs indicate that Clara cells, NEBs and type II pneumocytes are able to replicate (Evans et al., 1978; Evans et al., 1973; Peake et al., 2000). To confirm this in the ovine lung, expression of Ki-67 was colocalised with phenotypic markers (CCSP, synaptophysin, SP-C) using dual IHC labelling and the substrate chromogens DAB (brown) and VIP (purple). Optimisation of antibody concentration, sequence of incubation and substrate colour was necessary (Figure 4.6). Numbers of Ki-67 positive cells were then compared between different combinations of antibody incubation and visualisation substrates in serial sections of bronchiole to determine the optimal experimental procedure.

Dual labelling of Clara cells and NEBs with Ki-67 was successful (Figure 4.7 A-D). Detection of SP-C protein was masked by Ki-67 using DAB and VIP substrates, so immunofluorescent techniques were used (Figure 4.7 E, F) (see 2.3.5). There was dual labelling of Ki-67 with the phenotypic marker for all three cell types in the lungs of lambs 10 days PI. This demonstrated the ability of Clara cells, NEB cells and type II pneumocytes to proliferate in the ovine lung, and hence their potential as a target cell for JSRV.

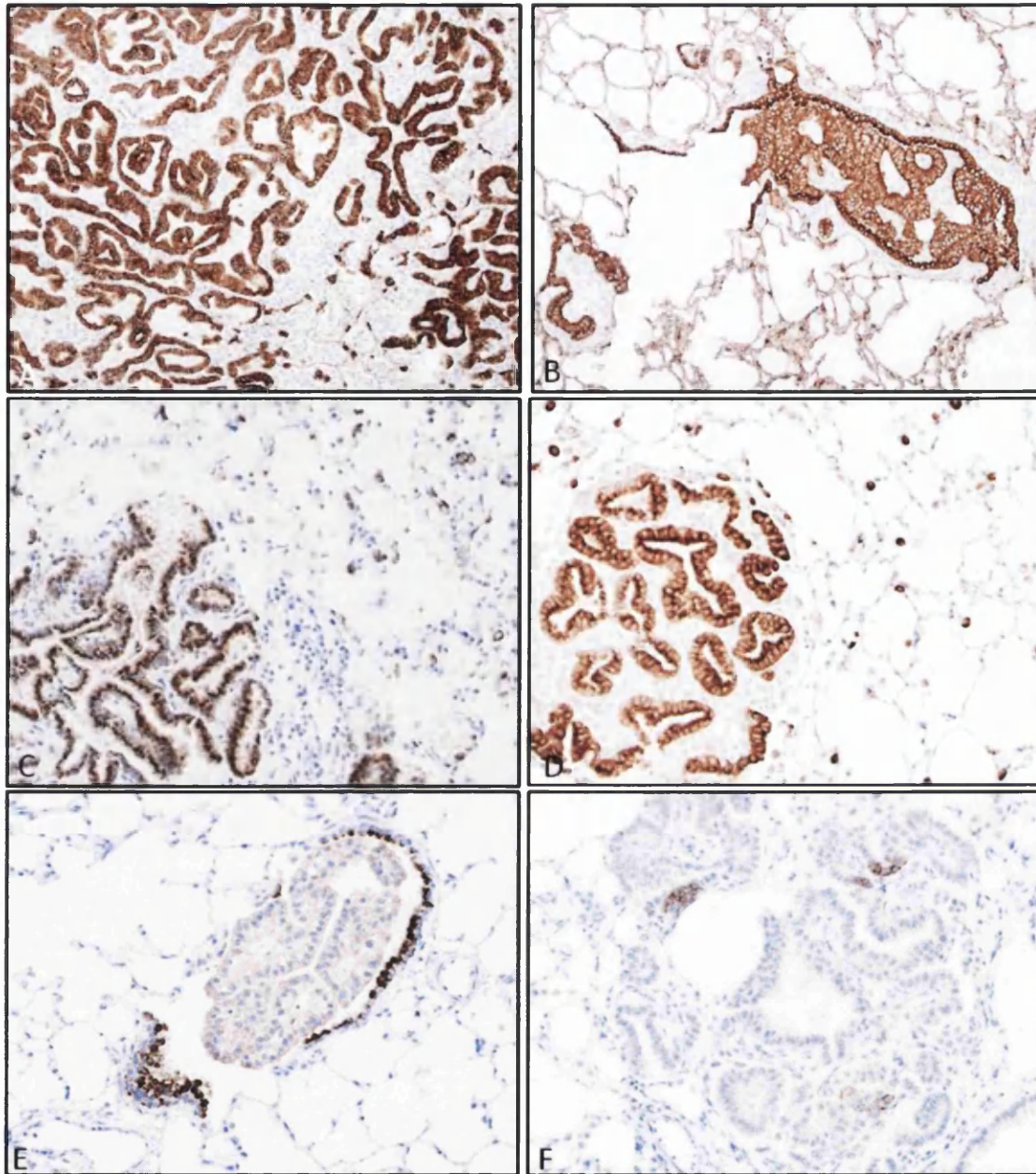


Figure 4.5 IHC analysis of tumours from OPA-N and OPA-E. (A,B) Diffuse labelling of tumour acini with anti-pancytokeratin antibody in OPA-N (left) and OPA-E (right), OM x100. (C,D) anti-SP-C antibody labels neoplastic cells and normal type II pneumocytes in OPA-N (left) and OPA-E (right) (arrow). (E) anti-CCSP antibody shows weak labelling of tumour and strong labelling of Clara cells in bronchial epithelium, OPA-E OM x100, OM x200. (F) anti-synaptophysin antibody shows focal labelling within tumour nodule of OPA-E. OM x200.

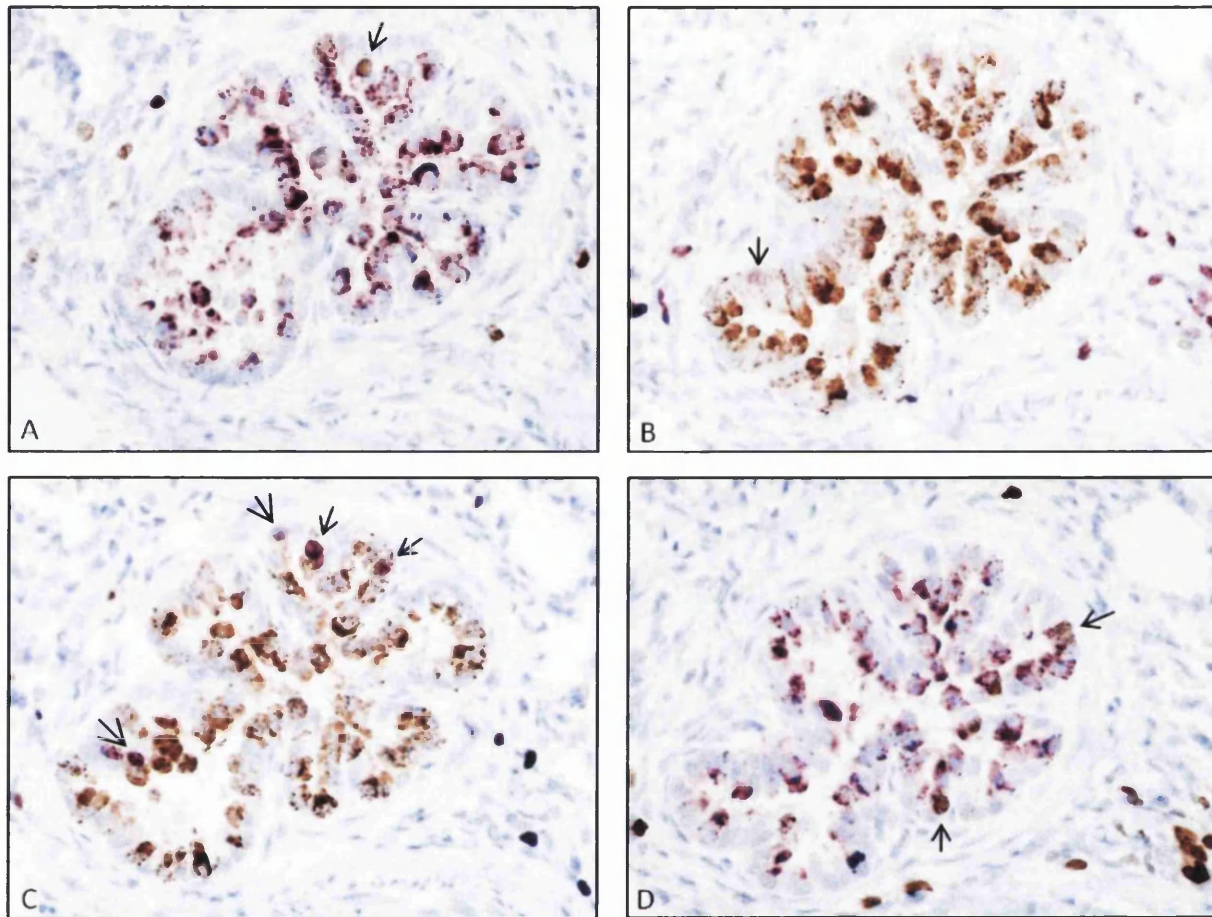


Figure 4.6 Optimisation of dual labelling IHC using anti-CCSP antibody (1/20 000) and anti-Ki-67 antibody (1/1000). (A) Bronchiole: anti-CCSP antibody VIP, anti-Ki-67 antibody DAB. Arrow points to single cell labelling for both antigens. (B) Bronchiole: anti-CCSP antibody DAB, anti-Ki-67 antibody VIP. Arrow points to single cell with faint labelling with both antigens. (C) Bronchiole: anti- Ki-67 VIP, anti-CCSP antibody DAB. 4 cells labelling with both antigens (arrows). (D) Bronchiole: anti-Ki-67 antibody DAB, anti-CCSP antibody VIP 4 cells show labelling for both antigens. The most sensitive method which was easiest to visualise used the weakest antibody first (Ki-67 1/1000) with the strongest substrate (DAB) shown in (D).

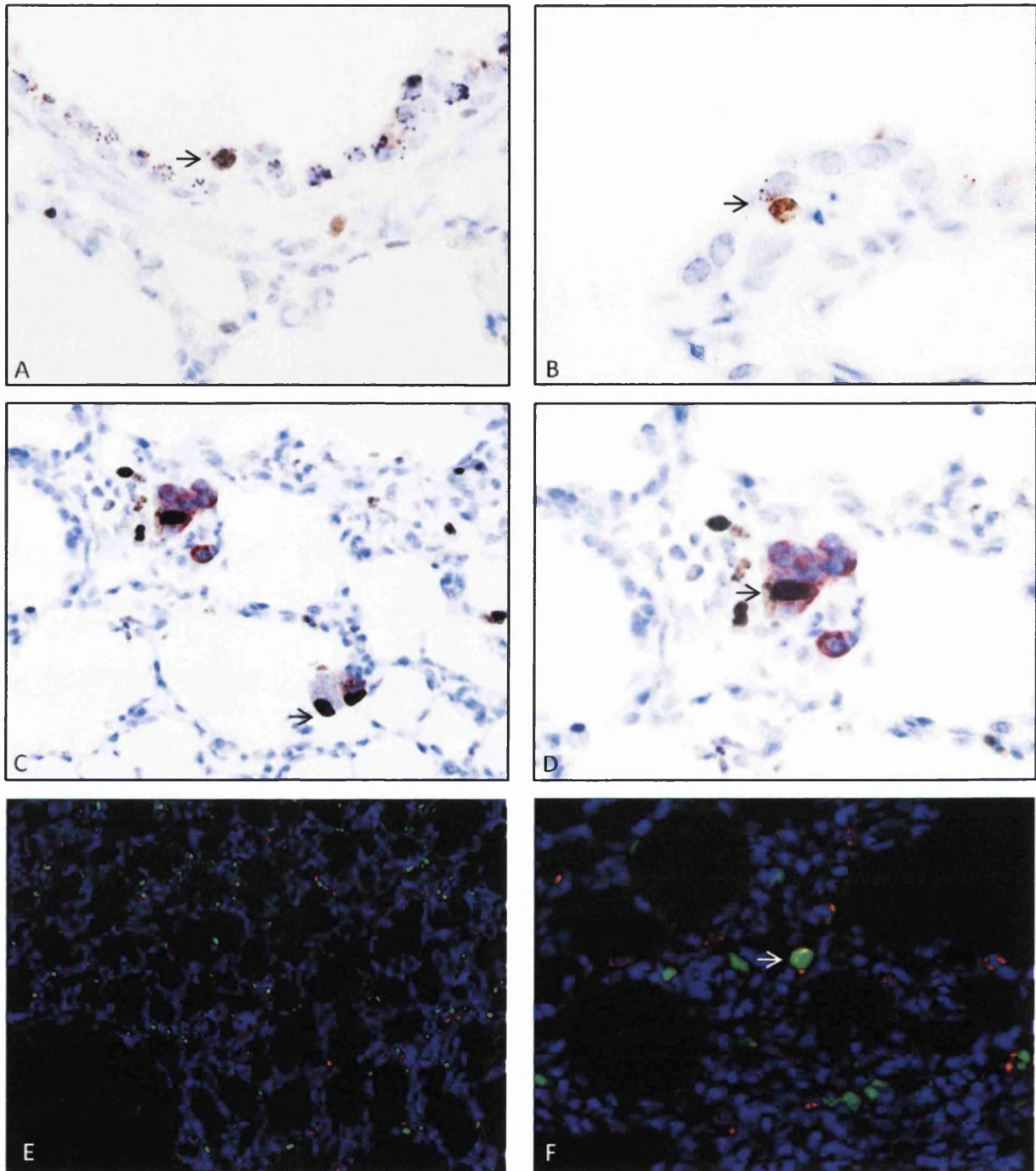


Figure 4.7 IHC to identify proliferative capacity of Clara cells, NEBs and type II pneumocytes on OPA-E 10 days PI. (A) Bronchiole: dual labelling of cell with anti-Ki-67 (DAB) and anti-CCSP (VIP) (arrow) OM x600. (B) Respiratory bronchiole dual labelling of cell with anti-Ki-67 (DAB) and anti-CCSP (VIP) (arrow) OM x1000. (C) NEBs: dual labelling of multiple cells in two NEBs with anti-Ki-67 (DAB) and anti-synaptophysin (VIP) (arrow) OM x400. (D) Detail of (C) OM x600. (E): Alveolar region. Green: anti-Ki-67. Red; anti-SP-C. Only occasional cells show dual labelling of Ki-67 and SP-C. OM x200. (F) Detail of (E) showing dual labelled cell (arrow) OM x400.

4.2.4 Validation of JSRV SU antibody using IHC.

To identify viral protein expression using IHC, a panel of anti-JSRV antibodies was tested on positive and negative control tissue (see Table 2.3). Of these, the anti-JSRV SU monoclonal pool gave the most satisfactory results (Figure 4.8 A, B). It was tested on OPA-N, and even in the presence of necrosis and mixed inflammatory cells labelling was highly sensitive and specific for neoplastic cells only (Figure 4.8 C, D). OPA-E tumours from animals 72 days post inoculation also labelled positively for JSRV SU (Figure 4.8 E, F).

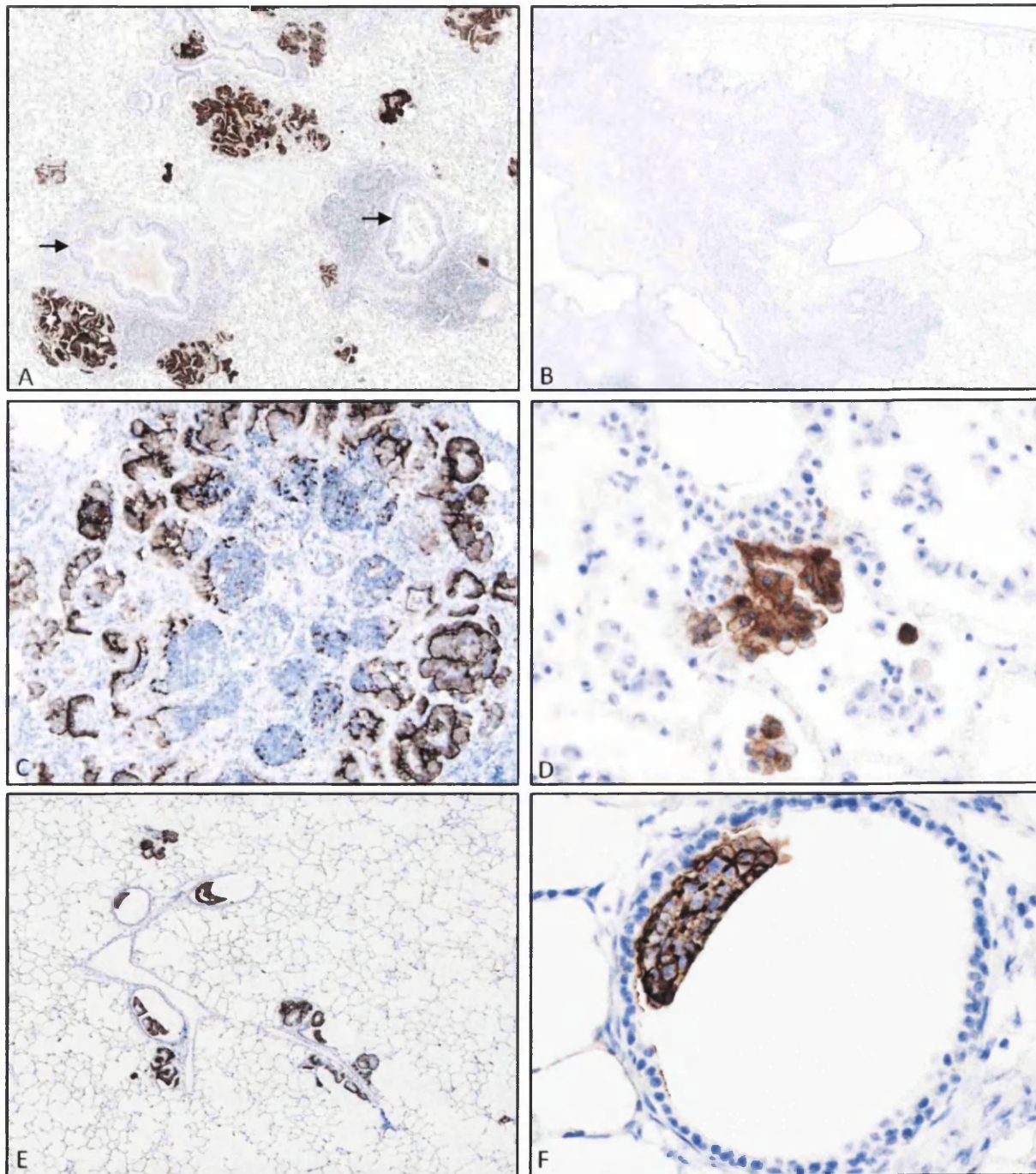


Figure 4.8 IHC using anti-JSRV SU antibody on cases from OPA-N and OPA-E. (A) OPA-N showing specific labelling of tumour foci (brown) but not normal bronchial epithelium (arrows) OM x 20. (B) Negative control ovine lung tumour from aged sheep not infected with JSRV, no labelling OM x20. (C) OPA-N tumour with central necrosis showing specific labelling of peripheral neoplastic tissue only OM x100. (D) OPA-N showing specific labelling of neoplastic cells but not surrounding inflammatory cells. OM x400. (E) OPA-E showing strong labelling of multiple tumour foci. (F) OPA-E with labelling of early tumour in bronchiole. Note cell surface staining pattern OM x 400.

4.2.4.1 Detection of single cells expressing JSRV SU

To identify single cells expressing JSRV SU protein, and hence the target cell for JSRV, the optimised anti-JSRV SU Mab was used to label lung tissue from lambs 10 days post-inoculation with JSRV₂₁. The sensitivity of JSRV SU antigen detection was compared between tissues fixed in ZS and FS. As formalin can mask antibody binding sites with cross linking, antigen retrieval (AR) methods were required to break these down before antibody incubation in FS tissue (see Table 2.2). The total number of single cells and clusters (two cells or more) visualised with DAB chromogen were counted for each animal. Initially all 24 ZS fixed sections from each lung were examined (96 slides in total). Very few single positive cells were detected and there was increased background and non specific labelling of some normal epithelial cells. The experiment was repeated using formalin fixed tissue with AR. This method proved to be more sensitive and specific, and as a result only five slides per lung were needed to provide adequate numbers of positive single cells for analysis (Table 4.1).

Formalin fixed tissue with AR was used for all further IHC experiments. All 96 sections of lung tissue from animals 3 days PI, and 10 sections from negative control mock and non-inoculated lambs from 3 and 10 days PI were also examined for JSRV SU protein expression, but none was found (Table 4.2).

Table 4.1 Comparison of fixation methods and detection of single/clusters of cells expressing virus in OPA-E lambs, 10 days PI using IHC.

Fixative	2852 E		2858 E		2854 E		2856 E	
	Single	Cluster	Single	Cluster	Single	Cluster	Single	Cluster
Zinc fixed 24 slides per animal	0	0	0	11	3	29	2	36
Formalin fixed + AR 5 slides per animal	3	2	2	14	12	20	10	15

Table 4.2 A summary of positive labelling for SU antibody on formalin fixed tissue from lambs 3 and 10 days PI.

Time PI	Total number of sections examined from all 8 animals at each time point			Number of sections with positive foci			Total number of positive single cells	Total number of positive clusters
	Infected	Mock	No inoculate	Infected	Mock	No inoculate		
3 days	96	10	10	0	0	0	0	0
10 days	20	10	10	13	0	0	27	51

4.2.4.2 Location of cells showing JSRV SU protein expression 10 days post inoculation

In order to obtain a more detailed phenotypic identification of JSRV SU positive cells, the location of single and clusters of cells were assigned to one of the five regions in the lung: bronchus, bronchiole, terminal bronchiole, respiratory bronchiole and alveolar region (Table 4.3, Figure 4.9 and 4.10.). No JSRV SU positive cells were found in the bronchi. Single and clusters of JSRV SU positive cells were found in all remaining regions of the lung. Both location and number of positive cells was seen to vary between the four JSRV₂₁ infected lambs (Figure 4.9).

These findings indicate that JSRV is expressed by single cells in all levels of conducting and respiratory airways. Previous work shows epithelial cells lining the tract in these areas to include ciliated epithelial cells, Clara cells, NE cells, NEBs and alveolar type I and type II pneumocytes (Table 3.3). Cells located at the BADJ, shown to harbour BASCs in mice (Kim et al., 2005), also appeared to be targeted on occasion (Figure 4.10 E,F).

Table 4.3 Summary of size and location of positive labelling cells in four lambs 10 days PI

Location	Number of positive single cells	Number of positive clusters
Bronchus	0	0
Bronchiole	10	4
Terminal bronchiole	4	6
Respiratory bronchiole	6	24
Alveolar region	7	18

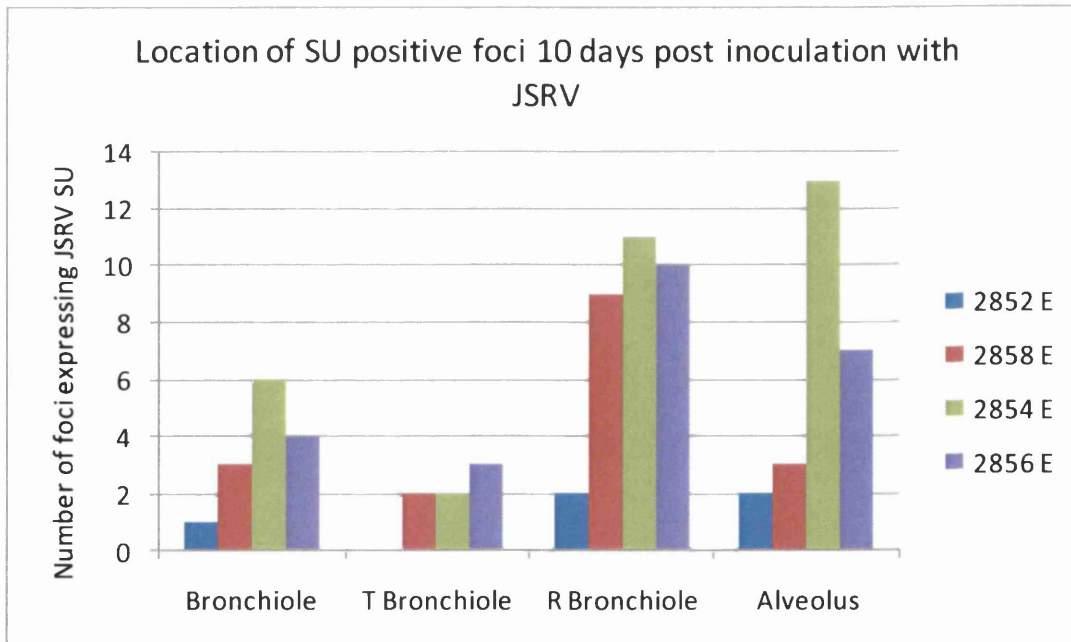


Figure 4.9 Variation in location of JSRV SU expression both within and between animals.

Note: JSRV SU expressing foci include single cells and clusters.

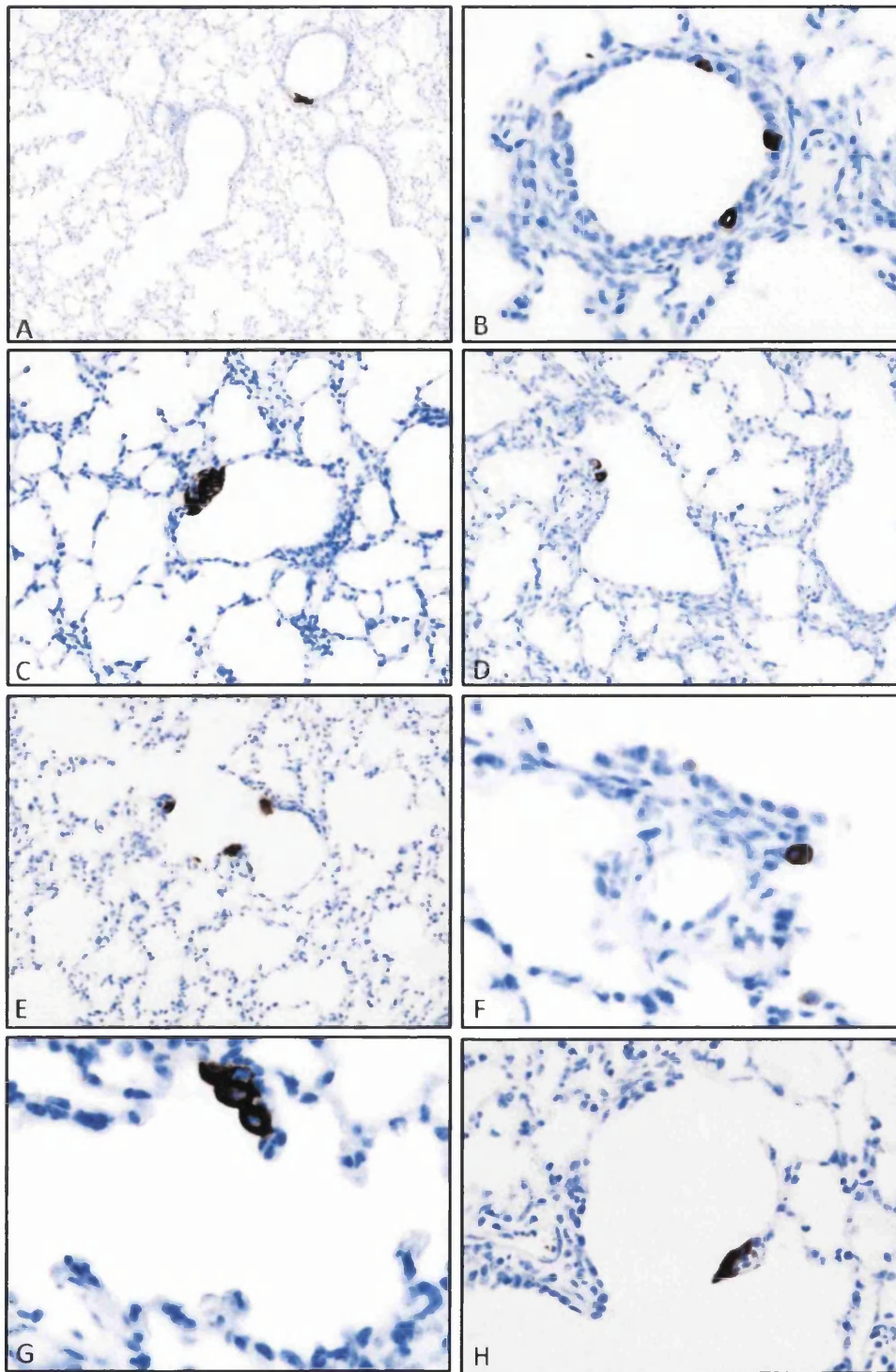


Figure 4.10 IHC using anti JSRV SU Mab to label cells in lung tissue from lambs 10 days post inoculation. (A) 2858E: positive cluster in terminal bronchiole.OM x 100. (B) Positive single cells in bronchiole.OM x600. (C) 2856 E: positive cluster in respiratory bronchiole.OM x200. (D) 2856 E: positive single cells in respiratory bronchiole. (E) 2854E: positive clusters in respiratory bronchioles at BADJs. (F) 2854 E Positive single cell in respiratory bronchiole at BADJ.OM x600. (G) 2854E: positive cluster lining the alveolar duct wall.OM x600. (H) 2856 E Positive cells lining the smooth muscle ring on the free edge of an alveolar septa.OM x400.

4.2.5 Identification of JSRV target cell using serial sections

Serial sections were cut from blocks showing JSRV SU positive cells. These were then labelled with cell specific markers to try and localise the presence of viral protein to cell type. Figure 4.12 shows that larger groups of cells were identified on multiple sections. However, even though tissue sections were thin (5 μm), it was rare to see the same cell in adjacent sections due to small changes in anatomy.

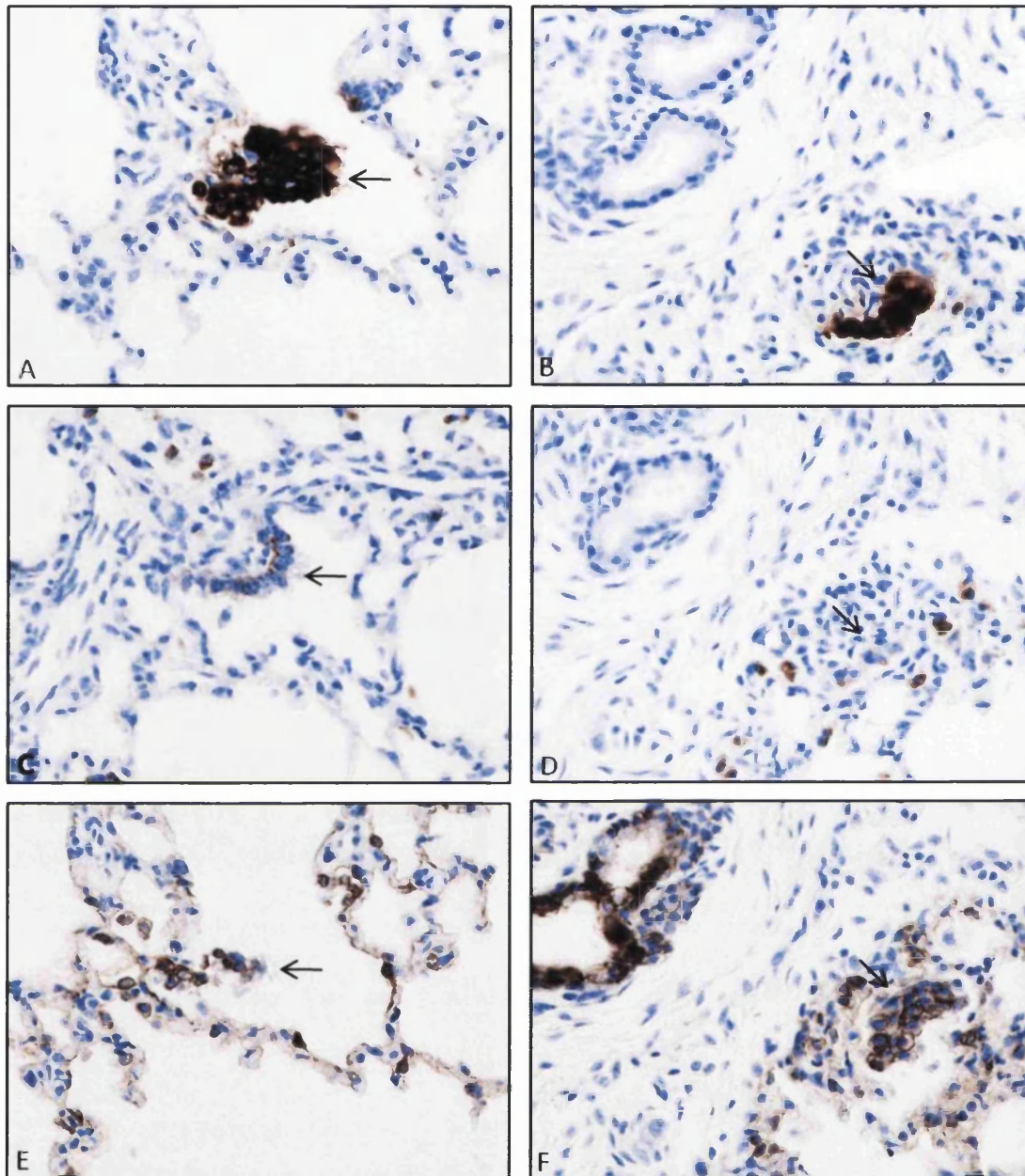


Figure 4.11 IHC of serial sections stained with anti-JSRV SU Mab (A,B), anti-DC-LAMP antibody (C,D) and anti-pancytokeratin antibody (E,F). The same cluster of cells (arrow) is visible in each of the three serial sections (A,C,E) and B,D,F). (A,B) Cells labelling for JSRV SU label faintly in (C,D) for DC LAMP (a type II pneumocyte marker). (E,F) show moderate labelling for pan cytokeratin (an epithelial cell marker).OM x400.

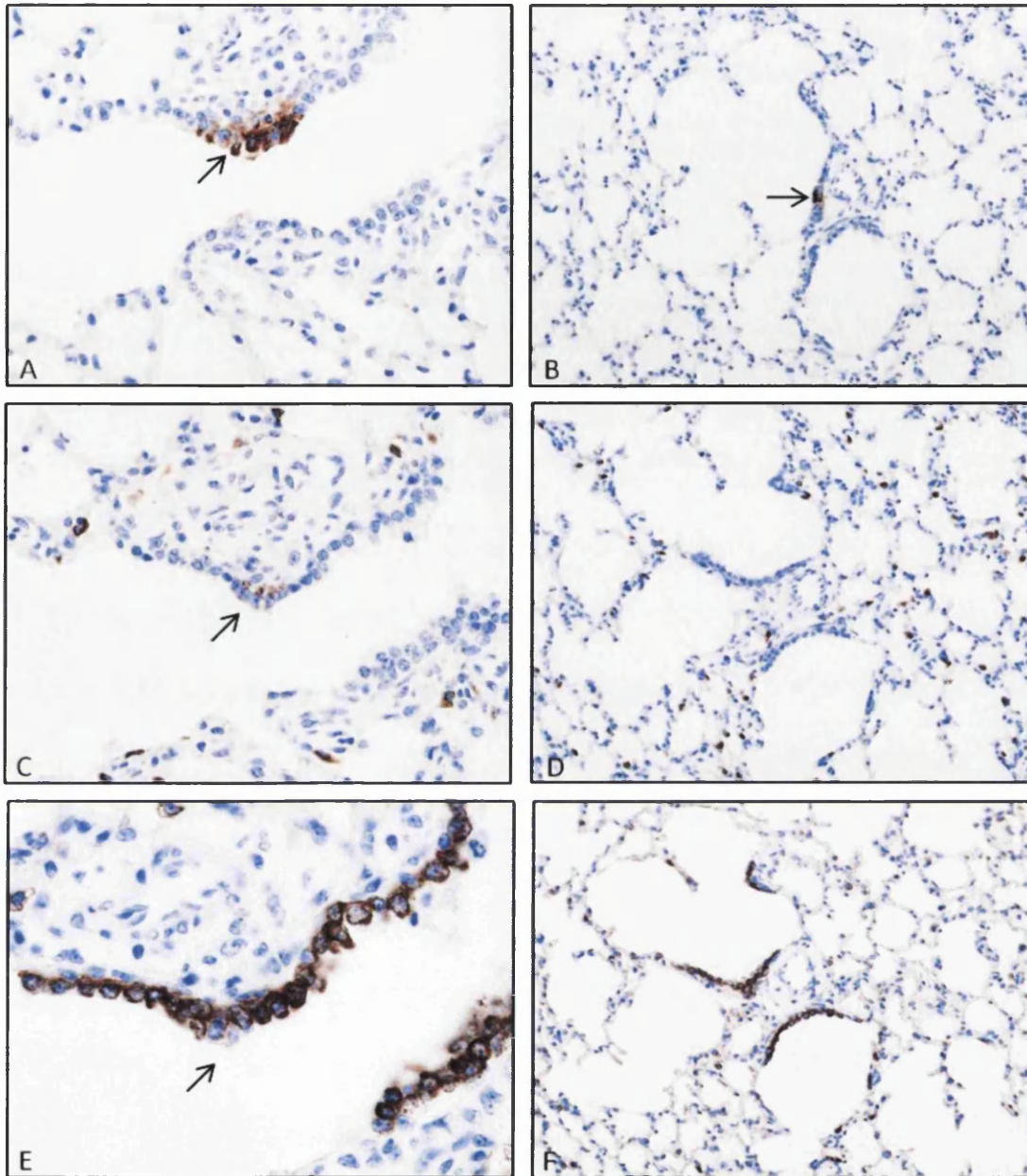


Figure 4.12 IHC of serial sections labelled with anti-JSRV SU, anti-DC LAMP, SP-C and anti-pancytokeratin antibodies. (A) A JSRV SU positive focus in the respiratory bronchiole. OM x400. (C) Same focus labels positively with anti- DC LAMP in serial section. OM x400. (E) Partial labelling of same focus in serial section with anti-cytokeratin. OM x 600. (B) A single JSRV SU positive cell in the respiratory bronchiole.. Focus lost on serial sectioning in (D) anti-DC-LAMP and (F) anti-cytokeratin.OM x200.

4.2.6 Identification of JSRV target cell using dual labelling

To enable better localisation of multiple antigens to a single cell, sections were labelled with two antibodies using DAB and VIP chromagen substrates to distinguish between the different antigens (see 2.5.3). To avoid cross reactions, only antibodies raised in different species were used together. FS sections from animals 71-92 PI were used to validate the technique, as JSRV SU positive cells were abundant in most of these sections. The weakest antibody (ie. the one used at the highest concentration) was incubated first for each experiment (Table 4.4).

Dual labelling with anti-JSRV SU and anti-CCSP antibodies showed that tumour foci and individual cells were positive for JSRV SU but not CCSP (Figure 4.13, 4.14). Comparison of the distinct labelling patterns of different cell types showed JSRV SU protein located predominantly on the surface of cells, and CCSP in the cytoplasm (Figure 4.13 C,D). Dual labelling for synaptophysin and JSRV SU showed virus to be associated with NEBs in the alveolar region, but not single NE cells in the bronchiole (Figure 4.15 A,B). As CCSP and SP-C antibodies were both polyclonal reagents from rabbits, tissues were incubated with another type II pneumocyte marker, anti-DC-LAMP antibody (rat monoclonal) instead of SP-C. (Salaun et al., 2004). These were shown to colocalise in a previous experiment (Appendix 2). In some sections, single cells in the bronchiolar epithelium and tumour foci were seen to label strongly for both JSRV SU and DC-LAMP proteins (Figure 4.15 C,D). One of these cells was located at the BADJ (Figure 4.15G). Cells labelling for SP-C in this region were previously identified (Figure 3.3L) and it is where BASCs have been found in mice (Kim et al., 2005). In other sections, cells labelled only for JSRV SU and not DC-LAMP, both in the bronchioles and the alveolar region (Figure 4.15A, B).

Table 4.4 Summary of antibodies used for dual labelling

First primary antibody	Dilution	Substrate	Second primary antibody	Dilution	Substrate
anti- SRV SU	1/400	VIP	anti-CCSP	1/20 000	DAB
anti-synaptophysin	1/50	DAB	anti- JSRV SU	1/400	VIP
anti-DC-LAMP	1/200	DAB	anti-JSRV SU	1/400	VIP

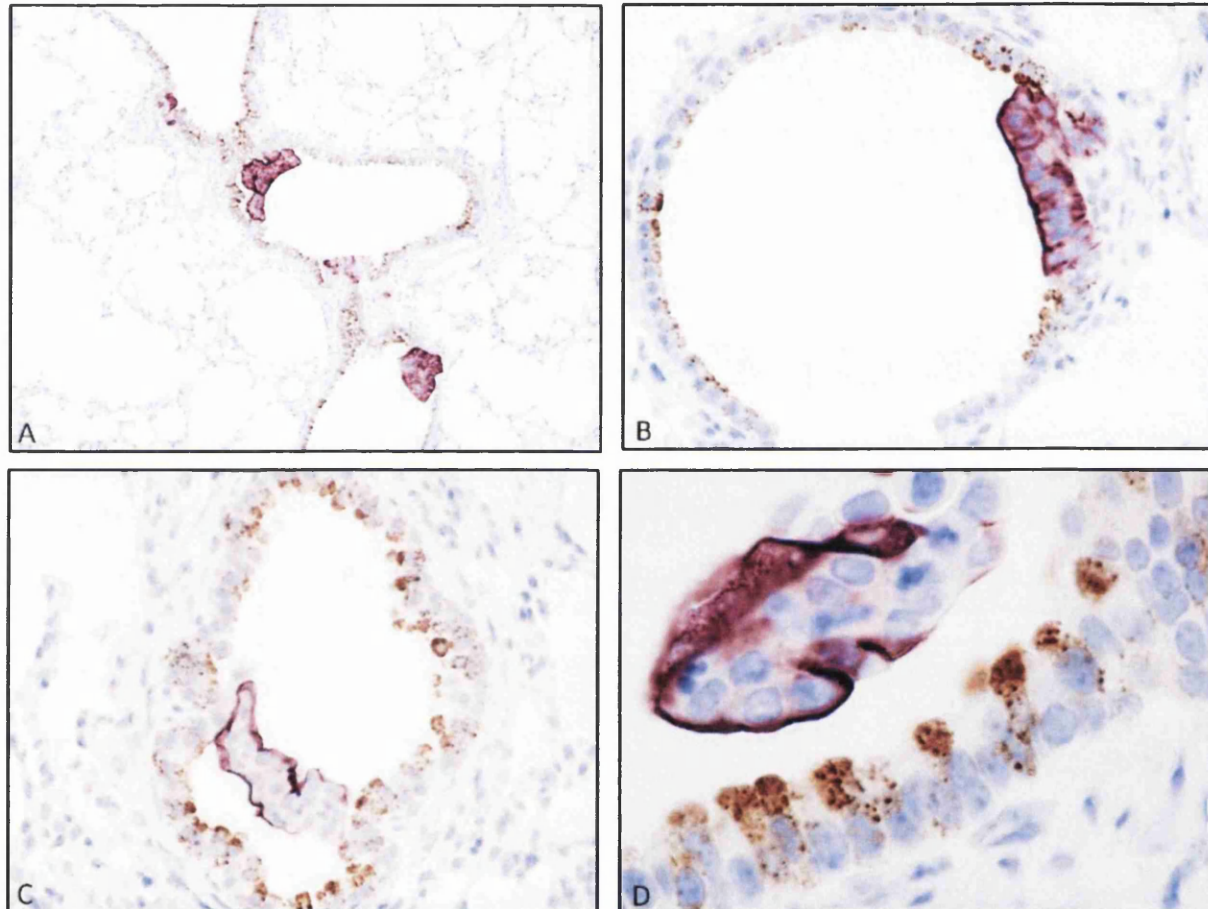


Figure 4.13 Dual IHC on lungs from experimental infections. Anti-JSRV SU antibody, VIP substrate (purple) and anti-CCSP antibody, DAB substrate (brown). (A) Bronchioles with tumour, OM x100. (B) Respiratory bronchiole with early tumour, OM x400. (C) Bronchiole with tumour in lumen displaying surface staining pattern of JSRV SU, OM x400. (D) Section comparing the labelling patterns between JSRV SU (strong surface labelling, faint cytoplasmic label) and CCSP (strong granular cytoplasmic). OM x1000.

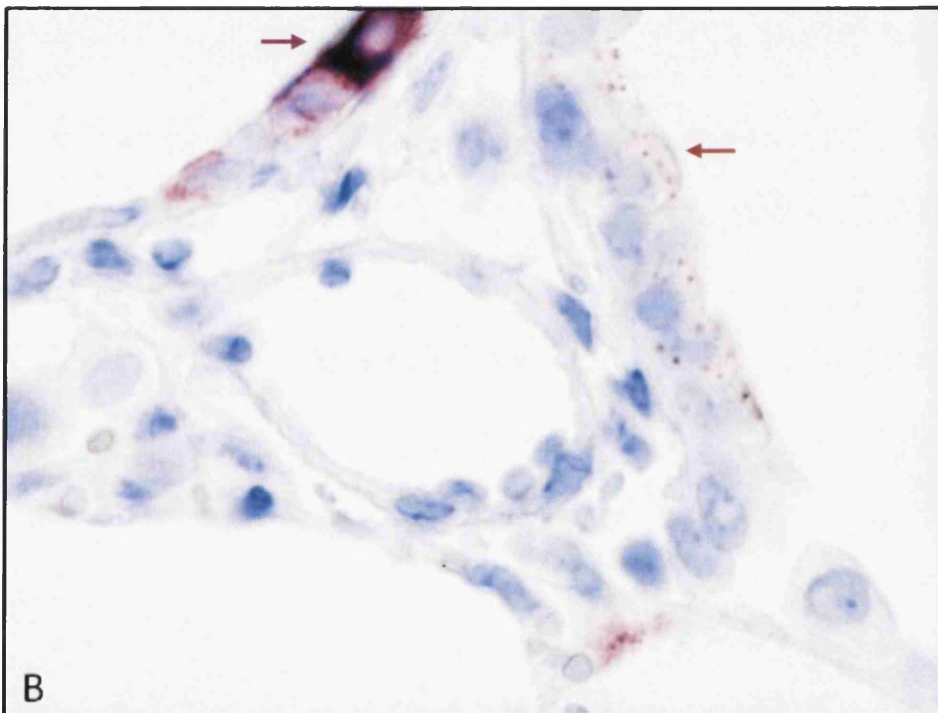
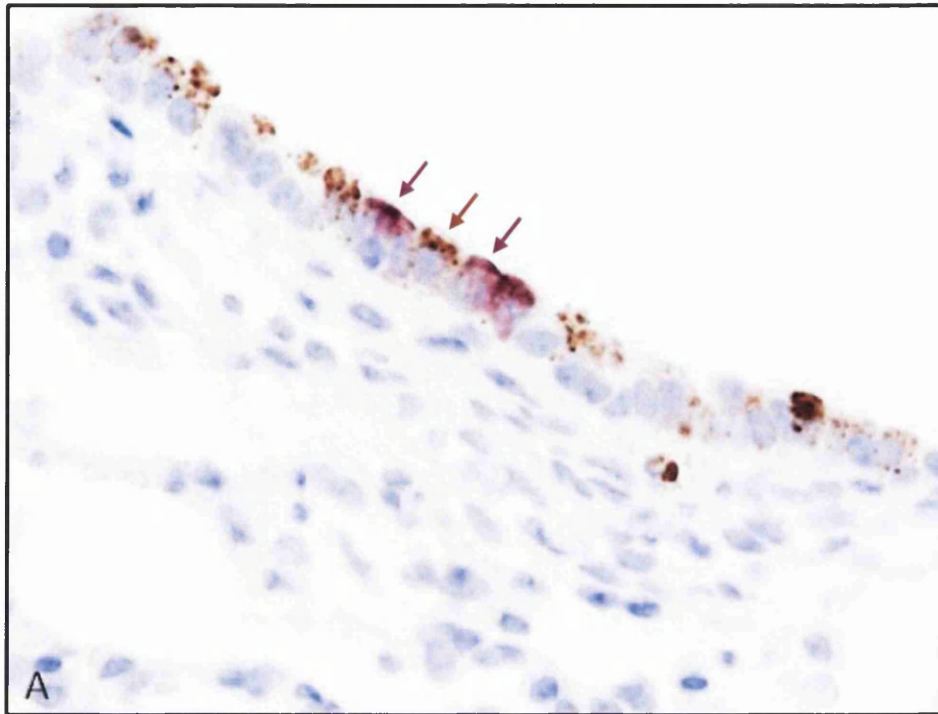


Figure 4.14 Dual labelling with anti-CCSP antibody (brown) and anti-JSRV antibody (purple). (A) Respiratory bronchiole with adjacent JSRV SU (purple arrow) and CCSP (brown arrow) positive cells, OM x400. (B) Respiratory bronchiole with separate JSRV SU (purple arrow) and CCSP (brown arrow) positive cells, OM x600. Due to the intensity of the purple stain, it is not possible to identify if these cells are also expressing CCSP.

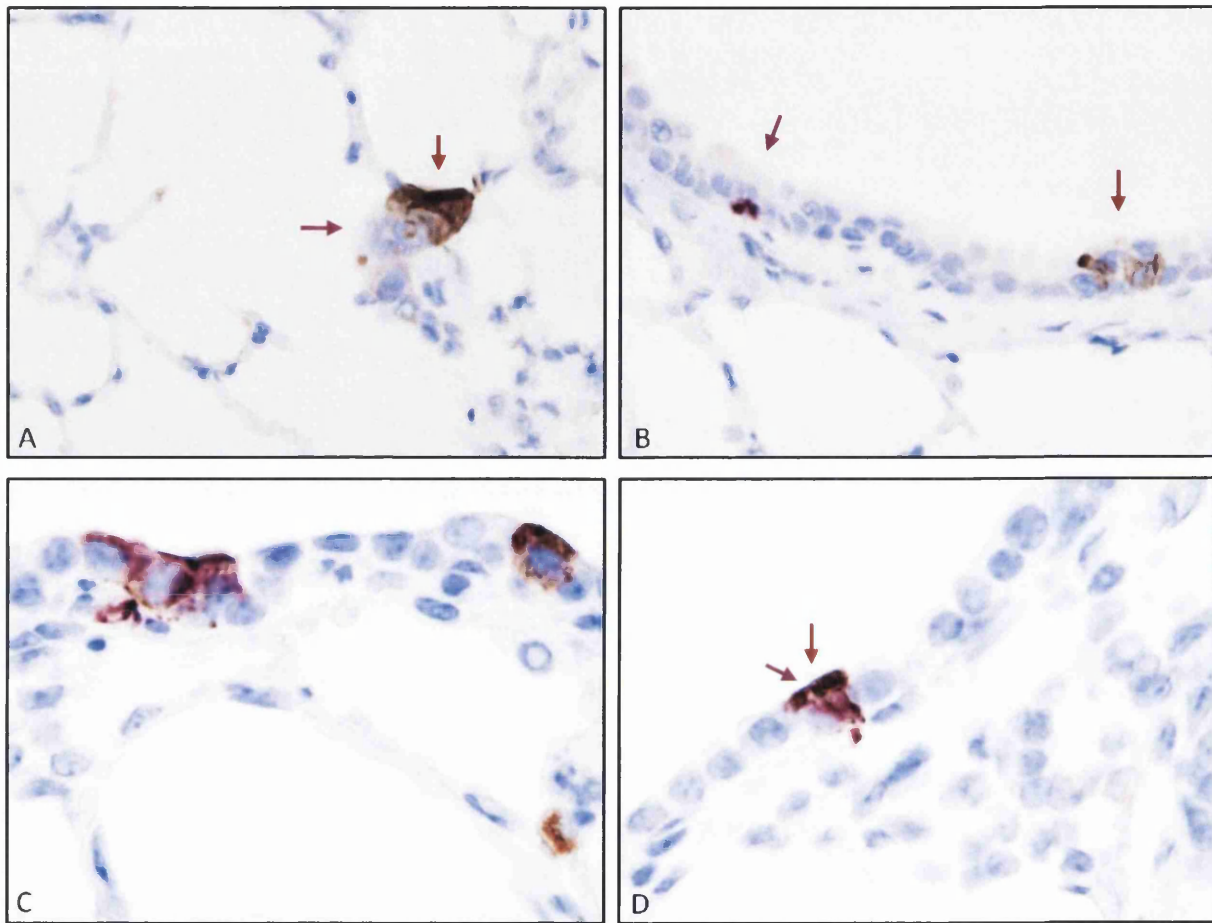


Figure 4.15 Double IHC to determine the phenotype of single and clusters of cells positive for JSRV SU. (A) Alveolar duct wall: NEB (purple, arrow) with associated JSRV SU (brown, arrow) label, OM x600. (B) Bronchiole: separate synaptophysin positive NE cell (purple arrow) and JSRV SU positive cells (brown arrow). OM x600. (C) Respiratory bronchiole: DC-LAMP (brown) and JSRV SU (purple) both labelling cluster, OM x1000. (D) Respiratory bronchiole: DC-LAMP (brown) and JSRV SU (purple) both labelling single cell (arrows), OM x1000.

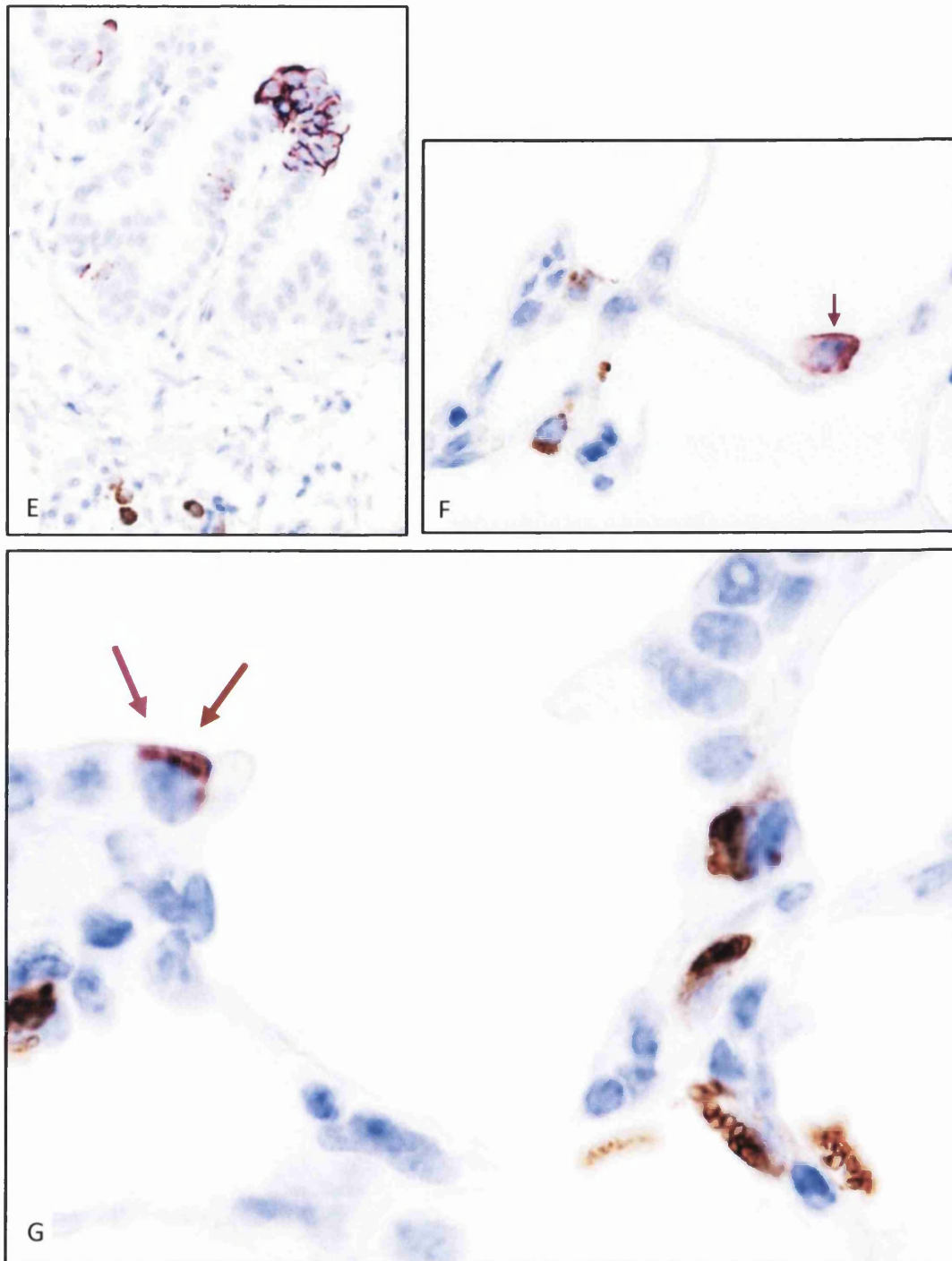


Figure 4.15 (cont.) Double IHC to determine the phenotype of single and clusters of cells positive for JSRV SU
 (E) Bronchiole , cluster of epithelial cells labelling with anti- JSRV SU antibody (purple) but not anti-DC-LAMP antibody (brown), OM x400. (F) Alveolus, single cell labelling for anti-JSRV SU antibody (purple arrow) but not anti-DC-LAMP antibody (brown), OM x1000. (G) BADJ: single cell positive for anti-JSRV SU (purple arrow) and DC-LAMP (brown arrow), OM x1000

4.2.7 Identification of JSRV target cell using immunofluorescence

4.2.7.1 Antibody optimisation

While the dual labelling techniques using DAB and VIP chromogens for antigen visualisation were effective for detecting antigens in separate cells, the similar hue (brown and purple) made it difficult to definitively identify one cell labelling for two antigens.

Immunofluorescence was chosen as a more sensitive and specific technique to detect multiple antigens in the same cell. It also provided the opportunity to localise antigens within the cell using a Z stack of optical sections. Two of the three primary antibodies of interest were derived from the same species (CCSP and SP-C) and so both indirect single colour labelling and primary antibody-Fab fragment complexes were used (see section 2.5). Fluorescent labels from separate ranges of the spectrum were chosen, and conditions for each antibody were re-optimised separately (Table 4.5). Multiple labelling was optimised on tissue from JSRV₂₁ infected lung 72-91 days PI (Figure 4.16).

Table 4.5 Optimised concentrations of antibody and fluorescent substrates / Fab fragments used for visualisation

Primary antibody	Original dilution	Antigen visualisation	Dilution for immunofluorescence	Antigen visualisation
anti-JSRV SU	1/800	DAB/VIP	1/400	Tyramide Alexa fluor [®] -488
anti-CCSP	1/20000	DAB/VIP	1/1000	Dylight™ 649 Fab
anti-SP-C	1/4000	DAB/VIP	1/2000	Tyramide Alexa fluor [®] 568
anti-synaptophysin	1/50	DAB/VIP	1/50	Tyramide Alexa fluor [®] -568

Using combinations of these antibodies, it was anticipated that the phenotypic protein expression of single cells expressing virus would be identified. The unexpected type II pneumocyte protein expression in cells of the respiratory epithelium from previous experiments (see Figure 3.3L) also raised the question of whether anti-JSRV SU antibody might be targeting these cells. Only one cell in all of the sections examined was found to express SP-C and CCSP. It was located at the BADJ of a respiratory bronchiole in a negative control animal (Figure 4.17).

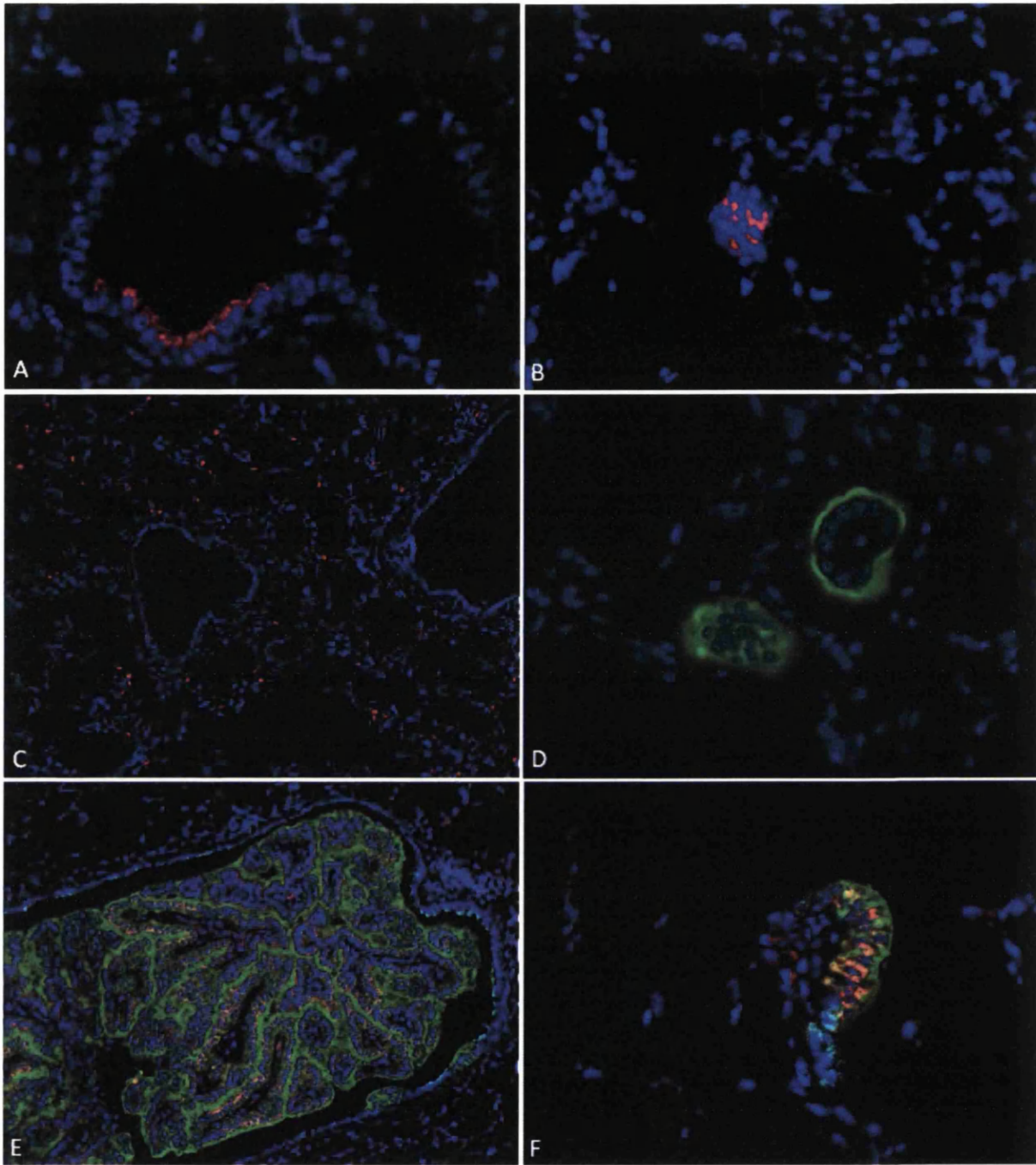


Figure 4.16 Optimisation of fluorescent antibodies for single and multiple labelling techniques in OPA-E lambs 72-91 days PI. (A) Respiratory bronchiole, cytoplasmic labelling of Clara cells. Red: anti-CCSP/Fab 649 fragment complex.OM x400. (B) Alveolar region, labelling of NEB. Red: anti-synaptophysin visualised with Tyramide-568.OMx400. (C) Alveolar region, labelling of type II pneumocytes. Red: anti-SP-C, visualised with Tyramide-568. OM x100. (D) OPA tumour foci. Green: anti-JSRV SU visualised with Tyramide-488.OM x400. (E) OPA in bronchiolar lumen. Green: anti-JSRV SU, red: anti SP-C, blue:anti-CCSP. OM x200. (D) OPA focus. Green: anti-JSRV SU, red: anti-SP-C, blue: anti-CCSP, yellow: colocalisation of SP-C and JSRV SU. OM x400.

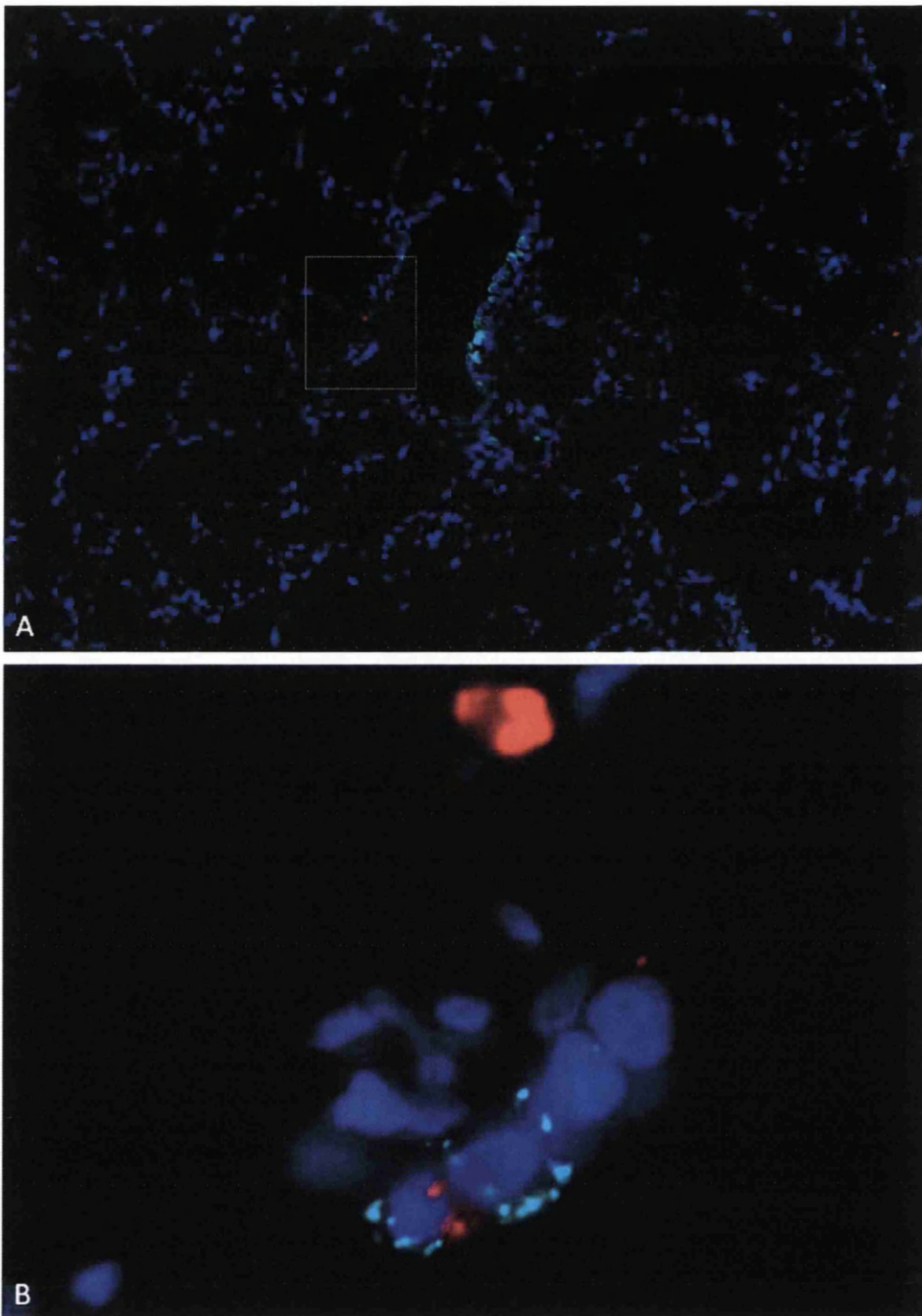


Figure 4.17 BADJ showing BASC-like cell in a negative control lamb. Red: anti-SP-C. Light blue: anti-CCSP. (A) Low power view to allow orientation of the respiratory bronchiole. Light blue highlights a length of respiratory epithelium. OM x100. (B) is detail of (A), showing dual labelling of one cell with SP-C (red) and CCSP (light blue) at the BADJ (arrow). OM x1000. Nuclei, DAPI (dark blue).

4.2.7.2 Tissue sectioning

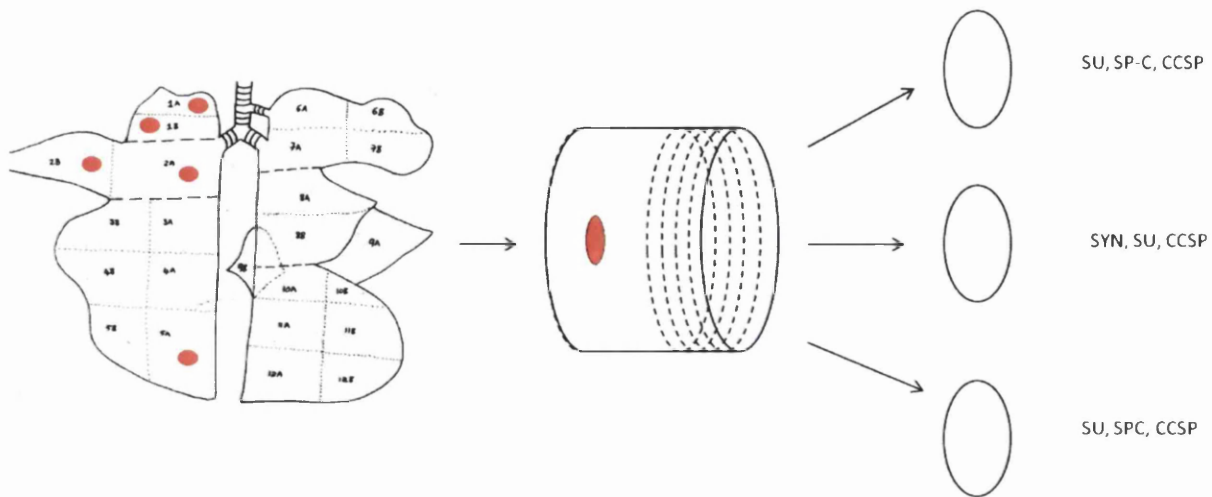


Figure 4.18 Sequential sectioning of lung tissue for multiple labelling using immunofluorescence. Slides from sites 1a,1b,2a,2b and 5a (red dots) were examined for JSRV SU expression using DAB substrate. Three serial sections were cut from those with JSRV SU expression, and triple labelled with SU, SP-C, CCSP/SYN, SU, CCSP/SU, SP-C, CCSP using immunofluorescence.

In order to identify suitable tissue sections for immunofluorescence, sections were first screened for JSRV SU expression using DAB substrate. Five sections from each of the four JSRV₂₁ infected lambs at 10 days post inoculation were examined. Sequential sections were cut from those with more than one single cell expressing virus (Figure 4.18). Three serial sections were labelled with multiple fluorescently labelled antibodies (Figure 4.16 E,F). The aim was to identify the same cell expressing virus in adjacent sections, and determine the expression of SP-C, CCSP and synaptophysin proteins.

4.2.7.3 Results of immunofluorescence

Results are shown in Figures 4.19-4.23. The phenotypes of a total of 13 single cells expressing JSRV SU were examined. 4/13 of these cells were examined for the expression of all three mature phenotypes, CCSP, SP-C and synaptophysin. Of these 3 labelled for JSRV SU only, and one labelled for JSRV SU and CCSP. 2/13 were examined for the expression of the two mature phenotypes CCSP and synaptophysin. Of these, both labelled for JSRV SU only. 7/13 were examined for the expression of the two mature phenotypes CCSP and SP-C. Of these, two labelled for JSRV SU only, two labelled for JSRV SU and CCSP only, one labelled for JSRV SU and SP-C only, and one labelled for JSRV SU, CCSP and SP-C. In summary, single cells expressing virus either labelled with no other marker, with CCSP, with SP-C or with CCSP and SP-C. None of these single cells labelled with synaptophysin.

Videos of the Z stacks which correspond to the following figures are shown in the accompanying CD. Z stacks are obtained by taking a series of photographs through the section at specified thickness intervals. An apotome grid is used for measurement. This enables a detailed analysis of the precise location of protein expression within the cell. Video 1 corresponds with Figure 4.19 B/C. Green, anti- JSRV SU. Light blue, anti-CCSP. Dark blue, DAPI nuclei. The slide is also labelled with anti-synaptophysin but no positive labelling is shown in this section. As the video runs, watch the green labelled cell in the centre. There is no evidence of light blue labelling, in contrast to the adjacent cells lining the respiratory epithelium. Video 2 corresponds with Figure 4.21. Green, anti-JSRV SU. Light blue, anti-CCSP. Dark blue, DAPI nuclei. Watch the green cell, and colocalisation of JSRV SU with CCSP. Video 3 corresponds with Figure 4.22. Green, anti-JSRV SU. Red, anti-SP-C. Viral expression is limited to a single cell expressing SP-C in the alveolar region. Video 5 has no corresponding figure. It shows another example of a single cell expressing JSRV SU (green) and SP-C (red).

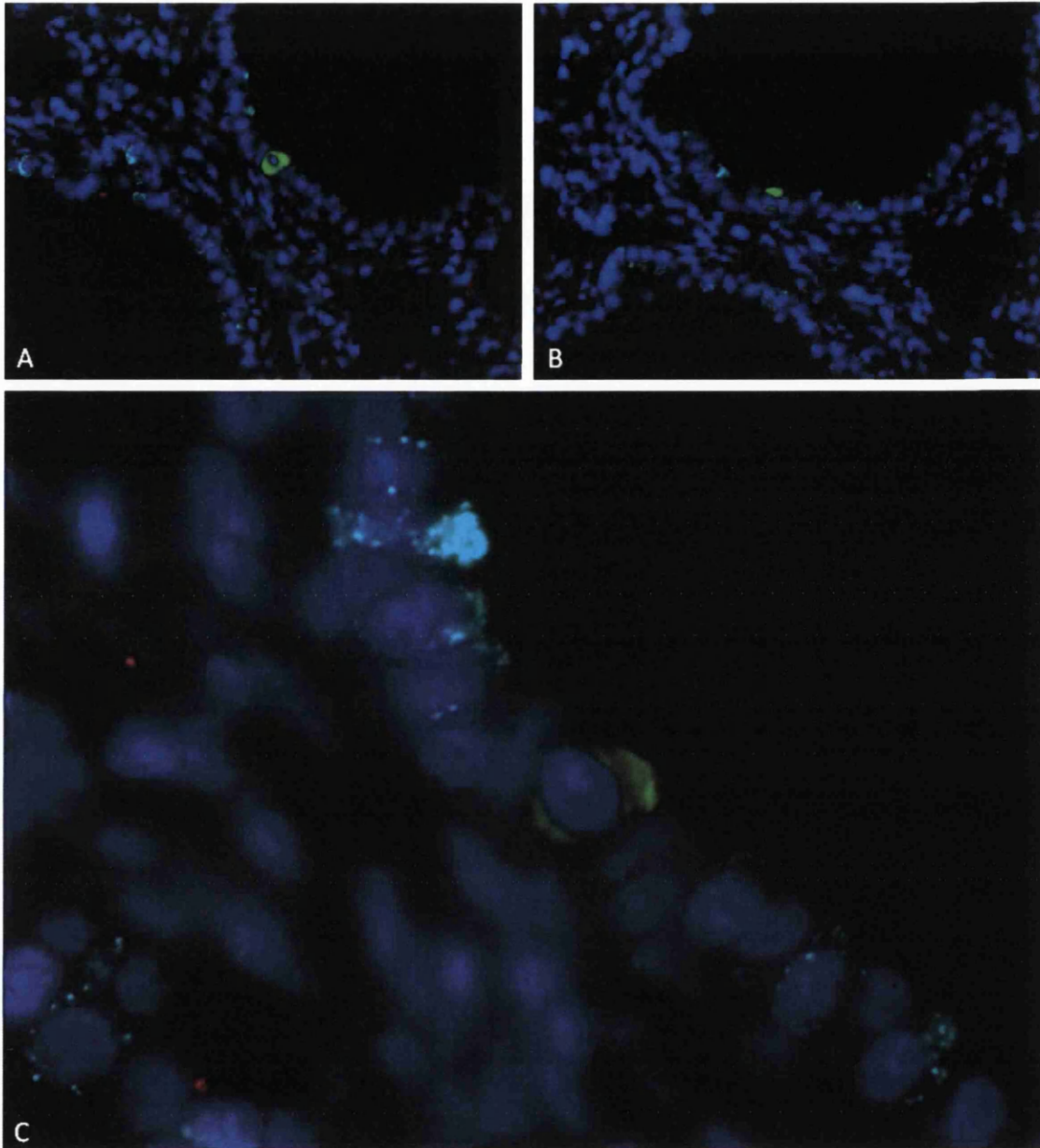


Figure 4.19 JSRV SU positive cell in respiratory bronchiole, which does not label with CCSP, SYN or SP-C. Serial sections (A) and (B) from lamb 2852 E. (A) Green: anti JSRV SU. Red: anti-SP-C. Light blue: anti-CCSP. OM x400. (B) Green: anti-JSRV SU. Red: anti-synaptophysin. Light blue: anti-CCSP. OM x400. (C) Detail of B showing single cell expressing JSRV SU. OM x1000. All nuclei DAPI (blue). **Z stack section on CD: AVI video 1.**

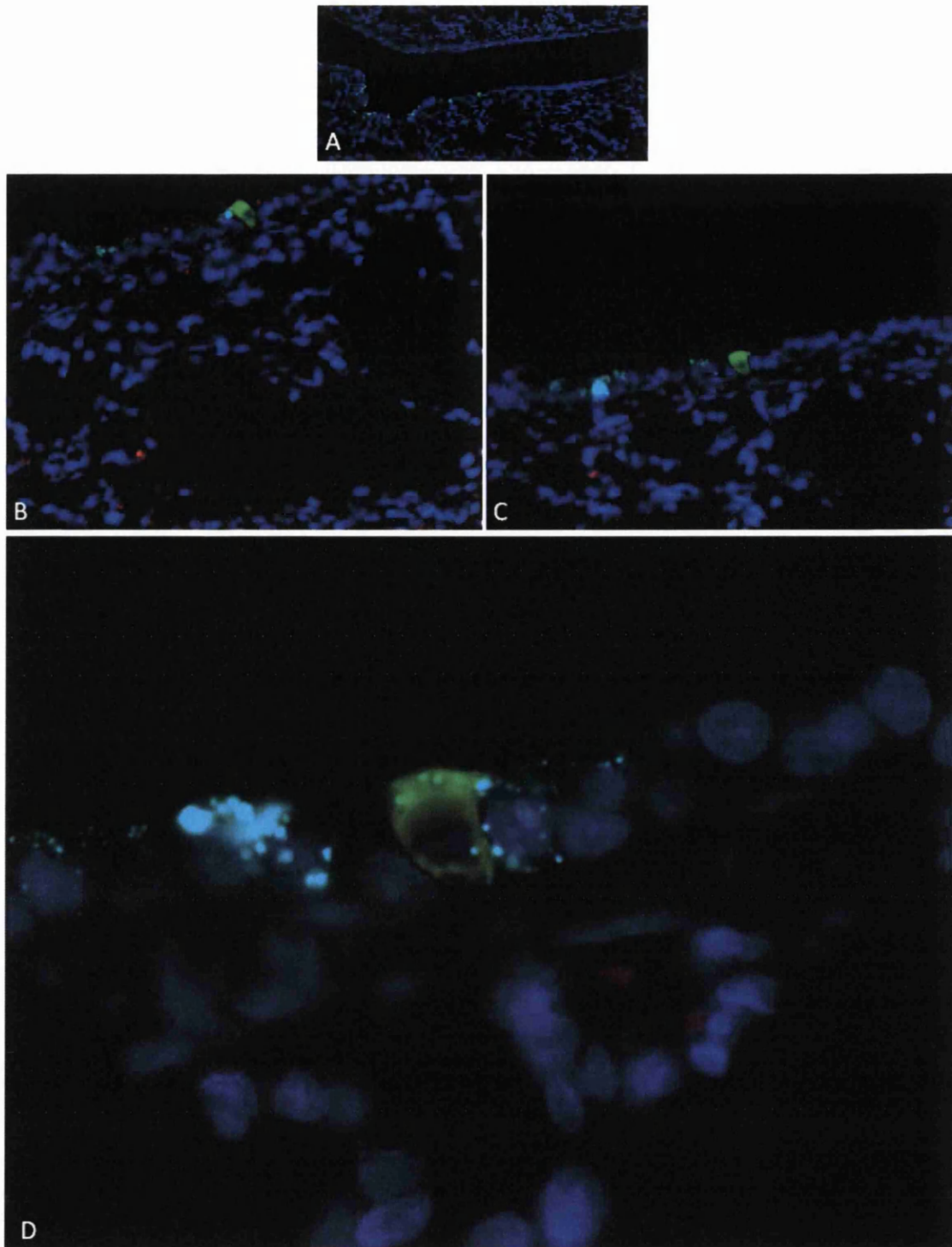


Figure 4.20 Single cell in terminal bronchiole with positive labelling for JSRV SU and CCSP only. Serial sections from 2858 E were cut. (A) Terminal bronchiole. Red: anti-synaptophysin. Green: anti-JSRV SU. Light blue: anti-CCSP. OM x100. (B) Red: anti-SP-C. Green: anti-JSRV SU. Light blue: anti-CCSP. OM x400. (C) Red: anti-synaptophysin. Green: anti- JSRV SU. Light blue: anti-CCSP, OM x400. (D) Detail of (C) OM x1000. CCSP colocalises with JSRV SU. All nuclei DAPI (blue).

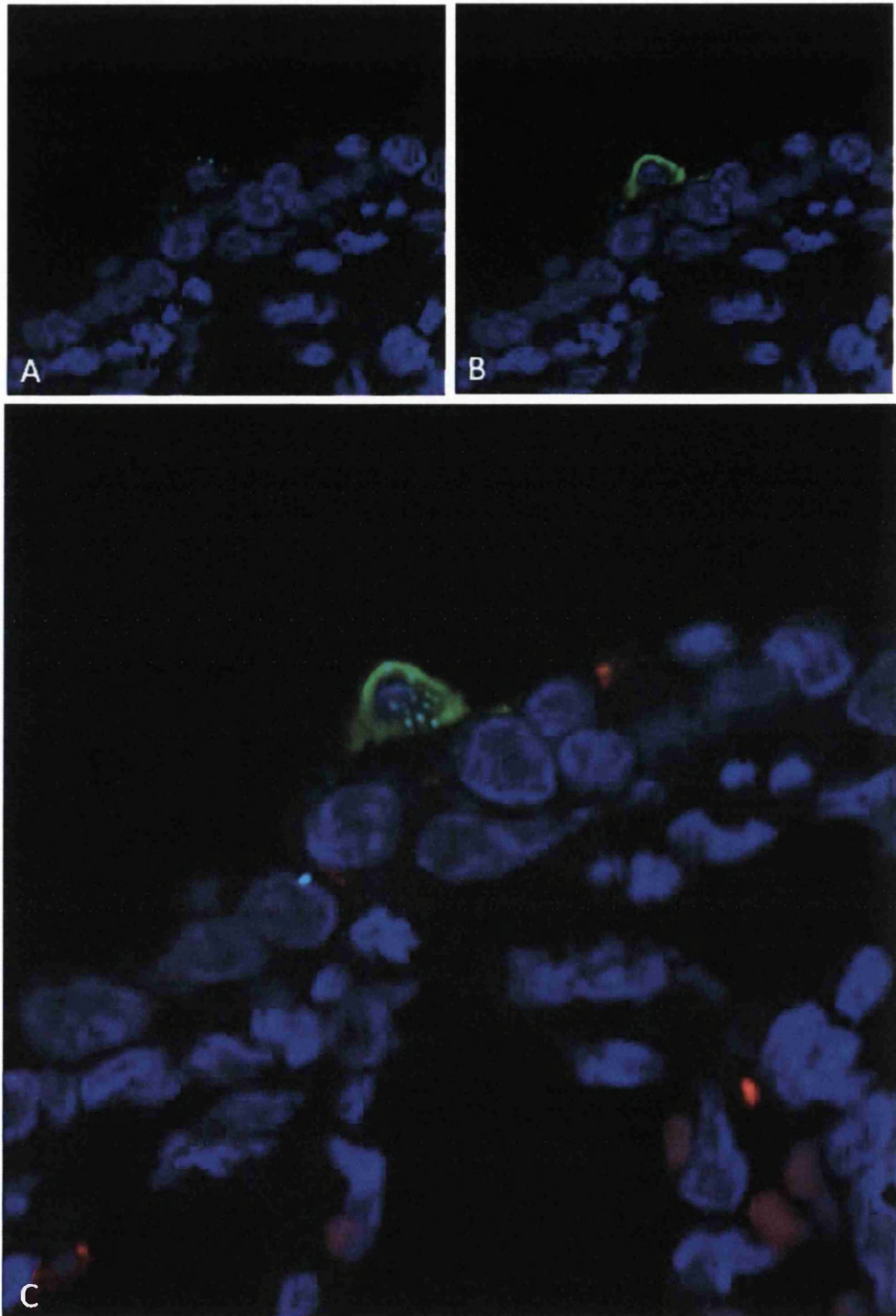


Figure 4.21 Single cell in terminal bronchiole expressing JSRV SU and CCSP only. Single section from 2856E.
(A) Light blue: anti-CCSP. (B) Green: anti-JSRV SU. (C) Green: anti-JSRV SU, light blue: anti-CCSP, red: anti-SP-C
blue: DAPI nuclei. OM x1000. Z stack section on CD: Video 2.

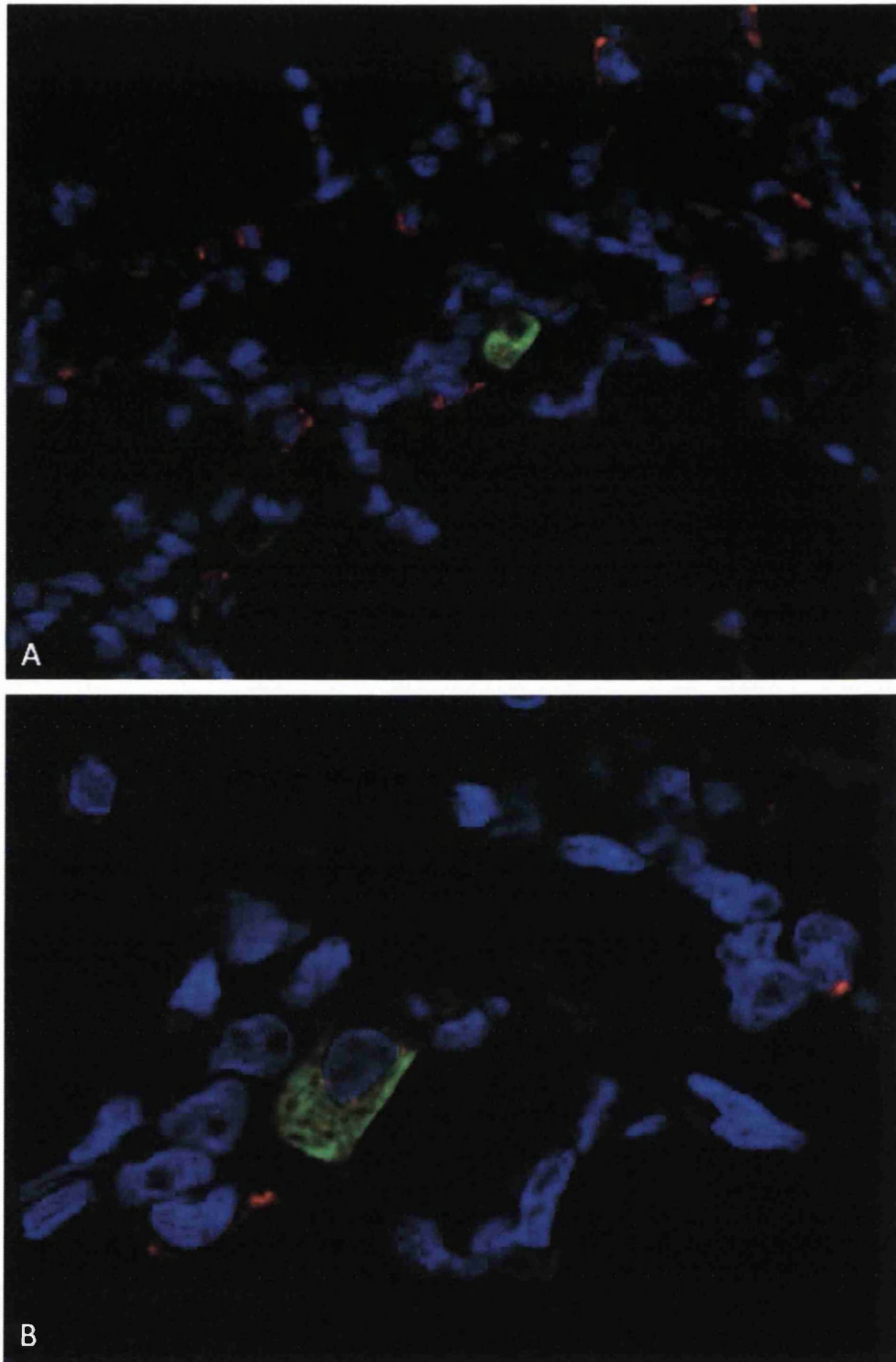


Figure 4.22 Single cell in alveolar region labels positively for JSRV SU and SP-C. (A) Alveolar region. Green : anti-JSRV SU. Red: anti SP-C. The location of the JSRV SU positive cell can be clearly seen. (B) is detail of (A) showing clear colocalisation of JSRV SU (green) and SP-C (red) to a single cell. This section was taken from a lamb 72 days PI as it was the best photographic example of JSRV infecting a type II pneumocytes. However, one similar cell was seen in lamb 2856 E 10 days PI. **Z stack section on CD: Video 3.**

Table 4.6 Summary of the protein expression of single SU positive cells in lambs 10 days PI. Yes/No denotes expression of protein as determined with IHC. Yellow highlight denotes cells examined for the expression of all three phenotypic markers. Green highlight denotes cells examined for CCSP and synaptophysin expression. Blue highlight denotes cells examined for expression of CCSP and SP-C. nd – not determined. NB. 2844 is a lamb from 72 days PI. **Z stacks can be seen on accompanying CD.**

Number	Cell number	Location	SU	CCSP	SP-C	SYN	Figure	Z stack
2852	1	R bronchiole	Yes	No	No	No	4.19	Video 1
2858	1	T bronchiole	Yes	No	No	No		
2858	1	T bronchiole	Yes	No	No	No		
2858	1	T bronchiole	Yes	Yes	No	No	4.20	
2858	1	R Bronchiole	Yes	No	nd	No		
2854	1	A D Wall	Yes	No	nd	No		
2858	1	R bronchiole	Yes	No	No	nd		
2854	1	T bronchiole	Yes	Yes	No	nd		
2856	1	R bronchiole	Yes	Yes	No	nd	4.21	Video 2
2856	1	Alveolar duct wall	Yes	No	Yes - low	Nd		
2856	1	Term bronchiole	Yes	Yes	Yes - low	Nd		
2856	1	Alveolar duct wall	Yes	No	No	Nd		
2856	1	R bronchiole	Yes	Yes	No	nd		
2844	1	Alveolar region	Yes	No	Yes	Nd	4.22	Video 3

4.2.7.3 Analysis of the phenotype of clusters of JSRV SU positive cells

The phenotype of clusters of cells (2 or more) found in these slides was also recorded (Figures 4.23-4.25 and Table 4.7). Clusters of cells in the bronchi were seen to label for SU and not CCSP or SP-C. In the terminal bronchiole clusters were positive for SU and CCSP but not synaptophysin (not labelled for SP-C). The respiratory bronchioles contained clusters labelling for SU only, SU and SP-C and SU and Synaptophysin.

Z stack sections can be seen on Video 4. This corresponds with Figure 4.23. Green, anti-JSRV. Light blue, anti-CCSP. Red, anti-SP-C. The two cells expressing virus do not label for the other two markers.

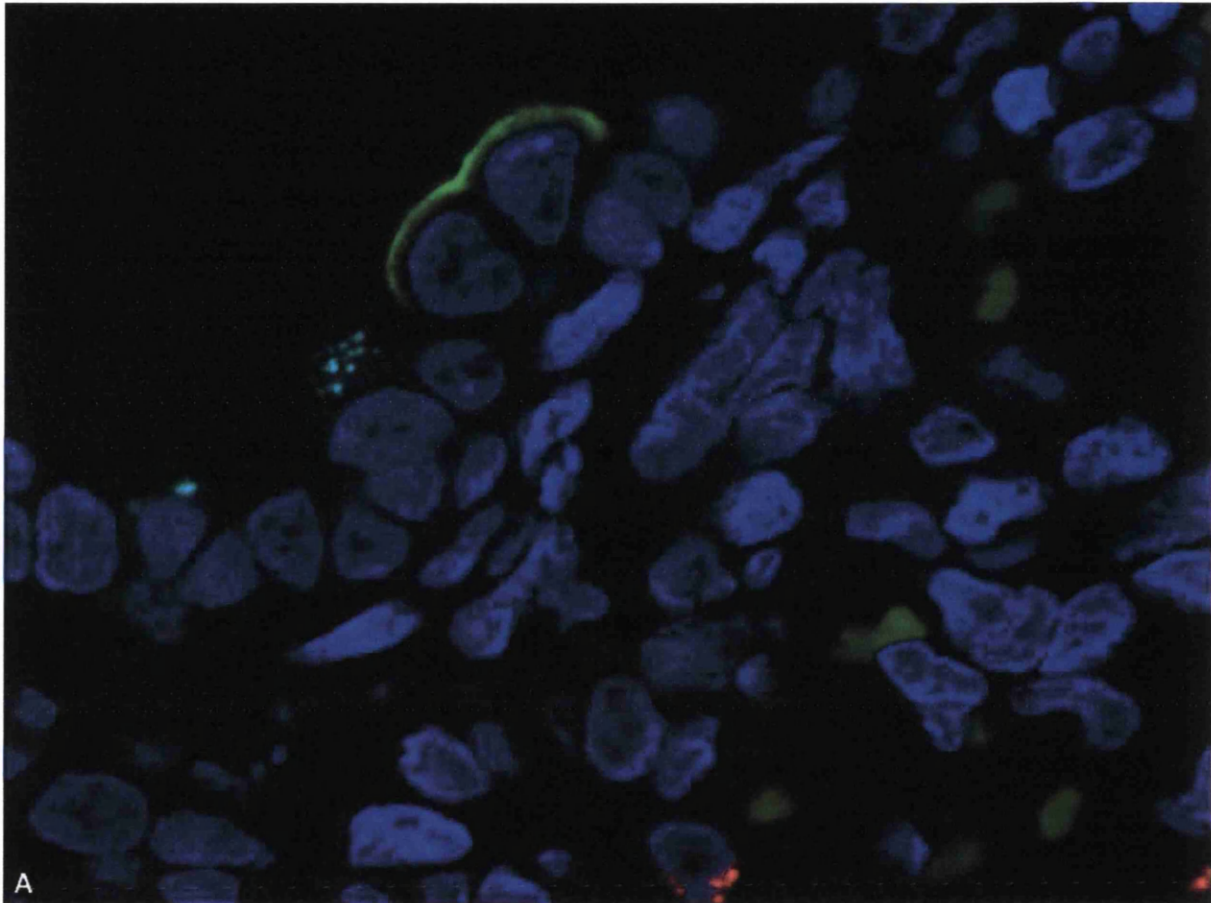


Figure 4.23 Respiratory bronchiole showing two cells expressing JSRV SU only. Lamb 2854E. Green (anti JSRV SU). Light blue (anti-CCSP). Red (anti-SP-C). Dark blue (DAPI, nuclei).OM x1000. The section shows two cells expressing JSRV SU on cell surface adjacent to a Clara cell in a respiratory bronchiole. A normal type II pneumocyte (red) can be seen towards the bottom of the section. Red blood cells are showing mild green autofluorescence. **Z stack section on CD: video 4.**

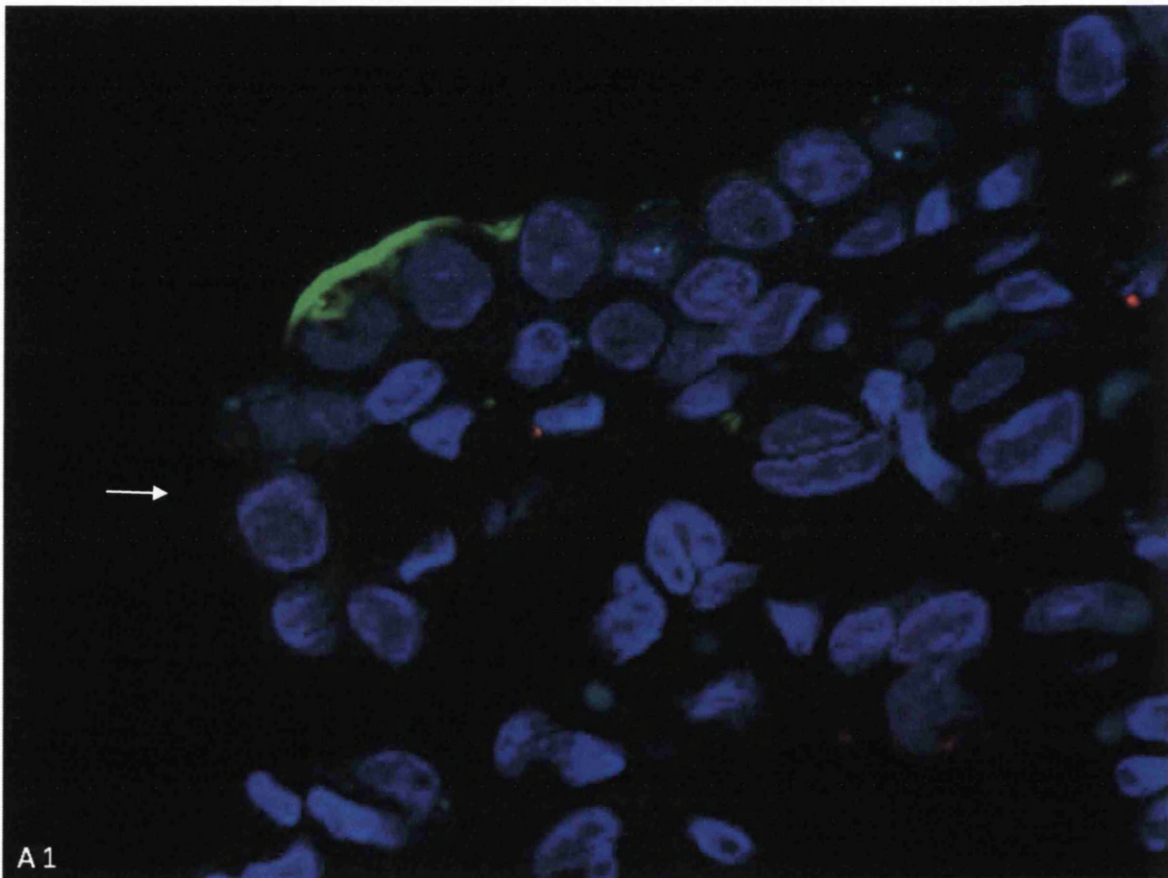
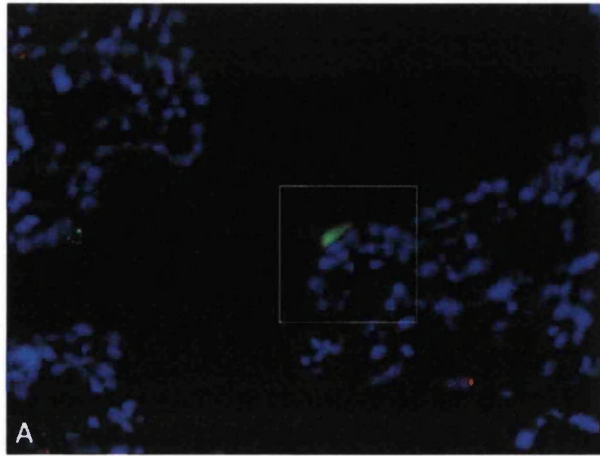


Figure 4.24 Respiratory bronchiole showing two cells adjacent to BADJ (arrow) expressing JSRV SU only. Lamb 2858 E. Green, anti-JSRV SU. Light blue, anti-CCSP. Red, anti-SP-C. Dark blue, DAPI nuclei . (A) Low power view to show location of JSRV SU positive cells. OM x 400, (A1) Detail of A. OM x1000.

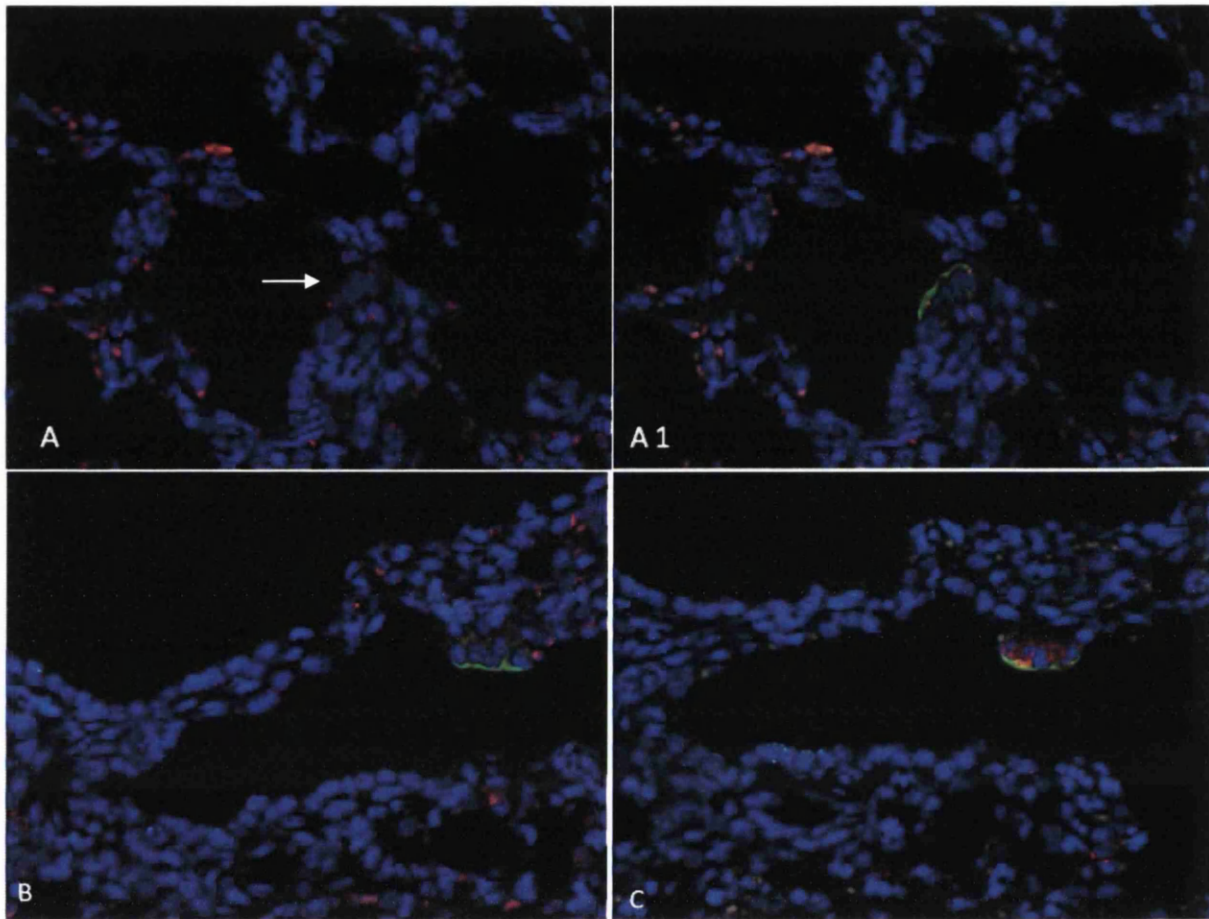


Figure 4.25 Phenotypic expressions of JSRV SU positive clusters. (A, A1) Single section from lamb 2856 E of respiratory bronchiole/alveolar region showing JSRV SU labelling of NEB. Red, anti-synaptophysin. Green, anti-JSRV SU. Arrow points to NEB to distinguish it from background autofluorescence of red blood cells. (B) JSRV SU cluster of cells in respiratory bronchiole from 2854E negative for synaptophysin. Green, anti-JSRV SU. Red, anti-synaptophysin. Light blue anti-CCSP. (C) Serial section to B, showing SP-C labelling of same JSRV SU positive cluster. Green, anti-JSRV SU. Red, anti-SP-C. Light blue, anti-CCSP. Dark blue, DAPI nuclei.

Table 4.7 Summary of protein expression of clusters of cells expressing virus in lambs 10 days PI

Case number	Number of cells in cluster	Location	SU	CCSP	SP-C	SYN	Figure	Z stack
2852	6	R bronchiole	Yes	Yes faint	Yes	nd		
2858	2	R bronchiole	Yes	No	No	nd		
2858	20	R bronchiole	Yes	No	Yes	nd		
2858	12	R bronchiole /ADW	Yes	No	No	nd		
2858	3	Bronchiole	Yes	No	No	No		
2858	4	R Bronchiole	Yes	No	nd	No		
2854	3	Alveolar cells	Yes	No	nd	No		Yes
2854	7	T bronchiole	Yes	Yes faint	nd	No		Yes
2854	2	R bronchiole	Yes	No	nd	Yes		Yes
2854	2	R bronchiole	Yes	No	No	nd	4.24	
2854	3	R bronchiole/ADW	Yes	No	nd	No		
2854	18	R bronchiole/ADW	Yes	No	nd	Yes		
2854	4	R bronchiole/alveoli	Yes	No	Yes	nd		
2854	2	R bronchiole/alveoli	Yes	No	nd	No		
2854	2	R bronchiole	Yes	No	No	nd	4.23	
2854	4	R bronchiole	Yes	No	Yes	No	4.25 B/C	
2856	4	R bronchiole/ADW	Yes	No	No	Yes	4.25,A/A1	
2856	2	Alveolar duct wall	Yes	No	Yes	nd		
2856	5	R bronchiole/ADW	Yes	No	nd	Yes		
2856	10	Alveolar duct wall	Yes	No	Yes	nd		Yes
2856	16	Alveolar duct wall	Yes	No	No	nd		

4.3 DISCUSSION

This study has characterised JSRV target cells *in vivo*, and the results suggest that the virus infects multiple cell types within the ovine lung. It is the first experiment to demonstrate *in vivo* expression of JSRV SU in single epithelial cells and to identify their phenotype. This information adds to the understanding of the early stages of pathogenesis of OPA.

JSRV SU expression was identified in single cells in the respiratory tract 10 days post intratracheal inoculation with JSRV₂₁ (Figure 4.10). These cells were located in conducting and respiratory airways which included the bronchioles, terminal bronchioles, respiratory bronchioles and alveolar ducts. Some cells expressed JSRV SU only and did not co-label with the phenotypic markers used (CCSP, SP-C, synaptophysin) (Figure 4.20). Others co-labelled with SU and CCSP, with SU and SP-C or with SU and CCSP and SP-C (Figures 4.21-4.23). This suggests that JSRV₂₁ can infect Clara cells, type II pneumocytes, cells expressing CCSP and SP-C, and a cell type which does not express the lineage specific lung markers used in this experiment.

Early speculation regarding JSRV target cells was based on the location of tumour nodules. These were identified as glandular epithelial cells arising from bronchi, bronchioles, alveolar ducts and alveoli (Cowdry, 1925a, b; Cuba-Cuparo A, 1960; de Kock, 1958; Wandera, 1968). The later development of antibodies to label viral proteins and lung epithelial cells allowed colocalisation of virus expression in tumour nodules with SP-C and CCSP. As a result of this, some authors proposed type II pneumocytes and Clara cells as the tumour cells of origin (Beytut et al., 2008; Palmarini et al., 1995; Platt et al., 2002). This principle was explored in transgenic mouse models of lung adenocarcinoma where oncogene expression is linked to SP-C or CCSP promoters (Wikenheiser et al., 1992; Wikenheiser and Whitsett, 1997). However, unpredictable results which showed varied correlation between promoter phenotype and mature tumour protein expression reduce the validity of this concept (Hicks et al., 2003). Nonetheless, the present study found single cells to express JSRV and CCSP or SP-C indicating both cell types are targets for the virus.

In order to improve the understanding of lung homeostasis, some studies have concentrated on further categorisation of these mature cell phenotypes according to their progenitor potential.

Lung injury models in mice have identified a subpopulation of ‘variant Clara cells’ which are found in stem cell niches at NEBs and the BADJ (Giangreco et al., 2002; Hong et al., 2001; Kim et al., 2005; Reynolds et al., 2000) (see section 1.1.5). These cells express CCSP, but unlike classical Clara cells they are resistant to naphthalene and have the ability to repopulate the damaged epithelium. They also lack the cytochrome p450 enzyme which metabolises xenobiotics in normal Clara cells (Singh and Katyal, 2000). Another study in mice which used lineage tracing techniques, noted variations in the ability of Clara cells in postnatal and mature animals to give rise to ciliated cells (Rawlins et al 2009). More detailed investigations are needed to confirm this finding. Differences between subpopulations of SP-C expressing cells have also been identified (Peers et al., 1990; Perl et al., 2005; Reddy et al., 2004; Roper et al., 2003; Sigurdson and Lwebuga-Mukasa, 1998). One study used FACS analysis of rat type II pneumocytes following hyperoxic injury to isolate two populations of cells distinguished by their expression of E-cadherin. E-cadherin negative cells appeared damage resistant, proliferative and exhibited high levels of telomerase activity when compared to E-cadherin positive cells (Reddy et al., 2004). It was proposed that they represented a transit amplifying population of type II pneumocytes, which would be responsible for the repopulation and repair of damaged epithelium. Additional work is required to see if any comparable subpopulations of Clara cells and type II pneumocytes exist in the sheep, and if they are specifically targeted by JSRV.

Another interpretation of the mixed tumour phenotype followed the cancer stem cell hypothesis (Eramo et al., 2010) (see section 1.1.6) and took this to indicate a stem cell origin for OPA (Platt et al., 2002). The theory was strengthened by evidence in mice where an oncogenic K-ras model of lung adenocarcinoma was shown to develop from BASCs residing at the BADJ (Jackson et al., 2001). Hyperplasia of these cells was also noted prior to tumour development (Kim et al., 2005). The possibility that JSRV might provide a tool to specifically target such vital cells in the sheep lung was an exciting concept and led to the search for JSRV infected BASC-like cells in sheep. Despite previous evidence of cells labelling with SP-C in respiratory bronchioles where BASCs might be expected (see Figure 3.4B), in these experiments very few BASC-like cells were identified (Figure 4.23) and only one cell in over 30 sections examined was found to express SP-C, CCSP and JSRV SU. This suggests that the availability of BASC-like cells in the sheep will not have a big influence on JSRV infection.

In addition there was no evidence of preneoplastic BASC hyperplasia which was seen in the mouse model (Kim et al 2005). Interestingly since this study began, multiple publications have questioned the validity of SPC/CCSP expression as a method for identifying cells with true stem cell properties (Giangreco et al., 2009; Kim et al., 2005; Rawlins et al., 2009; Stripp and Reynolds, 2008; Teisanu et al., 2009).

It is important to realise that the cancer stem cell does not have to originate from the endogenous stem cell of the tissue it is growing in (Visvader and Lindeman, 2008). While the permanency of a tissue stem cell does lend itself to an increased risk of mutation and oncogenic transformation, it is also possible that differentiated cells in the tumour can re-acquire self renewal capacity and stem-cell like properties from later mutations (Clarke et al., 2006). It could be that the single cell identified which expressed SP-C, CCSP and JSRV SU was actually in the process of dedifferentiating following viral infection. During embryonic development in the mouse, progenitor cells in the lung have been shown to express multiple lineage markers prior to restricted protein expression in the more differentiated cell lineages (Wuenschell et al., 1996). In the context of OPA both cell origins are possible and further investigations are limited until specific markers to identify stem cells in the ovine lung are better defined.

A proportion of the single cells expressing JSRV SU found in this study did not label for any of the three phenotypic markers (Table 4.6). Several hypotheses can be made regarding the identity of these cells. Firstly, they could represent infected Clara cells which are in the process of dedifferentiation and transformation. CCSP is thought to antagonise the neoplastic phenotype and reduced expression has been found in multiple solid tumours (Linnoila et al., 2000). Secondly, they could be an example of an immature progenitor type cell, as respiratory epithelium in the lungs of 16 day old lambs is still in the process of differentiating (see Table 3.4). Comparable cells may have been identified in the mouse lung following injury (Evans et al 1978). In that study, a population of intermediate type A Clara cells, distinguished by their lack of secretory granules and smooth ER, were identified and seen to increase dramatically in response to injury. As ciliated and Clara cells repopulated the epithelium, their numbers subsequently declined (Evans et al 1978). A final theory is that they could be an example of an as yet undefined population of progenitor cell in the ovine lung. Recent work with human lung

cancer has used the membrane antigen CD133+ to isolate a rare population of cells with stem cell properties from tumours. These cells also lacked any lineage-specific lung cell markers (Eramo et al., 2008). In the current study, efforts were made to optimise antibodies to label the potential stem cell proteins CD34, Oct-4 and CD 133+. Unfortunately it was not possible to optimise any of these on sheep tissue (see Table 2.3). A summary of possible cellular transformation events following JSRV infection of target cells is shown in Figure 4.26.

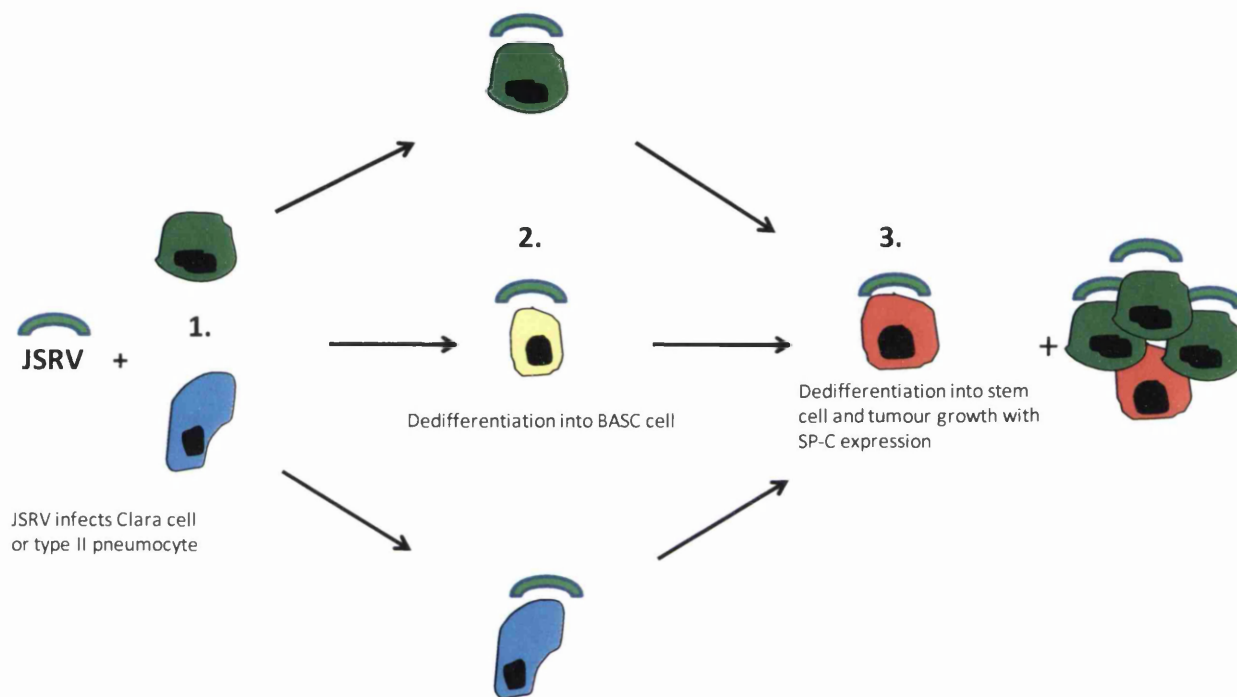


Figure 4.26 Schematic diagram to show possible target cells for JSRV infection in the ovine lung. 1. JSRV infects differentiated cells with progenitor capabilities Clara cells and type II pneumocytes. 2. JSRV infects BASCs. 3. JSRV infects stem cell with no phenotypic markers. Infection of all these potential target cells results in cancer stem cell formation and tumour growth with SP-C expression.

The phenotype of neoplastic clusters were also interesting to examine as they differed from some of the published literature on OPA. Over half of the 21 foci between 2-16 cells in diameter did not label with other differentiated cell type markers (Table 4.8). This is in contrast to other IHC studies of mature tumours where most tumours were found to express SP-C or CCSP (Beytut et al., 2008; Platt et al., 2002). 6/21 foci located in respiratory bronchioles and alveoli labelled positively for SP-C. One of these also showed faint CCSP expression. Similarly, other IHC studies on OPA have also demonstrated a greater positivity

for SP-C than CCSP within heterogenous mature tumours (Beytut et al., 2008; Platt et al., 2002). In contrast, examination of the K-ras induced mouse model of lung adenocarcinoma found dual positive CCSP and SP-C cells in the centre of tumours, which were continuous with the terminal bronchiolar epithelium (Jackson et al., 2001; Kim et al., 2005). This was not seen in OPA-E tumours. 3/21 foci labelled positively for synaptophysin were visually assessed (Figure 4.25A), and this is the first demonstration of neuroendocrine marker expression in OPA. It is uncertain whether these represent transdifferentiated tumour cells, or whether the tumour has grown around existing NEBS. Although more commonly found in small cell carcinomas, neuroendocrine differentiation has been recorded in human adenocarcinomas of the lung (Ionescu et al., 2007).

Up until this point, the assumption has been made that all single cells expressing virus represent JSRV target cells. However, there is a possibility that not all of the cells identified will continue to support viral protein expression and develop into tumour nodules. Instead virus expression may be subsequently repressed, leaving the cell to function normally. Alternatively these infected cells could apoptose, although there is no morphological evidence of this on H and E examination. *In vitro* models for JSRV transformation have demonstrated marked variations in transformation efficiency between cell lines (Palmarini et al., 2000a). This has been attributed to the preferential activity of JSRV LTRs in specific cell types which contain the appropriate transcription factors required for viral replication (McGee-Estrada and Fan, 2006, 2007; McGee-Estrada et al., 2002; Palmarini et al., 2000a). Similar requirements are likely for successful replication *in vivo*. In addition as demonstrated for other retroviruses, restriction factors may have a role in inhibiting viral expression and transformation *in vivo* (see 1.3.4).

From the data obtained in this study it appears that JSRV can infect multiple cell types in the ovine lung. Whether there are variations in the efficiency of virus expression between the different cell types is unknown from these experiments, and warrants further investigation.

CHAPTER 5 JSRV INFECTION AND THE HOST CYTOKINE RESPONSE

5.1 Introduction

This chapter continues the investigation into the early stages of OPA pathogenesis by examining the host innate response to infection with JSRV in terms of cytokine expression. How a virus interacts with the innate immune system plays a central role in determining the eventual outcome of infection. This is both through the immediate effect of the innate response and by the influence it has on the downstream adaptive response. Ideally for the host, Pattern recognition receptors (PRRs) identify viral components (pathogen associated molecular patterns), and trigger a cytokine signalling cascade to limit virus spread and attract innate immune cells (see section 1.3.5). Antigen presenting cells then prime the adaptive immune response and the virus is eliminated (Takeuchi and Akira, 2009). In return, viruses have adapted by developing various mechanisms of immune evasion which include virus encoded factors to affect cytokine activities (Haddad, 2002; Hansen and Bouvier, 2009; Lee et al., 2009).

The importance of the innate response in controlling infection by other respiratory viruses such as Respiratory Syncytial Virus (RSV) and Influenza is well recognised. Experiments show that the balance between virus elimination and disease pathogenesis is dependent on the spectrum of cytokine release from infected epithelial cells (Bueno et al., 2008; Julkunen et al., 2000; Tripp et al., 2005). For retroviruses, there is little information regarding these initial stages of infection in the literature (Browne and Littman, 2008) and the need for further work in this area has recently been acknowledged (Mogensen et al., 2010; Pereira and Ansari, 2009). Similarly, for JSRV understanding of this process is incomplete. There have been no detailed investigations into the innate response, and studies have been unable to demonstrate robust evidence of a JSRV specific adaptive immune response (Ortin et al., 1998; Summers et al., 2002; Summers et al., 2005).

This chapter used quantitative real-time reverse transcriptase polymerase chain reaction (qRT-PCR) to measure the expression of a number of inflammatory cytokines and chemokines

in the lungs and mediastinal lymph nodes of infected animals. Samples were taken at three time points post experimental infection of lambs with JSRV₂₁ and from naturally infected sheep. Cytokine mRNA levels were compared with age matched controls at each time point, and correlated with the stage of disease using histological examination of adjacent tissue sections.

5.2 Methods

5.2.1 Sample collection and storage

The host response to JSRV infection was assessed in lung samples from experimentally and naturally infected animals (see section 2.1). Lung and lymph node tissue was collected from SPF lambs inoculated with JSRV₂₁ at 6 days old, and euthanased 3, 10 and 72-91 days later. Age matched mock-infected and non-infected lambs were included as negative controls. Naturally infected adult sheep with clinical signs of OPA were collected from local farms, and lung samples were chosen from those with minimal gross evidence of secondary lung infections on post mortem examination. Adult negative control animals were obtained from a flock free of OPA for five years. A total of 12 lungs from experimentally infected lambs and 4 from naturally infected sheep with age matched controls were examined (Figure 5.1).

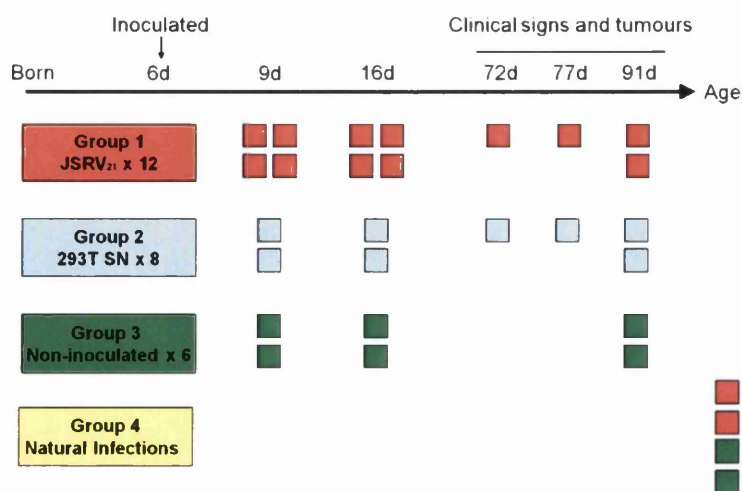


Figure 5.1 Summary of animals sampled to investigate cytokine response to infection with JSRV. Each coloured box represents the PME of one animal. Red: JSRV infected. Blue: mock inoculated. Green: controls.

Tissue samples were dissected from 24 fixed sites in each lung (see section 1.4). They were immediately placed in labelled cassettes and snap frozen in liquid nitrogen, before long term storage at -80 °C.

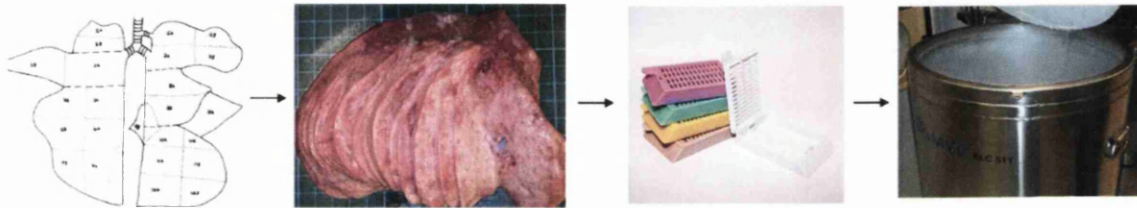


Figure 5.2 Summary of tissue sampling process before RNA extraction. 24 sites were sampled from each lung, and snap frozen in liquid nitrogen.

5.2.2 RNA extraction and purification

For each lung, tissue from sample sites 1a, 1b, 2a, 2b and 5a and mediastinal lymph nodes, were analysed. RNA was extracted from cryostats using the RNeasy mini kit (Qiagen), and any residual DNA was removed with DNase digest kit (Qiagen) (section 1.5). The quality of RNA was assessed using Agilent chip technology, and only samples with a RIN > 8 were included (appendix). A Nanodrop spectrophotometer was used to confirm the purity of the sample and measure the concentration of RNA extracted.



Figure 5.3 Procedure for RNA extraction and analysis. RNA was extracted from cryostats using an RNeasy kit and analysed using Agilent chip and nanodrop systems.

5.2.3 Establishment of reference genes for qRTPCR

For precise comparison of mRNA transcription levels between samples, results from the qRTPCR experiments were normalised to a fixed reference. Firstly, different reference genes were compared in order to select two stable reference genes for lung and lymph node tissue using the programme geNorm (Vandesompele et al., 2002). The use of multiple reference genes increases the accuracy of detecting small expression differences in candidate genes.

5.2.2.3 geNorm analysis

geNorm was used to assess the stability of five common reference genes, with different functions, in normal and OPA lung and lymph node (Figure 5.4). RNA for analysis was extracted from a variety of normal and diseased lung and lymph node tissue. qRTPCR was performed to determine mRNA levels of β -actin (ACT B), succinate dehydrogenase (SDHA), tyrosine 3-monooxygenase/tryptophan 5-monooxygenase activation protein zeta polypeptide (YWHAZ), beta-2-microglobulin (M2G1) and glyceraldehyde-3-phosphate dehydrogenase (GAPDH).

Ct values were transformed into relative quantification data by subtracting the highest Ct value from all other Ct values for each gene measured. This provided a delta Ct value, with the highest delta Ct value as 0, and all other values less than this. Then for each data point, the equation $2^{(-\text{delta Ct})}$ was applied. Therefore all data were expressed relative to the expression of the least expressed gene. These values were inserted into the geNorm Excel file, and analysis assigned an M (stability) value to each gene based on expression variation between tissues, where the lowest M value indicates the least variation/most stable. The two most stable were identified for each tissue (Figure 5.4). ACTB and SDHA showed the least expression variation in lung tissue, and ACT B and YWHAZ in lymph node tissue. These were therefore chosen as reference genes for each tissue type respectively.

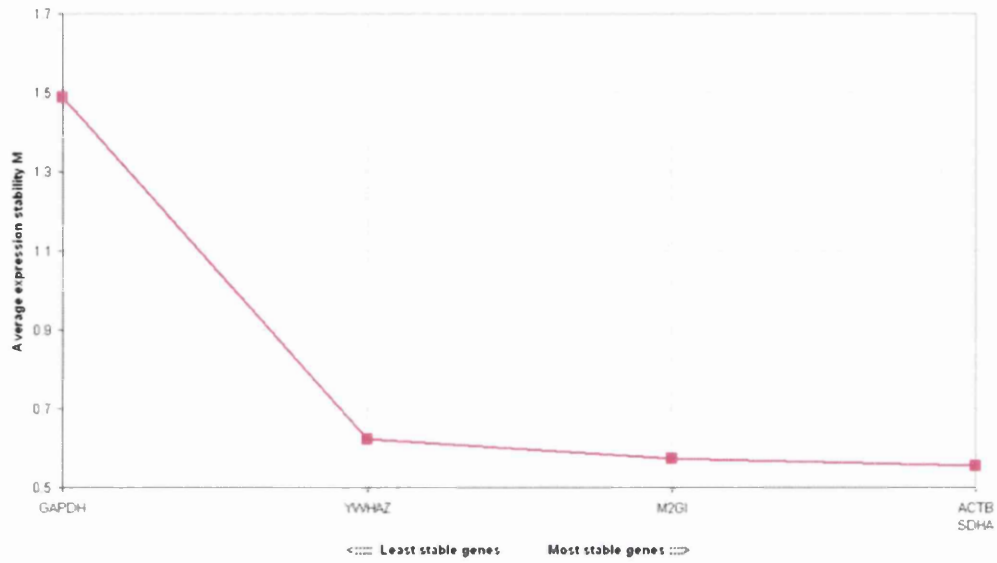
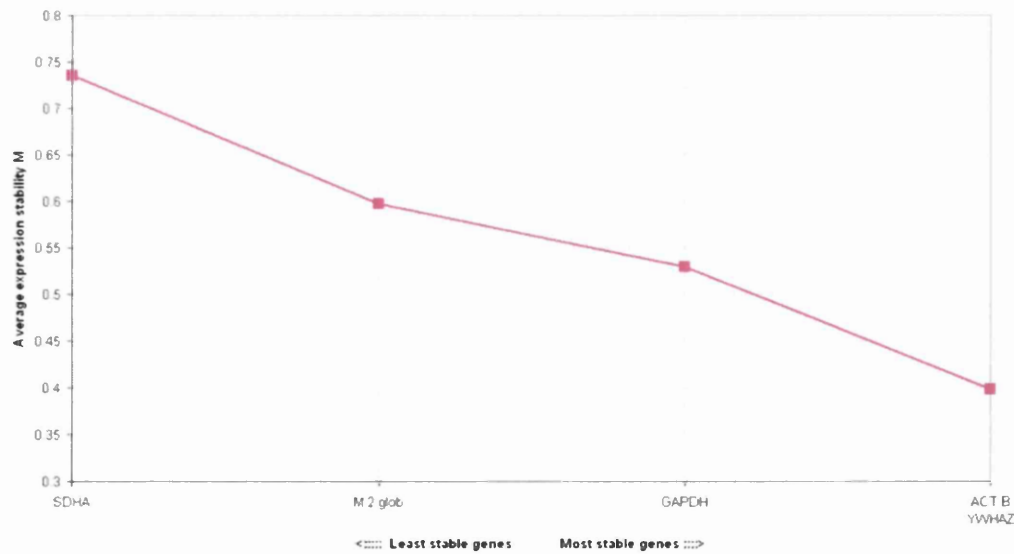
A**B**

Figure 5.4 geNorm analysis to determine the stability of reference genes in normal and diseased lung (A) and lymph node (B) tissue. These charts indicate the average expression stability value (M) for reference genes at each stage during stepwise exclusion of the least stable expressed reference gene. The least stable is on the left, and the most two stable on the right.

5.2.4 qRTPCR candidate gene analysis.

mRNA levels of JSRV and 15 cytokines were analysed by qRTPCR (Table 6.5). Primer sequences were taken from published literature (see Table 2.6) and reaction conditions were optimised using RNA from positive control samples (Li et al., 2008; Palmarini et al., 1996). These included plasmid DNA constructs, con A stimulated PBMCs and transfected cell lines expressing the gene of interest (see section 2.4.1). RNA from lung samples from all eight animals at each time point were examined on separate 96 well plates. Five samples were analysed per animal, and each was run in duplicate on a single plate (Figure 5.5). A dilution series of positive control RNA and water acted as positive and negative controls on every plate. All lymph node samples were run in duplicate and fitted onto one plate per primer set.

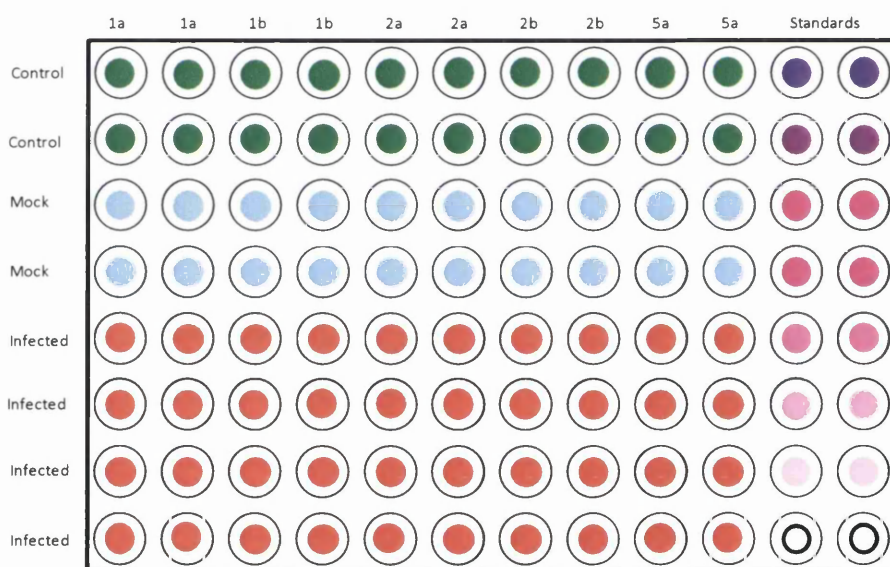


Figure 5.5 Arrangement of samples on 96 well plate. Each horizontal row contains five samples from one animal. Control (green), mock infected (blue) and infected (red) animals. Each vertical row contains samples taken from the same lung sampling site (1a-5a). An RNA dilution series (purple) and water (clear circles) were included as positive and negative controls.

Table 5.1 Summary of cytokines examined and their actions

Cytokine	Immune response type	Source in the lung	Action	Reference
IFN gamma	Th1 – cellular immunity	T cells , NK cells and macrophages	Drives CD 8 cells	(Fukuyama et al., 2007)
IL-2	Th1	T cells, dendritic cells	Induces proliferation of CD 4 and CD 8 cells.	(Granucci et al., 2002; Tripp et al., 2005)
IL-4	Th 2 – humoral immunity	T-cells, mast cells, bone marrow and stromal cells	Differentiates naïve T cells into Th2 cells, induces proliferation and isotype switching of B cells	(Haddad 2002)
IL-6	Th 2	T-cells, B-cells, monocytes/macrophages, fibroblasts, endothelial cells, stromal cells	Multifunction cytokine, regulates T and B cell functions and acute phase reactions. Increases malignancy in lung tumours	(Haddad 2002 (Schafer and Brugge, 2007)
IL-10	Th 2	T-cells, monocyte/macrophages, B-cells	Blocks cytokine synthesis by Th1 cells, activates monocytes, NK cells , enhances B cell proliferation ie. Immunostimulatory and immunosuppressive	(Hatanaka et al., 2000)
IL-18	Th1, Th2	Macrophage, T cells, B cells, dendritic cells	Enhances IL-12 driven Th1 response, can also stimulate Th2 when IL-12 not there.	(Nakanishi et al., 2001)
MCP-1	na	Tumour	Monocyte chemoattractant	(Fujimoto et al., 2009)
TGF-beta	Multifunctional	Multiple cell types	Inhibits lymphocyte proliferation. Inhibits proliferation and promotes differentiation in the lung	(Moreno et al., 1998)
TNF alpha	Th1	Monocytes/macrophages, T-cells, B-cells fibroblasts, neutrophils, NK cells, endothelial cells	Mediates inflammatory and immune functions. Can be pro angiogenic or anti vascular at high doses for tumours	(Haddad 2002)
GM-CSF	NA	Lung cancer epithelial cells, endothelial cells, fibroblasts,macrophages	Expands immunosuppressive tumour associated macrophages, tumour cell proliferation and angiogenesis.	(Whiteside 2006)
IDO	Anti-viral/immunoregulatory	Multiple cell types	Suppresses T cell responses	(Whiteside 2006 Mellor and Munn 2004)
IFN alpha	Anti viral /antiangiogenic	T-cells, B-cells, monocytes/macrophages, fibroblasts, epithelial cells	Anti-viral activity	(Persano et al 2009)
IL-8	Chemokine, angiogenic factor	Monocytes, T-cells, fibroblasts, endothelial cells, neutrophils and epithelial cells	Neutrophil chemoattractant, growth factor for lung cancer cells	(Zhu et al., 2004)
IL-1 beta	NA	Monocytes/macrophages, endothelial cells, fibroblasts, , keratinocytes, epithelial cells, dendritic cells, NK cells, T-cells and B-cells	Locally affects cells involved in inflammation, injury or infection. Pro- inflammatory and immunoregulatory	(Fan et al., 2004)

5.3.1 Histological analysis of experimental samples

In order to understand which cell types might be involved in cytokine production, a basic histological assessment on H and E stained sections was made for tissue from each time point. Tissue was taken from each animal at the same five locations as those taken for RNA extraction and examined histologically. The sections were assessed by eye for desmoplasia, tumour area and cellular infiltrates of lymphocytes, neutrophils and macrophage (Table 5.2). These were graded from 0-4 , increasing in intensity.

Table 5.2 Histopathological scoring of lung tissue for evaluation of infiltrating cell types and tumour pathology. Absent (-), mild (+), moderate (++) , marked (+++).

	Desmoplasia	Macrophages	Lymphocytes	Neutrophils	Necrosis	Tumour area
3 days PI	(-)	(-)	(-)	(-)	(-)	(-)
10 days PI	(-)	(-)	(-)	(-)	(-)	+
8 weeks PI	+	+	+	+	(-)	++
Natural infections	++	+++	++	++	(-)	+++

5.3.2 Candidate gene analysis

JSRV RNA was detected in the lung tissue of all infected animals at 10 days PI, lung tissue and lymph nodes of all at 72-91 days PI, and of all naturally infected OPA animals. JSRV₂₁ infected lambs 3 days PI and all mock/control animals were negative for JSRV expression. These results correlated with the IHC findings where JSRV SU was identified in lung tissue from the same individual animals and sites (section 4.2.2).

A total of 14 cytokines (Table 5.1) were examined at 3 days, 10 days and 72-91 days PI. Exceptions were that IL-2 and IL-4 were not examined at 3 days PI and IFN alpha was not examined at 10 and 72-91 days PI. mRNA levels of cytokines were quantified using the Pfaffl method (Pfaffl, 2001). This measures the relative expression of a target gene versus a reference gene. The relative expression software tool REST was used to analyse the data as this includes multiple reference genes and efficiencies for each candidate gene (Pfaffl et al., 2002) (see section 2.5.8). The results are based on the permuted expression data, not simply the raw Ct values, and are presented in whisker box plots (Figures 5.6-5.9). Each box area encompasses 50% of the observations, and the other 50% lies within the whiskers. The dotted line represents the median value. If one tail is longer than the other, then data is skewed in that direction. For each time point, cytokine expression was initially compared between mock infected and uninfected control animals. As no significant differences were seen between these groups, they were combined and compared as a single control group to infected animals.

The REST programme also performs a statistical test on the analysed C_T values using a *Pair-Wise Fixed Reallocation Randomisation Test*© (Pfaffl, 2001). This provides a P value (standard error <0.005 at P=0.05) to assess the significance of the expression ratio value given. The changes in mRNA detected are presented in the legends to Figure 5.6-5.9 and summarised in Table 5.3. In addition, IHC was used to identify the cellular location of IL-8 protein which was seen in neutrophils in OPA-E, and tumour cells, neutrophils and macrophages in OPA-N cases (Figure 5.10).

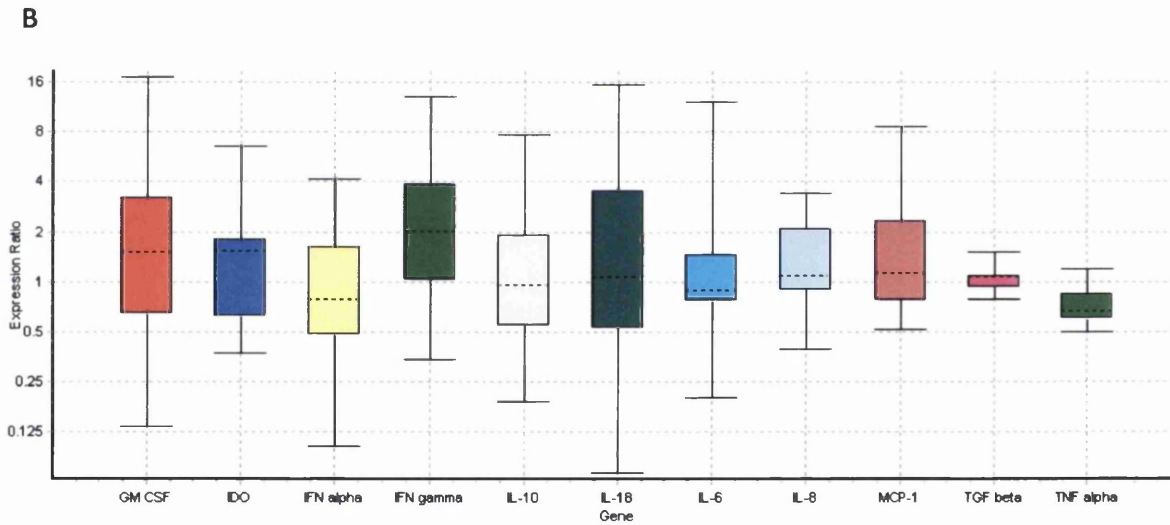
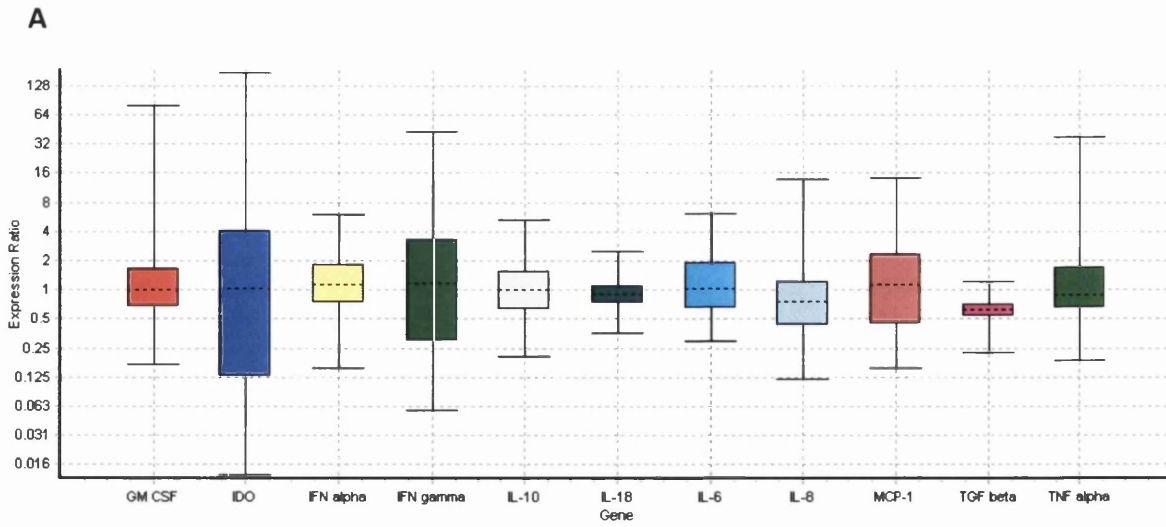


Figure 5.6 Whisker box plots of relative amounts of cytokine mRNA in lung (A) and lymph node (B) of JSRV infected vs mock/uninfected animals at 3 days PI. (A) TGF beta mRNA was reduced by a mean factor of 0.63 (1.6 x) in lung tissue (B) No significant changes detected in lymph node. Please note difference in scales on the Y axis between the two graphs.

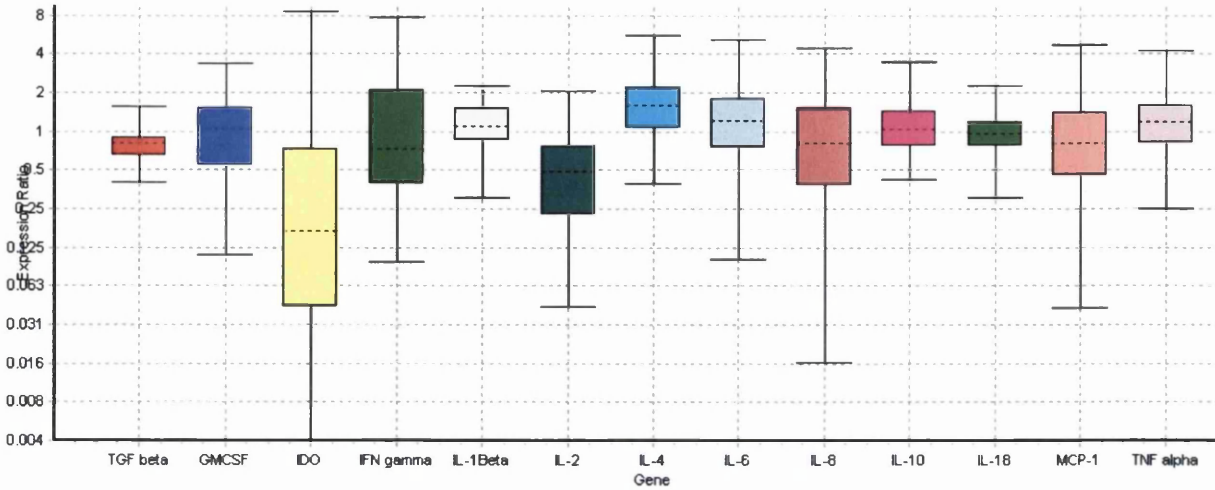
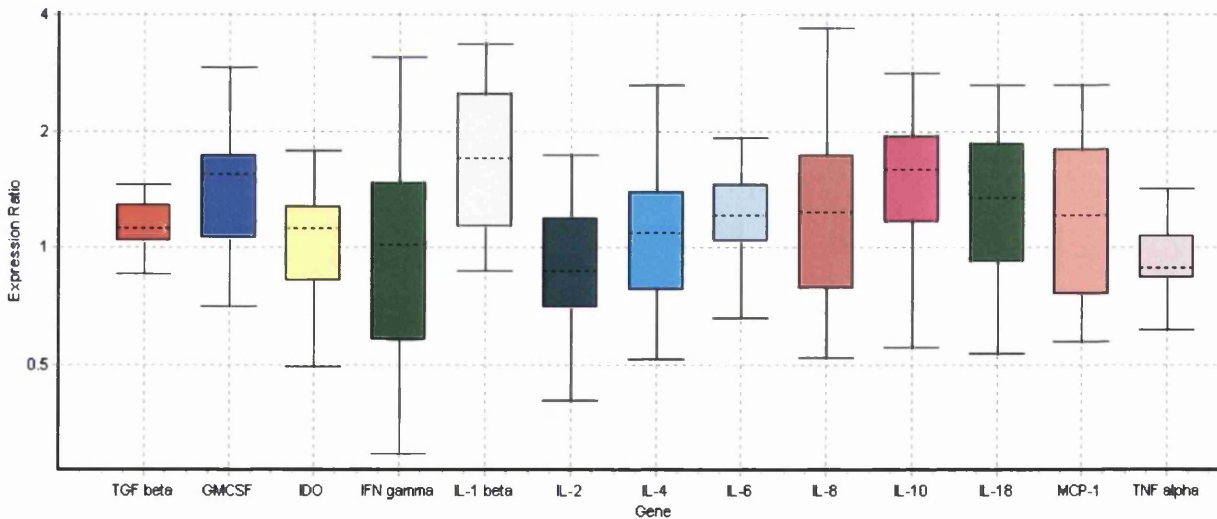
A**B**

Figure 5.7 Whisker box plots of relative cytokine expression in lung (A) and lymph node (B) tissue 10 days PI with JSRV₂₁ vs. mock/uninfected animals. (A) Levels of cytokine mRNA were reduced for TGF beta by a mean factor of 0.78 (1.3 x), IL-2 by a mean factor of 0.41 (2.4x) and IDO by a mean factor of 0.18 (5.6x). IL-4 mRNA levels were increased by a mean factor of 1.56. (B) No significant changes were identified in the cytokine levels in lymph node tissue. Please note difference in scales on the Y axis between the two graphs.

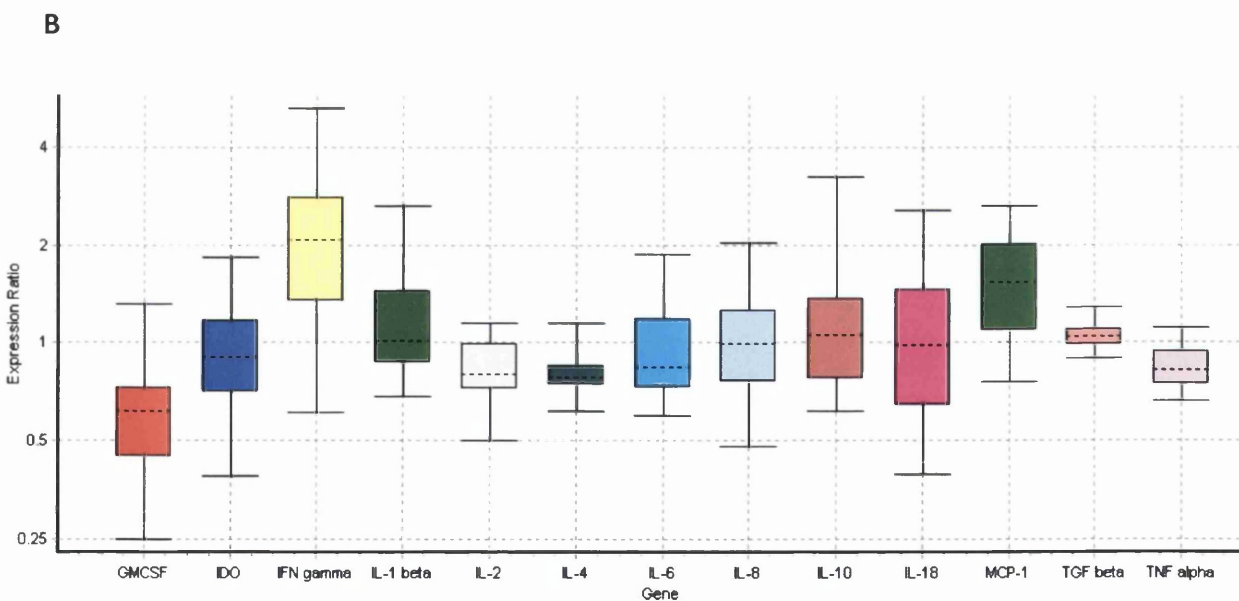
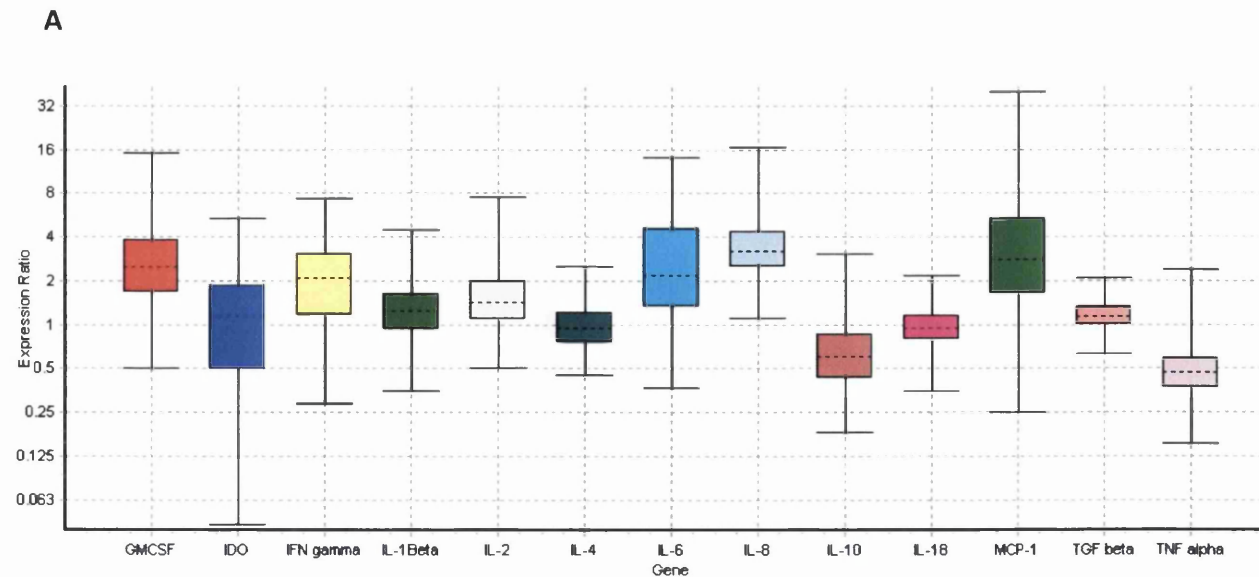


Figure 5.8 Whisker box plots of relative cytokine expression in lung and lymph node tissue vs controls, 72-91 days PI with JSRV₂₁. (A) Levels of cytokine mRNA in the lung were reduced for IL-10 by a mean factor of 0.6 (1.6x) and TNF alpha by a mean factor of 0.49 (2x). Increased levels were seen for GMCSF (2.5x), IFN gamma (1.85 x), IL-1 beta (1.2x), IL-2 (1.5x), IL-6 (2.5x), IL-8 (3.4 x), MCP-1 (2.9x) and TGF beta (1.2x). No significant changes were identified in the cytokine expression of lymph node tissue. Please note difference in scales on the Y axis between the two graphs.

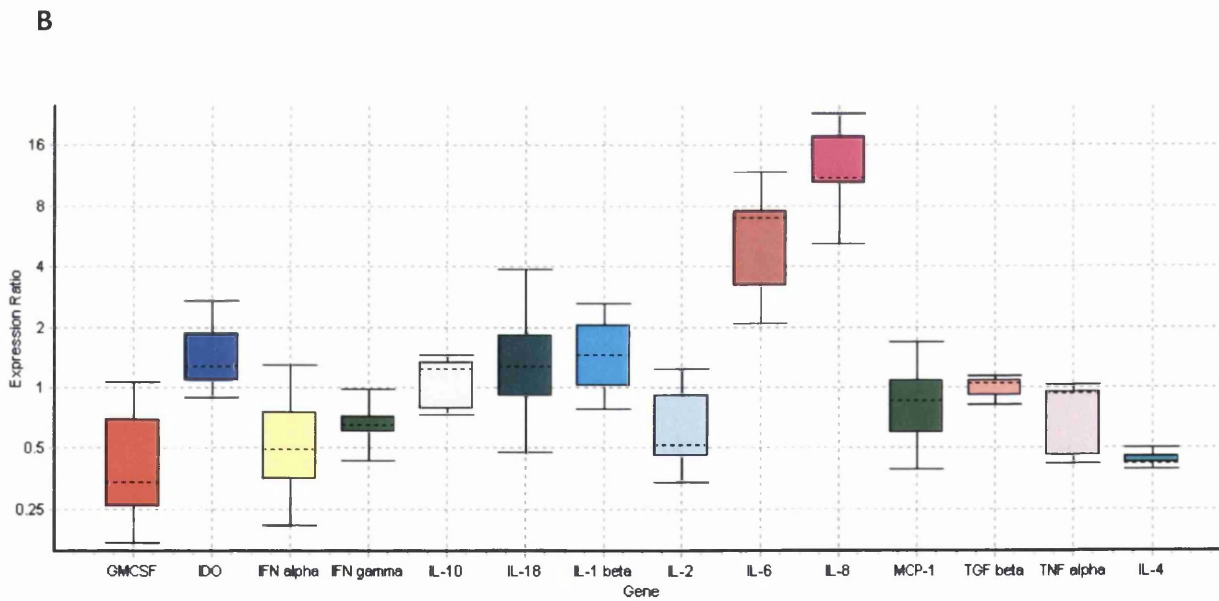
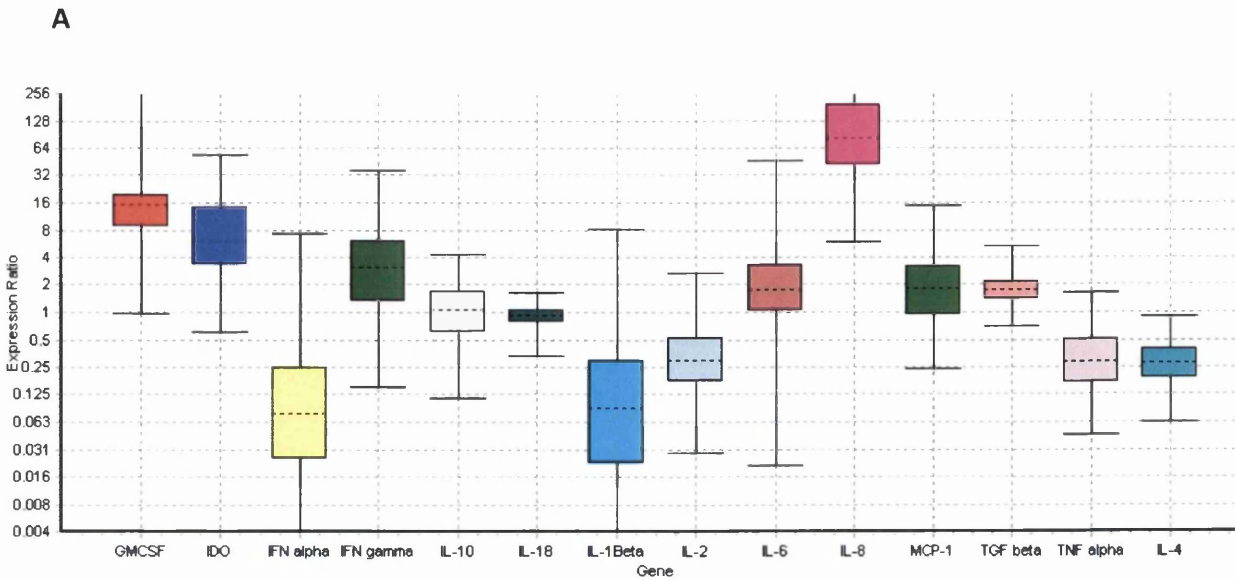


Figure 5.9 Whisker box plots of relative cytokine expression in lung (A) and lymph node (B) tissue from naturally infected animals vs. control group. (A) Increased cytokine mRNA was found for GM CSF (x15), IDO (x7), IFN gamma (2.8x), IL-8 (207x), MCP-1 (1.7x), TGF beta (1.8x). Reduced levels of cytokine mRNA were found for IFN alpha (11.9x), IL-1 beta (11.5x), TNF alpha (3.4x), IL-2 (3x) and IL-4 (3.7x). (B) In lymph nodes increased cytokine mRNA were detected for IL-8 (12.7x) and IL-6 (5.5 x) (P=0.067). Reduced cytokine mRNA was found for IFN gamma (1.5) and IL-4 (2.4). Please note difference in scales on the Y axis between the two graphs.

Table 5.3 Summary of changes in mRNA levels of a variety of cytokines. Those considered to be significant (P=0.05) are highlighted in green (increased) and yellow (reduced). Nc indicates no change in expression, ns indicates not significant, and na the analysis was non-diagnostic. Amounts of JSRV as determined by CT value are represented by +,++ or +++

Days PI	Tissue	JSRV	GMCSF	IDO	MCP-1	IL-8	IFN gamma	IL-2	IL-4	TNF alpha	IFN alpha	IL-1 beta	IL-6	TGF beta	IL-10	IL-18
3	Lung	None	nc	nc	nc	nc	nc	na	na	nc	nc	nc	nc	↓1.6	nc	nc
	Lymph node	None	nc	nc	nc	nc	nc	na	na	nc	nc	nc	nc	nc	nc	nc
10	Lung	Positive +	nc	↓5.6	nc	nc	nc	↓2.4	↑1.6	nc	na	nc	nc	↓1.3	nc	nc
	Lymph node	None	nc	nc	nc	nc	nc	nc	nc	nc	na	nc	nc	nc	nc	nc
72-91	Lung	Positive ++	↑2.5	nc	↑2.9	↑3.4	↑1.85	↑1.5	nc	↓2	na	↑1.2	↑2.5	↑1.2	↓1.6	nc
	Lymph node	Positive ++	nc	nc	nc	nc	nc	nc	nc	nc	na	nc	nc	nc	nc	nc
Natural infection	Lung	Positive +++	↑15	↑7	↑1.7	↑207	↑2.8	↓2.2	↓3.7	↓3.4	↓11.9	↓11.5	nc	↑1.8	nc	nc
	Lymph node	Positive +++	nc	nc	nc	↑12.7	↓1.5	nc	↓2.4	nc	nc	nc	↑5.5	nc	nc	nc

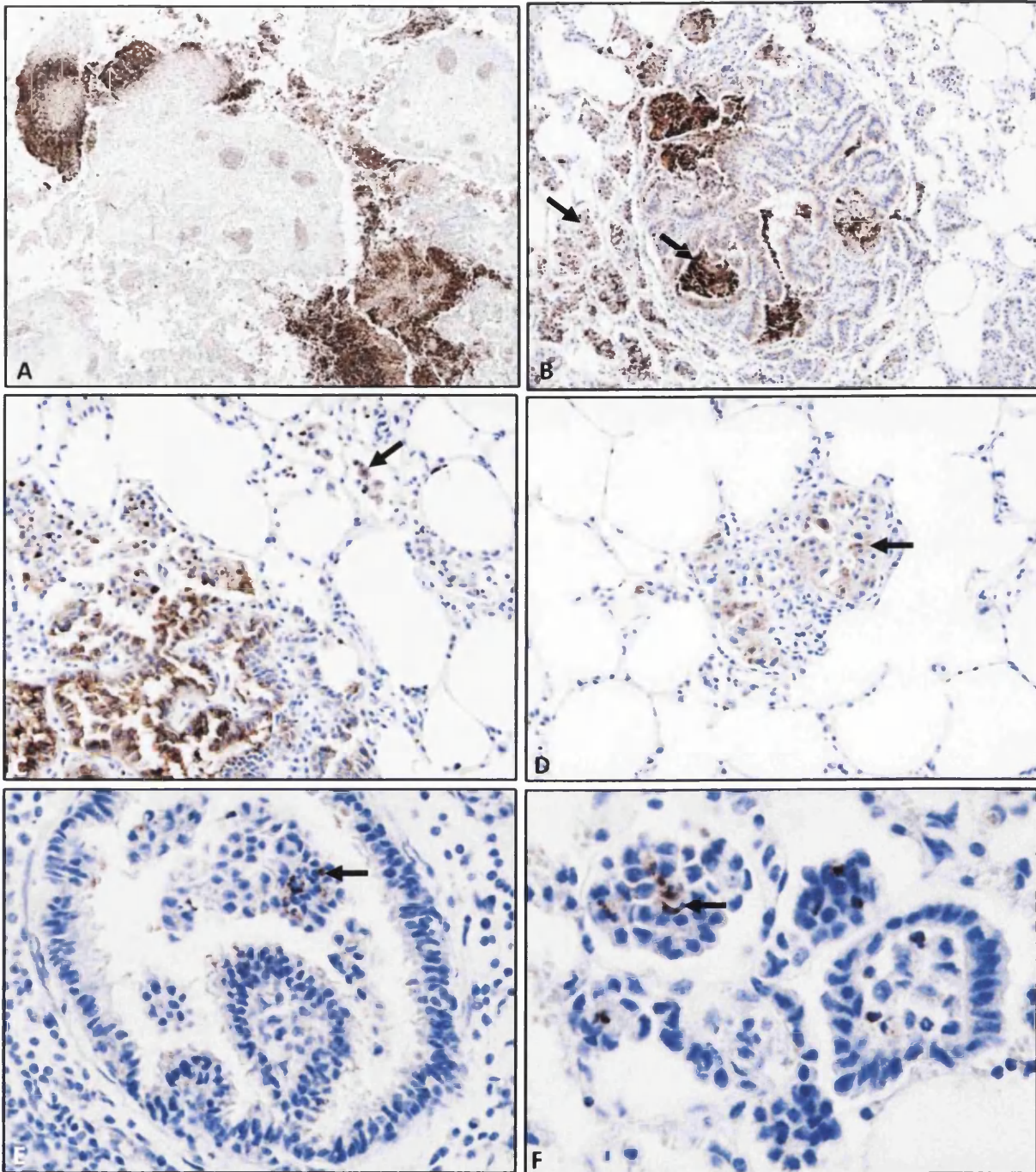


Figure 5.10 IHC showing labelling for IL-8 in lungs from OPA-N and OPA-E . (A) Positive control tissue, ovine placenta with Chlamydial infection. Brown labelling indicates antigen, OM x100. (B-D) Tumour from OPA-N. (B) Labelling of neutrophil clusters and peritumoural macrophages and neutrophils (arrows) OM x100. (C) Cytoplasmic labelling of neoplastic cells (left) and macrophages (arrow) OM x200. (D) Labelling of neoplastic cells (arrow) OM x200. (E and F) OPA-E showing positive labelling of intratumoural neutrophils (arrow)(E) OM x400, (F) OM x600 .

5.4 DISCUSSION

This is the first study to describe a preliminary investigation into the innate immune response to JSRV. The aim of the experiment was to see how the host innate response varied at different stages of disease pathogenesis. mRNA levels of JSRV and 14 inflammatory cytokines and chemokines representative of innate, cell mediated and humoral responses and tumour growth regulation were analysed by qRT-PCR at early and late time points following inoculation. These levels were compared to samples from age matched control animals. Corresponding histopathology was also recorded.

There was no change detected in levels of cytokine mRNA at 3 days PI (Figure 5.6 A). By 10 days, all infected lung samples were positive for JSRV mRNA. No inflammatory cell infiltrate was seen on histological examination but decreases in IL-2 and IDO mRNA were detected (Figure 5.7A). IL-2 can be produced by activated T lymphocytes and dendritic cells (APCs) and is involved in differentiation and survival of cytotoxic T cells and immune cell differentiation (Granucci et al., 2002). IDO is an immunomodulatory enzyme which degrades the essential amino acid tryptophan and has the potential to inhibit viral growth (Munn and Mellor, 2007). Another retrovirus (HIV) has been shown to modulate IDO expression (Maneglier et al., 2009), but the mechanism and effect of reduced mRNA levels at this time point is uncertain.

By 72-91 days PI, increased levels of JSRV mRNA were detected in all infected samples. Histology identified scattered tumour foci with small numbers of peritumoural macrophages, intratumoural lymphocytes and occasional neutrophils (Table 5.2). Concomitant increases in GM-CSF, IL-8 and MCP-1 mRNA, all cytokines known to promote tumour growth through angiogenesis and macrophage recruitment, were detected (Figure 5.8A). Macrophages are generally regarded as being essential for tumour progression, playing key roles in angiogenesis, cell survival and metastasis. Increased numbers in some human tumours correlates with a poor prognosis (Lewis and Pollard, 2006; Sica et al., 2008). Levels of mRNA for the pro and anti-inflammatory cytokine IL-6 were also increased at this time point. Any cytokine with less than a 2-fold change was not regarded as significant in this study. However, if this had been accepted then additional findings were small raises (<2 fold) in TH1 cytokines IL-2 and IFN gamma mRNA, and a reduction (<2 fold) in TH2 cytokine IL-10.

These levels of cytokine mRNA could reflect activation and proliferation of T cells and the early stages of an adaptive response, but whether this is in response to tumour or viral antigen is unknown.

In tissue from natural infections histological examination found large areas of tumour, with dense patches of infiltrating neutrophils, lymphocytes and peritumoural macrophages. The most dramatic change in cytokine mRNA was a 207- fold upregulation of IL-8 (Figure 5.9A). The presence of neutrophils seen on H and E and their positive IHC labelling for IL-8 (Figure 5.10 A-C), supports the original classification of IL-8 as a neutrophil chemoattractant with inflammatory activity (Baggiolini et al., 1989). However, IL-8 has also been shown to play an important role in tumour progression and metastasis (Yuan et al., 2005). In support of this, IHC showed positive labelling for IL-8 in tumour cells and infiltrating macrophages (Figure 5.10 C,D). IL-8 is now recognised as a potent angiogenic factor in several cancers including non-small cell lung cancer (NSCLC) in humans, and increased levels are associated with angiogenesis, tumour progression and poor survival. IL-8 also stimulates tumour associated macrophages to secrete growth factors (Waugh and Wilson, 2008). Studies on OPA conducted in the 1980's were able to identify a factor released by tumour cells into the supernatant, which stimulated chemotaxis of both alveolar macrophages and blood monocytes (Myer et al., 1987b). When normal alveolar macrophages were cultured with this supernatant the cells were stimulated to produce another 'factor' (Myer et al., 1987a). It is tempting to speculate that this 'factor' may have been IL-8.

Naturally infected lung samples also showed increased detection of GM-CSF, IDO and IFN gamma mRNA. In humans IDO activity is increased in lung cancer patients. It is expressed by cancer cells and tumour infiltrating antigen presenting cells, and increasing sera levels have been shown to correlate with disease progression (Karanikas et al., 2007; Suzuki et al., 2010). IDO acts to inhibit T cell proliferation, induce T cell apoptosis, modify natural killer cell function and enhance local Treg immunosuppression all of which lead to immune tolerance of the tumour (Munn and Mellor, 2007). IFN gamma has a variety of functions including antiviral, immunoregulatory and anti-tumour effects. It has also been shown to induce IDO expression (Mellor and Munn, 2004). There was decreased detection of IL-1 beta mRNA in OPA-N, which is an immunoregulatory and proinflammatory cytokine secreted by a variety of activated immune cells (Fan et al 2004), along with interferon alpha, which has potent

antiangiogenic properties (Persano et al., 2009). Smaller reductions in mRNA levels of TNF alpha, IL-4 and IL-2 suggest a lack of cell mediated or humoral response at this stage of disease.

While JSRV mRNA expression was detected in all mediastinal lymph nodes 8 weeks PI and naturally infected animals, only those of the naturally infected animals showed changes in cytokine mRNA levels (Figure 5.9B). Here there were increases in IL-8 and IL-6 ($P < 0.06$) mRNA and a decrease in IL-4 mRNA. IHC showed infiltrating neutrophils in the lymph nodes to label for IL-8, and this could explain the increase in detection of IL-8 mRNA. A summary of cytokine changes in naturally infected animals, including the stage of disease pathogenesis they might be detected in is shown in Figure 5.11.

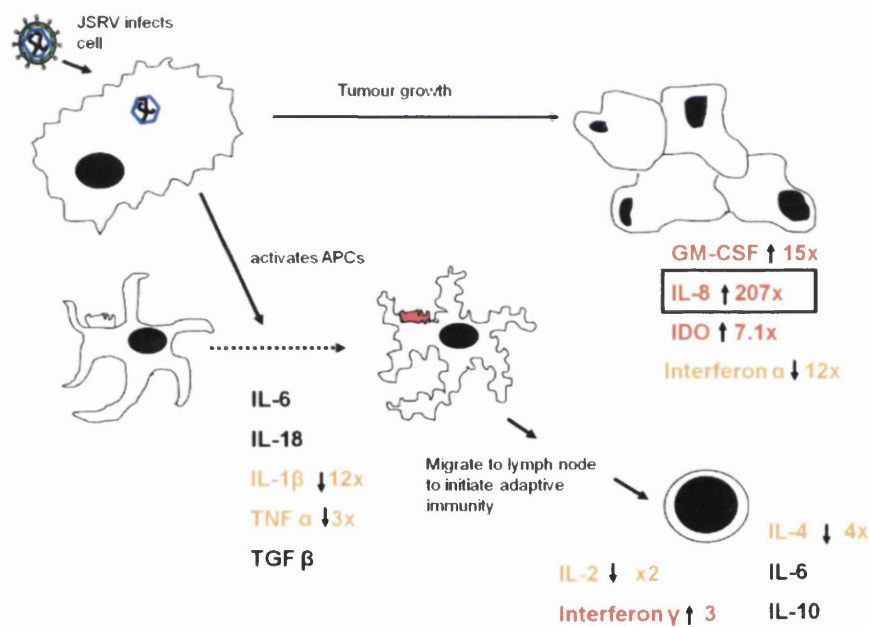


Figure 5.11 Summary of possible cytokine interactions following JSRV infection of a lung epithelial cell.

Of the cytokines examined, the biggest changes in mRNA expression ratios were seen in those known to promote tumour survival during the later stages of disease pathogenesis. Early virus expression was not accompanied by cytokine release or cellular infiltrate. In fact, at no point was there strong evidence of an adaptive immune response being made to viral antigen either detected by marked cellular infiltrates or increases in mRNA of cytokines commonly associated with TH1 or TH2 responses (Table 5.3).

qRT-PCR analysis has been used previously to successfully quantify levels of cytokine mRNA in the sheep (Budhia et al., 2006; Garcia-Crespo et al., 2005; Li et al., 2008; Ryan et al., 2008; Smeed et al., 2007). As it involves an exponential amplification of the gene of interest, the capacity to detect small changes in gene expression is maximised (Budhia et al., 2006). Sensitivity in this study was also enhanced by the use of multiple reference genes with tested stability, for data normalisation (Vandesompele et al., 2002). To further ensure reliable results, the experiment was carried out following the Minimum Information for Publication of Quantitative Real-Time PCR Experiments (MIQE) guidelines (Bustin et al., 2009). Despite these strict control measures, conclusive interpretation of mRNA cytokine levels is still a challenging task (Tripp et al., 2005), and there are certain limitations of the technique which must be recognised.

Cytokines are produced by a variety of cell types, frequently as part of a cascade, and act synergistically or antagonistically with autocrine and paracrine effects (Haddad, 2002). Measurements must take into account the short half-life and variable timing of peak expression post stimulation which is cytokine specific. It may be that the timing of sampling in this study did not reflect the maximum fluctuations in mRNA production. In addition, a broad range of cellular material was included in each tissue sample and it was not possible to assign changes in cytokine levels to particular cell types (apart from IL-8). This mix of cell types could also mean that detected changes in mRNA levels may not be due to upregulation or downregulation of mRNA, but simply that a different cell phenotype with a higher or lower baseline level of mRNA has been sampled. Alternatively, if only a few cells were affected, expression changes may have been diluted as RNA extraction was from a whole cross section of lung. Finally, interpretation of the qRT-PCR data in this study has assumed that levels of cytokine mRNA correlate with protein production and cytokine release. However, recent work

has highlighted methods of post-transcriptional control which act to regulate nuclear export, cytoplasmic localisation, translation initiation and mRNA decay (Anderson, 2008). These mechanisms are used to coordinate inflammatory responses, turning them on and off more rapidly than would otherwise be possible by transcriptional control alone. Post transcriptional regulation of the majority of cytokines used in this study has already been reported (Anderson, 2008). Methods to detect protein production eg. IHC would allow accurate correlation of mRNA levels with active cytokine release in this study.

To summarise the findings in this chapter, it appears that a majority of the cytokine response is related to tumour survival, with little evidence of a host response to virus expression. Further work should concentrate on looking at expression of a broader range of cytokines. Type I interferons are the key cytokines produced after a viral infection, and they coordinate additional innate responses and subsequent adaptive responses (Kawai and Akira, 2006). Future experiments should examine these cytokines in the early stages of disease, as techniques for evasion of the IFN related innate antiviral response have been reported for other viruses (Yoshikawa et al., 2010).

CHAPTER 6 GENERAL DISCUSSION AND CONCLUSIONS

Ovine pulmonary adenocarcinoma is a fatal respiratory disease of adult sheep. Since the first reports in the 19th century, research has successfully identified many important aspects of disease epidemiology and pathogenesis. However, a detailed analysis of the early stages of infection has not yet been described. The aim of this thesis was to examine some of these early interactions between JSRV and its ovine host. There were two main objectives. The first was to identify the target cell for JSRV infection in the lung, and the second to investigate the cytokine response to virus expression and tumour growth.

An experimental model of OPA was used to provide tissue for analysis which included these initial stages of pathogenesis (see 2.1). 6 day old SPF lambs received an intratracheal inoculation with an infectious molecular clone, JSRV₂₁. The lambs were euthanased 3, 10 and 72-91 days afterwards. IHC techniques to identify the phenotype of specific cells in the lung, and virus expression were then optimised (see 3.2 and 4.2). These methods were combined and applied to lung tissue from lambs 10 days post inoculation. Analysis of the phenotype of single cells expressing virus indicated that JSRV has multiple target cells in the ovine lung (see 4.2). Levels of cytokine mRNA were then measured in a range of lung samples (see 5.2). These were collected 3 and 10 days post inoculation (pre and post viral expression respectively) and between 72-91 days PI when tumour growth was prominent. Tissues from advanced field cases of OPA were included for comparison. Levels of cytokine mRNA remained unaffected by viral inoculation and early virus expression. However changes were seen in samples with prominent tumour growth, particularly in lungs from field cases of OPA. This was primarily noted for cytokines known to promote tumour survival.

The first experimental chapter concentrated on developing IHC techniques for respiratory epithelial cell identification in the ovine lung. These cells examined were ciliated epithelial cells, Clara cells, NEBs and type II pneumocytes. The specificity of antibodies was determined in several ways. For ciliated epithelial cells and Clara cells histochemical stains were used to highlight the morphological appearance of these cells prior to antibody labelling (Figure 3.2). For type II pneumocytes, SP-C specificity was confirmed by demonstrating colocalisation of labelling in the same cells with another published type II marker DC-LAMP (Salaun et al., 2004). A number of antibodies were evaluated to label NEBS (Table 2.3), but

only synaptophysin was successful. A study on human lung tissue also found synaptophysin to be the most reliable marker of neuroendocrine differentiation (Kasprzak et al., 2007). The unique morphology of NEBs, and positive control tissue containing other neuroendocrine cells, validated the specificity of this antibody. Inclusion of anti-aquaporin-5 antibody to label type I pneumocytes (Warburton et al., 2000) and anti-surfactant protein B antibody, which is expressed by both Clara cells and type II pneumocytes (Beytut et al., 2008), would have made this analysis more complete. Unfortunately the timescale of the project did not allow for this.

These techniques were initially developed to provide a tool for analysis of the JSRV target cell. However during the optimisation procedure on control lungs from experimental lambs, variations in protein expression were noticed between the age groups, and the possibility that these cells were undergoing postnatal cytodifferentiation was introduced. These observations were confirmed using Image J to numerically quantify IHC labelling for CCSP and beta tubulin (Figure 2.4). Protein expression in the bronchi, bronchioles, terminal bronchioles and respiratory bronchioles was examined in lung tissue from 9, 16 and 91 day old lambs. Increased protein detection was taken as an indicator of cell maturation, which was found to be both age and site specific. Maturation of ciliated epithelial cells was unchanged between 9-16 days, but showed an increase in all regions of the lung by 91 days. In contrast, Clara cells appeared to mature earlier in the proximal airways (bronchioles) than the distal ones (terminal and respiratory bronchioles). Populations of NEBs and type II pneumocytes were counted manually, but no significant changes were observed within these time points.

To complement this analysis of postnatal maturation the same samples were used to assess the proliferative state of different anatomical areas. The number of cells expressing Ki-67 were calculated as a percentage of the total number of cells in each of five predefined regions of the lung, to give the proliferative index of the epithelium in that area. Interestingly the biggest change was seen in the alveolar compartment where the proliferation index decreased between 16 and 91 days. As this calculation included all cell types in the region, it was thought to be due to a decrease in microvascular maturation, which has been identified as the final stage of lung maturation in other animals (Burri, 2006). Smaller but still significant reductions were seen in the bronchi, bronchioles and terminal bronchioles over the same time period. These measurements were of epithelial cells only, and likely reflect a decrease in growth rate of each

anatomical structure. However, the lack of samples between these time points may have failed to detect more dramatic changes in the proliferative index of these regions.

These techniques to identify and quantify epithelial cells in the ovine lung can now be applied to aid investigations into the pathogenesis of ovine respiratory disease. They will also be helpful for further analysis of progenitor cell types and cell subpopulations using lung injury models in the sheep lung, as has been performed in the mouse (Peake et al., 2000; Stevens et al., 1997; Stripp et al., 1995). In turn this may lead to a greater understanding of human respiratory disease. Recognition of similarities in lung anatomy and physiology between sheep and humans has led to a recent increase in the use of the sheep as a model for human respiratory disease. Lambs are now the leading model for diaphragmatic hernia and premature development of the lung (Scheerlinck et al., 2008). They are also used as a model for studying RSV infection, one of the most important infectious respiratory diseases of children (Meyerholz et al., 2004).

The second experimental chapter used immunofluorescent techniques to analyse the phenotype of JSRV target cells *in vivo*. Previously optimised antibodies which labelled respiratory epithelial cells were used in combination with an anti-JSRV SU antibody to identify the phenotype of single cells expressing virus. These cells were present in the lamb lung 10 days post inoculation, and were located in the distal conducting and respiratory airways. Multiple target cells were identified. They included SP-C and CCSP positive cells, both of which have been previously suggested as target cells for JSRV (Beytut et al., 2008; Palmarini et al., 1995; Platt et al., 2002). More interesting were several cells which labelled for JSRV SU but none of the other phenotypic markers. Evidence of cytodifferentiation in control lambs during this developmental period raised the possibility of JSRV targeting an immature type cell with an undifferentiated phenotype.

The ability of other respiratory viruses to infect their target cells can be affected by the stage of cell differentiation. For example, the expression of receptors for influenza virus are dependent on the state of differentiation of epithelial cells (Chan et al., 2010). For JSRV it is not known how Hyal-2 expression varies with cell maturity, but it is possible that the presence of other permissive and restrictive factors necessary for JSRV replication could be altered by the differentiation state of the target cell. It is interesting that an age related susceptibility to

infection has been previously recorded for JSRV (Salvatori et al., 2004). At the time this was attributed to a reduction in proliferation, and therefore the number of dividing (target) cells, for JSRV infection in older lambs. However, the present study found only small reductions in the proliferative index of multiple regions in the lung during maturation, suggesting additional factors may be involved. There is also a possibility that this undifferentiated cell could be similar to a type A Clara cell, previously described in mice following injury of respiratory epithelium (Evans et al., 1978). If the same repair mechanisms were to occur in sheep, then these undifferentiated cell types would increase in injured lungs, resulting in increased susceptibility to infection with JSRV. One of the early experiments by Dungal in 1938 found that addition of bacteria or lung worms to viral inoculate resulted in greater disease transmission (Table 1.4). Whether this was due to a change in the state of cell proliferation or differentiation needs further investigation.

There is also a possibility that this undifferentiated cell is some kind of previously undescribed stem cell. Respiratory viruses capable of infecting stem cells in the lung have already been described. For example, the SARS virus has been shown to replicate in lung progenitor cells *in vitro* (Ling et al., 2006). This could have an important role in the pathogenicity of infection *in vivo* as damage to these cell types would prevent efficient repair. Other malignant retroviruses which induce haematopoietic tumours have also been shown to infect haematopoietic and progenitor cell types to generate leukemic stem cells (Banerjee et al., 2010). Undifferentiated cells with stem cell characteristics have recently been isolated from lung tumours in humans (Eramo et al., 2008). If JSRV were to specifically target a stem cell in the lung, this would have huge implications for the field of respiratory research.

At the beginning of this study, Kim and co-workers reported an experiment using a K-ras mouse model of lung adenocarcinoma which identified stem cells in the lung (BASCs) expressing CCSP and SP-C (Kim et al., 2005). It was proposed that these BASCs were the progenitor stem cells for tumour growth, and additional experiments confirmed their stem cell characteristics *in vitro*. Initially, it was thought that a similar situation might be happening in the sheep, and JSRV was targeting BASCs. However, dual labelling using immunofluorescence failed to detect significant numbers of BASCs in the sheep. In the mouse, BASCs were detected in the majority of BADJ which occur at the junction of the terminal bronchioles and alveoli. In the sheep lung anatomy is slightly different (Figure 3.1F,

G). The presence of respiratory bronchioles effectively increases the number of BADI and therefore potential stem cell niches. However, out of all the sections examined from control and infected lambs, only two cells were identified with convincing dual expression of CCSP and SP-C (Figure 4.17). One of these also expressed JSRV SU. While this does suggest primary infection of a BASC, the low numbers detected imply that variations in this cell type will not greatly affect the ability for JSRV to infect the lung. It is still possible that JSRV does target the 'sheep equivalent of a BASC' but that the cell markers are different to the mouse. The variation in anatomy in this region of the lung gives weight to this theory, but further work needs to be done to verify this.

There are several ways in which the phenotype of the JSRV target cell could be further analysed. To investigate the immature progenitor cell theory, dual labelling of normal lung sections with beta tubulin and CCSP would demonstrate if there was a population of undifferentiated (ie. unlabelled) cells which diminished with increasing age. If this was the case, then the number of available target cells for JSRV would also decrease and an experimental infection would show a reduced number of cells expressing virus in older animals. Comparison of the infection of animals with and without lung injury, and a detailed IHC analysis of the cell types present and infected in both situations would also help target cell identification. A more thorough investigation of these cell types could be possible if lambs were infected with a fluorescently tagged virus and euthanased after 10 days. The target cells could be isolated using FACS, and their *in vitro* properties could then be examined in more detail. Methods for live imaging of *in vivo* virus infection or the use of *in vitro* lung tissue culture slices would also be helpful. In order to determine the efficiency of infection within this range of potential target cells, variations in inoculation dose and route of inoculation would be beneficial.

The second aim of this thesis was to investigate the host innate response to viral inoculation in terms of cytokine production. RNA was extracted from adjacent lung samples to those already analysed with IHC, and qRT-PCR was used to confirm the presence of JSRV mRNA. The cytokines analysed were chosen to represent indicators of innate, cell mediated and humoral responses and tumour growth regulation (Table 5.1). Little response, as detected by changes in mRNA levels, was seen in samples 3 and 10 days post inoculation. By 8 weeks PI, small increases in GM-CSF, IL-8 and MCP-1 mRNA were detected. In natural infections, larger

increases were detected in GMCSF and IL-8 mRNA, which are cytokines previously associated with neovascularisation and macrophage recruitment. Evidence of immunoregulation was also apparent due to an increase in IDO, and reduction in IL-1 beta. IHC was able to detect labelling for IL-8 in tumour cells, neutrophils and infiltrating macrophages. These results indicate that the host is responding to tumour growth, but provide little evidence of an acute or cell mediated/humoral response to viral infection. Interestingly, expression changes in some of these cytokines have also been recognised during the growth of human lung tumours (Karanikas et al., 2007; Yuan et al., 2005).

These findings are in agreement with much of the literature on OPA as several studies have been unable to detect JSRV specific T cell or antibody responses (Ortin et al., 1998; Summers et al., 2002). There are various explanations for this. The first involves a mechanism of central tolerance whereby expression of closely related enJSRV during fetal development results in the removal of any anti-JSRV T cells (see 1.3.7). This would make the sheep immunotolerant of JSRV antigens. Another idea is based on the propensity for JSRV to infect sheep lymphoid tissue (Palmarini et al 1996). Viral RNA and proviral DNA have been found in monocytes, macrophages, B cells and T cells early on in disease pathogenesis before clinical signs are apparent (Holland et al 1999). Although evidence of transformation is lacking, impairment of the normal function of these cells is possible and a reduced responsiveness of lymphoid cells to the T-cell mitogen Con A from naturally and experimentally infected animals has been reported (Summers et al 2002). Mechanisms of local immunosuppression have also been suggested. Several retroviruses encode an immunosuppressive domain within their Env protein which is well conserved between some genera (Haraguchi et al., 1995). Although a similar peptide sequence is not present on JSRV, it is still possible that JSRV Env could be causing immunosuppressive effects. Another theory is based on the immunoregulatory properties of surfactant proteins (SP-A, SP-B and SP-C) produced in large amounts by neoplastic cells (Beytut et al., 2008; Summers et al., 2002).

It is also important that the normal immunoregulatory properties of the respiratory tract and tumours in general are not overlooked. All previously mentioned surfactant proteins are constitutively produced by respiratory epithelial cells as immune modulators to limit innate inflammation and maintain lung homeostasis (Hussell and Goulding, 2010). This could also limit inflammatory reactions to small amounts of virus produced during the early stages of

infection with JSRV. Tumours, like viruses, have developed a multitude of mechanisms to evade rejection by the host immune response (see 1.3.6). One study on OPA reported downregulation of MHC I within tumour nodules (Summers et al., 2005). This study has detected increased mRNA levels of the immunoregulatory cytokine IDO in tissues containing mature tumours from naturally infected animals. Additional methods of tumour immunomodulation by OPA have still to be investigated.

In contrast to these theories, there are occasional reports of a host response to JSRV infection in certain situations. Vaccination trials showed that recombinant JSRV capsid antigen was able to induce antibody production and specific T cell responses in vaccinated sheep (Summers et al., 2006), and some histological studies found infiltrating lymphocytes within tumours (Garcia-Goti et al., 2000). One experiment looked for evidence of an adaptive immune response using IHC and found strong labelling for IFN gamma in macrophages and MHC II upregulation in tumour associated cells in advanced clinical cases of OPA (Summers et al., 2005). In a more recent investigation (Hudachek et al., 2010) experimentally infected lambs showed evidence of OPA lesion regression as detected using computed tomography. Low titres of serum neutralising antibodies were detected in 4/12 lambs (maximum titre 1:100 compared to 1:3000 in mice expressing JSRV Env). Two of these showed partial lesion regression and one did not develop tumour during the 3 month course of the experiment. A CD3+ T cell infiltration in association with tumours was also reported. However, all lambs were coinfecting with MVV which does induce strong antibody responses and could have had a role in OPA tumour rejection in these animals. While the ability to detect even a very low anti-JSRV Env antibody titre in these lambs (Hudachek et al., 2010) and an anti-CA response following vaccination (Summers et al., 2006) does indicate that the central tolerance proposition cannot be absolute, it is unlikely that adaptive immunity plays an important role in disease control in the majority of cases in the field.

Further work should include analysis of samples using a more global gene analysis system such as SAGE or microarray analysis. This would allow variations in many more cytokines to be assessed. Samples from additional time points, particularly in the early stages prior to extensive tumour growth, would provide a more thorough analysis of the host response to infection. Other techniques such as *in situ* hybridisation or laser capture microdissection could also help to link cytokine production to specific cell phenotypes and reduce the potential for

signal dilution experienced in this study. Proteomic analysis would allow correlation of mRNA levels with protein production, hence identifying any evidence of post transcriptional control.

In summary, these experiments are some of the first to analyse the early stages of infection of JSRV in the ovine lung. They have been successful in identifying some specifics of disease pathogenesis, including the identification of multiple target cells *in vivo*. However, of equal importance is the number of additional questions that have been raised, highlighting the need for further work in this area. As well as contributing towards the knowledge of JSRV pathogenesis, there have also been advances in the potential for the use of OPA as a model for human lung cancer. Research in this area is hindered by the lack of a good experimental model, particularly for examining early stages of oncogenesis. The infectious model used in the study, in combination with the robust IHC techniques developed to identify virus expression and cell phenotype, provides a unique and easily manipulated model with which to study the early stages of lung cancer. The similarity in cytokine response to tumour growth between sheep and humans, along with a lack of detectable response to virus, further recommends the OPA model as a tool for studying therapeutics for lung cancer.

Original reports of OPA described it as '*a rather puzzling disease*' (McFadyean, 1894). It is hoped that this thesis contributes towards addressing some of these confusing issues.

Appendix 1

Table A1 A summary of experimental animal numbers and their corresponding age of euthanasia and infection status.

Animal number	Time of euthanasia in days post inoculation	JSRV₂₁ infected/mock infected/control
2851	3	Control
2849	3	Control
2840	3	Mock
2846	3	Mock
2841	3	JSRV ₂₁
2848	3	JSRV ₂₁
2845	3	JSRV ₂₁
2850	3	JSRV ₂₁
2857	10	Control
2859	10	Control
2855	10	Mock
2853	10	Mock
2854	10	JSRV ₂₁
2858	10	JSRV ₂₁
2852	10	JSRV ₂₁
2856	10	JSRV ₂₁
2844	72	JSRV ₂₁
2842	72	Control
2863	91	JSRV ₂₁
2864	91	Control
2865	90	JSRV ₂₁
2861	90	JSRV ₂₁
2866	91	Mock
2862	91	Mock

Appendix 2

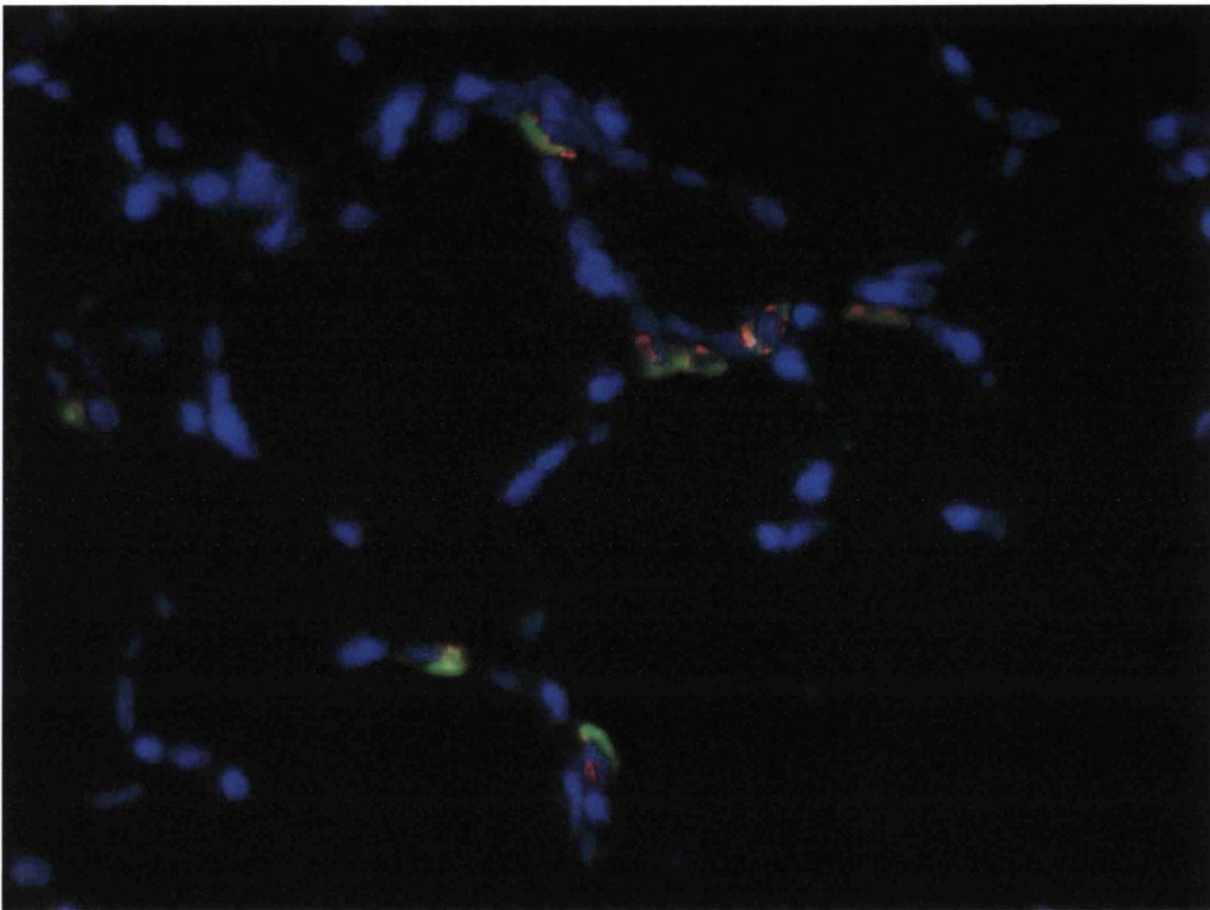


Figure A1 Alveolar region showing colocalisation of labelling for DC-LAMP and SP-C in type II pneumocytes. Green, anti-DC-LAMP. Red, anti-SP-C. Blue, DAPI nuclei.

Akira, S., Uematsu, S., and Takeuchi, O. (2006). Pathogen recognition and innate immunity. *Cell* **124**, 783-801.

Al-Zubaidy, A., and Sokkar, S.M. (1979). Studies on Ovine Pulmonary Adenomatosis in Iraq. *Indian Veterinary Journal* **56**, 360-362.

Alcorn, D.G., Adamson, T.M., Maloney, J.E., and Robinson, P.M. (1981). A morphologic and morphometric analysis of fetal lung development in the sheep. *Anat Rec* **201**, 655-667.

Allen, T.E., Sherrill, K.J., Crispell, S.M., Perrott, M.R., Carlson, J.O., and DeMartini, J.C. (2002). The jaagsiekte sheep retrovirus envelope gene induces transformation of the avian fibroblast cell line DF-1 but does not require a conserved SH2 binding domain. *J Gen Virol* **83**, 2733-2742.

Anderson, P. (2008). Post-transcriptional control of cytokine production. *Nat Immunol* **9**, 353-359.

Archer, F., Jacquier, E., Lyon, M., Chastang, J., Cottin, V., Mornex, J.F., and Leroux, C. (2007). Alveolar type II cells isolated from pulmonary adenocarcinoma: a model for JSRV expression in vitro. *Am J Respir Cell Mol Biol* **36**, 534-540.

Arnaud, F., Black, S.G., Murphy, L., Griffiths, D.J., Neil, S.J., Spencer, T.E., and Palmarini, M. (2010). Interplay between ovine bone marrow stromal cell antigen 2/tetherin and endogenous retroviruses. *J Virol* **84**, 4415-4425.

Arnaud, F., Caporale, M., Varela, M., Biek, R., Chessa, B., Alberti, A., Golder, M., Mura, M., Zhang, Y.P., Yu, L., *et al.* (2007a). A Paradigm for Virus-Host Coevolution: Sequential Counter-Adaptations between Endogenous and Exogenous Retroviruses. *PLoS Pathog* **3**, e170.

Arnaud, F., Murcia, P.R., and Palmarini, M. (2007b). Mechanisms of late restriction induced by an endogenous retrovirus. *J Virol* **81**, 11441-11451.

Arsalane, K., Broeckert, F., Knoops, B., Wiedig, M., Toubeau, G., and Bernard, A. (2000). Clara cell specific protein (CC16) expression after acute lung inflammation induced by intratracheal lipopolysaccharide administration. *Am J Respir Crit Care Med* **161**, 1624-1630.

Asabe, K., Jennings, R.W., Harrison, M.R., and Suita, S. (2004). Quantitative study of pulmonary endocrine cells in fetal, postnatal and adult sheep. *J Vet Med Sci* **66**, 373-380.

Aso, Y., Yoneda, K., and Kikkawa, Y. (1976). Morphologic and biochemical study of pulmonary changes induced by bleomycin in mice. *Lab Invest* **35**, 558-568.

Azzopardi, A., and Thurlbeck, W.M. (1969). The histochemistry of the nonciliated bronchiolar epithelial cell. *Am Rev Respir Dis* **99**, 516-525.

Baggiolini, M., Walz, A., and Kunkel, S.L. (1989). Neutrophil-activating peptide-1/interleukin 8, a novel cytokine that activates neutrophils. *J Clin Invest* **84**, 1045-1049.

Bai, J., Bishop, J.V., Carlson, J.O., and DeMartini, J.C. (1999). Sequence comparison of JSRV with endogenous proviruses: envelope genotypes and a novel ORF with similarity to a G-protein-coupled receptor. *Virology* **258**, 333-343.

Balaguer, L., and Romano, J. (1991). Solitary neuroendocrine cells and neuroepithelial bodies in the lower airways of embryonic, fetal, and postnatal sheep. *Anat Rec* **231**, 333-338.

Baltimore, D. (1970). RNA-dependent DNA polymerase in virions of RNA tumour viruses. *Nature* **226**, 1209-1211.

Bancroft J.D., C.H.C. (1994). *Manual of Histological Techniques and their Diagnostic application* (Longman Group UK Limited).

Banerjee, P., Crawford, L., Samuelson, E., and Feuer, G. (2010). Hematopoietic stem cells and retroviral infection. *Retrovirology* **7**, 8.

Barre-Sinoussi, F., Chermann, J.C., Rey, F., Nugeyre, M.T., Chamaret, S., Gruest, J., Dautet, C., Axler-Blin, C., Vezinet-Brun, F., Rouzioux, C., *et al.* (1983). Isolation of a T-lymphotropic retrovirus from a patient at risk for acquired immune deficiency syndrome (AIDS). *Science* **220**, 868-871.

Barth, P.J., Koch, S., Muller, B., Unterstab, F., von Wichert, P., and Moll, R. (2000). Proliferation and number of Clara cell 10-kDa protein (CC10)-reactive epithelial cells and basal cells in normal, hyperplastic and metaplastic bronchial mucosa. *Virchows Arch* **437**, 648-655.

Bernard, A., Marchandise, F.X., Depelchin, S., Lauwerys, R., and Sibille, Y. (1992). Clara cell protein in serum and bronchoalveolar lavage. *Eur Respir J* 5, 1231-1238.

Bertolini, G., Roz, L., Perego, P., Tortoreto, M., Fontanella, E., Gatti, L., Pratesi, G., Fabbri, A., Andriani, F., Tinelli, S., *et al.* (2009). Highly tumorigenic lung cancer CD133+ cells display stem-like features and are spared by cisplatin treatment. *Proc Natl Acad Sci U S A* 106, 16281-16286.

Beytut, E., Sozmen, M., and Erginsoy, S. (2008). Immunohistochemical Detection of Pulmonary Surfactant Proteins and Retroviral Antigens in the Lungs of Sheep with Pulmonary Adenomatosis. *J Comp Pathol*.

Bhattacharjee, A., Richards, W.G., Staunton, J., Li, C., Monti, S., Vasa, P., Ladd, C., Beheshti, J., Bueno, R., Gillette, M., *et al.* (2001). Classification of human lung carcinomas by mRNA expression profiling reveals distinct adenocarcinoma subclasses. *Proc Natl Acad Sci U S A* 98, 13790-13795.

Bieniasz, P.D. (2003). Restriction factors: a defense against retroviral infection. *Trends Microbiol* 11, 286-291.

Blakemore, F.B., TJ (1941). The occurrence of Jaagsiekte in England. *The Veterinary Record* 53, 35-37.

Blenkinsopp, W.K. (1967). Proliferation of respiratory tract epithelium in the rat. *Exp Cell Res* 46, 144-154.

Boers, J.E., Ambergen, A.W., and Thunnissen, F.B. (1999). Number and proliferation of clara cells in normal human airway epithelium. *Am J Respir Crit Care Med* 159, 1585-1591.

Bolton, S.J., Pinnion, K., Marshall, C.V., Wilson, E., Barker, J.E., Oreffo, V., and Foster, M.L. (2008). Changes in Clara cell 10 kDa protein (CC10)-positive cell distribution in acute lung injury following repeated lipopolysaccharide challenge in the rat. *Toxicol Pathol* 36, 440-448.

Bonne (1939). Morphological resemblance of pulmonary adenomatosis (Jaagsiekte) in sheep and certain cases of cancer of the lung in man. *The American Journal of Cancer* 34, 491-501.

Bouljihad, M., and Leipold, H.W. (1994). An ultrastructural study of pulmonary bronchiolar and alveolar epithelium in sheep. *Zentralbl Veterinarmed A* 41, 573-586.

Brackenbury, J.H. (1972). Lung-air-sac anatomy and respiratory pressures in the bird. *J Exp Biol* 57, 543-550.

Breeze, R.G., and Wheeldon, E.B. (1977). The cells of the pulmonary airways. *Am Rev Respir Dis* 116, 705-777.

Browne, E.P., and Littman, D.R. (2008). Species-specific restriction of apobec3-mediated hypermutation. *J Virol* 82, 1305-1313.

Brudek, T., Christensen, T., Aagaard, L., Petersen, T., Hansen, H.J., and Moller-Larsen, A. (2009). B cells and monocytes from patients with active multiple sclerosis exhibit increased surface expression of both HERV-H Env and HERV-W Env, accompanied by increased seroreactivity. *Retrovirology* 6, 104.

Budhia, S., Haring, L.F., McConnell, I., and Blacklaws, B.A. (2006). Quantitation of ovine cytokine mRNA by real-time RT-PCR. *J Immunol Methods* 309, 160-172.

Bueno, S.M., Gonzalez, P.A., Pacheco, R., Leiva, E.D., Cautivo, K.M., Tobar, H.E., Mora, J.E., Prado, C.E., Zuniga, J.P., Jimenez, J., *et al.* (2008). Host immunity during RSV pathogenesis. *Int Immunopharmacol* 8, 1320-1329.

Burri, P.H. (2006). Structural aspects of postnatal lung development - alveolar formation and growth. *Biol Neonate* 89, 313-322.

Bustin, S.A., Benes, V., Garson, J.A., Hellemans, J., Huggett, J., Kubista, M., Mueller, R., Nolan, T., Pfaffl, M.W., Shipley, G.L., *et al.* (2009). The MIQE guidelines: minimum information for publication of quantitative real-time PCR experiments. *Clin Chem* 55, 611-622.

Caporale, M., Cousens, C., Centorame, P., Pinoni, C., De las Heras, M., and Palmarini, M. (2006). Expression of the jaagsiekte sheep retrovirus envelope glycoprotein is sufficient to induce lung tumors in sheep. *J Virol* 80, 8030-8037.

Cardoso, W.V. (2000). Lung morphogenesis revisited: old facts, current ideas. *Dev Dyn* 219, 121-130.

Cardoso, W.V., and Lu, J. (2006). Regulation of early lung morphogenesis: questions, facts and controversies. *Development* 133, 1611-1624.

Castleman, W.L. (1984). Alterations in pulmonary ultrastructure and morphometric parameters induced by parainfluenza (Sendai) virus in rats during postnatal growth. *Am J Pathol* 114, 322-335.

Castleman, W.L., and Lay, J.C. (1990). Morphometric and ultrastructural study of postnatal lung growth and development in calves. *Am J Vet Res* 51, 789-795.

Castro, C.M., Yang, Y., Zhang, Z., and Linnoila, R.I. (2000). Attenuation of pulmonary neuroendocrine differentiation in mice lacking Clara cell secretory protein. *Lab Invest* 80, 1533-1540.

Chan, R.W., Yuen, K.M., Yu, W.C., Ho, C.C., Nicholls, J.M., Peiris, J.S., and Chan, M.C. (2010). Influenza H5N1 and H1N1 virus replication and innate immune responses in bronchial epithelial cells are influenced by the state of differentiation. *PLoS One* 5, e8713.

Chilosi, M., and Murer, B. (2010). Mixed adenocarcinomas of the lung: place in new proposals in classification, mandatory for target therapy. *Arch Pathol Lab Med* 134, 55-65.

Chitra, E., Yu, S.L., Hsiao, K.N., Shao, H.Y., Sia, C., Chen, I.H., Hsieh, S.Y., Chen, J.H., and Chow, Y.H. (2009). Generation and characterization of JSRV envelope transgenic mice in FVB background. *Virology* 393, 120-126.

Clara, M. (1937). Zur Histobiologie des Bronchialepithels. *Z mikrosk-anatForsch* 4, 321-347.

Clarke, M.F., Dick, J.E., Dirks, P.B., Eaves, C.J., Jamieson, C.H., Jones, D.L., Visvader, J., Weissman, I.L., and Wahl, G.M. (2006). Cancer stem cells--perspectives on current status and future directions: AACR Workshop on cancer stem cells. *Cancer Res* 66, 9339-9344.

Coetzee, S., Els, H.J., and Verwoerd, D.W. (1976). Transmission of jaagsiekte (ovine pulmonary adenomatosis) by means of a permanent epithelial cell line established from affected lungs. *Onderstepoort J Vet Res* 43, 133-141.

Coffin, J.M., Hughes, S.H., and Varmus, H.E. (1997). *Retroviruses* (Cold Spring Harbour Laboratory Press).

Coppens, J.T., Van Winkle, L.S., Pinkerton, K., and Plopper, C.G. (2007). Distribution of Clara cell secretory protein expression in the tracheobronchial airways of rhesus monkeys. *Am J Physiol Lung Cell Mol Physiol* 292, L1155-1162.

Corrin, B. (2000). *Pathology of the Lungs* (Hardcourt Publishers Ltd).

Cote, M., Zheng, Y.M., and Liu, S.L. (2009). Receptor binding and low pH coactivate oncogenic retrovirus envelope-mediated fusion. *J Virol* 83, 11447-11455.

Cousens, C., Bishop, J.V., Philbey, A.W., Gill, C.A., Palmarini, M., Carlson, J.O., DeMartini, J.C., and Sharp, J.M. (2004). Analysis of integration sites of Jaagsiekte sheep retrovirus in ovine pulmonary adenocarcinoma. *J Virol* 78, 8506-8512.

Cousens, C., Minguillon, E., Dalziel, R.G., Ortin, A., Garcia, M., Park, J., Gonzalez, L., Sharp, J.M., and de las Heras, M. (1999). Complete sequence of enzootic nasal tumor virus, a retrovirus associated with transmissible intranasal tumors of sheep. *J Virol* 73, 3986-3993.

Cowdry, E.V. (1925a). Studies on the Etiology of Jagziekte : I. The Primary Lesions. *J Exp Med* 42, 323-333.

Cowdry, E.V. (1925b). Studies on the Etiology of Jagziekte : ii. Origin of the Epithelial Proliferations, and the Subsequent Changes. *J Exp Med* 42, 335-345.

Cregger, M., Berger, A.J., and Rimm, D.L. (2006). Immunohistochemistry and quantitative analysis of protein expression. *Arch Pathol Lab Med* 130, 1026-1030.

Cuba-Cuparo, A., de la Vega, E., and Copaira, M. (1960). Pulmonary Adenomatosis of Sheep - Metastasizing Bronchiolar Tumors. *American journal of Veterinary Research July*, 673-682.

Cuba-Cuparo A, d.I.V.E., Copaira M (1960). Pulmonary Adenomatosis of Sheep - Metastasizing Bronchiolar Tumors. *American journal of Veterinary Research July*, 673-682.

Cutlip, R.C., and Young, S. (1982). Sheep pulmonary adenomatosis (jaagsiekte) in the United States. *Am J Vet Res* 43, 2108-2113.

Cutz, E., Chan, W., Wong, V., and Conen, P.E. (1975). Ultrastructure and fluorescence histochemistry of endocrine (APUD-type) cells in tracheal mucosa of human and various animal species. *Cell Tissue Res* 158, 425-437.

Cvjetanovic, V., Forsek, Z., Nevjestic, A., and Rukavina, L. (1972). Isolation of the Sheep Pulmonary Adenomatosis (SPA) Virus. *Veterinaria* 21, 493-496.

Dakessian, R.M., and Fan, H. (2008). Specific in vivo expression in type II pneumocytes of the Jaagsiekte sheep retrovirus long terminal repeat in transgenic mice. *Virology* 372, 398-408.

Dakessian, R.M., Inoshima, Y., and Fan, H. (2007). Tumors in mice transgenic for the envelope protein of Jaagsiekte sheep retrovirus. *Virus Genes* 35, 73-80.

Danilkovitch-Miagkova, A., Duh, F.M., Kuzmin, I., Angeloni, D., Liu, S.L., Miller, A.D., and Lerman, M.I. (2003). Hyaluronidase 2 negatively regulates RON receptor tyrosine kinase and mediates transformation of epithelial cells by jaagsiekte sheep retrovirus. *Proc Natl Acad Sci U S A* 100, 4580-4585.

Dave, V., Wert, S.E., Tanner, T., Thitoff, A.R., Loudy, D.E., and Whitsett, J.A. (2008). Conditional deletion of Pten causes bronchiolar hyperplasia. *Am J Respir Cell Mol Biol* 38, 337-345.

De Boer, G., F. (1970). Zwoegerziekte. Een persisterende virusinfectie bij Schapen. Diss Utrecht.

de Kock, G. (1958). The transformation of the lining of the pulmonary alveoli with special reference to adenomatosis in the lungs (Jagziekte) of sheep. *American journal of Veterinary Research* 19, 261-269.

De las Heras, M., Barsky, S.H., Hasleton, P., Wagner, M., Larson, E., Egan, J., Ortin, A., Gimenez-Mas, J.A., Palmarini, M., and Sharp, J.M. (2000). Evidence for a protein related immunologically to the jaagsiekte sheep retrovirus in some human lung tumours. *Eur Respir J* 16, 330-332.

De Las Heras, M., Murcia, P., Ortin, A., Azua, J., Borderias, L., Alvarez, R., Jimenez-Mas, J.A., Marchetti, A., and Palmarini, M. (2007). Jaagsiekte sheep retrovirus is not detected in human lung adenocarcinomas expressing antigens related to the Gag polyprotein of betaretroviruses. *Cancer Lett* 258, 22-30.

De Las Heras, M., Ortin, A., Benito, A., Summers, C., Ferrer, L.M., and Sharp, J.M. (2006). In-situ demonstration of mitogen-activated protein kinase Erk 1/2 signalling pathway in contagious respiratory tumours of sheep and goats. *J Comp Pathol* 135, 1-10.

De las Heras, M., Ortin, A., Cousens, C., Minguijon, E., and Sharp, J.M. (2003). Enzootic nasal adenocarcinoma of sheep and goats. *Curr Top Microbiol Immunol* 275, 201-223.

De las Heras, M., Ortin A., Cousens C., Minguijon E., Sharp J.M., (2003). Enzootic nasal adenocarcinoma of sheep and goats. *Current Topics in Microbiology and Immunology* 275, 201-223.

de Villiers, E.M., Els, H.J., and Verwoerd, D.W. (1975). Characteristics of an ovine herpesvirus associated with pulmonary adenomatosis (jaagsiekte) in sheep. *S Afr J Med Sci* 40, 165-175.

de Visser, K.E., and Coussens, L.M. (2005). The interplay between innate and adaptive immunity regulates cancer development. *Cancer Immunol Immunother* 54, 1143-1152.

Deimling, J., Thompson, K., Tseu, I., Wang, J., Keijzer, R., Tanswell, A.K., and Post, M. (2007). Mesenchymal maintenance of distal epithelial cell phenotype during late fetal lung development. *Am J Physiol Lung Cell Mol Physiol* 292, L725-741.

Delves, P.J., and Roitt, I.M. (2000a). The immune system. First of two parts. *N Engl J Med* 343, 37-49.

Delves, P.J., and Roitt, I.M. (2000b). The immune system. Second of two parts. *N Engl J Med* 343, 108-117.

Demartini, J.C., Rosadio, R.H., and Lairmore, M.D. (1988). The etiology and pathogenesis of ovine pulmonary carcinoma (sheep pulmonary adenomatosis). *Vet Microbiol* 17, 219-236.

Dungal, N. (1946). Experiments with Jaagsiekte. *Am J Pathol* 22, 737-759.

Dungal, N., Gislason, G., and Taylor, E., L. (1938). Epizootic Adenomatosis in the lungs of sheep - comparisons with Jaagsiekte, verminous pneumonia and progressive pneumonia. *Journal of Comparative Pathology*, 46-68.

Dungal, N., Gislason, G., and Taylor, E.L. (1938). Epizootic Adenomatosis in the lungs of sheep - comparisons with Jaagsiekte, verminous pneumonia and progressive pneumonia. *Journal of Comparative Pathology*, 46-68.

Dunlap, K.A., Palmarini, M., Adelson, D.L., and Spencer, T.E. (2005). Sheep endogenous betaretroviruses (enJSRVs) and the hyaluronidase 2 (HYAL2) receptor in the ovine uterus and conceptus. *Biol Reprod* **73**, 271-279.

Dunlap, K.A., Palmarini, M., Varela, M., Burghardt, R.C., Hayashi, K., Farmer, J.L., and Spencer, T.E. (2006). Endogenous retroviruses regulate periimplantation placental growth and differentiation. *Proc Natl Acad Sci U S A* **103**, 14390-14395.

Dunphy, J., Horvath, A., Barcham, G., Balic, A., Bischof, R., and Meeusen, E. (2001). Isolation, characterisation and expression of mRNAs encoding the ovine CC chemokines, monocyte chemoattractant protein (MCP)-1 α and -2. *Vet Immunol Immunopathol* **82**, 153-164.

Dupressoir, A., Vernochet, C., Bawa, O., Harper, F., Pierron, G., Opolon, P., and Heidmann, T. (2009). Syncytin-A knockout mice demonstrate the critical role in placentation of a fusogenic, endogenous retrovirus-derived, envelope gene. *Proc Natl Acad Sci U S A* **106**, 12127-12132.

Dykes, J.R., and McFadyean, J. (1888). Lung disease in sheep, caused by the strongylus rufescens. *Journal of Comparative Pathology and Therapeutics* **1**, 139-146.

Ellermann, V., and Bang, O. (1908). Experimentelle Leukämie bei Hühnern. *Zentralbl Bakteriol Parasite Infekt* **46**, 595-609.

Eramo, A., Haas, T.L., and De Maria, R. (2010). Lung cancer stem cells: tools and targets to fight lung cancer. *Oncogene*.

Eramo, A., Lotti, F., Sette, G., Pilozi, E., Biffoni, M., Di Virgilio, A., Conticello, C., Ruco, L., Peschle, C., and De Maria, R. (2008). Identification and expansion of the tumorigenic lung cancer stem cell population. *Cell Death Differ* **15**, 504-514.

Erlwein, O., Kaye, S., McClure, M.O., Weber, J., Wills, G., Collier, D., Wessely, S., and Cleare, A. (2010). Failure to detect the novel retrovirus XMRV in chronic fatigue syndrome. *PLoS One* **5**, e8519.

Evans, M.J., Cabral-Anderson, L.J., and Freeman, G. (1978). Role of the Clara cell in renewal of the bronchiolar epithelium. *Lab Invest* **38**, 648-653.

Evans, M.J., Cabral, L.J., Stephens, R.J., and Freeman, G. (1973). Renewal of alveolar epithelium in the rat following exposure to NO₂. *Am J Pathol* **70**, 175-198.

Evans, M.J., Johnson, L.V., Stephens, R.J., and Freeman, G. (1976). Renewal of the terminal bronchiolar epithelium in the rat following exposure to NO₂ or O₃. *Lab Invest* **35**, 246-257.

Fan, H., Longacre, A., Meng, F., Patel, V., Hsiao, K., Koh, J.S., and Levine, J.S. (2004). Cytokine dysregulation induced by apoptotic cells is a shared characteristic of macrophages from nonobese diabetic and systemic lupus erythematosus-prone mice. *J Immunol* **172**, 4834-4843.

Fanucchi, M.V., Buckpitt, A.R., Murphy, M.E., and Plopper, C.G. (1997a). Naphthalene cytotoxicity of differentiating Clara cells in neonatal mice. *Toxicol Appl Pharmacol* **144**, 96-104.

Fanucchi, M.V., Murphy, M.E., Buckpitt, A.R., Philpot, R.M., and Plopper, C.G. (1997b). Pulmonary cytochrome P450 monooxygenase and Clara cell differentiation in mice. *Am J Respir Cell Mol Biol* **17**, 302-314.

Feyrter, F. (1938). Über wucherung der Brunnerschen Drüsen. *Virchows Arch* **293**, 509-526.

Flecknoe, S., Harding, R., Maritz, G., and Hooper, S.B. (2000). Increased lung expansion alters the proportions of type I and type II alveolar epithelial cells in fetal sheep. *Am J Physiol Lung Cell Mol Physiol* **278**, L1180-1185.

Flecknoe, S.J., Wallace, M.J., Cock, M.L., Harding, R., and Hooper, S.B. (2003). Changes in alveolar epithelial cell proportions during fetal and postnatal development in sheep. *Am J Physiol Lung Cell Mol Physiol* **285**, L664-670.

Fuchs, E., Tumber, T., and Guasch, G. (2004). Socializing with the neighbors: stem cells and their niche. *Cell* **116**, 769-778.

Fujimoto, H., Sangai, T., Ishii, G., Ikehara, A., Nagashima, T., Miyazaki, M., and Ochiai, A. (2009). Stromal MCP-1 in mammary tumors induces tumor-associated macrophage infiltration and contributes to tumor progression. *Int J Cancer* **125**, 1276-1284.

Fukuyama, T., Ichiki, Y., Yamada, S., Shigematsu, Y., Baba, T., Nagata, Y., Mizukami, M., Sugaya, M., Takenoyama, M., Hanagiri, T., *et al.* (2007). Cytokine production of lung cancer cell lines: Correlation between their production and the inflammatory/immunological responses both in vivo and in vitro. *Cancer Sci* 98, 1048-1054.

Galon, J., Costes, A., Sanchez-Cabo, F., Kirilovsky, A., Mlecnik, B., Lagorce-Pages, C., Tosolini, M., Camus, M., Berger, A., Wind, P., *et al.* (2006). Type, density, and location of immune cells within human colorectal tumors predict clinical outcome. *Science* 313, 1960-1964.

Garcia-Crespo, D., Juste, R.A., and Hurtado, A. (2005). Selection of ovine housekeeping genes for normalisation by real-time RT-PCR; analysis of PrP gene expression and genetic susceptibility to scrapie. *BMC Vet Res* 1, 3.

Garcia-Goti, M., Gonzalez, L., Cousens, C., Cortabarria, N., Extramiana, A.B., Minguñon, E., Ortin, A., De las Heras, M., and Sharp, J.M. (2000). Sheep pulmonary adenomatosis: characterization of two pathological forms associated with jaagsiekte retrovirus. *J Comp Pathol* 122, 55-65.

Giangreco, A., Arwert, E.N., Rosewell, I.R., Snyder, J., Watt, F.M., and Stripp, B.R. (2009). Stem cells are dispensable for lung homeostasis but restore airways after injury. *Proc Natl Acad Sci U S A* 106, 9286-9291.

Giangreco, A., Reynolds, S.D., and Stripp, B.R. (2002). Terminal bronchioles harbor a unique airway stem cell population that localizes to the bronchoalveolar duct junction. *Am J Pathol* 161, 173-182.

Goff, S.P. (2004). Retrovirus restriction factors. *Mol Cell* 16, 849-859.

Gonzalez, R.F., Allen, L., and Dobbs, L.G. (2009). Rat alveolar type I cells proliferate, express OCT-4, and exhibit phenotypic plasticity in vitro. *Am J Physiol Lung Cell Mol Physiol* 297, L1045-1055.

Gosney, J.R. (1990). Pulmonary endocrine cells in native Peruvian guinea-pigs at low and high altitude. *J Comp Pathol* 102, 7-12.

Granucci, F., Andrews, D.M., Degli-Esposti, M.A., and Ricciardi-Castagnoli, P. (2002). IL-2 mediates adjuvant effect of dendritic cells. *Trends Immunol* 23, 169-171.

Griffiths, D.J. (2001). Endogenous retroviruses in the human genome sequence. *Genome Biol* 2, REVIEWS1017.

Griffiths, D.J., Martineau, H.M., and Cousens, C. (2010). Pathology and pathogenesis of ovine pulmonary adenocarcinoma. *J Comp Pathol* 142, 260-283.

Gross, L. (1951). "Spontaneous" leukemia developing in C3H mice following inoculation in infancy, with AK-leukemic extracts, or AK-embryos. *Proc Soc Exp Biol Med* 76, 27-32.

Gross, L. (1957). Development and serial cellfree passage of a highly potent strain of mouse leukemia virus. *Proc Soc Exp Biol Med* 94, 767-771.

Guth, A.M., Janssen, W.J., Bosio, C.M., Crouch, E.C., Henson, P.M., and Dow, S.W. (2009). Lung environment determines unique phenotype of alveolar macrophages. *Am J Physiol Lung Cell Mol Physiol* 296, L936-946.

Haddad, J.J. (2002). Cytokines and related receptor-mediated signaling pathways. *Biochem Biophys Res Commun* 297, 700-713.

Hall, P.A., and Levison, D.A. (1990). Review: assessment of cell proliferation in histological material. *J Clin Pathol* 43, 184-192.

Hanahan, D., and Weinberg, R.A. (2000). The hallmarks of cancer. *Cell* 100, 57-70.

Hansen, T.H., and Bouvier, M. (2009). MHC class I antigen presentation: learning from viral evasion strategies. *Nat Rev Immunol* 9, 503-513.

Haraguchi, S., Good, R.A., and Day, N.K. (1995). Immunosuppressive retroviral peptides: cAMP and cytokine patterns. *Immunol Today* 16, 595-603.

Harel, J., Rassart, E., and Jolicoeur, P. (1981). Cell cycle dependence of synthesis of unintegrated viral DNA in mouse cells newly infected with murine leukemia virus. *Virology* 110, 202-207.

Harrington, N.P., Surujballi, O.P., and Prescott, J.F. (2006). Cervine (*Cervus elaphus*) cytokine mRNA quantification by real-time polymerase chain reaction. *J Wildl Dis* 42, 219-233.

Hatanaka, H., Abe, Y., Kamiya, T., Morino, F., Nagata, J., Tokunaga, T., Oshika, Y., Suemizu, H., Kijima, H., Tsuchida, T., *et al.* (2000). Clinical implications of interleukin (IL)-10 induced by non-small-cell lung cancer. *Ann Oncol* 11, 815-819.

Heidmann, O., Vernochet, C., Dupressoir, A., and Heidmann, T. (2009). Identification of an endogenous retroviral envelope gene with fusogenic activity and placenta-specific expression in the rabbit: a new "syncytin" in a third order of mammals. *Retrovirology* 6, 107.

Herring, A.J., Sharp, J.M., Scott, F.M., and Angus, K.W. (1983). Further evidence for a retrovirus as the aetiological agent of sheep pulmonary adenomatosis (jaagsiekte). *Vet Microbiol* 8, 237-249.

Hiatt, K.M., and Highsmith, W.E. (2002). Lack of DNA evidence for jaagsiekte sheep retrovirus in human bronchioloalveolar carcinoma. *Hum Pathol* 33, 680.

Hicks, S.M., Vassallo, J.D., Dieter, M.Z., Lewis, C.L., Whiteley, L.O., Fix, A.S., and Lehman-McKeeman, L.D. (2003). Immunohistochemical analysis of Clara cell secretory protein expression in a transgenic model of mouse lung carcinogenesis. *Toxicology* 187, 217-228.

Ho, M.M., Ng, A.V., Lam, S., and Hung, J.Y. (2007). Side population in human lung cancer cell lines and tumors is enriched with stem-like cancer cells. *Cancer Res* 67, 4827-4833.

Hofacre, A., and Fan, H. (2004). Multiple domains of the Jaagsiekte sheep retrovirus envelope protein are required for transformation of rodent fibroblasts. *J Virol* 78, 10479-10489.

Holland, M.J., Palmarini, M., Garcia-Goti, M., Gonzalez, L., McKendrick, I., de las Heras, M., and Sharp, J.M. (1999). Jaagsiekte retrovirus is widely distributed both in T and B lymphocytes and in mononuclear phagocytes of sheep with naturally and experimentally acquired pulmonary adenomatosis. *J Virol* 73, 4004-4008.

Holt, P.G., Strickland, D.H., Wikstrom, M.E., and Jahnsen, F.L. (2008). Regulation of immunological homeostasis in the respiratory tract. *Nat Rev Immunol* 8, 142-152.

Hong, K.U., Reynolds, S.D., Giangreco, A., Hurley, C.M., and Stripp, B.R. (2001). Clara cell secretory protein-expressing cells of the airway neuroepithelial body microenvironment include a label-retaining subset and are critical for epithelial renewal after progenitor cell depletion. *Am J Respir Cell Mol Biol* 24, 671-681.

Hong, K.U., Reynolds, S.D., Watkins, S., Fuchs, E., and Stripp, B.R. (2004a). Basal cells are a multipotent progenitor capable of renewing the bronchial epithelium. *Am J Pathol* 164, 577-588.

Hong, K.U., Reynolds, S.D., Watkins, S., Fuchs, E., and Stripp, B.R. (2004b). In vivo differentiation potential of tracheal basal cells: evidence for multipotent and unipotent subpopulations. *Am J Physiol Lung Cell Mol Physiol* 286, L643-649.

Hopwood, P., Wallace, W.A., Cousens, C., Dewar, P., Muldoon, M., Norval, M., and Griffiths, D.J. (2010). Absence of markers of betaretrovirus infection in human pulmonary adenocarcinoma. *Hum Pathol*.

Hudachek, S.F., Kraft, S.L., Thamm, D.H., Bielefeldt-Ohmann, H., DeMartini, J.C., Miller, A.D., and Dernell, W.S. (2010). Lung tumor development and spontaneous regression in lambs coinfectd with Jaagsiekte sheep retrovirus and ovine lentivirus. *Vet Pathol* 47, 148-162.

Hunter, A.R., and Munro, R. (1983). The diagnosis, occurrence and distribution of sheep pulmonary adenomatosis in Scotland 1975 to 1981. *Br Vet J* 139, 153-164.

Hussell, T., and Goulding, J. (2010). Structured regulation of inflammation during respiratory viral infection. *Lancet Infect Dis* 10, 360-366.

Hyde, D.M., Plopper, C.G., Kass, P.H., and Alley, J.L. (1983). Estimation of cell numbers and volumes of bronchiolar epithelium during rabbit lung maturation. *Am J Anat* 167, 359-370.

Ionescu, D.N., Treaba, D., Gilks, C.B., Leung, S., Renouf, D., Laskin, J., Wood-Baker, R., and Gown, A.M. (2007). Non-small cell lung carcinoma with neuroendocrine differentiation--an entity of no clinical or prognostic significance. *Am J Surg Pathol* 31, 26-32.

Jackson, E.L., Willis, N., Mercer, K., Bronson, R.T., Crowley, D., Montoya, R., Jacks, T., and Tuveson, D.A. (2001). Analysis of lung tumor initiation and progression using conditional expression of oncogenic K-ras. *Genes Dev* 15, 3243-3248.

Jassim, F.A., Sharp, J.M., and Marinello, P.D. (1987). Three-step procedure for isolation of epithelial cells from the lungs of sheep with jaagsiekte. *Res Vet Sci* 43, 407-409.

Jeffery, P.K., and Reid, L. (1975). New observations of rat airway epithelium: a quantitative and electron microscopic study. *J Anat* 120, 295-320.

Jiang, F., Qiu, Q., Khanna, A., Todd, N.W., Deepak, J., Xing, L., Wang, H., Liu, Z., Su, Y., Stass, S.A., *et al.* (2009). Aldehyde dehydrogenase 1 is a tumor stem cell-associated marker in lung cancer. *Mol Cancer Res* 7, 330-338.

Johnson, R., and Kaneene, J.B. (1992). Bovine leukemia virus and enzootic bovine leukosis. *Veterinary Bulletin* 62, 287-312.

Julkunen, I., Melen, K., Nyqvist, M., Pirhonen, J., Sareneva, T., and Matikainen, S. (2000). Inflammatory responses in influenza A virus infection. *Vaccine* 19 Suppl 1, S32-37.

Karanikas, V., Zamanakou, M., Kerenidi, T., Dahabreh, J., Hevas, A., Nakou, M., Gourgoulianis, K.I., and Germenis, A.E. (2007). Indoleamine 2,3-dioxygenase (IDO) expression in lung cancer. *Cancer Biol Ther* 6, 1258-1262.

Kasprzak, A., Zabel, M., and Biczysko, W. (2007). Selected markers (chromogranin A, neuron-specific enolase, synaptophysin, protein gene product 9.5) in diagnosis and prognosis of neuroendocrine pulmonary tumours. *Pol J Pathol* 58, 23-33.

Kauffman, S.L. (1980). Cell Proliferation in the Mammalian lung. *International review of experimental pathology* 22, 131-184.

Kawai, T., and Akira, S. (2006). Innate immune recognition of viral infection. *Nat Immunol* 7, 131-137.

Kawashima, K., Meyerholz, D.K., Gallup, J.M., Grubor, B., Lazic, T., Lehmkuhl, H.D., and Ackermann, M.R. (2006). Differential expression of ovine innate immune genes by preterm and neonatal lung epithelia infected with respiratory syncytial virus. *Viral Immunol* 19, 316-323.

Kennedy, A.R., Desrosiers, A., Terzaghi, M., and Little, J.B. (1978). Morphometric and histological analysis of the lungs of Syrian golden hamsters. *J Anat* 125, 527-553.

Kikkawa, Y., Motoyama, E.K., and Cook, C.D. (1965). The ultrastructure of the lungs of lambs. The relation of osmiophilic inclusions and alveolar lining layer to fetal maturation and experimentally produced respiratory distress. *Am J Pathol* 47, 877-903.

Kim, C.F., Jackson, E.L., Woolfenden, A.E., Lawrence, S., Babar, I., Vogel, S., Crowley, D., Bronson, R.T., and Jacks, T. (2005). Identification of bronchioalveolar stem cells in normal lung and lung cancer. *Cell* 121, 823-835.

Kleeberger, W., Versmold, A., Rothamel, T., Glockner, S., Brecht, M., Haverich, A., Lehmann, U., and Kreipe, H. (2003). Increased chimerism of bronchial and alveolar epithelium in human lung allografts undergoing chronic injury. *Am J Pathol* 162, 1487-1494.

Klymiuk, N., Muller, M., Brem, G., and Aigner, B. (2003). Characterization of endogenous retroviruses in sheep. *J Virol* 77, 11268-11273.

Kolliker, A. (1882). Zur erkenntniss des Baues der Lunge des Menschen. *Verth Phys-MedGes Wurzburg* 16.

Kotton, D.N., and Fine, A. (2008). Lung stem cells. *Cell Tissue Res* 331, 145-156.

Krause, D.S., Theise, N.D., Collector, M.I., Henegariu, O., Hwang, S., Gardner, R., Neutzel, S., and Sharkis, S.J. (2001). Multi-organ, multi-lineage engraftment by a single bone marrow-derived stem cell. *Cell* 105, 369-377.

Kwang, J., Keen, J., Rosati, S., and Tolari, F. (1995). Development and application of an antibody ELISA for the marker protein of ovine pulmonary carcinoma. *Vet Immunol Immunopathol* 47, 323-331.

Lange, A.W., Keiser, A.R., Wells, J.M., Zorn, A.M., and Whitsett, J.A. (2009). Sox17 promotes cell cycle progression and inhibits TGF-beta/Smad3 signaling to initiate progenitor cell behavior in the respiratory epithelium. *PLoS One* 4, e5711.

Larruskain, A., Minguillon, E., Garcia-Etxebarria, K., Moreno, B., Arostegui, I., Juste, R.A., and Jugo, B.M. (2010). MHC class II DRB1 gene polymorphism in the pathogenesis of Maedi-Visna and pulmonary adenocarcinoma viral diseases in sheep. *Immunogenetics* 62, 75-83.

Lee, H.R., Kim, M.H., Lee, J.S., Liang, C., and Jung, J.U. (2009). Viral interferon regulatory factors. *J Interferon Cytokine Res* 29, 621-627.

Leutenegger, C.M., Alluwaimi, A.M., Smith, W.L., Perani, L., and Cullor, J.S. (2000). Quantitation of bovine cytokine mRNA in milk cells of healthy cattle by real-time TaqMan polymerase chain reaction. *Vet Immunol Immunopathol* 77, 275-287.

Levina, V., Marrangoni, A.M., DeMarco, R., Gorelik, E., and Lokshin, A.E. (2008). Drug-selected human lung cancer stem cells: cytokine network, tumorigenic and metastatic properties. *PLoS One* 3, e3077.

Lewis, C.E., and Pollard, J.W. (2006). Distinct role of macrophages in different tumor microenvironments. *Cancer Res* 66, 605-612.

Lewis, P.F., and Emerman, M. (1994). Passage through mitosis is required for oncoretroviruses but not for the human immunodeficiency virus. *J Virol* 68, 510-516.

Li, H., Cunha, C.W., Davies, C.J., Gailbreath, K.L., Knowles, D.P., Oaks, J.L., and Taus, N.S. (2008). Ovine herpesvirus 2 replicates initially in the lung of experimentally infected sheep. *J Gen Virol* 89, 1699-1708.

Ling, T.Y., Kuo, M.D., Li, C.L., Yu, A.L., Huang, Y.H., Wu, T.J., Lin, Y.C., Chen, S.H., and Yu, J. (2006). Identification of pulmonary Oct-4+ stem/progenitor cells and demonstration of their susceptibility to SARS coronavirus (SARS-CoV) infection in vitro. *Proc Natl Acad Sci U S A* 103, 9530-9535.

Linial, M., Fan, H., Hahn, B., Lower, R., and Neil, J. (2005).

Linnoila, R.I. (2006). Functional facets of the pulmonary neuroendocrine system. *Lab Invest* 86, 425-444.

Linnoila, R.I., Szabo, E., DeMayo, F., Witschi, H., Sabourin, C., and Malkinson, A. (2000). The role of CC10 in pulmonary carcinogenesis: from a marker to tumor suppression. *Ann N Y Acad Sci* 923, 249-267.

Liu, S.L., and Miller, A.D. (2005). Transformation of madin-darby canine kidney epithelial cells by sheep retrovirus envelope proteins. *J Virol* 79, 927-933.

Liu, S.L., and Miller, A.D. (2006). Oncogenic transformation by the jaagsiekte sheep retrovirus envelope protein. *Oncogene*.

Lombardi, V.C., Ruscetti, F.W., Das Gupta, J., Pfof, M.A., Hagen, K.S., Peterson, D.L., Ruscetti, S.K., Bagni, R.K., Petrow-Sadowski, C., Gold, B., *et al.* (2009). Detection of an infectious retrovirus, XMRV, in blood cells of patients with chronic fatigue syndrome. *Science* 326, 585-589.

Mackay, J.M. (1969). Tissue culture studies of sheep pulmonary adenomatosis (Jaagsiekte). I. Direct cultures of affected lungs. *J Comp Pathol* 79, 141-146.

Mackay, J.M., Nisbet, D.I., and Slee, J. (1971). A high incidence of jaagsiekte following experimental cold exposures in housed sheep. *Int J Biometeorol* 15, 65-69.

Madoz-Gurpide, J., Kuick, R., Wang, H., Misek, D.E., and Hanash, S.M. (2007). Integral protein microarrays for the identification of lung cancer antigens in sera that induce a humoral immune response. *Mol Cell Proteomics*.

Maeda, N., Fan, H., and Yoshikai, Y. (2008). Oncogenesis by retroviruses: old and new paradigms. *Rev Med Virol* 18, 387-405.

Maeda, N., Inoshima, Y., Fruman, D.A., Brachmann, S.M., and Fan, H. (2003). Transformation of mouse fibroblasts by Jaagsiekte sheep retrovirus envelope does not require phosphatidylinositol 3-kinase. *J Virol* 77, 9951-9959.

Maeda, N., Palmarini, M., Murgia, C., and Fan, H. (2001). Direct transformation of rodent fibroblasts by jaagsiekte sheep retrovirus DNA. *Proc Natl Acad Sci U S A* 98, 4449-4454.

Mallick, B., Ghosh, Z., and Chakrabarti, J. (2009). MicroRNome analysis unravels the molecular basis of SARS infection in bronchoalveolar stem cells. *PLoS One* 4, e7837.

Malmquist, W.A., Krauss, H.H., Moulton, J.E., and Wandera, J.G. (1972). Morphologic study of virus-infected lung cell cultures from sheep pulmonary adenomatosis (Jaagsiekte). *Lab Invest* 26, 528-533.

Maneglier, B., Malleret, B., Guillemin, G.J., Spreux-Varoquaux, O., Devillier, P., Rogez-Kreuz, C., Porcheray, F., Therond, P., Dormont, D., and Clayette, P. (2009). Modulation of indoleamine-2,3-

dioxygenase expression and activity by HIV-1 in human macrophages. *Fundam Clin Pharmacol* 23, 573-581.

Marei, H.E., and Abd el-Gawad, M. (2001). Differentiation of ciliated cells in the terminal bronchioles of neonatal calves. *Eur J Morphol* 39, 269-276.

Mariassy, A.T., and Plopper, C.G. (1983). Tracheobronchial epithelium of the sheep: I. Quantitative light-microscopic study of epithelial cell abundance, and distribution. *Anat Rec* 205, 263-275.

Mariassy, A.T., and Plopper, C.G. (1984). Tracheobronchial epithelium of the sheep: II. Ultrastructural and morphometric analysis of the epithelial secretory cell types. *Anat Rec* 209, 523-534.

Martin, W.B., Angus, K.W., Robinson, G.W., and Scott, F.M. (1979). The herpesvirus of sheep pulmonary adenomatosis. *Comp Immunol Microbiol Infect Dis* 2, 313-325.

Martin, W.B., Scott, F.M., Sharp, J.M., Angus, K.W., and Norval, M. (1976). Experimental production of sheep pulmonary adenomatosis (Jaagsiekte). *Nature* 264, 183-185.

Mayer, A.K., Bartz, H., Fey, F., Schmidt, L.M., and Dalpke, A.H. (2008). Airway epithelial cells modify immune responses by inducing an anti-inflammatory microenvironment. *Eur J Immunol* 38, 1689-1699.

McFadyean, J. (1894). Verminous pneumonia in the sheep. *Journal of Comparative Pathology and Therapeutics* 7, 31-42.

McFadyean, J. (1920). Transformation of the alveolar epithelium in verminous pneumonia in the sheep. *The Journal of Comparative Pathology and Therapeutics* 33, 1-10.

McGee-Estrada, K., and Fan, H. (2006). In vivo and in vitro analysis of factor binding sites in Jaagsiekte sheep retrovirus long terminal repeat enhancer sequences: roles of HNF-3, NF- κ B, and C/EBP for activity in lung epithelial cells. *J Virol* 80, 332-341.

McGee-Estrada, K., and Fan, H. (2007). Comparison of LTR enhancer elements in sheep beta retroviruses: insights into the basis for tissue-specific expression. *Virus Genes* 35, 303-312.

McGee-Estrada, K., Palmarini, M., and Fan, H. (2002). HNF-3 β is a critical factor for the expression of the Jaagsiekte sheep retrovirus long terminal repeat in type II pneumocytes but not in Clara cells. *Virology* 292, 87-97.

McNeilly, T.N., Baker, A., Brown, J.K., Collie, D., Maclachlan, G., Rhind, S.M., and Harkiss, G.D. (2008). Role of alveolar macrophages in respiratory transmission of visna/maedi virus. *J Virol* 82, 1526-1536.

Mellor, A.L., and Munn, D.H. (2004). IDO expression by dendritic cells: tolerance and tryptophan catabolism. *Nat Rev Immunol* 4, 762-774.

Metzger, M.J., Holguin, C.J., Mendoza, R., and Miller, A.D. (2010). The prostate cancer-associated human retrovirus XMRV lacks direct transforming activity but can induce low rates of transformation in cultured cells. *J Virol* 84, 1874-1880.

Metzger, R.J., Klein, O.D., Martin, G.R., and Krasnow, M.A. (2008). The branching programme of mouse lung development. *Nature* 453, 745-750.

Meyerholz, D.K., DeGraaff, J.A., Gallup, J.M., Olivier, A.K., and Ackermann, M.R. (2006). Depletion of alveolar glycogen corresponds with immunohistochemical development of CD208 antigen expression in perinatal lamb lung. *J Histochem Cytochem* 54, 1247-1253.

Meyerholz, D.K., Grubor, B., Fach, S.J., Sacco, R.E., Lehmkuhl, H.D., Gallup, J.M., and Ackermann, M.R. (2004). Reduced clearance of respiratory syncytial virus infection in a preterm lamb model. *Microbes Infect* 6, 1312-1319.

Miller, A.D. (2008). Hyaluronidase 2 and its intriguing role as a cell-entry receptor for oncogenic sheep retroviruses. *Semin Cancer Biol* 18, 296-301.

Mogensen, T.H., Melchjorsen, J., Larsen, C.S., and Paludan, S.R. (2010). Innate immune recognition and activation during HIV infection. *Retrovirology* 7, 54.

Moreno, B., Woodall, C.J., Watt, N.J., and Harkiss, G.D. (1998). Transforming growth factor-beta 1 (TGF-beta1) expression in ovine lentivirus-induced lymphoid interstitial pneumonia. *Clin Exp Immunol* 112, 74-83.

Mornex, J.F. (2003). [The sheep, model for human lung pathology]. *Rev Prat* 53, 241-244.

Mornex, J.F., Thivolet, F., De las Heras, M., and Leroux, C. (2003). Pathology of human bronchioloalveolar carcinoma and its relationship to the ovine disease. *Curr Top Microbiol Immunol* 275, 225-248.

Morozov, V.A., Lagaye, S., Lower, J., and Lower, R. (2004). Detection and characterization of betaretroviral sequences, related to sheep Jaagsiekte virus, in Africans from Nigeria and Cameroon. *Virology* 327, 162-168.

Munn, D.H., and Mellor, A.L. (2007). Indoleamine 2,3-dioxygenase and tumor-induced tolerance. *J Clin Invest* 117, 1147-1154.

Mura, M., Murcia, P., Caporale, M., Spencer, T.E., Nagashima, K., Rein, A., and Palmarini, M. (2004). Late viral interference induced by transdominant Gag of an endogenous retrovirus. *Proc Natl Acad Sci U S A* 101, 11117-11122.

Murcia, P.R., Arnaud, F., and Palmarini, M. (2007). The transdominant endogenous retrovirus enJS56A1 associates with and blocks intracellular trafficking of Jaagsiekte sheep retrovirus Gag. *J Virol* 81, 1762-1772.

Myer, M.S., Verwoerd, D.W., and Garnett, H.M. (1987a). Demonstration of growth-inhibitory as well as growth-stimulatory factors in medium conditioned by lung lavage cells stimulated with a chemotactic factor secreted by jaagsiekte tumour cells. *Onderstepoort J Vet Res* 54, 123-130.

Myer, M.S., Verwoerd, D.W., and Garnett, H.M. (1987b). Production of a macrophage chemotactic factor by cultured jaagsiekte tumour cells. *Onderstepoort J Vet Res* 54, 9-15.

Nakanishi, K., Yoshimoto, T., Tsutsui, H., and Okamura, H. (2001). Interleukin-18 regulates both Th1 and Th2 responses. *Annu Rev Immunol* 19, 423-474.

Nisbet, D.I., Mackay, J.M., Smith, W., and Gray, E.W. (1971). Ultrastructure of sheep pulmonary adenomatosis (Jaagsiekte). *J Pathol* 103, 157-162.

Nobel, T.A., Neumann, F., and Klopfer, U. (1969). Histological patterns of the metastases in pulmonary adenomatosis of sheep (jaagsiekte). *J Comp Pathol* 79, 537-540.

Ortin, A., Cousens, C., Minguijon, E., Pascual, Z., Villarreal, M.P., Sharp, J.M., and Heras Mde, L. (2003). Characterization of enzootic nasal tumour virus of goats: complete sequence and tissue distribution. *J Gen Virol* 84, 2245-2252.

Ortin, A., Minguijon, E., Dewar, P., Garcia, M., Ferrer, L.M., Palmarini, M., Gonzalez, L., Sharp, J.M., and De las Heras, M. (1998). Lack of a specific immune response against a recombinant capsid protein of Jaagsiekte sheep retrovirus in sheep and goats naturally affected by enzootic nasal tumour or sheep pulmonary adenomatosis. *Vet Immunol Immunopathol* 61, 229-237.

Ortin, A., Perez de Villarreal, M., Minguijon, E., Cousens, C., Sharp, J.M., and De las Heras, M. (2004). Coexistence of enzootic nasal adenocarcinoma and jaagsiekte retrovirus infection in sheep. *J Comp Pathol* 131, 253-258.

Orzalesi, M.M., Motoyama, E.K., Jacobson, H.N., Kikkawa, Y., Reynolds, E.O., and Cook, C.D. (1965). The Development of the Lungs of Lambs. *Pediatrics* 35, 373-381.

Otto, W.R. (1997). Lung stem cells. *Int J Exp Pathol* 78, 291-310.

Palmarini, M., Datta, S., Omid, R., Murgia, C., and Fan, H. (2000a). The long terminal repeat of Jaagsiekte sheep retrovirus is preferentially active in differentiated epithelial cells of the lungs. *J Virol* 74, 5776-5787.

Palmarini, M., Dewar, P., De las Heras, M., Inglis, N.F., Dalziel, R.G., and Sharp, J.M. (1995). Epithelial tumour cells in the lungs of sheep with pulmonary adenomatosis are major sites of replication for Jaagsiekte retrovirus. *J Gen Virol* 76 (Pt 11), 2731-2737.

Palmarini, M., and Fan, H. (2001). Retrovirus-induced ovine pulmonary adenocarcinoma, an animal model for lung cancer. *J Natl Cancer Inst* 93, 1603-1614.

Palmarini, M., Gray, C.A., Carpenter, K., Fan, H., Bazer, F.W., and Spencer, T.E. (2001a). Expression of endogenous betaretroviruses in the ovine uterus: effects of neonatal age, estrous cycle, pregnancy, and progesterone. *J Virol* 75, 11319-11327.

Palmarini, M., Hallwirth, C., York, D., Murgia, C., de Oliveira, T., Spencer, T., and Fan, H. (2000b). Molecular cloning and functional analysis of three type D endogenous retroviruses of sheep reveal a different cell tropism from that of the highly related exogenous jaagsiekte sheep retrovirus. *J Virol* 74, 8065-8076.

Palmarini, M., Holland, M.J., Cousens, C., Dalziel, R.G., and Sharp, J.M. (1996). Jaagsiekte retrovirus establishes a disseminated infection of the lymphoid tissues of sheep affected by pulmonary adenomatosis. *J Gen Virol* 77 (Pt 12), 2991-2998.

Palmarini, M., Maeda, N., Murgia, C., De-Fraja, C., Hofacre, A., and Fan, H. (2001b). A phosphatidylinositol 3-kinase docking site in the cytoplasmic tail of the Jaagsiekte sheep retrovirus transmembrane protein is essential for envelope-induced transformation of NIH 3T3 cells. *J Virol* 75, 11002-11009.

Palmarini, M., Mura, M., and Spencer, T.E. (2004). Endogenous betaretroviruses of sheep: teaching new lessons in retroviral interference and adaptation. *J Gen Virol* 85, 1-13.

Palmarini, M., Sharp, J.M., de las Heras, M., and Fan, H. (1999a). Jaagsiekte sheep retrovirus is necessary and sufficient to induce a contagious lung cancer in sheep. *J Virol* 73, 6964-6972.

Palmarini, M., Sharp, J.M., Lee, C., and Fan, H. (1999b). In vitro infection of ovine cell lines by Jaagsiekte sheep retrovirus. *J Virol* 73, 10070-10078.

Palsson, P., A. (1985). Maedi/visna of sheep in Iceland, introduction of the disease in Iceland, clinical features, control measures and eradication. (Commission of the European Communities, Luxembourg).

Park, K.S., Wells, J.M., Zorn, A.M., Wert, S.E., Laubach, V.E., Fernandez, L.G., and Whitsett, J.A. (2006). Transdifferentiation of ciliated cells during repair of the respiratory epithelium. *Am J Respir Cell Mol Biol* 34, 151-157.

Patierno, S.R., Manyak, M.J., Fernandez, P.M., Baker, A., Weeraratna, A.T., Chou, D.S., Szlyk, G., Geib, K.S., Walsh, C., and Patteras, J. (2002). Uteroglobin: a potential novel tumor suppressor and molecular therapeutic for prostate cancer. *Clin Prostate Cancer* 1, 118-124.

Payne, A.L., and Verwoerd, D.W. (1984). A scanning and transmission electron microscopy study of jaagsiekte lesions. *Onderstepoort J Vet Res* 51, 1-13.

Payne, A.L., Verwoerd, D.W., and Garnett, H.M. (1983). The morphology and morphogenesis of jaagsiekte retrovirus (JSRV). *Onderstepoort J Vet Res* 50, 317-322.

Peake, J.L., Reynolds, S.D., Stripp, B.R., Stephens, K.E., and Pinkerton, K.E. (2000). Alteration of pulmonary neuroendocrine cells during epithelial repair of naphthalene-induced airway injury. *Am J Pathol* 156, 279-286.

Peers, C., Kemp, P.J., Boyd, C.A., and Nye, P.C. (1990). Whole-cell K⁺ currents in type II pneumocytes freshly isolated from rat lung: pharmacological evidence for two subpopulations of cells. *Biochim Biophys Acta* 1052, 113-118.

Pereira, L.E., and Ansari, A.A. (2009). A case for innate immune effector mechanisms as contributors to disease resistance in SIV-infected sooty mangabeys. *Curr HIV Res* 7, 12-22.

Perk, K., and Hod, I. (1982). Sheep lung carcinoma: an endemic analogue of a sporadic human neoplasm. *J Natl Cancer Inst* 69, 747-749.

Perk, K., Hod, I., and Nobel, T.A. (1971). Pulmonary adenomatosis of sheep (jaagsiekte). I. Ultrastructure of the tumor. *J Natl Cancer Inst* 46, 525-537.

Perk, K., Michalides, R., Spiegelman, S., and Schlom, J. (1974). Biochemical and morphologic evidence for the presence of an RNA tumor virus in pulmonary carcinoma of sheep (Jaagsiekte). *J Natl Cancer Inst* 53, 131-135.

Perk, K., and Yaniv, A. (1977). Lack of maedi viral related RNA in pulmonary carcinoma of sheep (jaagsiekte). *Res Vet Sci* 24, 46-48.

Perl, A.K., Wert, S.E., Loudy, D.E., Shan, Z., Blair, P.A., and Whitsett, J.A. (2005). Conditional recombination reveals distinct subsets of epithelial cells in trachea, bronchi, and alveoli. *Am J Respir Cell Mol Biol* 33, 455-462.

Persano, L., Moserle, L., Esposito, G., Bronte, V., Barbieri, V., Iafrate, M., Gardiman, M.P., Larghero, P., Pfeffer, U., Naschberger, E., *et al.* (2009). Interferon-alpha counteracts the angiogenic switch and reduces tumor cell proliferation in a spontaneous model of prostatic cancer. *Carcinogenesis* *30*, 851-860.

Pfaffl, M.W. (2001). A new mathematical model for relative quantification in real-time RT-PCR. *Nucleic Acids Res* *29*, e45.

Pfaffl, M.W., Horgan, G.W., and Dempfle, L. (2002). Relative expression software tool (REST) for group-wise comparison and statistical analysis of relative expression results in real-time PCR. *Nucleic Acids Res* *30*, e36.

Phalen, R.F., Yeh, H.C., Schum, G.M., and Raabe, O.G. (1978). Application of an idealized model to morphometry of the mammalian tracheobronchial tree. *Anat Rec* *190*, 167-176.

Philbey, A.W., Cousens, C., Bishop, J.V., Gill, C.A., DeMartini, J.C., and Sharp, J.M. (2006). Multiclonal pattern of Jaagsiekte sheep retrovirus integration sites in ovine pulmonary adenocarcinoma. *Virus Res* *117*, 254-263.

Pinkerton, K.E., and Joad, J.P. (2000). The mammalian respiratory system and critical windows of exposure for children's health. *Environ Health Perspect* *108 Suppl 3*, 457-462.

Platt, J.A., Kraipowich, N., Villafane, F., and DeMartini, J.C. (2002). Alveolar type II cells expressing jaagsiekte sheep retrovirus capsid protein and surfactant proteins are the predominant neoplastic cell type in ovine pulmonary adenocarcinoma. *Vet Pathol* *39*, 341-352.

Plopper, C., St George, J., Cardoso, W., Wu, R., Pinkerton, K., and Buckpitt, A. (1992). Development of airway epithelium. Patterns of expression for markers of differentiation. *Chest* *101*, 2S-5S.

Plopper, C.G., Hill, L.H., and Mariassy, A.T. (1980a). Ultrastructure of the nonciliated bronchiolar epithelial (Clara) cell of mammalian lung. III. A study of man with comparison of 15 mammalian species. *Exp Lung Res* *1*, 171-180.

Plopper, C.G., Mariassy, A.T., and Hill, L.H. (1980b). Ultrastructure of the nonciliated bronchiolar epithelial (Clara) cell of mammalian lung: II. A comparison of horse, steer, sheep, dog, and cat. *Exp Lung Res* *1*, 155-169.

Plopper, C.G., Mariassy, A.T., and Lollini, L.O. (1983). Structure as revealed by airway dissection. A comparison of mammalian lungs. *Am Rev Respir Dis* *128*, S4-7.

Plopper, C.G., Weir, A.J., Nishio, S.J., Chang, A., Voit, M., Philpot, R.M., and Buckpitt, A.R. (1994). Elevated susceptibility to 4-ipomeanol cytotoxicity in immature Clara cells of neonatal rabbits. *J Pharmacol Exp Ther* *269*, 867-880.

Poiesz, B.J., Ruscetti, F.W., Reitz, M.S., Kalyanaraman, V.S., and Gallo, R.C. (1981). Isolation of a new type C retrovirus (HTLV) in primary uncultured cells of a patient with Sezary T-cell leukaemia. *Nature* *294*, 268-271.

Rai, S.K., DeMartini, J.C., and Miller, A.D. (2000). Retrovirus vectors bearing jaagsiekte sheep retrovirus Env transduce human cells by using a new receptor localized to chromosome 3p21.3. *J Virol* *74*, 4698-4704.

Rai, S.K., Duh, F.M., Vigdorovich, V., Danilkovitch-Miagkova, A., Lerman, M.I., and Miller, A.D. (2001). Candidate tumor suppressor HYAL2 is a glycosylphosphatidylinositol (GPI)-anchored cell-surface receptor for jaagsiekte sheep retrovirus, the envelope protein of which mediates oncogenic transformation. *Proc Natl Acad Sci U S A* *98*, 4443-4448.

Ramos-Vara, J.A. (2005). Technical aspects of immunohistochemistry. *Vet Pathol* *42*, 405-426.

Rawlins, E.L., Clark, C.P., Xue, Y., and Hogan, B.L. (2009). The Id2+ distal tip lung epithelium contains individual multipotent embryonic progenitor cells. *Development* *136*, 3741-3745.

Rawlins, E.L., and Hogan, B.L. (2006). Epithelial stem cells of the lung: privileged few or opportunities for many? *Development* *133*, 2455-2465.

Rawlins, E.L., and Hogan, B.L. (2008). Ciliated epithelial cell lifespan in the mouse trachea and lung. *Am J Physiol Lung Cell Mol Physiol* *295*, L231-234.

Rawlins, E.L., Okubo, T., Que, J., Xue, Y., Clark, C., Luo, X., and Hogan, B.L. (2008). Epithelial stem/progenitor cells in lung postnatal growth, maintenance, and repair. *Cold Spring Harb Symp Quant Biol* 73, 291-295.

Rawlins, E.L., Ostrowski, L.E., Randell, S.H., and Hogan, B.L. (2007). Lung development and repair: contribution of the ciliated lineage. *Proc Natl Acad Sci U S A* 104, 410-417.

Raz, D.J., He, B., Rosell, R., and Jablons, D.M. (2006). Current concepts in bronchioloalveolar carcinoma biology. *Clin Cancer Res* 12, 3698-3704.

Raz, E. (2007). Organ-specific regulation of innate immunity. *Nat Immunol* 8, 3-4.

Reader, J.R., Tepper, J.S., Schelegle, E.S., Aldrich, M.C., Putney, L.F., Pfeiffer, J.W., and Hyde, D.M. (2003). Pathogenesis of mucous cell metaplasia in a murine asthma model. *Am J Pathol* 162, 2069-2078.

Reddy, R., Buckley, S., Doerken, M., Barsky, L., Weinberg, K., Anderson, K.D., Warburton, D., and Driscoll, B. (2004). Isolation of a putative progenitor subpopulation of alveolar epithelial type 2 cells. *Am J Physiol Lung Cell Mol Physiol* 286, L658-667.

Reynolds, S.D., Hong, K.U., Giangreco, A., Mango, G.W., Guron, C., Morimoto, Y., and Stripp, B.R. (2000). Conditional clara cell ablation reveals a self-renewing progenitor function of pulmonary neuroendocrine cells. *Am J Physiol Lung Cell Mol Physiol* 278, L1256-1263.

Reynolds, S.D., and Malkinson, A.M. (2010). Clara cell: progenitor for the bronchiolar epithelium. *Int J Biochem Cell Biol* 42, 1-4.

Reynolds, S.D., Reynolds, P.R., Snyder, J.C., Whyte, F., Paavola, K.J., and Stripp, B.R. (2007). CCSP regulates cross talk between secretory cells and both ciliated cells and macrophages of the conducting airway. *Am J Physiol Lung Cell Mol Physiol* 293, L114-123.

Rizvi, S.M., Goodwill, J., Lim, E., Yap, Y.K., Wells, A.U., Hansell, D.M., Davis, P., Abdel-Ghani, S., Goldstraw, P., and Nicholson, A.G. (2009). The frequency of neuroendocrine cell hyperplasia in patients with pulmonary neuroendocrine tumours and non-neuroendocrine cell carcinomas. *Histopathology* 55, 332-337.

Robertson, W. (1904). Jagziekte pr chronic Catarrhal Pneumonia (sheep). *Journal of Comparative Pathology and Therapeutics* 17, 221-224.

Roper, J.M., Staversky, R.J., Finkelstein, J.N., Keng, P.C., and O'Reilly, M.A. (2003). Identification and isolation of mouse type II cells on the basis of intrinsic expression of enhanced green fluorescent protein. *Am J Physiol Lung Cell Mol Physiol* 285, L691-700.

Rosadio, R.H., Lairmore, M.D., Russell, H.I., and DeMartini, J.C. (1988a). Retrovirus-associated ovine pulmonary carcinoma (sheep pulmonary adenomatosis) and lymphoid interstitial pneumonia. I. Lesion development and age susceptibility. *Vet Pathol* 25, 475-483.

Rosadio, R.H., Sharp, J.M., Lairmore, M.D., Dahlberg, J.E., and De Martini, J.C. (1988b). Lesions and retroviruses associated with naturally occurring ovine pulmonary carcinoma (sheep pulmonary adenomatosis). *Vet Pathol* 25, 58-66.

Rosati, S., Pittau, M., Alberti, A., Pozzi, S., York, D.F., Sharp, J.M., and Palmarini, M. (2000). An accessory open reading frame (orf-x) of jaagsiekte sheep retrovirus is conserved between different virus isolates. *Virus Res* 66, 109-116.

Roth, J. (1973). The Clara cells and the pulmonary surfactant system. Light and electron microscopic studies on the function of Clara cells. *Exp Pathol (Jena)* 8, 305-313.

Rous, P. (1911). A Sarcoma of the Fowl Transmissible by an Agent Separable from the Tumor Cells. *J Exp Med* 13, 397-411.

Ruifrok, A.C., and Johnston, D.A. (2001). Quantification of histochemical staining by color deconvolution. *Anal Quant Cytol Histol* 23, 291-299.

Ryan, E., Horsington, J., Brownlie, J., and Zhang, Z. (2008). Foot-and-Mouth Disease Virus Infection in Fetal Lambs: Tissue Tropism and Cytokine Response. *J Comp Pathol* 138, 108-120.

Ryerse, J.S., Hoffmann, J.W., Mahmoud, S., Nagel, B.A., and deMello, D.E. (2001). Immunolocalization of CC10 in Clara cells in mouse and human lung. *Histochem Cell Biol* 115, 325-332.

Sage, E.K., Loebinger, M.R., Polak, J., and Janes, S.M. (2008). The role of bone marrow-derived stem cells in lung regeneration and repair.

Sakamoto, O., Iwama, A., Amitani, R., Takehara, T., Yamaguchi, N., Yamamoto, T., Masuyama, K., Yamanaka, T., Ando, M., and Suda, T. (1997). Role of macrophage-stimulating protein and its receptor, RON tyrosine kinase, in ciliary motility. *J Clin Invest* 99, 701-709.

Salaun, B., de Saint-Vis, B., Pacheco, N., Pacheco, Y., Riesler, A., Isaac, S., Leroux, C., Clair-Moninot, V., Pin, J.J., Griffith, J., *et al.* (2004). CD208/dendritic cell-lysosomal associated membrane protein is a marker of normal and transformed type II pneumocytes. *Am J Pathol* 164, 861-871.

Salvatori, D., Gonzalez, L., Dewar, P., Cousens, C., de las Heras, M., Dalziel, R.G., and Sharp, J.M. (2004). Successful induction of ovine pulmonary adenocarcinoma in lambs of different ages and detection of viraemia during the preclinical period. *J Gen Virol* 85, 3319-3324.

Sauter, D., Specht, A., and Kirchhoff, F. (2010). Tetherin: holding on and letting go. *Cell* 141, 392-398.

Schafer, Z.T., and Brugge, J.S. (2007). IL-6 involvement in epithelial cancers. *J Clin Invest* 117, 3660-3663.

Scheerlinck, J.P., Snibson, K.J., Bowles, V.M., and Sutton, P. (2008). Biomedical applications of sheep models: from asthma to vaccines. *Trends Biotechnol* 26, 259-266.

Scheuermann, D.W., Klika, E., De Groot-Lasseel, M.H., Bazantova, I., and Switka, A. (1997). An electron microscopic study of the parabronchial epithelium in the mature lung of four bird species. *Anat Rec* 249, 213-225.

Scholzen, T., and Gerdes, J. (2000). The Ki-67 protein: from the known and the unknown. *J Cell Physiol* 182, 311-322.

Sharp, J.M., and Angus, K.W. (1990). Sheep Pulmonary Adenomatosis Chapters 9 and 10. *Maedi-visna and related diseases*, 157-185.

Sharp, J.M., and DeMartini, J.C. (2003). Natural History of JSRV in sheep. *Current Topics in Microbiology and Immunology* 275, 55-79.

Sharp, J.M., and Herring, A.J. (1983). Sheep pulmonary adenomatosis: demonstration of a protein which cross-reacts with the major core proteins of Mason-Pfizer monkey virus and mouse mammary tumour virus. *J Gen Virol* 64 (Pt 10), 2323-2327.

Shijubo, N., Itoh, Y., Shigehara, K., Yamaguchi, T., Itoh, K., Shibuya, Y., Takahashi, R., Ohchi, T., Ohmichi, M., Hiraga, Y., *et al.* (2000). Association of Clara cell 10-kDa protein, spontaneous regression and sarcoidosis. *Eur Respir J* 16, 414-419.

Shijubo, N., Itoh, Y., Yamaguchi, T., Shibuya, Y., Morita, Y., Hirasawa, M., Okutani, R., Kawai, T., and Abe, S. (1997). Serum and BAL Clara cell 10 kDa protein (CC10) levels and CC10-positive bronchiolar cells are decreased in smokers. *Eur Respir J* 10, 1108-1114.

Shirlaw, J.F. (1959). Studies on Jaagsiekte in Kenya. *Bulletin of Epizootic Diseases in Africa* 1, 287-302.

Sica, A., Larghi, P., Mancino, A., Rubino, L., Porta, C., Totaro, M.G., Rimoldi, M., Biswas, S.K., Allavena, P., and Mantovani, A. (2008). Macrophage polarization in tumour progression. *Semin Cancer Biol* 18, 349-355.

Sigurdson, S.L., and Lwebuga-Mukasa, J.S. (1998). Adhesive characteristics of type II pneumocyte subpopulations from saline- and silica-treated rats. *Exp Lung Res* 24, 307-320.

Singh, G., and Katyal, S.L. (2000). Clara cell proteins. *Ann N Y Acad Sci* 923, 43-58.

Sisson, S., and Grossman, J.D. (1975). *The Anatomy of the Domestic Animals*. In, G. R, ed. (W.B Saunders), pp. 916-936.

Smeed, J.A., Watkins, C.A., Rhind, S.M., and Hopkins, J. (2007). Differential cytokine gene expression profiles in the three pathological forms of sheep paratuberculosis. *BMC Vet Res* 3, 18.

Smiley-Jewell, S.M., Nishio, S.J., Weir, A.J., and Plopper, C.G. (1998). Neonatal Clara cell toxicity by 4-ipomeanol alters bronchiolar organization in adult rabbits. *Am J Physiol* 274, L485-498.

Snyder, J.C., Teisanu, R.M., and Stripp, B.R. (2009). Endogenous lung stem cells and contribution to disease. *J Pathol* 217, 254-264.

Sorokin, S.P., Hoyt, R.F., Jr., and Shaffer, M.J. (1997). Ontogeny of neuroepithelial bodies: correlations with mitogenesis and innervation. *Microsc Res Tech* 37, 43-61.

Spencer, T.E., Mura, M., Gray, C.A., Griebel, P.J., and Palmarini, M. (2003). Receptor usage and fetal expression of ovine endogenous betaretroviruses: implications for coevolution of endogenous and exogenous retroviruses. *J Virol* 77, 749-753.

Stevens, T.P., McBride, J.T., Peake, J.L., Pinkerton, K.E., and Stripp, B.R. (1997). Cell proliferation contributes to PNEC hyperplasia after acute airway injury. *Am J Physiol* 272, L486-493.

Stripp, B.R., Maxson, K., Mera, R., and Singh, G. (1995). Plasticity of airway cell proliferation and gene expression after acute naphthalene injury. *Am J Physiol* 269, L791-799.

Stripp, B.R., and Reynolds, S.D. (2008). Maintenance and repair of the bronchiolar epithelium. *Proc Am Thorac Soc* 5, 328-333.

Suau, F., Cottin, V., Archer, F., Croze, S., Chastang, J., Cordier, G., Thivolet-Bejui, F., Mornex, J.F., and Leroux, C. (2006). Telomerase activation in a model of lung adenocarcinoma. *Eur Respir J* 27, 1175-1182.

Summers, C., Dewar, P., van der Molen, R., Cousens, C., Salvatori, D., Sharp, J.M., Griffiths, D.J., and Norval, M. (2006). Jaagsiekte sheep retrovirus-specific immune responses induced by vaccination: a comparison of immunisation strategies. *Vaccine* 24, 1821-1829.

Summers, C., Neill, W., Dewar, P., Gonzalez, L., van der Molen, R., Norval, M., and Sharp, J.M. (2002). Systemic immune responses following infection with Jaagsiekte sheep retrovirus and in the terminal stages of ovine pulmonary adenocarcinoma. *J Gen Virol* 83, 1753-1757.

Summers, C., Norval, M., De Las Heras, M., Gonzalez, L., Sharp, J.M., and Woods, G.M. (2005). An influx of macrophages is the predominant local immune response in ovine pulmonary adenocarcinoma. *Vet Immunol Immunopathol* 106, 285-294.

Suratt, B.T., Cool, C.D., Serls, A.E., Chen, L., Varella-Garcia, M., Shpall, E.J., Brown, K.K., and Worthen, G.S. (2003). Human pulmonary chimerism after hematopoietic stem cell transplantation. *Am J Respir Crit Care Med* 168, 318-322.

Suzuki, Y., Suda, T., Furuhashi, K., Suzuki, M., Fujie, M., Hahimoto, D., Nakamura, Y., Inui, N., Nakamura, H., and Chida, K. (2010). Increased serum kynurenine/tryptophan ratio correlates with disease progression in lung cancer. *Lung Cancer* 67, 361-365.

Takeuchi, O., and Akira, S. (2009). Innate immunity to virus infection. *Immunol Rev* 227, 75-86.

Taylor, E. (1937). Does Jaagsiekte occur in great Britain. *Journal of Comparative Pathology and Therapeutics*, 317-320.

Teisanu, R.M., Lagasse, E., Whitesides, J.F., and Stripp, B.R. (2009). Prospective isolation of bronchiolar stem cells based upon immunophenotypic and autofluorescence characteristics. *Stem Cells* 27, 612-622.

Temin, H.M., and Mizutani, S. (1970). RNA-dependent DNA polymerase in virions of Rous sarcoma virus. *Nature* 226, 1211-1213.

Temin, H.M., and Rubin, H. (1958). Characteristics of an assay for Rous sarcoma virus and Rous sarcoma cells in tissue culture. *Virology* 6, 669-688.

Travis, K. (2004). Lung cancer screening for all? Not yet, panel says. *J Natl Cancer Inst* 96, 900-901.

Travis, W.D., Brambilla, E., Konrad Muller-Hermelink, H., and Harris, C.C. (2004a). *Tumours of the Lung, Pleura, Thymus and Heart*.

Travis, W.D., Brambilla, E., Muller-Hermelink, H.K., and Harris, C.C., eds. (2004b). *Pathology and Genetics of Tumours of the Lung, Pleura, thymus and Heart* (Lyon, IARC Press).

Tripp, R.A., Oshansky, C., and Alvarez, R. (2005). Cytokines and respiratory syncytial virus infection. *Proc Am Thorac Soc* 2, 147-149.

Tustin, R.C. (1969). Ovine Jaagsiekte. *Journal of the South African Veterinary Medical Association* 40, 2-23.

Tyler, W.S. (1983). Comparative subgross anatomy of lungs. Pleuras, interlobular septa, and distal airways. *Am Rev Respir Dis* 128, S32-36.

Tyner, J.W., Kim, E.Y., Ide, K., Pelletier, M.R., Roswit, W.T., Morton, J.D., Battaile, J.T., Patel, A.C., Patterson, G.A., Castro, M., *et al.* (2006). Blocking airway mucous cell metaplasia by inhibiting EGFR antiapoptosis and IL-13 transdifferentiation signals. *J Clin Invest* **116**, 309-321.

Van Hoeven, N.S., and Miller, A.D. (2005). Improved enzootic nasal tumor virus pseudotype packaging cell lines reveal virus entry requirements in addition to the primary receptor Hyal2. *J Virol* **79**, 87-94.

Van Lommel, A. (2001). Pulmonary neuroendocrine cells (PNEC) and neuroepithelial bodies (NEB): chemoreceptors and regulators of lung development. *Paediatr Respir Rev* **2**, 171-176.

Van Lommel, A., and Lauweryns, J.M. (1997). Postnatal development of the pulmonary neuroepithelial bodies in various animal species. *J Auton Nerv Syst* **65**, 17-24.

Vandesompele, J., De Preter, K., Pattyn, F., Poppe, B., Van Roy, N., De Paepe, A., and Speleman, F. (2002). Accurate normalization of real-time quantitative RT-PCR data by geometric averaging of multiple internal control genes. *Genome Biol* **3**, RESEARCH0034.

Varela, M., Chow, Y.H., Sturkie, C., Murcia, P., and Palmarini, M. (2006). Association of RON tyrosine kinase with the Jaagsiekte sheep retrovirus envelope glycoprotein. *Virology* **350**, 347-357.

Varela, M., Golder, M., Archer, F., de las Heras, M., Leroux, C., and Palmarini, M. (2008). A large animal model to evaluate the effects of Hsp90 inhibitors for the treatment of lung adenocarcinoma. *Virology* **371**, 206-215.

Varela, M., Spencer, T.E., Palmarini, M., and Arnaud, F. (2009). Friendly viruses: the special relationship between endogenous retroviruses and their host. *Ann N Y Acad Sci* **1178**, 157-172.

Vargas, A., Moreau, J., Landry, S., LeBellego, F., Toufaily, C., Rassart, E., Lafond, J., and Barbeau, B. (2009). Syncytin-2 plays an important role in the fusion of human trophoblast cells. *J Mol Biol* **392**, 301-318.

Ventura, J.J., Tenbaum, S., Perdiguero, E., Huth, M., Guerra, C., Barbacid, M., Pasparakis, M., and Nebreda, A.R. (2007). p38alpha MAP kinase is essential in lung stem and progenitor cell proliferation and differentiation. *Nat Genet* **39**, 750-758.

Verwoerd, D.W., De Villiers, E.M., and Tustin, R.C. (1980a). Aetiology of jaagsiekte: experimental transmission to lambs by means of cultured cells and cell homogenates. *Onderstepoort J Vet Res* **47**, 13-18.

Verwoerd, D.W., Payne, A.L., York, D.F., and Myer, M.S. (1983). Isolation and preliminary characterization of the jaagsiekte retrovirus (JSRV). *Onderstepoort J Vet Res* **50**, 309-316.

Verwoerd, D.W., Williamson, A.L., and De Villiers, E.M. (1980b). Aetiology of jaagsiekte: transmission by means of subcellular fractions and evidence for the involvement of a retrovirus. *Onderstepoort J Vet Res* **47**, 275-280.

Visvader, J.E., and Lindeman, G.J. (2008). Cancer stem cells in solid tumours: accumulating evidence and unresolved questions. *Nat Rev Cancer* **8**, 755-768.

Voigt, K., Brugmann, M., Huber, K., Dewar, P., Cousens, C., Hall, M., Sharp, J.M., and Ganter, M. (2007). PCR examination of bronchoalveolar lavage samples is a useful tool in pre-clinical diagnosis of ovine pulmonary adenocarcinoma (Jaagsiekte). *Res Vet Sci* **83**, 419-427.

Voisset, C., Weiss, R.A., and Griffiths, D.J. (2008). Human RNA "rumor" viruses: the search for novel human retroviruses in chronic disease. *Microbiol Mol Biol Rev* **72**, 157-196.

Voswinkel, R., Motejl, V., Fehrenbach, A., Wegmann, M., Mehling, T., Fehrenbach, H., and Seeger, W. (2004). Characterisation of post-pneumonectomy lung growth in adult mice. *Eur Respir J* **24**, 524-532.

Walsh, S.R., Linnerth-Petrik, N.M., Laporte, A.N., Menzies, P.I., Foster, R.A., and Wootton, S.K. (2010). Full-length genome sequence analysis of enzootic nasal tumor virus reveals an unusually high degree of genetic stability. *Virus Res* **151**, 74-87.

Wandera, J.G. (1968). Experimental transmission of sheep pulmonary adenomatosis (Jaagsiekte). *Vet Rec* **83**, 478-482.

Warburton, D., Schwarz, M., Tefft, D., Flores-Delgado, G., Anderson, K.D., and Cardoso, W.V. (2000). The molecular basis of lung morphogenesis. *Mech Dev* **92**, 55-81.

Watson, W.L., and Smith, R.R. (1951). Terminal bronchiolar or "alveolar cell" cancer of the lung; report of thirty-three cases. *J Am Med Assoc* **147**, 7-13.

Waugh, D.J., and Wilson, C. (2008). The interleukin-8 pathway in cancer. *Clin Cancer Res* **14**, 6735-6741.

Weiss, R. (2001). Retroviruses and cancer. *Current science* **81**, 528-534.

Wells, A.B. (1970). The kinetics of cell proliferation in the tracheobronchial epithelia of rats with and without chronic respiratory disease. *Cell Tissue Kinet* **3**, 185-206.

Whiteside, T.L. (2006). Immune suppression in cancer: effects on immune cells, mechanisms and future therapeutic intervention. *Semin Cancer Biol* **16**, 3-15.

Wikenheiser, K.A., Clark, J.C., Linnoila, R.I., Stahlman, M.T., and Whitsett, J.A. (1992). Simian virus 40 large T antigen directed by transcriptional elements of the human surfactant protein C gene produces pulmonary adenocarcinomas in transgenic mice. *Cancer Res* **52**, 5342-5352.

Wikenheiser, K.A., and Whitsett, J.A. (1997). Tumor progression and cellular differentiation of pulmonary adenocarcinomas in SV40 large T antigen transgenic mice. *Am J Respir Cell Mol Biol* **16**, 713-723.

William, H. (1961). *Lectures on the Whole of Anatomy : An Annotated Translation of Prelectiones anatomiae universalis* (University of California Press).

Wootton, S.K., Halbert, C.L., and Miller, A.D. (2005). Sheep retrovirus structural protein induces lung tumours. *Nature* **434**, 904-907.

Wootton, S.K., Halbert, C.L., and Miller, A.D. (2006a). Envelope proteins of Jaagsiekte sheep retrovirus and enzootic nasal tumor virus induce similar bronchioalveolar tumors in lungs of mice. *J Virol* **80**, 9322-9325.

Wootton, S.K., Metzger, M.J., Hudkins, K.L., Alpers, C.E., York, D., DeMartini, J.C., and Miller, A.D. (2006b). Lung cancer induced in mice by the envelope protein of jaagsiekte sheep retrovirus (JSRV) closely resembles lung cancer in sheep infected with JSRV. *Retrovirology* **3**, 94.

Wuenschell, C.W., Sunday, M.E., Singh, G., Minoo, P., Slavkin, H.C., and Warburton, D. (1996). Embryonic mouse lung epithelial progenitor cells co-express immunohistochemical markers of diverse mature cell lineages. *J Histochem Cytochem* **44**, 113-123.

Yanagi, S., Kishimoto, H., Kawahara, K., Sasaki, T., Sasaki, M., Nishio, M., Yajima, N., Hamada, K., Horie, Y., Kubo, H., *et al.* (2007). Pten controls lung morphogenesis, bronchioalveolar stem cells, and onset of lung adenocarcinomas in mice. *J Clin Invest* **117**, 2929-2940.

Yeatman, T.J. (2004). A renaissance for SRC. *Nat Rev Cancer* **4**, 470-480.

York, D.F., Vigne, R., Verwoerd, D.W., and Querat, G. (1991). Isolation, identification, and partial cDNA cloning of genomic RNA of jaagsiekte retrovirus, the etiological agent of sheep pulmonary adenomatosis. *J Virol* **65**, 5061-5067.

York, D.F., Vigne, R., Verwoerd, D.W., and Querat, G. (1992). Nucleotide sequence of the jaagsiekte retrovirus, an exogenous and endogenous type D and B retrovirus of sheep and goats. *J Virol* **66**, 4930-4939.

Yoshikawa, T., Hill, T.E., Yoshikawa, N., Popov, V.L., Galindo, C.L., Garner, H.R., Peters, C.J., and Tseng, C.T. (2010). Dynamic innate immune responses of human bronchial epithelial cells to severe acute respiratory syndrome-associated coronavirus infection. *PLoS One* **5**, e8729.

Yousem, S.A., Finkelstein, S.D., Swalsky, P.A., Bakker, A., and Ohori, N.P. (2001). Absence of jaagsiekte sheep retrovirus DNA and RNA in bronchioalveolar and conventional human pulmonary adenocarcinoma by PCR and RT-PCR analysis. *Hum Pathol* **32**, 1039-1042.

Yuan, A., Chen, J.J., Yao, P.L., and Yang, P.C. (2005). The role of interleukin-8 in cancer cells and microenvironment interaction. *Front Biosci* **10**, 853-865.

Zavala, G., Pretto, C., Chow, Y.H., Jones, L., Alberti, A., Grego, E., De las Heras, M., and Palmarini, M. (2003). Relevance of Akt phosphorylation in cell transformation induced by Jaagsiekte sheep retrovirus. *Virology* **312**, 95-105.

Zhu, Y.M., Webster, S.J., Flower, D., and Woll, P.J. (2004). Interleukin-8/CXCL8 is a growth factor for human lung cancer cells. *Br J Cancer* 91, 1970-1976.

